STRINGQFT

String-Theoretic Construction
of Quantum Field Theory

VOLUME XVI

M5-Brane Theories and Class S

Xingyang Yu

StringQFT v1.0 / Source build candidate

Drafted with AI assistance under the supervision of the author.
Manuscript free to read. All rights reserved.

Contents

XVI.1 The six-dimensional parent **1**
XVI.1.1 The parent behind the compactifications 1
XVI.1.2 Separated five-branes and tensor strings 2
XVI.1.3 A circle and the five-dimensional gauge coupling 4
XVI.1.4 An instanton carries circle momentum 6
XVI.1.5 A torus and the four-dimensional coupling 9
XVI.1.6 Cycles, duality frames and the data still needed 12
XVI.1.7 Exercises 14

XVI.2 Twisting on a curve and the first class S building block **18**
XVI.2.1 Canceling the curve holonomy 18
XVI.2.2 From transverse scalars to differentials 21
XVI.2.3 What a regular puncture fixes 23
XVI.2.4 The three-punctured sphere and its free fields 25
XVI.2.5 Masses and flavor moment maps 28
XVI.2.6 Exercises 31

XVI.3 From three-punctured spheres to four-dimensional theories **34**
XVI.3.1 What a gauge tube does 34
XVI.3.2 Two trinions give four flavors 36
XVI.3.3 Pants counts and a handle 39
XVI.3.4 The sphere and its elliptic cover 42
XVI.3.5 Degeneration channels and coupling coordinates 44

XVI.4 Hitchin systems and Seiberg–Witten geometry **51**
XVI.4.1 The BPS equations after the twist 51
XVI.4.2 From a Higgs field to its spectral cover 54
XVI.4.3 Masses stay fixed while Coulomb parameters vary 55
XVI.4.4 The differential and its actual periods 58
XVI.4.5 A node and a weak-coupling cusp are different limits 61

XVI.5 Regular punctures and partial closure **67**
XVI.5.1 From a boundary condition to a partition 67
XVI.5.2 Invariant poles and puncture flavor 69
XVI.5.3 Counting parameters on a trinion 72

XVI.5.4 A nilpotent moment-map expectation value 74
XVI.5.5 Closure and gauging in a complete example 75

XVI.6 The T_N theories and non-Lagrangian fixtures 81
XVI.6.1 Three full punctures 81
XVI.6.2 Protected operators and the exceptional T_3 symmetry 83
XVI.6.3 Gauging a flavor subgroup 85
XVI.6.4 The Argyres–Seiberg comparison 87
XVI.6.5 Two T_4 blocks and a complete gluing 89

XVI.7 From six-dimensional to four-dimensional anomalies 94
XVI.7.1 Insert the twist into I8 94
XVI.7.2 The bulk result on closed curves 97
XVI.7.3 Anomalies of punctures 99
XVI.7.4 Central charges and flavor levels 101
XVI.7.5 Comparing a non-Lagrangian frame 104

XVI.8 Higgs branches and three-dimensional mirrors 109
XVI.8.1 Circle reduction and the branches being compared 109
XVI.8.2 From a partition to a tail 111
XVI.8.3 Gluing the star and removing its ineffective U1 113
XVI.8.4 Monopoles and a finite Hilbert series 115
XVI.8.5 Enhancement and the domain of the calculation 118

XVI.9 Irregular ends and Argyres–Douglas theories 124
XVI.9.1 Colliding regular ends and decoupling a flavor 124
XVI.9.2 Boundary data at infinity 128
XVI.9.3 Scaling from the Seiberg–Witten differential 130
XVI.9.4 Matching the IIB singularity direction by direction 132
XVI.9.5 Deformations and singular fibers 134

XVI.10 Outer twists and orthogonal–symplectic constructions 139
XVI.10.1 Why a twist line is needed 139
XVI.10.2 Twisted differentials and their spectral curve 141
XVI.10.3 Twisted puncture labels and boundary data 143
XVI.10.4 Gluing two fixtures into a complete theory 145
XVI.10.5 Reading D- and E-type fixture tables 148

XVI.11 Global forms and genuine line operators 154
XVI.11.1 From wrapped surfaces to lines 154
XVI.11.2 Mutual locality and a choice of genuine lines 156
XVI.11.3 SU(2), SO(3) and the discrete theta choice 158
XVI.11.4 Mapping classes and the line-preserving subgroup 160
XVI.11.5 Punctures, screening and flavor backgrounds 162

XVI.12 A class-S construction atlas 166
XVI.12.1 Choosing a theory from geometry 166

XVI.12.2 Comparing recurring constructions 168
XVI.12.3 Searching backwards from observables 171
XVI.12.4 Gluing, closure and collision 173
XVI.12.5 Inputs for protected calculations 176

Chapter XVI.1

The six-dimensional parent

XVI.1.1 The parent behind the compactifications

A four-dimensional gauge coupling can be the shape of a two-dimensional surface. To understand that statement, we first need a parent theory in which the surface is an actual part of spacetime. The parent in this volume is the six-dimensional $(2,0)$ theory. Compactification on a flat torus preserves all sixteen supercharges and gives four-dimensional $\mathcal{N}=4$ supersymmetry. Replacing the torus by a curved punctured surface, with a suitable twist, will instead produce the $\mathcal{N}=2$ theories of class S. The flat example is therefore a useful place to learn exactly which data a compactification carries.

The interacting parents are labelled by simply-laced Lie algebras $\mathfrak{g}$ of type A, D or E. Their existence and their realization in string or M-theory are physical inputs. We will use the A_{N-1} realization by N coincident M5-branes for explicit calculations. A collection of parallel M5-branes also has a free center-of-mass tensor multiplet; the interacting theory associated with $\mathfrak{su}(N)$ is the relative sector. A single M5-brane has a free tensor multiplet and does not supply a nontrivial A_0 interacting theory. The general ADE classification is broader than this elementary parallel-brane picture.

There is no ordinary nonabelian six-dimensional gauge-field action from which we will derive the interacting parent. This absence does not prevent a local free tensor description on a generic tensor branch, and it does not preclude formulations of the free chiral tensor. It does mean that a lower-dimensional Yang–Mills Lagrangian cannot simply be lifted by adding a sixth coordinate. Our calculations instead start from physical fields, brane charges, protected tensions and a controlled low-energy reduction.

The chapter follows one chain of questions. How do separated five-branes encode tensor multiplets and charged strings? How does a circle turn them into vectors and charged particles? Why does a five-dimensional instanton have the mass of a Kaluza–Klein mode? Finally, which part of the four-dimensional coupling is the shape of the torus, and which additional choices are needed to specify a theory with definite line operators? The calculations fix the numerical factors in this chain. They do not turn a classical soliton into a proof of the complete quantum spectrum.

XVI.1.2 Separated five-branes and tensor strings

What changes when the five-branes separate? Take an M5-brane along $x^{0,1,2,3,4,5}$ in flat eleven-dimensional spacetime. Its five transverse positions are scalar fields, and rotations of the transverse space give the R-symmetry group

$$\mathrm{Spin}(5)_R \simeq \mathrm{USp}(4)_R. \tag{XVI.1.1}$$

Together with the fermions, the five scalars belong to a tensor multiplet containing a two-form potential B. Choose the orientation of this flat M5 worldvolume so that its three-form field strength obeys

$$H = dB, \qquad H = *_6 H. \tag{XVI.1.2}$$

The metric has mostly plus signature. The sign in this equation is an orientation convention; the supersymmetry label alone should not be used to transfer a Hodge-star sign between different geometric constructions.

The physical little group of a massless particle in six dimensions is Spin(4). A nonchiral two-form has $\binom{4}{2} = 6$ transverse polarizations. Self-duality selects one of its two three-dimensional pieces. Thus the on-shell bosonic count is

$$n_B = \frac{1}{2}\binom{4}{2} + 5 = 3 + 5 = 8. \tag{XVI.1.3}$$

Supersymmetry pairs these with eight fermionic polarizations. In particular, the tensor is not a six-dimensional vector: a massless vector would have four polarizations. This distinction will matter when we identify the vector that appears after compactification.

For N separated parallel branes, write their positions as y_a^I, where $a = 1, \ldots, N$ and $I = 6, \ldots, 10$. The common translation and the relative positions are

$$y^I_{\mathrm{cm}} = \frac{1}{N}\sum_{a=1}^{N} y_a^I, \qquad \widehat{y}_a^I = y_a^I - y^I_{\mathrm{cm}}, \qquad \sum_a \widehat{y}_a^I = 0. \tag{XVI.1.4}$$

This split can be made without selecting a particular transverse direction. With $u = (1, \ldots, 1)^t$, the projector onto the relative subspace is

$$P = \mathbf{1}_N - \frac{uu^t}{N}, \qquad P^2 = P, \quad Pu = 0, \quad \mathrm{tr}\, P = N - 1. \tag{XVI.1.5}$$

Indeed, $u^t u = N$ makes the two quadratic terms in P^2 combine to $-uu^t/N$. The rank is therefore $N - 1$, as required for the Cartan tensor multiplets of A_{N-1}. This is a statement about local free fields on the generic branch. It is not a claim that every global partition function factors into an independent center-of-mass partition function and an absolute interacting theory.

An M2-brane stretched between two M5-branes has an endpoint on each worldvolume. Its boundary is a string, electrically coupled to the two-form. Writing e_a for the standard orthonormal basis vectors of $\mathbb{R}^N$, opposite endpoint orientations give the charge vector $e_a - e_b$, which is orthogonal to u. Choosing neighboring branes as simple charges gives

$$\alpha_i = e_i - e_{i+1}, \qquad i = 1, \ldots, N-1, \qquad \alpha_i \cdot \alpha_j = 2\delta_{ij} - \delta_{i,j+1} - \delta_{i+1,j}. \tag{XVI.1.6}$$

The relative-coordinate construction has produced the A_{N-1} Cartan matrix. The root lattice is carried by endpoint charges, rather than by hypothetical nonabelian two-form matrix components. Permutations of indistinguishable parallel branes act as the Weyl group. Locally, away from coincidences, the tensor branch therefore has five real scalar directions for each Cartan tensor; its A-series description is

$$\mathcal{M}_{\text{tensor,loc}} \simeq \left\{ (\widehat{y}_1, \ldots, \widehat{y}_N) \in (\mathbb{R}^5)^N : \sum_a \widehat{y}_a = 0 \right\} / S_N. \tag{XVI.1.7}$$

At a coincidence the free-field approximation ceases to include all light objects.

For three branes, these operations can be seen explicitly:

$$P_{A_2} = \frac{1}{3} \begin{pmatrix} 2 & -1 & -1 \\ -1 & 2 & -1 \\ -1 & -1 & 2 \end{pmatrix}, \qquad C_{A_2} = \begin{pmatrix} 2 & -1 \\ -1 & 2 \end{pmatrix}, \qquad \det C_{A_2} = 3. \tag{XVI.1.8}$$

Take the positions in one transverse direction to be $(0, d, 3d)$, with $d > 0$. Their center is $4d/3$, and projection gives

$$(\widehat{y}_1, \widehat{y}_2, \widehat{y}_3) = \frac{d}{3}(-4, -1, 5), \qquad (|y_1 - y_2|, |y_2 - y_3|, |y_1 - y_3|) = (d, 2d, 3d). \tag{XVI.1.9}$$

The sum of the two simple charges is $e_1 - e_3$. In this aligned example its tension is the sum of the two simple-string tensions. The equality concerns central-charge alignment; root addition by itself is not a proof that arbitrary charges support stable one-particle states in every vacuum.

To calculate the tension, let the stretched membrane occupy (x^0, x^1, x^6), with the two five-branes a distance d apart in x^6. Write ℓ_p for the eleven-dimensional Planck length. The membrane area per unit length in x^1 is d, hence

$$T_{\text{M2}} = \frac{1}{(2\pi)^2 \ell_p^3}, \qquad T_{\text{string}} = T_{\text{M2}} d = \frac{d}{(2\pi)^2 \ell_p^3}. \tag{XVI.1.10}$$

The M5 and M2 supersymmetry conditions can be written, with compatible orientation signs, as

$$\Gamma_{012345}\epsilon = \epsilon, \qquad \Gamma_{016}\epsilon = \epsilon. \tag{XVI.1.11}$$

The two independent compatible projectors leave eight of the eleven-dimensional thirty-two supercharges, or half of the sixteen preserved by the M5. This explains why the tension is a BPS quantity. The string is called self-dual because its electric and magnetic tensor charges are related by the self-duality of H.

Figure XVI.1.1 separates two configurations that should not be conflated. A string along x^1 is still an extended string after compactifying x^5. To obtain a particle, one must orient the membrane boundary along the compact direction instead. At $d = 0$, the stretched-string tension vanishes, and the generic tensor-branch effective theory no longer suffices. For $N = 1$, by contrast, $P = 0$ and there are no relative endpoint charges. The surviving free tensor multiplet should not be mistaken for an interacting rank-one parent.

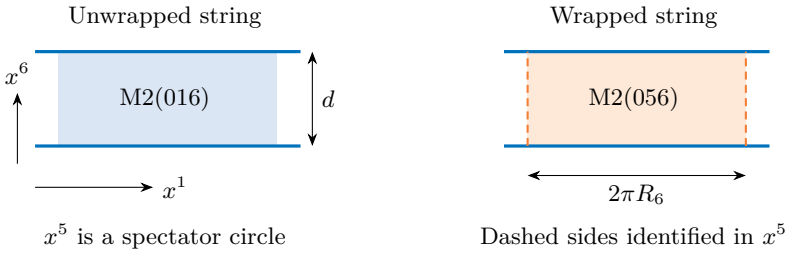


Figure XVI.1.1: Two different membrane strips between parallel M5-branes. The unwrapped M2 along (016) gives a string extending along x^1. The M2 along (056) wraps the longitudinal x^5 circle and gives a particle after reduction. The strip width is the transverse separation d in both cases.

The decoupled M5 worldvolume theory and the interacting coincident-brane limit are physical premises. The projector, charge Gram matrix and membrane area calculation explain how those premises organize a tractable branch. They also identify the objects whose winding will become gauge-theory electric charge.

XVI.1.3 A circle and the five-dimensional gauge coupling

How does a chiral tensor become a vector with a definite gauge coupling? Compactify the M5 direction x^5 on a circle of circumference $2\pi R_6$, keeping periodic fermions. The subscript on R_6 refers to the six-dimensional origin of the circle; it is not a transverse coordinate index. At energies

$$ER_6 \ll 1, \tag{XVI.1.12}$$

we can retain the circle-independent modes. Let $\vartheta_6 = x^5/R_6$, of period 2π, and use the orthonormal one-form $e^5 = R_6 d\vartheta_6$. Decompose a zero-mode three-form as

$$H = h_3 + f_2 \wedge e^5. \tag{XVI.1.13}$$

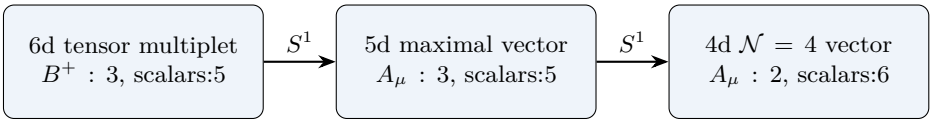
The components of f_2 arise from $B_{\mu 5}$. The six-dimensional self-duality condition expresses h_3 as the five-dimensional Hodge dual of f_2, with the sign fixed by the chosen orientation. Thus h_3 and f_2 are not independent fields. The Bianchi identity becomes the Maxwell equation together with the ordinary Bianchi identity:

$$df_2 = 0, \qquad d(*_5 f_2) = 0. \tag{XVI.1.14}$$

Locally f_2 is a vector field strength. An overall normalization of this free field is fixed by its charged objects, rather than by counting polarizations alone.

The zero-mode multiplet has precisely the required degrees of freedom:

$$\underbrace{3+5}_{\text{six-dimensional tensor}} \longrightarrow \underbrace{3+5}_{\text{five-dimensional vector}} . \tag{XVI.1.15}$$



Eight bosonic zero-mode polarizations at each step; periodic fermions.

Figure XVI.1.2: The same eight bosonic polarizations in successive zero-mode descriptions. Self-duality ties the five-dimensional two-form and vector descriptions together. On the second circle, the component of the five-dimensional vector along that circle becomes an additional scalar. Periodic fermions preserve sixteen supercharges.

The five-dimensional vector has $5-2=3$ physical polarizations. Adding an independent vector from the dualized $B_{\mu\nu}$ would count these same modes twice. Figure XVI.1.2 also shows the later four-dimensional reduction, where a Wilson-line scalar supplies the sixth scalar of $\mathcal{N}=4$ Yang–Mills.

The interacting low-energy identification is maximally supersymmetric Yang–Mills with algebra $\mathfrak{g}$. On a generic branch we first see only its Cartan vectors. For the A series, wrapped stretched membranes supply the charged particles that become the root W bosons. Let g_s be the type-IIA string coupling and $\ell_s = \sqrt{\alpha'}$ the string length. The ordinary longitudinal M-theory/type-IIA relation gives an independent way to fix their masses and the gauge kinetic coefficient:

$$R_6 = g_s \ell_s, \qquad \ell_p^3 = R_6 \ell_s^2, \qquad \text{M5}(012345) \longrightarrow \text{D4}(01234). \tag{XVI.1.16}$$

This is a dual description of the specified flat circle background, not an additional construction of the six-dimensional parent from a nonabelian tensor action.

Now use the wrapped configuration M2(056) in Figure XVI.1.1. A once-wrapped string of tension (XVI.1.10) has mass

$$M_W = (2\pi R_6) T_{\text{string}} = \frac{R_6 d}{2\pi \ell_p^3} = \frac{d}{2\pi \ell_s^2}. \tag{XVI.1.17}$$

The reduced membrane is the fundamental string stretching between the D4-branes, whose tension is $T_{\text{F1}} = 1/(2\pi\ell_s^2)$. The last expression is therefore also $T_{\text{F1}} d$. The circumference, rather than the radius alone, is essential to this equality. A winding number w changes the mass to $|w| M_W$ for a static pure winding configuration and reverses the oriented charge when w changes sign.

Let the generators be Hermitian, and use the fundamental matrix trace and curvature

$$\operatorname{tr}_f(T_a T_b) = \frac{1}{2}\delta_{ab}, \qquad F = dA - iA \wedge A, \qquad S_{\text{YM}} = -\frac{1}{2g_5^2} \int d^5x \, \operatorname{tr}_f F_{\mu\nu} F^{\mu\nu}. \tag{XVI.1.18}$$

In components this is $-F^a_{\mu\nu} F^{a\mu\nu}/(4g_5^2)$. Specifying both the matrix trace and the coefficient removes a common factor-of-two ambiguity.

At quadratic order the D4 Dirac–Born–Infeld action gives

$$S_{\text{D4}} \supset -\frac{\tau_4 (2\pi\alpha')^2}{4} \int d^5x \, \operatorname{tr}_f F_{\mu\nu} F^{\mu\nu}, \qquad \tau_4 = \frac{1}{(2\pi)^4 g_s \ell_s^5}, \quad \alpha' = \ell_s^2. \tag{XVI.1.19}$$

Only the unambiguous quadratic trace is needed; no prescription for the full nonabelian DBI action enters this calculation. Evaluating its coefficient before naming a coupling gives

$$\frac{\tau_4(2\pi\alpha')^2}{4} = \frac{4\pi^2\ell_s^4}{4(2\pi)^4 g_s \ell_s^5} = \frac{1}{16\pi^2 g_s \ell_s} = \frac{1}{2g_5^2}. \tag{XVI.1.20}$$

Consequently,

$$\boxed{g_5^2 = 8\pi^2 g_s \ell_s = 8\pi^2 R_6.} \tag{XVI.1.21}$$

The dimension is correct: g_5^2 has units of length. Expanding DBI assumes small field strengths in string units and neglects higher derivatives. The coefficient extracted in this regime is the one used in the long-wavelength gauge action.

Suppose instead that a source writes $-\operatorname{tr}_f F^2/(4g_{\rm n}^2)$ with exactly the same matrix trace. Equality of actions, not equality of the symbols for the couplings, requires

$$\frac{1}{2g_5^2} = \frac{1}{4g_{\rm n}^2}, \qquad g_5^2 = 2g_{\rm n}^2, \qquad R_6 = \frac{g_{\rm n}^2}{4\pi^2}. \tag{XVI.1.22}$$

Both radius formulas describe the same normalization of the action. Importing the last formula while leaving the first action unchanged would produce an incorrect instanton mass.

For a scale comparison, take $R_6 = 1/(10u)$ and $T_{\rm string} = 3u^2$, with u an energy unit. Then

$$M_W = \frac{3\pi}{5}u, \qquad M_{\rm KK}^{(1)} = 10u, \qquad g_5^2 = \frac{4\pi^2}{5u}, \qquad \frac{M_W}{M_{\rm KK}^{(1)}} = \frac{3\pi}{50}. \tag{XVI.1.23}$$

This branch has charged particles below the first geometric KK scale. Reducing R_6 at fixed six-dimensional string tension makes the winding particles lighter and the KK momentum modes heavier. Alternatively, fixing a finite W mass while shrinking the circle requires the tensor expectation value, and hence the string tension, to scale as $1/R_6$. The choice of what is held fixed is part of the compactification limit.

The circle has now explained the Cartan vector, its charged particles and the coefficient of its nonabelian low-energy completion. We next test that coefficient against a different charged object: a smooth instanton in the five-dimensional gauge theory.

XVI.1.4 An instanton carries circle momentum

Can the gauge theory remember momentum in a direction that has been removed? Its candidate charge is the instanton number on spatial $\mathbb{R}^4$. For the calculation in this section, return to the unbroken $SU(2)$ scalar origin and set the electric fields to zero. More generally, scalar fields can be covariantly constant and commute with the embedded $SU(2)$, with zero scalar potential. A generic separated-brane scalar expectation value does not satisfy these conditions. In that case scalar gradients contribute to the energy, and the pure magnetic answer below is not the total energy.

Use the Euclidean spatial orientation $dx^1 \wedge dx^2 \wedge dx^3 \wedge dx^4 > 0$ and write $*_4$ for its Hodge star. A smooth finite-action connection approaching a pure gauge at infinity extends to a bundle on the compactification S^4. Its charge is

$$k = \frac{1}{8\pi^2} \int_{\mathbb{R}^4} \operatorname{tr}_f (F \wedge F) \in \mathbb{Z}. \tag{XVI.1.24}$$

The energy following from (XVI.1.18) is

$$E = \frac{1}{2g_5^2} \int d^4x \, \operatorname{tr}_f F_{ij} F_{ij} = \frac{1}{g_5^2} \int \operatorname{tr}_f (F \wedge *_4 F). \tag{XVI.1.25}$$

The factor $1/2$ in the component-to-form identity is crucial. Since $*_4^2 = 1$ on two-forms, expansion of a nonnegative square yields

$$E = \frac{1}{2g_5^2} \int \operatorname{tr}_f \big[(F - *_4 F) \wedge *_4 (F - *_4 F) \big] + \frac{8\pi^2 k}{g_5^2}. \tag{XVI.1.26}$$

For negative k choose the opposite sign in the square. Thus

$$E \geq \frac{8\pi^2 |k|}{g_5^2}, \qquad E = \frac{8\pi^2 |k|}{g_5^2} \quad \text{when} \quad F = \operatorname{sgn}(k) *_4 F. \tag{XVI.1.27}$$

The bound alone does not exhibit a finite-action field that attains it. We now construct one and evaluate its integrals.

For $a = 1, 2, 3$, define the self-dual 't Hooft symbols by

$$\eta^a_{ij} = \epsilon_{aij} \quad (i, j \leq 3), \qquad \eta^a_{i4} = \delta_{ai}, \qquad \eta^a_{4i} = -\delta_{ai}. \tag{XVI.1.28}$$

Take $T_a = \sigma_a / 2$, set $r^2 = \sum_i (x^i)^2$, and choose a size $\rho > 0$. The regular-gauge BPST connection is

$$A_i = A^a_i T_a, \qquad A^a_i = \frac{2 \eta^a_{ij} x^j}{r^2 + \rho^2}. \tag{XVI.1.29}$$

With $D = r^2 + \rho^2$, the derivative term is

$$\partial_i A^a_j - \partial_j A^a_i = -\frac{4\eta^a_{ij}}{D} - \frac{4}{D^2} \big(x_i \eta^a_{j\ell} x^\ell - x_j \eta^a_{i\ell} x^\ell \big). \tag{XVI.1.30}$$

The commutator is not optional: because $F = dA - iA \wedge A$, it contributes $+\epsilon_{abc} A^b_i A^c_j$. Substitution of the symbols in (XVI.1.28) gives the identity

$$\epsilon_{abc} \eta^b_{i\ell} \eta^c_{jm} x^\ell x^m = r^2 \eta^a_{ij} + x_i \eta^a_{j\ell} x^\ell - x_j \eta^a_{i\ell} x^\ell. \tag{XVI.1.31}$$

Its second and third terms cancel the nonradial derivative terms. The remaining curvature is

$$F^a_{ij} = -\frac{4\rho^2 \eta^a_{ij}}{(r^2 + \rho^2)^2}, \qquad F = *_4 F. \tag{XVI.1.32}$$

For example, at $x = (0, 0, 0, r)$ both F^3_{12} and F^3_{34} equal $-4\rho^2/(r^2 + \rho^2)^2$. This checks the relative spatial orientation, not merely the radial falloff. At infinity the leading

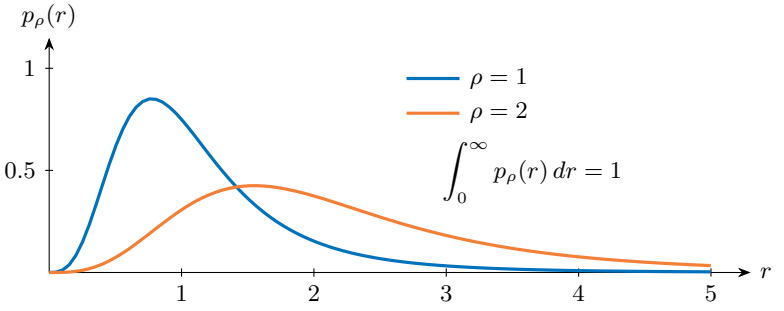


Figure XVI.1.3: The radial distribution of unit topological charge, $p_\rho(r) = 12\rho^4 r^3/(r^2+\rho^2)^4$, for two sizes. Each curve integrates to one. Increasing the size spreads the same charge over a larger spatial region; it does not change the classical mass.

connection is pure gauge, while the curvature falls as r^{-4}. At the origin the connection is smooth for positive ρ.

There are twelve nonzero entries of magnitude one in η^a_{ij} when both orders of i, j are included. The fundamental trace then gives

$$\operatorname{tr}_f F_{ij}F_{ij} = \frac{1}{2}\sum_{a,i,j}(F^a_{ij})^2 = \frac{96\rho^4}{(r^2+\rho^2)^4}. \tag{XVI.1.33}$$

To integrate it, use $\operatorname{Vol}(S^3) = 2\pi^2$ and set $t = r^2/\rho^2$. The radial integral is

$$\int_0^\infty \frac{r^3\,dr}{(r^2+\rho^2)^4} = \frac{1}{2\rho^4}\int_0^\infty \frac{t\,dt}{(1+t)^4} = \frac{1}{12\rho^4}. \tag{XVI.1.34}$$

The last integral is $1/6$, obtainable by writing $t = (1+t)-1$ and integrating two inverse powers. Consequently,

$$\int d^4x\ \operatorname{tr}_f F_{ij}F_{ij} = 16\pi^2, \qquad \int \operatorname{tr}_f F\wedge F = 8\pi^2, \qquad k = 1. \tag{XVI.1.35}$$

This evaluates a field configuration rather than inserting an assumed integer into the bound. Its energy and the circle coefficient agree:

$$E_{\mathrm{BPST}} = \frac{8\pi^2}{g_5^2} = \frac{1}{R_6}. \tag{XVI.1.36}$$

The size dependence is particularly informative. Equation (XVI.1.35) defines the normalized radial density

$$p_\rho(r) = \frac{12\rho^4 r^3}{(r^2+\rho^2)^4}, \qquad \int_0^\infty p_\rho(r)\,dr = 1, \qquad p_{2\rho}(2r) = \frac{1}{2}p_\rho(r). \tag{XVI.1.37}$$

Figure XVI.1.3 illustrates the last relation. As ρ tends to zero, the density tends to zero at each fixed $r > 0$, yet its integral remains one. The limiting charge concentrates

at the origin. Substituting the pointwise limit under the integral would erase a physical charge and leave the space of smooth solutions.

The charge interpretation has a separate brane check. In the RR convention where $\mu_p = (2\pi)^{-p}\alpha'^{-(p+1)/2}$, the D4 Wess–Zumino action couples to the RR one-form C_1 through

$$S_{\mathrm{WZ}} \supset \frac{\mu_4(2\pi\alpha')^2}{2}\int C_1 \wedge \mathrm{tr}_f(F\wedge F). \tag{XVI.1.38}$$

For a localized instanton, the spatial integral reduces this coupling to a worldline coupling. Its coefficient is

$$\frac{\mu_4(2\pi\alpha')^2}{2}(8\pi^2 k) = 16\pi^4\alpha'^2\mu_4\, k = \mu_0 k, \qquad \mu_0 = \alpha'^{-1/2}. \tag{XVI.1.39}$$

Thus the instanton has k units of D0 charge. Ordinary M/IIA duality identifies D0 charge with momentum around the M-theory circle. Choosing the circle orientation consistently gives

$$n = k, \qquad p_5 = \frac{k}{R_6}, \qquad M_{\mathrm{D0}} = \frac{1}{g_s\ell_s} = \frac{1}{R_6}. \tag{XVI.1.40}$$

The energy equality alone fixes only $|n| = |k|$; the WZ coupling and orientation carry the sign information. An anti-self-dual configuration has $k = -1$ and the same positive mass.

These calculations explain why instanton charge is the appropriate remnant of circle momentum. They do not quantize the instanton moduli space or establish a normalizable quantum state for every integer charge. The zero-size region and the absence of ordinary smooth commutative $U(1)$ instantons are important boundaries: the free tensor still has KK excitations, although its abelian five-dimensional zero-mode action has no BPST solution. Moreover, $1/R_6$ lies at the KK threshold, outside the strict regime (XVI.1.12). Protected mass and charge matching can remain meaningful there without proving that pure five-dimensional Yang–Mills is an all-energy definition of the parent. We will need the charge identification, together with its limitations, when the next circle carries a nontrivial holonomy.

XVI.1.5 A torus and the four-dimensional coupling

Which geometric modulus becomes the complex Yang–Mills coupling? A marked torus has an ordered pair of primitive cycles, A and B. Use two angles ϑ_6, ϑ_5, each of period 2π, and the flat metric

$$ds^2_{T^2} = R_6^2(d\vartheta_6 + \kappa\, d\vartheta_5)^2 + R_5^2 d\vartheta_5^2, \qquad R_5, R_6 > 0. \tag{XVI.1.41}$$

Here A is the first circle. The radius R_5 is the radius of the quotient base after reducing along A. It is not generally the length of the slanted B cycle divided by 2π. The dimensionless real number κ measures shear.

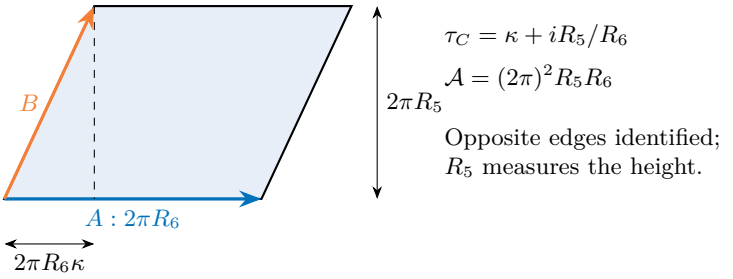


Figure XVI.1.4: A marked flat torus, with opposite edges identified. The horizontal edge is A; the slanted edge is B. Its horizontal projection determines κ, while the height is $2\pi R_5$. The area and complex structure are independent geometric data.

Represent the torus by a lattice in a complex plane. Its periods and complex structure are

$$\omega_A = 2\pi R_6, \qquad \omega_B = 2\pi(R_6\kappa + iR_5), \qquad \tau_C = \frac{\omega_B}{\omega_A} = \kappa + i\frac{R_5}{R_6}. \tag{XVI.1.42}$$

The metric on the angular coordinates is the Gram matrix

$$G = \begin{pmatrix} R_6^2 & R_6^2\kappa \\ R_6^2\kappa & R_5^2 + R_6^2\kappa^2 \end{pmatrix}, \qquad \det G = R_6^2 R_5^2, \qquad \mathcal{A} = (2\pi)^2 R_6 R_5. \tag{XVI.1.43}$$

The area is independent of shear. The two marked cycle lengths, however, are

$$L_A = 2\pi R_6, \qquad L_B = 2\pi\sqrt{R_5^2 + \kappa^2 R_6^2}. \tag{XVI.1.44}$$

Figure XVI.1.4 displays the distinction between the slanted edge and its perpendicular height. It is the height that appears in the second dimensional reduction.

First compactify along A. The five-dimensional gauge coupling is (XVI.1.21), and the quotient direction has circumference $2\pi R_5$. For fields independent of this second circle, integrating the gauge kinetic term gives

$$-\frac{1}{2g_5^2}\int_0^{2\pi R_5} dy \int d^4x \ \mathrm{tr}_f \, F_{\mu\nu}F^{\mu\nu} = -\frac{1}{2g_4^2}\int d^4x \ \mathrm{tr}_f \, F_{\mu\nu}F^{\mu\nu}. \tag{XVI.1.45}$$

Therefore

$$g_4^2 = \frac{g_5^2}{2\pi R_5} = 4\pi\frac{R_6}{R_5}, \qquad \frac{4\pi}{g_4^2} = \frac{R_5}{R_6}. \tag{XVI.1.46}$$

The five-dimensional vector contributes its component along the second circle as a scalar. Together with the original five scalars, the zero modes form the $2+6$ bosonic polarizations of a four-dimensional $\mathcal{N}=4$ vector multiplet. A torus with periodic spin structure preserves all sixteen supercharges; no compensating R-symmetry twist is required for its flat metric.

The real part of the coupling comes from the same metric. Reducing the first circle leaves the dimensionless KK connection

$$a = \kappa\, d\vartheta_5, \qquad \oint_B a = 2\pi\kappa. \tag{XVI.1.47}$$

A state of integer KK charge n acquires phase $\exp(in \oint a)$. Since instanton charge is $k = n$ with our orientation, a unit instanton winding the second circle acquires precisely the four-dimensional theta-angle phase. In the normalization

$$\exp\left(-\frac{8\pi^2 k}{g_4^2} + ik\theta_4\right) \quad (k > 0), \qquad \theta_4 = 2\pi\kappa, \tag{XVI.1.48}$$

the connection holonomy supplies θ_4. This is the topological part of the reduction; it is not visible if one keeps only the diagonal kinetic terms of the torus metric.

Define the complex coupling using the same fundamental trace as before:

$$\tau_{\mathrm{YM}} = \frac{\theta_4}{2\pi} + \frac{4\pi i}{g_4^2}. \tag{XVI.1.49}$$

Combining the real and imaginary parts gives the result

$$\boxed{\tau_{\mathrm{YM}} = \kappa + i\frac{R_5}{R_6} = \tau_C}, \qquad q_{\mathrm{inst}} = e^{2\pi i \tau_C}. \tag{XVI.1.50}$$

The equality concerns the actual compactification torus of the six-dimensional parent. A spectral torus describing an $\mathcal{N} = 2$ low-energy effective theory is a different object. Its modulus, a chosen ultraviolet coordinate and a cross-ratio need not be identical functions. This distinction will prevent a misleading transfer of the simple result (XVI.1.50) to every curve that appears later in class S.

For a sheared example, measure lengths in a common unit L and choose

$$R_6 = 2L, \qquad R_5 = 3L, \qquad \kappa = \frac{1}{3}. \tag{XVI.1.51}$$

Then the kinetic and topological reductions give

$$\tau_C = \frac{1}{3} + \frac{3i}{2}, \qquad g_4^2 = \frac{8\pi}{3}, \qquad \theta_4 = \frac{2\pi}{3}, \qquad q_{\mathrm{inst}} = e^{-3\pi} e^{2\pi i/3}. \tag{XVI.1.52}$$

The corresponding geometric measurements are

$$\mathcal{A} = 24\pi^2 L^2, \qquad L_A^2 = 16\pi^2 L^2, \qquad L_B^2 = \frac{340\pi^2}{9} L^2. \tag{XVI.1.53}$$

Using $L_B/(2\pi)$ in (XVI.1.46) would replace $3L$ by $\sqrt{85}L/3$ and give the wrong coupling. The base metric and the KK connection together already encode the shear; it must not be counted a second time by using the full slanted length.

To obtain a four-dimensional theory at fixed external energy, both compactification scales must become large compared with that energy. A simple limit keeps the shape fixed and scales

$$(R_6, R_5) \longmapsto (\epsilon R_6, \epsilon R_5), \qquad \epsilon \longrightarrow 0, \qquad \tau_C \text{ fixed}, \quad \mathcal{A} \longmapsto \epsilon^2 \mathcal{A}. \tag{XVI.1.54}$$

Every geometric KK energy of a fixed nonzero momentum mode then scales as $1/\epsilon$. Area tending to zero is not sufficient by itself. On a rectangular torus, take R_6 fixed and $R_5 \to 0$. The area vanishes, but modes with momentum along the first circle still have masses $|n|/R_6$. They remain in the problem unless the external energy is also much smaller than that scale. Shape fixes the dimensionless coupling; size controls the accuracy of the lower-dimensional description.

The derivation identifies the local gauge theory and its coupling. It has also used a marking, which chooses an electric description. We now change that marking and ask what additional information must travel with it.

XVI.1.6 Cycles, duality frames and the data still needed

Does changing the basis of torus cycles leave one fixed gauge theory unchanged? The geometric operation is straightforward, but its physical interpretation depends on charges and global choices. First consider a string wrapped on an oriented cycle

$$\gamma = nA + mB, \qquad (n, m) \in \mathbb{Z}^2. \tag{XVI.1.55}$$

Its geometric length is

$$L_{n,m} = |n\omega_A + m\omega_B| = 2\pi R_6 |n + m\tau_C|, \qquad M_{n,m} = T_{\text{string}} L_{n,m} \tag{XVI.1.56}$$

for a static straight wrapped string of tension T_{string}. The geometric calculation is exact for that configuration. It does not establish an occupied stable one-particle BPS state for every pair (n, m). Nonprimitive pairs and marginal binding require further dynamics.

The example (XVI.1.51) is useful because its shear makes sign and basis errors visible. For the primitive cycle $A + 2B$,

$$|1 + 2\tau_C|^2 = \left(\frac{5}{3}\right)^2 + 3^2 = \frac{106}{9}, \qquad L_{1,2}^2 = \frac{1696\pi^2}{9} L^2. \tag{XVI.1.57}$$

Replacing this cycle by $A - 2B$ changes the interference term and hence the length. Simultaneously reversing both signs preserves the length but reverses the oriented charge. A mass comparison alone cannot distinguish a particle from its antiparticle.

Let E denote the matrix whose two columns are the real two-vectors representing A and B. The modular S change of marking is

$$(A', B') = (B, -A), \qquad E' = ES, \qquad S = \begin{pmatrix} 0 & -1 \\ 1 & 0 \end{pmatrix}. \tag{XVI.1.58}$$

To describe the same oriented cycle, transform the coordinate column contragrediently:

$$q = \begin{pmatrix} n \\ m \end{pmatrix}, \qquad q' = S^{-1} q = \begin{pmatrix} m \\ -n \end{pmatrix}, \qquad E' q' = Eq. \tag{XVI.1.59}$$

For example, $(n, m) = (1, 2)$ becomes $(2, -1)$, and $2A' - B' = A + 2B$. Choosing $(-2, 1)$ would instead give the negative cycle. Both choices have the same length, so checking only a norm would miss the orientation error.

The Gram matrix transforms together with the coordinates:

$$G' = S^t G S, \qquad q'^t G' q' = q^t G q, \qquad \tau'_C = \frac{-\omega_A}{\omega_B} = -\frac{1}{\tau_C}. \tag{XVI.1.60}$$

For the sheared example this gives

$$\tau'_C = -\frac{1}{1/3 + 3i/2} = -\frac{12}{85} + \frac{54i}{85}. \tag{XVI.1.61}$$

The positive imaginary part confirms that the oriented area is preserved. Simply interchanging the symbols R_5 and R_6 would miss the transformed shear. On a rectangular torus, $\kappa = 0$, the exchange reduces to the familiar reciprocal ratio, and (XVI.1.46) yields

$$g'^2_4 = \frac{16\pi^2}{g_4^2}. \tag{XVI.1.62}$$

The electric and magnetic descriptions exchange roles. Establishing the full quantum duality requires the parent-theory interpretation, beyond the matrix identity that preserves geometric lengths.

There is also a global qualification. An algebra, a coupling and a local Lagrangian do not uniquely specify which Wilson–'t Hooft lines are genuine operators. For algebra $\mathfrak{su}(2)$, the center-valued electric and magnetic charges can be represented by

$$(e, m) \in \mathbb{F}_2^2, \qquad \langle (e, m), (e', m') \rangle = em' - me' \pmod 2. \tag{XVI.1.63}$$

Mutually local line charges have zero pairing. A maximal allowed subgroup has two elements and is generated by one of the three nonzero vectors. They are

$$\begin{aligned} L_{SU(2)} &= \{(0,0), (1,0)\}, \\ L_{SO(3)_+} &= \{(0,0), (0,1)\}, \\ L_{SO(3)_-} &= \{(0,0), (1,1)\}. \end{aligned} \tag{XVI.1.64}$$

This list is complete: a one-dimensional subspace over $\mathbb{F}_2$ has exactly one nonzero element, and $\mathbb{F}_2^2$ has exactly three such elements. Each generator pairs trivially with itself. The whole two-dimensional space is not isotropic, since $(1, 0)$ and $(0, 1)$ pair to one. Isotropy of a few displayed subgroups, without completeness and distinctness, would not establish this classification.

Modulo two, the sign in the S transformation is invisible, so the action exchanges electric and magnetic charges. Therefore

$$S : L_{SU(2)} \longleftrightarrow L_{SO(3)_+}, \qquad S : L_{SO(3)_-} \longmapsto L_{SO(3)_-}. \tag{XVI.1.65}$$

Figure XVI.1.5 makes the effect explicit. The full modular group can act on a family of absolute theories, rather than as a symmetry of one chosen line spectrum. A choice of global gauge form and discrete theta data is therefore not dispensable information.

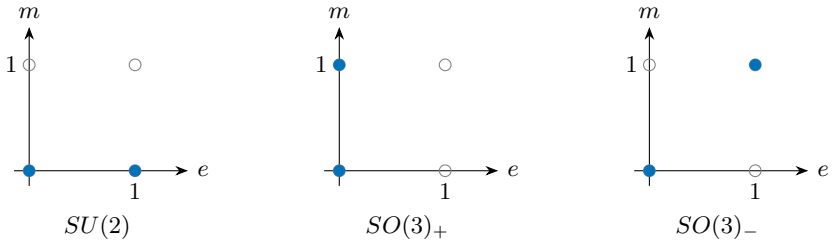


Figure XVI.1.5: The three maximal mutually local center-charge choices for algebra $\mathfrak{su}(2)$. Filled blue points are the allowed subgroup; gray points are excluded. Each choice contains the origin and exactly one nonzero vector. Modular S exchanges the first two choices and preserves the third as a center-charge set.

Removing the center-of-mass tensor in (XVI.1.5) addresses a different issue. That projection separates local common translations from relative brane motion. The relative/absolute distinction for the interacting six-dimensional theory concerns global topological data and the choice needed to obtain definite partition functions and line operators after compactification. One operation does not automatically perform the other. We will return to those global choices in Chapter 11.

The flat torus has supplied a local four-dimensional gauge theory, its complex coupling, a geometric origin for changes of electric frame, and a warning about the remaining global data. On a curved surface the first obstruction is more elementary: constant supersymmetry parameters need not exist. The next chapter explains the twist that compensates the spin connection and makes the class S construction possible.

XVI.1.7 Exercises

Show the derivation and explain the physical interpretation in each problem. For benchmark submissions, see `benchmark/PROTOCOL.md`. All traces, orientations and radii follow the conventions of this chapter.

1. **Four separated five-branes.** Place four branes at $(0, 2, 5, 9)d$ along one transverse direction. Calculate y_{cm}/d, the four relative positions in units of d, and the Gram matrix of $e_1 - e_2, e_2 - e_3, e_3 - e_4$. Give its determinant. Find the three simple-string tensions and the tension of the $e_1 - e_4$ string in units of $T_{\mathrm{M2}}d$. Explain why adding the same displacement to all four positions changes none of these tensions, and why the local projection does not choose a global line spectrum.

2. **Winding and the trace.** Take $R_6 = 1/(12u)$ and $T_{\mathrm{string}} = 5u^2$. Find the static mass for winding $w = -2$ in units of πu, the first KK mass in units of u, and g_5^2 in units of π^2/u. A source uses $-\operatorname{tr}_f F^2/(4g_{\mathrm{n}}^2)$ with the same trace. Find g_{n}^2 in the same units. What information is lost by recording only the winding mass?

3. **Where is the instanton charge?** For the radial density (XVI.1.37), derive the charge inside a ball of radius $r = \rho$. Also compute the charge inside $r = 2\rho$ as an exact rational number. Finally, double the instanton size from ρ to 2ρ and compute the charge inside the fixed ball whose radius is the original ρ. Explain why the total energy is independent of size in the stated background, and why neither a generic scalar expectation value nor the limit $\rho = 0$ can be inserted without further work.

4. **A different sheared torus.** Set $R_6 = 3L$, $R_5 = 2L$ and $\kappa = -1/2$. Give the real and imaginary parts of τ_C, g_4^2/π, θ_4/π, $\mathcal{A}/(\pi^2 L^2)$ and $L_B^2/(\pi^2 L^2)$. Calculate $L_{2,1}^2/(\pi^2 L^2)$. Explain why the quotient radius is needed in the coupling calculation. Compare uniform shrinking at fixed shape with shrinking only R_5 at fixed R_6.

5. **Transport an oriented charge.** On the torus of Problem 4, replace (A, B) by $(B, -A)$. Give the real and imaginary parts of τ_C' and the new coordinates of $2A + B$. Verify the equality of oriented cycles before verifying their lengths. Explain why a test of mass invariance alone cannot distinguish the correct charge transport from its overall negative.

6. **Complete the global choice.** Enumerate all maximal isotropic subspaces of $\mathbb{F}_2^2$ under (XVI.1.63), recording each by its nonzero generator. Give the image under S of the three generators in the order $(1,0), (0,1), (1,1)$. Explain why checking isotropy alone would allow an incomplete catalog containing a duplicate subgroup. State which two absolute theories are exchanged, and distinguish this global choice from removing the free center-of-mass multiplet.

Sources and scope

The parent and the tensor branch. The ADE interacting parent, its generic tensor branch and the M5 realization of the A series are [GEO-E]; the non-gravitational worldvolume decoupling is [DEC]. See Witten 1995, arXiv:hep-th/9507121v1, §1 and §1.1, physical PDF pp. 2–6, and Witten 2009, arXiv:0905.2720v1, §4, (4.1)–(4.6), physical PDF pp. 9–12. The latter uses the opposite chirality naming convention, $(0, 2)$; its §5.2.2, physical PDF p. 18, directly describes the coincident-M5 realization. The local polarization, projection and root calculations (XVI.1.3)–(XVI.1.9) are [MATH], conditional on these field and charge identifications. The M2 endpoint and compatible projector premises are [GEO-E]; see Strominger 1996, arXiv:hep-th/9512059v1, (7)–(8), physical PDF pp. 4–6. The membrane tension uses the normalization of Volume III and the M-theory units specified in this chapter; its half-supersymmetric interpretation is [BPS:1/2|short]. The local center-of-mass split makes no global factorization claim.

Circle reduction and its coefficient. The zero-mode equations, wrapped area, quadratic DBI expansion and trace conversion in (XVI.1.13)–(XVI.1.22) are conditional [MATH]. The DBI premise is the low-field, low-derivative D-brane action of Volume III ([WS]); only its coefficient arithmetic is performed here. The longitudinal M5/D4 and wrapped M2/F1 identifications [DUAL] assume the flat ordinary M/IIA circle background of (XVI.1.16). The resulting nonabelian low-energy gauge identification is [GEO-E], not an

all-energy equality derived from a tensor action. See Witten 2009, (4.1), and Lambert et al. 2011, arXiv:1012.2882v3, (2.2), physical PDF p. 4, for the native action whose coefficient is converted in (XVI.1.22). The result $g_5^2 = 8\pi^2 R_6$ retains the established fundamental trace.

The explicit instanton and KK interpretation. The square completion, differentiated BPST connection, charge integral and radial-size relation (XVI.1.24)–(XVI.1.37) are [MATH]. They concern a smooth $SU(2)$ configuration with $\rho > 0$, zero electric fields and the stated unbroken or commuting-scalar background. For the instanton/KK interpretation see Lambert et al. 2011, §2, (2.8) and (2.18), physical PDF pp. 4–6. The protected charge and quantum-state interpretation remains [GEO-E]; the calculation does not supply a full instanton Hilbert space. The absolute WZ coefficient in (XVI.1.38) is the Volume III RR convention, $\tau_p = \mu_p / g_s$, with the exponential $\exp(B + 2\pi\alpha' F)$. Compare Myers 1999, arXiv:hep-th/9910053v2, (3), physical PDF p. 2, and (21)–(23), p. 7. That source uses $\mu_p^{\mathrm{M}} = \mu_p / g_s$ and $C^{\mathrm{M}} = g_s C$; their product reproduces the coefficient here. Its opposite connection sign leaves $F \wedge F$ unchanged. The D0 charge arithmetic is [MATH]; in the stated M/IIA circle background, D0 charge is circle momentum. A merely proportional WZ expression is insufficient to fix this coefficient.

The marked torus and the coupling. The metric, periods, reduction integrals, examples and scale limits (XVI.1.41)–(XVI.1.54) are conditional [MATH]. The identification of the protected instanton charge with KK charge and the infrared $\mathcal{N} = 4$ theory is [GEO-E]; these are the physical premises behind the holonomy-to-theta step. See Witten 1995, §1.1, physical PDF pp. 5–6, and Witten 2009, §3, (3.1)–(3.5), physical PDF pp. 7–9. For the KK connection coupled to instanton current, see the latter source, §5.1, (5.2), physical PDF p. 15. The geometric modulus refers to the actual compactification torus, with periodic fermions and sixteen preserved supercharges.

Cycle transport and global data. The oriented basis transport, metric identities and finite isotropic-subspace enumeration (XVI.1.55)–(XVI.1.65) are [MATH]. Geometric cycle lengths alone do not establish a stable BPS spectrum. The physical line-operator and relative/absolute qualifications use Aharony et al. 2013, arXiv:1305.0318v5, §1.1–1.2, (1.4) and Fig. 1, physical PDF pp. 2–6, and Witten 2009, §4.1, (4.7)–(4.9), physical PDF pp. 12–14. The global classification is used at the stated $\mathfrak{su}(2)$ center-charge level. Chapter 11 develops the additional global data; no fixed absolute theory is claimed to be invariant under the full modular group.

References

Aharony, O., N. Seiberg, and Y. Tachikawa (2013). "Reading between the lines of four-dimensional gauge theories". In: *JHEP* 08, p. 115. DOI: 10.1007/JHEP08(2013)115. arXiv: 1305.0318 [hep-th].

Lambert, N., C. Papageorgakis, and M. Schmidt-Sommerfeld (2011). "M5-Branes, D4-Branes and Quantum 5D Super-Yang–Mills". In: *JHEP* 01, p. 083. DOI: 10.1007/JHEP01(2011)083. arXiv: 1012.2882 [hep-th].

Myers, R. C. (1999). "Dielectric-branes". In: *JHEP* 12, p. 022. DOI: 10.1088/1126-6708/1999/12/022. arXiv: hep-th/9910053.

Strominger, A. (1996). "Open p-branes". In: *Phys. Lett. B* 383. Ed. by M. J. Duff, pp. 44–47. DOI: 10.1016/0370-2693(96)00712-5. arXiv: hep-th/9512059.
Witten, E. (1995). "Some Comments on String Dynamics". In: arXiv: hep-th/9507121.
Witten, E. (2009). "Geometric Langlands From Six Dimensions". In: arXiv: 0905.2720 [hep-th].

Chapter XVI.2

Twisting on a curve and the first class S building block

The circle and torus reductions of the previous chapter used flat compact directions. A curved surface introduces a new obstruction: a spinor transported around the surface generally returns rotated. To retain supersymmetry we must cancel that rotation with an R-symmetry background. This chapter performs the cancellation, follows the resulting scalar fields into differential forms, and works out the smallest punctured-sphere example.

The reader needs the representation meaning of a supercharge, the four-dimensional $\mathcal{N} = 2$ hypermultiplet, and elementary complex coordinates. We recall the spinor branches and the symplectic description of a half-hypermultiplet when they enter. No knowledge of the Hitchin equations is required. We use only their holomorphicity equation to explain why protected spectral data contain meromorphic differentials. By the end, the reader should be able to count the surviving supercharges, reconstruct a quadratic differential from fixed puncture masses, and describe the fields and flavor moment maps of the three-punctured sphere.

XVI.2.1 Canceling the curve holonomy

What replaces a constant supersymmetry parameter when the compactification surface is curved? Locally, the spin connection on an oriented surface is an abelian connection. A field of spin s acquires a phase under a rotation of the tangent frame. A background connection for an abelian subgroup of the R-symmetry can supply a second phase. We choose the background so that the combined charge is zero for some of the supercharges. This is a partial topological twist: four-dimensional Lorentz transformations are unaffected.

Let C be the oriented curve and let s denote its rotation weight. The complexification of a positive-chirality six-dimensional spinor branches under the four-dimensional Lorentz

algebra and rotations of C as

$$S_6^+ = (\mathbf{2},\mathbf{1})_{+1/2} \oplus (\mathbf{1},\mathbf{2})_{-1/2}. \tag{XVI.2.1}$$

The two entries in parentheses are the left and right Weyl representations in four dimensions. Each summand therefore has two complex components. The $(2,0)$ supercharges also transform in the four-dimensional spinor representation of $\mathrm{Spin}(5)_R$. Choose an R-symmetry plane, with rotation weight t. Its commuting $\mathfrak{su}(2)$ acts on the doublets in

$$\mathbf{4}_R = \mathbf{2}_{+1/2} \oplus \mathbf{2}_{-1/2}, \qquad Q_{\mathbb{C}} \in S_6^+ \otimes \mathbf{4}_R. \tag{XVI.2.2}$$

We have first complexified the supersymmetry representation; its reality condition will be imposed below. The tensor product has complex dimension sixteen. This number by itself is not the number of independent complex physical supercharges.

Choose the R connection equal to the curve spin connection in the convention that the covariant derivative on a component reads

$$D_C Q_{s,t} = \big(d + \mathrm{i}(s+t)\omega_C\big) Q_{s,t}, \qquad s' = s + t. \tag{XVI.2.3}$$

The cancellation can now be done before solving any differential equation. The four tensor-product sectors give

s	t	s'	complex multiplicity
$+\frac{1}{2}$	$+\frac{1}{2}$	$+1$	4
$+\frac{1}{2}$	$-\frac{1}{2}$	0	4
$-\frac{1}{2}$	$+\frac{1}{2}$	0	4
$-\frac{1}{2}$	$-\frac{1}{2}$	-1	4

$$\dim_{\mathbb{C}} \ker s' = 8. \tag{XVI.2.4}$$

Each neutral sector is a four-dimensional Weyl spinor tensored with the remaining R-symmetry doublet. Figure XVI.2.1 displays the cancellation as a diagonal in the two charge directions. Neutrality removes the local holonomy obstruction. We assume compatible global spin and R lifts, and later choose puncture conditions that preserve these parameters.

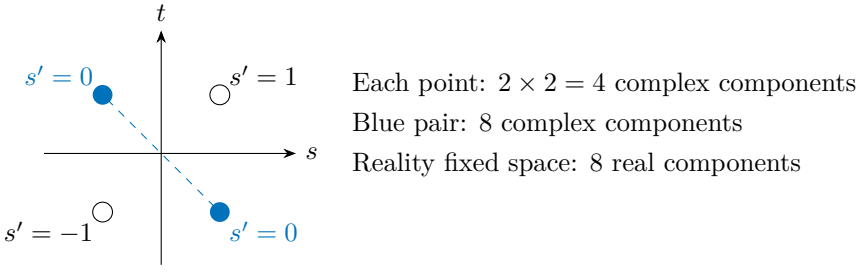


Figure XVI.2.1: The four spin/R sectors. Blue points lie on $s + t = 0$; each point represents four complex components. The inherited reality condition acts between the two neutral sectors and leaves eight real supercharges.

It is useful to make that last reality statement explicit. Otherwise an eight-dimensional complex kernel can easily be mistaken for sixteen real supercharges. Order each of the spin and R bases with two positive weights followed by two negative weights. A representative of the inherited symplectic reality maps is supplied by

$$E = \begin{pmatrix} 0 & 1 \\ -1 & 0 \end{pmatrix}, \qquad B_6 = \begin{pmatrix} 0 & I_2 \\ -I_2 & 0 \end{pmatrix}, \qquad B_R = \begin{pmatrix} 0 & E \\ E & 0 \end{pmatrix}. \tag{XVI.2.5}$$

Here the map on the tensor product is antilinear. These matrices specify the real structure used in the calculation; constructing a six-dimensional Clifford representation is not needed for this weight computation. Their squares and their tensor product satisfy

$$B_6\overline{B}_6 = -I_4, \qquad B_R\overline{B}_R = -I_4, \qquad \mathcal{R}(v) = (B_6 \otimes B_R)\overline{v}, \qquad \mathcal{R}^2 = 1. \tag{XVI.2.6}$$

Each factor exchanges positive and negative weights, so their tensor product preserves the condition $s + t = 0$. Write the neutral vector as (a, b), where a belongs to spin-positive/R-negative and b to spin-negative/R-positive. With $L = I_2 \otimes E$, the restricted real matrix multiplying complex conjugation is

$$R_0 = \begin{pmatrix} 0 & L \\ -L & 0 \end{pmatrix}, \qquad L^2 = -I_4, \qquad R_0^2 = I_8. \tag{XVI.2.7}$$

For example, its eigenvectors of sign $\eta = \pm 1$ obey $b = -\eta La$; either sign permits arbitrary $a \in \mathbb{R}^4$. Writing a neutral complex vector as $v = x + \mathrm{i}y$, the fixed-point condition thus becomes

$$\begin{gathered} R_0 x = x, \qquad R_0 y = -y, \\ \dim_{\mathbb{R}} \operatorname{Fix} \mathcal{R} = \dim \ker(R_0 - I) + \dim \ker(R_0 + I) = 4 + 4 = 8. \end{gathered} \tag{XVI.2.8}$$

The left and right neutral rows form conjugate parts of the physical supersymmetry algebra. The resulting four-dimensional theory has $\mathcal{N} = 2$, with R-symmetry Lie algebra $\mathfrak{su}(2)_R \oplus \mathfrak{u}(1)_r$. The local branching calculation does not fix the central quotients of its global symmetry group.

Two comparisons clarify what the cancellation achieves. If the background is multiplied by a coefficient k, the four weights are

$$s'_k \in \left\{ \frac{1+k}{2}, \frac{1-k}{2}, \frac{-1+k}{2}, \frac{-1-k}{2} \right\}. \tag{XVI.2.9}$$

For $k = 0$ or $k = 2$, no row is neutral on a generic curved surface. For $k = -1$, the other diagonal is neutral; this is an equally possible choice after reversing the R-plane convention. The sign choice is therefore different from omitting the required cancellation.

A flat unpunctured torus provides a second comparison. With periodic spin structure and trivial background holonomy, the connection imposes no local or global rotation on any component. In that case

$$\omega_{T^2} = 0 : \qquad \dim_{\mathbb{R}} \operatorname{Fix} \mathcal{R}\big|_{Q_{\mathbb{C}}} = 16, \tag{XVI.2.10}$$

consistent with the enhanced supersymmetry of the previous chapter. The eight-supercharge result concerns the generic twisted curved situation, with compatible defects. The class S construction further uses the interacting $(2,0)$ parent and an appropriate four-dimensional low-energy, small-area limit. Canceling the spin connection is the kinematic step that makes that physical compactification possible; it does not by itself determine its finite-area dynamics.

XVI.2.2 From transverse scalars to differentials

The same twist changes the geometric meaning of the scalar fields. Which field can record positions in the chosen transverse R-symmetry plane once that plane is tied to the tangent frames of C? The answer follows from its rotation charge. We assign a holomorphic one-form dz curve spin $+1$. The scalar in the transverse plane must have the same charge if it is to become a one-form after twisting.

This charge is fixed by the vector representation of Spin(5), not by the spinor weights alone. In a real basis for its defining five-dimensional vector representation, use the Hermitian plane-rotation generator

$$H_R = \begin{pmatrix} 0 & -\mathrm{i} & 0 & 0 & 0 \\ \mathrm{i} & 0 & 0 & 0 & 0 \\ 0 & 0 & 0 & 0 & 0 \\ 0 & 0 & 0 & 0 & 0 \\ 0 & 0 & 0 & 0 & 0 \end{pmatrix}, \qquad \operatorname{spec} H_R = \{-1,0,0,0,+1\}. \tag{XVI.2.11}$$

The eigenvectors in the selected plane have charges ± 1; the three orthogonal components are neutral. Consequently

$$\mathbf{5}_R = \mathbf{3}_0 \oplus \mathbf{1}_{+1} \oplus \mathbf{1}_{-1}, \qquad s = 0 \implies s' = t. \tag{XVI.2.12}$$

The positive component becomes a smooth section of the canonical line bundle K_C, the bundle whose local sections are $f(z,\bar{z})\,dz$. The negative component is its complex conjugate, of smooth $(0,1)$ type. The triplet remains scalar on C. Changing the vector charges to ± 2 would instead assign a different tensor power of the canonical bundle and would contradict the explicit plane rotation above.

At this stage "section of K_C" means a smooth section, not necessarily a holomorphic one. A change of frame constrains transformation laws, while a field equation constrains dependence on position. In a description obtained after an additional circle reduction, one has a connection A on C and an effective Higgs field Φ valued in K_C. Here P is the gauge bundle, and $\operatorname{ad} P$ is its associated bundle of Lie algebras in the adjoint representation. The notation $\Omega^{1,0}(C, \operatorname{ad} P)$ means smooth adjoint-valued one-forms of type $(1,0)$, while $\bar{\partial}_A$ is the connection-corrected antiholomorphic derivative. The protected supersymmetric configurations obey, among other equations,

$$\Phi \in \Omega^{1,0}(C, \operatorname{ad} P), \qquad \bar{\partial}_A \Phi = 0. \tag{XVI.2.13}$$

This separate equation supplies the holomorphicity away from defects. In particular, a smooth twisted configuration with a nonzero $\bar{\partial}_A \Phi$ has the correct bundle type but is outside this protected locus. We use this effective description, or tensor-branch eigenvalues, without assuming a local interacting six-dimensional adjoint scalar Lagrangian.

For type A_1, the two eigenvalues are opposite. Introduce a local eigenvalue coefficient x_z, its one-form λ, and the quadratic invariant ϕ_2:

$$\lambda = x_z\, dz, \qquad \phi_2 = f_z(z)\,(dz)^2, \qquad \lambda^2 = \phi_2 \quad \Longleftrightarrow \quad x_z^2 = f_z(z). \tag{XVI.2.14}$$

The invariant is single-valued on the base even when the two eigenvalues exchange around a branch point. Equation (XVI.2.14) defines a spectral cover $\pi : \Sigma \to C$; λ is naturally a one-form on that cover. The marked surface C and the cover Σ have different jobs. Marked-point positions and the complex structure of C specify coupling data of the construction. Coefficients of ϕ_2, with its singular parts appropriately fixed, describe Coulomb data.

We can see the bundle transformation directly, without a metric. On an overlap let $z = z(w)$. Equality of the one-form and its square in the two coordinates requires

$$x_w = x_z\big(z(w)\big)\frac{dz}{dw}, \qquad f_w = f_z\big(z(w)\big)\left(\frac{dz}{dw}\right)^2. \tag{XVI.2.15}$$

For the second coordinate patch of a sphere, $z = 1/w$, these become

$$x_w = -\frac{x_z(1/w)}{w^2}, \qquad f_w = \frac{f_z(1/w)}{w^4}. \tag{XVI.2.16}$$

The fourth power is essential when checking the puncture at infinity. A rational function that appears to decrease at large z can still define a singular quadratic differential at $w = 0$.

Consider a simple local example relevant to a massless regular puncture:

$$\phi_2 = \left(\frac{c}{z} + O(1)\right)(dz)^2, \qquad c \neq 0. \tag{XVI.2.17}$$

The eigenvalue coefficient behaves as $x_z \sim \sqrt{c/z}$, which has a square-root branch. This is a statement about eigenvalues, not a fractional pole order for an ordinary meromorphic matrix Φ_z. Pass to the ramified coordinate $z = t^2$. The symbol π^* denotes pullback along the covering map, which includes the coordinate Jacobian. Since $dz = 2t\, dt$,

$$\pi^*\phi_2 = \big(4c + O(t^2)\big)(dt)^2, \qquad \lambda = \big(\pm 2\sqrt{c} + O(t^2)\big)dt. \tag{XVI.2.18}$$

The one-form is regular on the normalized cover near this point. Figure XVI.2.2 shows why a singular eigenvalue coefficient on the base need not mean a singular one-form on the cover. If $c = 0$, the leading local model changes and this ramification argument must be redone.

Finally, the twist should not be confused with a change of engineering dimension. A tensor-multiplet scalar in six dimensions has mass dimension two. Compactification and the choice of effective normalization enter before we interpret λ as the four-dimensional Seiberg–Witten differential. In the effective convention used here,

$$[z] = 0, \qquad [\lambda] = [x_z] = [m] = 1, \qquad [\phi_2] = 2, \qquad [\varphi_{6d}] = 2. \tag{XVI.2.19}$$

The equality of bundle types does not identify the dimensionful fields without the intervening compactification scales. This distinction will let us compare masses with residues consistently while using dimensionless coordinates for the punctures.

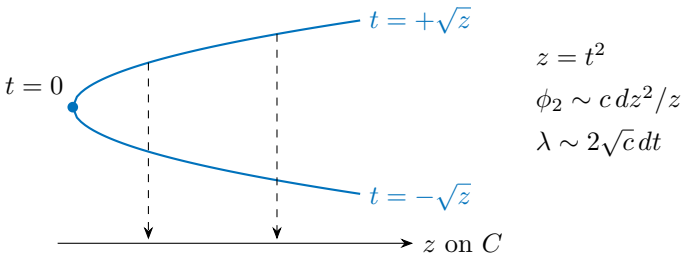


Figure XVI.2.2: A real slice of the local map $z = t^2$. The two branches of t lie over the same positive z. The sketch depicts the covering coordinate, not the value of x_z. A simple pole of ϕ_2 on the base pulls back to a regular λ when $c \neq 0$.

XVI.2.3 What a regular puncture fixes

How much of ϕ_2 is a choice of vacuum, and how much is already fixed by the punctures? We answer on a sphere, where every step reduces to rational functions. The physical input is the regular A_1 puncture dictionary: a puncture has a flavor mass m_i, with residue eigenvalues $\pm m_i$, and its leading quadratic singularity is their square. In a local coordinate ζ_i vanishing at the puncture,

$$\phi_2 = \left(\frac{m_i^2}{\zeta_i^2} + \frac{b_i}{\zeta_i} + O(1) \right) (d\zeta_i)^2. \tag{XVI.2.20}$$

We hold the masses fixed while varying Coulomb data. At zero mass the quadratic differential has at most a simple pole. The remaining simple-pole coefficient is not determined by specifying that the puncture is regular. The word "regular" here describes the allowed defect singularity, not a claim that every coefficient is nonsingular.

Take $n \geq 3$ distinct marked points on $\mathbb{P}^1$, put one at infinity, and call the finite ones $p_1, \ldots, p_{n-1}$. Let D denote their reduced divisor: the sum of the distinct punctures, including infinity, each counted with multiplicity one. To represent every differential with at most double poles at these points, set

$$d(z) = \prod_{i=1}^{n-1} (z - p_i), \qquad \phi_2 = \frac{P(z)}{d(z)^2} (dz)^2. \tag{XVI.2.21}$$

Multiplication by d^2 removes all finite poles. The numerator is therefore a polynomial. Its allowed degree follows from infinity rather than from guesswork. If $P(z) \sim a_k z^k$, then in $w = 1/z$

$$f_z(z) \sim a_k z^{k-2n+2}, \qquad f_w(w) \sim a_k w^{2n-6-k}. \tag{XVI.2.22}$$

A double pole permits exponent no smaller than -2. Thus $k \leq 2n - 4$. The coefficient at that highest allowed power is precisely the double-pole coefficient at infinity. At a finite point, remove its vanishing factor from d and evaluate the rest. The mass

constraints are

$$P(p_i) = m_i^2 \prod_{j \neq i} (p_i - p_j)^2, \qquad [z^{2n-4}]P = m_\infty^2. \tag{XVI.2.23}$$

There are $2n-3$ polynomial coefficients and n constraints. A subtraction alone would not establish the answer: the constraints must be independent and consistent. Both facts are easy to see constructively. First set the top coefficient equal to m_∞^2. Interpolate the remaining required values at the $n-1$ finite points using a polynomial of degree at most $n-2$. Since $n-2 < 2n-4$ for $n \geq 3$, this does not disturb the chosen top coefficient. Every list of mass squares is therefore attained.

Now subtract two solutions with the same masses. Their difference vanishes at every finite p_i and has no coefficient of degree $2n-4$. Since the points are distinct, the factor theorem gives

$$\delta P = d(z)R(z), \qquad \deg \delta P \leq 2n-5, \qquad \deg R \leq n-4. \tag{XVI.2.24}$$

It follows that the fixed-mass fiber is an affine space with translation space

$$\delta\phi_2 = \frac{R(z)}{d(z)}(dz)^2, \qquad \dim_{\mathbb{C}}\{R : \deg R \leq n-4\} = n-3. \tag{XVI.2.25}$$

For $n = 3$, the degree bound is negative, meaning that $R = 0$. For comparison with bundle notation, $K_{\mathbb{P}^1}$ has degree -2 and the difference has at most simple poles. The bundle $K^2(D)$ permits precisely those simple poles at D. We write H^0 for its global holomorphic sections, and $\mathcal{O}(d)$ for the degree-d line bundle on the sphere. In this notation,

$$\delta\phi_2 \in H^0\big(\mathbb{P}^1, K^2(D)\big) = H^0\big(\mathbb{P}^1, \mathcal{O}(n-4)\big). \tag{XVI.2.26}$$

The elementary polynomial argument both proves the dimension here and identifies the actual differentials counted by the bundle formula.

An independent way to expose the infinity conditions is to use partial fractions. Since the coefficient function must decrease at least as z^{-2}, it has the form

$$f_z(z) = \sum_{i=1}^{n-1} \left(\frac{m_i^2}{(z-p_i)^2} + \frac{b_i}{z-p_i} \right). \tag{XVI.2.27}$$

Expanding at large z gives the first two terms explicitly:

$$f_z(z) = \frac{\sum_i b_i}{z} + \frac{\sum_i (m_i^2 + p_i b_i)}{z^2} + O(z^{-3}). \tag{XVI.2.28}$$

The first term would make a triple pole at infinity after multiplication by w^{-4}. The second sets its prescribed double coefficient. Thus

$$\sum_i b_i = 0, \qquad \sum_i p_i b_i = m_\infty^2 - \sum_i m_i^2. \tag{XVI.2.29}$$

For at least two distinct finite points these are independent equations on $n-1$ variables, again leaving $n-3$. This form is useful when tracking local singular terms; the polynomial form is more convenient for constructing a global answer.

For four massless punctures at $0, 1, q, \infty$, with $q \neq 0, 1$, the polynomial R is a constant:

$$\phi_2 = \frac{u}{z(z-1)(z-q)}(dz)^2. \tag{XVI.2.30}$$

Here q specifies the marked surface, while u, of mass dimension two, is the Coulomb coefficient. They enter different parts of the rational function and are varied for different physical purposes. This is the first surface that will admit the gauge-theory gluing studied in the next chapter.

For five massless punctures at $0, 1, 2, 4, \infty$, one degree is added to R, giving a changed example that can be checked at every puncture:

$$\phi_2 = \frac{u_0 + u_1 z}{z(z-1)(z-2)(z-4)}(dz)^2. \tag{XVI.2.31}$$

Both terms have at most simple poles, including at infinity: the constant numerator gives a regular coefficient there, and the linear numerator gives a simple pole. Figure XVI.2.3 counts the same freedom before the masses are set to zero. With seven numerator coefficients and five fixed double coefficients, there are two vacuum parameters.

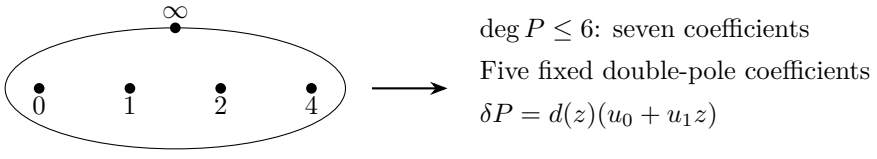


Figure XVI.2.3: Five distinct marked points on a sphere, with the affine chart $0, 1, 2, 4$ and its point at infinity. The numerator of the general double-pole differential has degree at most six. Fixing all five mass squares leaves the two variations displayed on the right.

The hypotheses matter in practical calculations. Omitting the condition at infinity leaves an extra variation that changes its mass. If two marked points collide, the divisor is no longer the reduced divisor used above, and the pole problem must be reformulated. A sphere with only 0 and ∞ is also outside the $n \geq 3$ argument: its double coefficients cannot be independently prescribed, since $m^2(dz)^2/z^2$ gives the same square at both ends. These examples distinguish a fixed external source from an allowed variation of the vacuum.

XVI.2.4 The three-punctured sphere and its free fields

The three-punctured sphere, often called a trinion, has no Coulomb coefficient at fixed masses. What physical theory can nevertheless live on this surface? We first determine its spectral data completely. We then introduce the free matter theory assigned to it by the class S construction and inspect its representation. This order makes clear what the differential calculation does, and what additional physical identification is needed.

Put the three punctures at $0, 1, \infty$. The numerator has degree at most two, so write

$$\phi_2 = \frac{Az^2 + Bz + C}{z^2(z-1)^2}(dz)^2. \tag{XVI.2.32}$$

At zero the double coefficient is C. At one it is $A + B + C$, and at infinity it is A. The three residue equations can be displayed as a nonsingular linear system:

$$\begin{pmatrix} 1 & 0 & 0 \\ 1 & 1 & 1 \\ 0 & 0 & 1 \end{pmatrix} \begin{pmatrix} C \\ B \\ A \end{pmatrix} = \begin{pmatrix} m_0^2 \\ m_1^2 \\ m_\infty^2 \end{pmatrix}, \qquad \det \begin{pmatrix} 1 & 0 & 0 \\ 1 & 1 & 1 \\ 0 & 0 & 1 \end{pmatrix} = 1. \tag{XVI.2.33}$$

Solving yields

$$\phi_2 = \frac{m_\infty^2 z^2 + (m_1^2 - m_0^2 - m_\infty^2)z + m_0^2}{z^2(z-1)^2}(dz)^2. \tag{XVI.2.34}$$

Every numerator coefficient is fixed by the masses. In particular, if all three masses vanish, the entire differential vanishes. This establishes the absence of a Coulomb modulus in this example. It supplies no count of matter fields, because hypermultiplet scalars need not parameterize the Coulomb branch.

For a numerical example, take $(m_0, m_1, m_\infty) = (1, 2, 4)$ in a common mass unit. The result and its infinity expansion are

$$f_z(z) = \frac{16z^2 - 13z + 1}{z^2(z-1)^2}, \qquad f_w(w) = \frac{16 - 13w + w^2}{w^2(1-w)^2}. \tag{XVI.2.35}$$

Multiplication by the squared local coordinate gives 1, 4, and 16 at 0, 1, and ∞, respectively. The last check is especially useful: incorrectly transforming a quadratic differential as a function would lose the infinity mass entirely.

The physical identification now enters: this regular A_1 trinion is the free theory T_2, consisting of one half-hypermultiplet in

$$V = \mathbf{2}_0 \otimes \mathbf{2}_1 \otimes \mathbf{2}_\infty, \qquad q = (q_{abc}), \qquad a, b, c = 1, 2. \tag{XVI.2.36}$$

The three factors are flavor groups associated with the marked punctures; none is gauged in this isolated building block. Figure XVI.2.4 shows the three actions on a single array of fields. The identification is part of the compactification dictionary. It is not a consequence of finding zero Coulomb parameters, since that count alone cannot distinguish different free matter theories.

Why is a half-hypermultiplet possible in this representation? Recall that a complex representation is pseudoreal if it admits a commuting antilinear map whose square is -1. A doublet of $SU(2)$ has the invariant form E used above. On the threefold tensor product define

$$J = E \otimes E \otimes E, \qquad J^T = -J, \qquad J\overline{J} = -I_8, \qquad \mathcal{J}(q) = J\overline{q}. \tag{XVI.2.37}$$

The transpose gives one minus sign per factor; the square gives the same three minus signs. The form is nondegenerate, and for $g = g_0 \otimes g_1 \otimes g_\infty$ its invariance follows factor

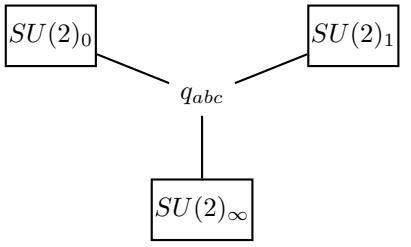


Figure XVI.2.4: The T_2 matter block. Each square is a flavor $SU(2)$ acting on one index of q_{abc}; the lines indicate tensor factors, not quiver arrows or gauge nodes. The three visible factors form a subgroup of the full flavor symmetry of four free hypermultiplets.

by factor from $g_i^T E g_i = E$. This proves pseudoreality of the specified representation, which permits the half-hyper field content.

In an $\mathcal{N} = 1$ description, that half-hyper has eight independent chiral coordinates q_{abc}. Thus its scalar count is

$$\dim_{\mathbb{C}} V = 8, \qquad \dim_{\mathbb{R}} \mathcal{H} = 16, \qquad n_h = \dim_{\mathbb{H}} \mathcal{H} = 4. \tag{XVI.2.38}$$

Here n_h is the number of quaternionic scalar dimensions, including representation multiplicity. A full hypermultiplet in the same eight-dimensional representation would double this count. Pseudoreality does not impose $q = J\overline{q}$ on these eight chiral coordinates: applying that equation twice would give $q = -q$. The multiplet reality condition involves the additional R-symmetry structure; the chiral coordinates themselves remain complex and independent.

The tensor product with only two doublet factors gives a useful test of the logic. In that case

$$J_2 = E \otimes E, \qquad J_2^T = +J_2, \qquad J_2 \overline{J}_2 = +I_4. \tag{XVI.2.39}$$

The representation is real rather than pseudoreal. Merely being a tensor product of $SU(2)$ doublets is therefore insufficient for the particular half-hyper construction above; the parity of the number of factors matters.

For later gluing, focus on one marked factor and regard the other two indices as multiplicity labels. The representation branches as

$$V\big|_{SU(2)_0} = \mathbf{2} \otimes \mathbb{C}^4, \qquad 4 \text{ half-doublets} = 2 \text{ full doublet hypers}. \tag{XVI.2.40}$$

With Hermitian generators $T_a = \sigma_a/2$ in a fundamental, our trace normalization is $\mathrm{tr}_{\mathbf{2}}(T_a T_b) = \delta_{ab}/2$. For the generator acting on the first tensor factor this gives the direct check

$$T_3^{(0)} = \tfrac{1}{2}\,\mathrm{diag}(1, -1) \otimes I_2 \otimes I_2, \qquad \mathrm{tr}_V\big((T_3^{(0)})^2\big) = 4\,\mathrm{tr}_{\mathbf{2}}(T_3^2) = 2. \tag{XVI.2.41}$$

The multiplicity will be doubled again when two independent trinion blocks are joined through a common flavor factor.

The marked $SU(2)^3$ action is smaller than the full flavor symmetry of the free theory. In the chiral coordinates, the free metric is the standard Hermitian metric and

the holomorphic symplectic form is specified by J. Their common compact invariance group is

$$USp(8) = \{U \in U(8) : U^T J U = J\}, \qquad SU(2)^3 \longrightarrow USp(8). \tag{XVI.2.42}$$

To see the size of this enhancement, choose a symplectic basis in which J takes the standard block form. The complexified infinitesimal condition $X^T J + JX = 0$ then reads

$$\begin{gathered} X = \begin{pmatrix} A & B \\ C & -A^T \end{pmatrix}, \qquad B = B^T, \quad C = C^T, \\ \dim \mathfrak{sp}(8, \mathbb{C}) = 16 + 10 + 10 = 36. \end{gathered} \tag{XVI.2.43}$$

A Cartan subalgebra has A diagonal and $B = C = 0$, with four independent entries. Generic entries distinct up to sign leave only these four commuting directions. The full free mass space therefore has rank four; the three marked-puncture masses select only three directions in it.

Even the visible tensor action is not faithful on the product of centers. For $\epsilon_i = \pm 1$, its actual action on the local fields is

$$\begin{gathered} (\epsilon_0 I_2) \otimes (\epsilon_1 I_2) \otimes (\epsilon_\infty I_2) = (\epsilon_0 \epsilon_1 \epsilon_\infty) I_8, \\ \ker = \{(+,+,+), (+,-,-), (-,+,-), (-,-,+)\}. \end{gathered} \tag{XVI.2.44}$$

The four product-positive signs contain the identity and close under multiplication. The product-negative set has the same cardinality but acts as $-I_8$, so it is not the kernel. This determines the center action on these local fields. Choosing allowed background bundles or genuine line operators requires further global information about the compactification.

XVI.2.5 Masses and flavor moment maps

To join two matter blocks, we will need more than the names of their flavor groups. We need the operators to which a vector multiplet couples. For the free trinion these operators are quadratic moment maps. Constructing them also gives a direct route to the mass matrix and a useful comparison with the trinion differential.

Use the lexicographic order $111, 112, 121, 122, 211, 212, 221, 222$ for the components of the column q. The holomorphic symplectic form and the Poisson bracket convention are

$$\Omega = \tfrac{1}{2} J_{ij}\, dq_i \wedge dq_j, \qquad \{F, G\} = (\partial F)^T J^{-1} (\partial G), \qquad J^{-1} = -J. \tag{XVI.2.45}$$

A flavor generator T preserves the form precisely when $T^T J + JT = 0$. It follows that JT is symmetric, allowing the quadratic function

$$\mu_T = \tfrac{1}{2} q^T J T q, \qquad (JT)^T = JT, \qquad \partial \mu_T = JTq. \tag{XVI.2.46}$$

Multiplying the gradient by the inverse symplectic form recovers the desired infinitesimal action:

$$X_T = J^{-1} \partial \mu_T = Tq, \qquad \iota_{X_T} \Omega = -d\mu_T. \tag{XVI.2.47}$$

The factor of one-half is fixed by differentiation of a symmetric quadratic form. Omitting it would generate $2Tq$, changing both the moment-map and coupling normalization.

For an explicit component example, use $T = T_3^{(0)}$ from (XVI.2.41). The nonzero anti-diagonal entries of J alternate signs according to the number of index values equal to two. Combining the two equal contributions to each monomial gives

$$\mu_{T_3^{(0)}} = \tfrac{1}{2}\big(-q_1q_8 + q_2q_7 + q_3q_6 - q_4q_5\big). \tag{XVI.2.48}$$

For instance $\partial\mu/\partial q_8 = -q_1/2$, while $(J^{-1})_{18} = -1$. Their product gives $(X_T)_1 = q_1/2$, the positive weight of the first factor. The complementary component has the negative weight. This elementary check ties the abstract symplectic formula to the actual flavor charges of the fields.

The moment maps also remember the Lie algebra. Direct substitution in the Poisson bracket yields

$$\{\mu_T, \mu_S\} = q^T JTSq = \tfrac{1}{2}q^T J[T,S]q = \mu_{[T,S]}. \tag{XVI.2.49}$$

For the middle equality, transpose the scalar quadratic expression and use $T^TJ = -JT$ and $S^TJ = -JS$; its symmetric part is $J(TS - ST)/2$. Thus the quadratic operators have the required flavor brackets before any gauging is introduced. In the next chapter they become the matter operators coupled to the adjoint chiral field of an $\mathcal{N} = 2$ vector multiplet.

Now turn on the three puncture masses. Our residue eigenvalues are $\pm m_i$, so the mass matrix uses $H = \mathrm{diag}(1,-1) = 2T_3$, not T_3 itself:

$$M = m_0 H \otimes I_2 \otimes I_2 + m_1 I_2 \otimes H \otimes I_2 + m_\infty I_2 \otimes I_2 \otimes H. \tag{XVI.2.50}$$

Each basis vector has one sign from each tensor factor. Its eigenvalue is therefore $\pm m_0 \pm m_1 \pm m_\infty$. Opposite weights are paired by J. Choose the four representatives with a positive m_0 sign:

$$\begin{pmatrix} M_1 \\ M_2 \\ M_3 \\ M_4 \end{pmatrix} = \begin{pmatrix} 1 & 1 & 1 \\ 1 & 1 & -1 \\ 1 & -1 & 1 \\ 1 & -1 & -1 \end{pmatrix} \begin{pmatrix} m_0 \\ m_1 \\ m_\infty \end{pmatrix}. \tag{XVI.2.51}$$

These are holomorphic mass eigenvalues; their signs depend on the choice of representative within each opposite pair. The three columns of this matrix are mutually orthogonal and have length squared four. Its rank is three, and its one-dimensional left kernel gives

$$M_1 - M_2 - M_3 + M_4 = 0, \qquad m_0 = \tfrac{1}{4}(M_1 + M_2 + M_3 + M_4), \tag{XVI.2.52}$$

with $m_1 = (M_1 + M_2 - M_3 - M_4)/4$ and $m_\infty = (M_1 - M_2 + M_3 - M_4)/4$. Thus the residue masses give a rank-three subfamily of the rank-four free $USp(8)$ mass space. An arbitrary fourth independent free-theory mass need not preserve this marked-trinion description. Counting three punctures must not erase the extra symmetry of the isolated free theory.

There is a precise algebraic comparison between these masses and the spectral cover. Homogenize the numerator of (XVI.2.34) to a binary quadratic:

$$N_h(Z,W) = m_\infty^2 Z^2 + (m_1^2 - m_0^2 - m_\infty^2)ZW + m_0^2 W^2. \tag{XVI.2.53}$$

The variable $[Z : W]$ is a point of $\mathbb{P}^1$, with $z = Z/W$ on the finite chart. The discriminant is the fixed-degree binary quadratic discriminant $B^2 - 4AC$. Factor it in two stages:

$$\Delta = \left(m_1^2 - m_0^2 - m_\infty^2\right)^2 - 4m_0^2 m_\infty^2 \tag{XVI.2.54}$$

$$= \left(m_1^2 - (m_0 + m_\infty)^2\right)\left(m_1^2 - (m_0 - m_\infty)^2\right) = M_1 M_2 M_3 M_4. \tag{XVI.2.55}$$

The paired signs in the four factors multiply to plus one. A generic zero of one chosen mass eigenvalue coincides with a repeated root of the binary quadratic. This is a comparison of algebraic zero loci within the specified mass family. It does not determine a full BPS spectrum or fix an additional overall convention for physical central charges.

For $(m_0, m_1, m_\infty) = (1, 2, 4)$, the four representatives and the two numerator roots are

$$(M_1, M_2, M_3, M_4) = (7, -1, 3, -5), \qquad \Delta = 105, \qquad z_\pm = \frac{13 \pm \sqrt{105}}{32}. \tag{XVI.2.56}$$

Both roots are distinct and away from $0, 1, \infty$; approximately they are 0.0860 and 0.7265. Keeping $m_0 = 1, m_1 = 2$ and varying $m_\infty = c$ gives the four massless loci in Figure XVI.2.5. At $c = 3$, for example,

$$N(z) = (3z - 1)^2, \qquad (M_1, M_2, M_3, M_4) = (6, 0, 2, -4), \qquad \dim_{\mathbb{C}} \ker M = 2. \tag{XVI.2.57}$$

The two zero-weight coordinates form one opposite pair. This supplies a direct free-field interpretation of a generic factor of the discriminant.

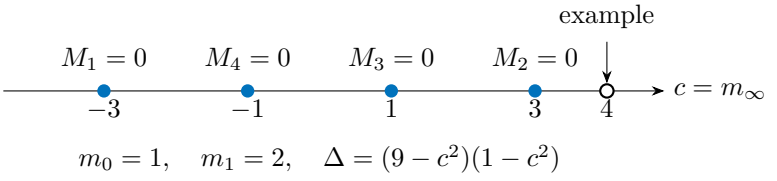


Figure XVI.2.5: The real slice $m_0 = 1, m_1 = 2, m_\infty = c$ of the holomorphic mass family. Each filled point sets one chosen opposite-pair mass to zero and makes the binary quadratic discriminant vanish. The open point $c = 4$ is the nonsingular numerical example in the text.

Homogenization is necessary at the boundary of this family. Set $m_\infty = 0$, but keep $m_1^2 \neq m_0^2$. The affine numerator has degree one, yet the fixed degree-two polynomial is

$$N_h = W\left((m_1^2 - m_0^2)Z + m_0^2 W\right), \qquad \Delta = (m_1^2 - m_0^2)^2 \neq 0. \tag{XVI.2.58}$$

One root lies at $W = 0$, that is, at infinity, and the other remains finite. They are distinct. Taking the discriminant of a new degree-one affine problem would discard the infinity root and would no longer be the quantity in (XVI.2.55).

For generic nonzero masses with two distinct numerator zeros away from the punctures, the double poles have even order and do not branch the cover. The two simple zeros do branch it. The Riemann–Hurwitz formula for the normalized connected double cover therefore gives

$$2g(\Sigma) - 2 = 2\big(2g(\mathbb{P}^1) - 2\big) + 2 = -4 + 2 = -2, \qquad g(\Sigma) = 0. \tag{XVI.2.59}$$

This calculation has a smoothness hypothesis. When all masses vanish, $\lambda^2 = 0$ is a nonreduced spectral equation, so it is not a smooth double cover to which the displayed genus argument applies. The eight chiral coordinates of the free theory still exist. Their survival is the concrete reason that vanishing Coulomb data cannot be read as absence of degrees of freedom.

Take-home message of this chapter

The twist cancels the curve rotation on eight real supercharges and makes the charged scalar a smooth one-form. Protected equations then select meromorphic spectral data. Fixing all regular-puncture mass squares on a sphere with $n \geq 3$ distinct punctures leaves $n - 3$ Coulomb coefficients. The trinion has none, but its assigned theory T_2 contains a free trifundamental half-hypermultiplet with $n_h = 4$. Its three marked flavor factors and their moment maps provide the inputs for gluing. They sit inside the full $USp(8)$ symmetry of the isolated free theory.

XVI.2.6 Exercises

For benchmark submissions, see `benchmark/PROTOCOL.md`. Include the requested written derivations and explanations.

1. **Change the twist.** Use the four spin/R rows in (XVI.2.4), each with complex multiplicity four. Compute the neutral complex dimensions for $k = 0, 1, 2, -1$ in $s'_k = s + kt$. For $k = 1$, calculate the two real eigenspace dimensions of R_0, then recover the real supersymmetry count. Submit the four neutral dimensions and the two eigenspace dimensions. Explain in writing why complex kernel dimension alone is insufficient, and why a periodic flat torus is not a counterexample to the curved-surface count.

2. **Five fixed sources.** Put five punctures at $0, 1, 2, 4, \infty$. Use coefficients in ascending powers of z and calculate the 5×7 map from P to its five double-pole coefficients. Derive its rank and a basis for its kernel. Submit that matrix, its rank, and two kernel vectors. Any rational basis is accepted. Explain why removing the last row changes a source, and why a collision of marked points is outside this linear problem.

3. **Reconstruct a different trinion.** Use masses $(m_0, m_1, m_\infty) = (2, 3, 5)$. Determine the ascending coefficient vector of the numerator and the three double-pole coefficients, including the one obtained after $w = 1/z$. Compute the fixed-degree binary quadratic discriminant. Explain why the repeated root at these masses does not introduce a Coulomb parameter.

4. **Reality and field counts.** Form $E \otimes E$ and $E \otimes E \otimes E$. Submit the signs of their transpose symmetries and squares, the value of n_h for a half-hyper in the latter representation, and every central sign triple acting trivially. Explain why the two-factor representation is not the same kind of half-hyper representation and why $q = J\overline{q}$ cannot be imposed on the eight independent chiral coordinates of the three-factor half-hyper.

5. **Recover a flavor action.** In the component order of this chapter, use $T = T_3^{(0)}$. Starting from J, determine the coefficients of $q_1q_8, q_2q_7, q_3q_6, q_4q_5$ in μ_T. Submit these four coefficients and the eight diagonal entries of the resulting linear Hamiltonian vector field. Derive the Poisson-bracket relation in (XVI.2.49) in writing, with its sign convention.

6. **A root goes to infinity.** Take $(m_0, m_1, m_\infty) = (1, 3, 0)$. Compute the four paired masses, the ascending affine numerator coefficients (retain its zero quadratic coefficient), and the binary discriminant. Submit the finite root and the number of roots at infinity counted with multiplicity. Verify the linear relation among the four masses. Explain why the reduced-degree affine discriminant is a different object, why the family has only three mass directions, and why the all-zero mass point cannot be treated by the smooth-cover genus calculation.

Sources and scope

§XVI.2.1. The spin/R branching, weight kernel and the fixed real space of the supplied symplectic reality map are representation calculations [MATH]. The compactification of the $(2, 0)$ parent with preserving defects and the appropriate four-dimensional limit is physical input [GEO-E]. Gaiotto (2012), arXiv:0904.2715v1, printed pp. 21–23, especially (2.27)–(2.30), supplies the twist and compactification setting. Gaiotto et al. (2013), arXiv:1110.2657v1, pp. 1–4, (1.1) and footnote 2, distinguishes finite area from the four-dimensional limit. The argument here assumes compatible global lifts and does not classify the global R group.

§XVI.2.2. The defining vector generator, bundle pullback and local ramified-coordinate calculation are explicit [MATH]. The protected holomorphic description uses the additional circle/Hitchin framework, separate from the smooth twist: Hollands and Kidwai (2018), published pp. 1717–1718, (1.14)–(1.15), and pp. 1726–1727, (2.4)–(2.7). The scalar twist is also described after (2.27)–(2.28) of Gaiotto (2012). Our effective λ has mass dimension one; this does not reassign the dimension of the original six-dimensional scalar.

§XVI.2.3. The regular A_1 defect/mass dictionary is sourced physical input [GEO-E]: Gaiotto (2012), printed pp. 14–18 and 22–23, (2.12)–(2.13), (2.25), (2.29)–(2.30); Hollands and Kidwai (2018), published (2.4)–(2.9). The fixed-residue interpolation, homogeneous kernel, partial-fraction constraints and sphere examples are derived here [MATH], for distinct punctures and fixed masses. They do not establish a complete Hitchin metric or an all-genus counting theorem.

§XVI.2.4. The trinion/free-half-hyper identification is [GEO-E]: Gaiotto (2012), printed pp. 8–10 and p. 18, (2.21), and Hollands and Kidwai (2018), published p. 1728. The massive differential, pseudoreality, scalar count, symplectic flavor algebra and center action are explicit consequences [MATH]. The center result concerns the displayed local fields, not a choice of global background or line data. The marked $SU(2)^3$ is a subgroup of the free $USp(8)$ flavor group.

§XVI.2.5. The moment maps, rank-three mass map, fixed-degree binary discriminant and generic-cover genus are derived in the text [MATH]. The mass comparison is consistent with Hollands and Kidwai (2018), published pp. 1728–1729, (2.9)–(2.10). To translate that source, use $\varphi_2^{\mathrm{HK}} = -\phi_2$ in its equation $\lambda^2 + \varphi_2^{\mathrm{HK}} = 0$, and $m_i^{\mathrm{HK}} = 2m_i$. These anchors use the published journal pagination. Our internal E is a flavor invariant tensor, and $\mu_T = q^T JTq/2$ uses J^{-1} as the Poisson matrix. The discriminant retains roots at infinity; the smooth genus calculation excludes the nonreduced all-massless curve. No complete BPS spectrum or arbitrary fourth free mass deformation is inferred.

References

Gaiotto, D. (2012). "N=2 dualities". In: *JHEP* 08, p. 034. DOI: 10.1007/JHEP08(2012)034. arXiv: 0904.2715 [hep-th].

Gaiotto, D., G. W. Moore, and Y. Tachikawa (2013). "On 6d N=(2,0) theory compactified on a Riemann surface with finite area". In: *PTEP* 2013, 013B03. DOI: 10.1093/ptep/pts047. arXiv: 1110.2657 [hep-th].

Hollands, L. and O. Kidwai (2018). "Higher length-twist coordinates, generalized Heun's opers, and twisted superpotentials". In: *Adv. Theor. Math. Phys.* 22.7, pp. 1713–1822. DOI: 10.4310/ATMP.2018.v22.n7.a2. arXiv: 1710.04438 [hep-th].

Chapter XVI.3

From three-punctured spheres to four-dimensional theories

The three-punctured sphere of the previous chapter gives a four-dimensional matter sector with three distinguished $SU(2)$ flavor symmetries. We now join two such spheres and ask what connects their matter fields. The answer is a gauge multiplet. A long neck makes its coupling weak, so a geometric decomposition produces a Lagrangian description that we can examine field by field.

Our first construction is $SU(2)$ gauge theory with four fundamental hypermultiplets. It will remain the example while we change the description from matter representations to a punctured sphere and then to its elliptic double cover. These descriptions emphasize different quantities. A puncture carries flavor data, a neck carries a gauge coupling, and periods of the double cover describe the abelian low-energy system. Keeping those roles separate is essential even in this rank-one example.

We use the circle reduction of Chapter 1, the twist and half-hypermultiplet convention of Chapter 2, and the $\mathcal{N} = 2$ multiplets reviewed in Volume 0. The new work is the sewing operation itself: its gauge and matter content, its superpotential, and its geometric limits. A second example, obtained by sewing two legs of the same trinion, will show why a neutral hypermultiplet can survive a construction whose interacting sector is familiar.

XVI.3.1 What a gauge tube does

A pair of pants is a sphere with three small disks removed. Its boundary circles can be extended to semi-infinite cylindrical ends. In the class-S description these ends represent the three full regular punctures of the A_1 theory. Sewing two ends replaces them by a finite cylinder. The flavor symmetry at each end then participates in a common gauge interaction.

To see the weak-coupling limit, give the middle of the cylinder a product metric.

Let t measure its length, let ϑ be an angle, and let R be its circle radius:

$$ds_C^2 = dt^2 + R^2 d\vartheta^2, \qquad 0 \le t \le L, \qquad \vartheta \sim \vartheta + 2\pi. \tag{XVI.3.1}$$

First reduce the six-dimensional theory on the small circle. Chapter 1 identifies the resulting low-energy gauge algebra as $\mathfrak{su}(2)$. In the trace convention used throughout this book, the five-dimensional kinetic term and coupling are

$$S_5 = -\frac{1}{2g_5^2}\int d^4x \int_0^L dt\ \mathrm{tr}_{\mathbf{2}}\, F_{MN}F^{MN}, \qquad g_5^2 = 8\pi^2 R, \qquad \mathrm{tr}_{\mathbf{2}}\, T_i T_j = \frac{1}{2}\delta_{ij}. \tag{XVI.3.2}$$

The gauge field that is constant along the segment has the same value at both ends. Inserting that zero mode into the action performs the reduction directly:

$$S_4 = -\frac{L}{2g_5^2}\int d^4x\ \mathrm{tr}_{\mathbf{2}}\, F_{\mu\nu}F^{\mu\nu}, \qquad \frac{1}{g_4^2} = \frac{L}{g_5^2}. \tag{XVI.3.3}$$

Thus a long segment suppresses the four-dimensional interaction. The zero-mode approximation concerns energies below the segment and circle excitation scales. It gives a weak description near a degeneration; it is not an exact metric formula for the conformal theory throughout its parameter space.

We normalize the dimensionless coupling as

$$\tau_{\mathrm{h}} = \frac{\theta}{2\pi} + \frac{4\pi i}{g_4^2}, \qquad \mathrm{Im}\,\tau_{\mathrm{h}} = \frac{L}{2\pi R}. \tag{XVI.3.4}$$

Both sides are dimensionless. A common rescaling of L and R leaves this leading coupling unchanged, while reducing their absolute sizes separates the four-dimensional theory from its compactification modes. The six-dimensional construction uses the physical assumption that the appropriate four-dimensional limit depends on the complex structure of the punctured surface. The product-cylinder calculation explains the weak limit of that dictionary.

A complex coordinate on an annulus makes the same limit visible without a metric. Choose

$$z = \exp(-t/R + i\vartheta), \qquad e^{-L/R} < |z| < 1. \tag{XVI.3.5}$$

The ratio of its boundary radii is exponentially small when the cylinder is long. More generally, two local coordinates z_L, z_R near the ends are sewn by a complex parameter p:

$$z_L z_R = p, \qquad |p| = e^{-L/R}. \tag{XVI.3.6}$$

This relation is called plumbing. Changing the phase of p rotates the two ends relative to one another. At $p = 0$ the neck is pinched to a node. For the two-trinion sphere, its normalization separates into two components. Pinching a self-glued handle instead lowers the genus and creates two punctures on one connected normalization, as in Section XVI.3.3. The relation to the weak microscopic coupling has the leading magnitude

$$\left|e^{2\pi i \tau_{\mathrm{h}}}\right| = e^{-8\pi^2/g_4^2} = e^{-L/R} = |p|. \tag{XVI.3.7}$$

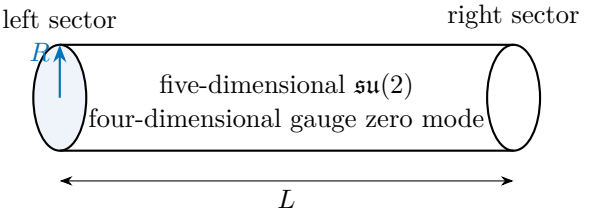


Figure XVI.3.1: The middle of a sewn neck, with circle radius R and segment length L. Reducing around the circle gives a five-dimensional gauge field. Its segment zero mode couples the two end sectors and has $1/g_4^2 = L/g_5^2$. The drawing specifies the product-metric region used in the weak-limit calculation.

A choice of local coordinates can multiply p by a nonzero constant and alter higher-order terms. Consequently this calculation fixes a logarithmic weak-coupling behavior, not a universal exact identification between a global cross-ratio and a microscopic coupling.

The boundary flavor symmetries specify how the gauge zero mode acts. If the two sectors have flavor transformations g_L and g_R, gauging the diagonal subgroup means

$$g_L = g_R = g, \qquad D_\mu Q_L = \partial_\mu Q_L - iA_\mu^i T_i Q_L, \qquad D_\mu Q_R = \partial_\mu Q_R - iA_\mu^i T_i Q_R. \tag{XVI.3.8}$$

The new field is a vector multiplet; the matter already belongs to the two end sectors. Supersymmetry also couples its adjoint chiral multiplet to their moment maps. We will construct that coupling explicitly rather than infer the matter content from the picture alone.

For orientation, take $L/R = 20$. The leading reduction gives

$$g_4^2 = \frac{2\pi^2}{5}, \qquad \operatorname{Im}\tau_{\mathrm{h}} = \frac{10}{\pi}, \qquad |p| = e^{-20}. \tag{XVI.3.9}$$

Increasing the length to $40R$ halves g_4^2 and squares $|p|$. This is why a small plumbing coordinate is more useful than a large real cylinder length near a weak-coupling cusp. Away from that cusp, the complex geometry remains useful while this simple metric reduction loses its quantitative control.

XVI.3.2 Two trinions give four flavors

Let Q_{abi} be the chiral coordinates of the left T_2 block and P_{icd} those of the right block. Every index takes two values. The index i will be gauged, while a, b, c, d label four remaining puncture symmetries. In representation notation the matter is

$$\frac{1}{2}(\mathbf{2}_a, \mathbf{2}_b, \mathbf{2}_g) \;\oplus\; \frac{1}{2}(\mathbf{2}_g, \mathbf{2}_c, \mathbf{2}_d). \tag{XVI.3.10}$$

The factor $1/2$ denotes a half-hypermultiplet in the pseudoreal trifundamental. It does not divide the dimension of each $\mathcal{N} = 1$ chiral coordinate space. There are eight chiral components in each summand.

Under $SU(2)_g$, the pairs (a,b) label four chiral doublets. The right sector supplies four more. Two such doublets make one full fundamental hyper, giving

$$\begin{aligned} &4+4=8 \text{ chiral doublets}, \quad N_f=\frac{8}{2}=4, \\ &n_h=\frac{8+8}{2}=8, \qquad\qquad n_v=\dim \mathfrak{su}(2)=3. \end{aligned} \tag{XVI.3.11}$$

Here n_h is a quaternionic component count. Four full hypers in a two-dimensional gauge representation give $n_h=8$. Confusing n_h with the number of fundamental flavors would double the matter content.

The one-loop screening can be calculated without relying on that verbal count. Set $t_i=\sigma_i/2$ on a fundamental and choose the gauged leg to be the last factor in each ordered tensor product. Its Cartan generator is

$$T_3=I_4\otimes\frac{1}{2}\begin{pmatrix}1&0\\0&-1\end{pmatrix}, \qquad \operatorname{tr}_{\mathbf{8}} T_3^2=4\left(\frac{1}{4}+\frac{1}{4}\right)=2. \tag{XVI.3.12}$$

The adjoint Cartan weights are $1,0,-1$, so its index is 2. The $\mathcal{N}=2$ vector contributes $2h^\vee=4$ to the beta coefficient. The sum subtracted from it runs over *hypermultiplet matter chirals*; the adjoint chiral inside the vector has already been included. Hence

$$b_0=2h^\vee-\sum_{\text{hypermatter chirals}} T(R)=4-2-2=0. \tag{XVI.3.13}$$

For comparison, replacing both half-trifundamentals by full trifundamentals gives $4-4-4=-4$. Removing one full fundamental from the correct theory gives $4-3=1$. Vanishing screening therefore depends on the actual half-hyper assignment.

The massless $SU(2)$ theory with four fundamentals is a conformal $\mathcal{N}=2$ theory with an exactly marginal complex coupling. The calculation above isolates the vanishing logarithmic coefficient. The identification of the full conformal theory also uses the protected $\mathcal{N}=2$ dynamics. In particular, absence of logarithmic running does not forbid finite holomorphic changes of the coordinate used for the coupling. That distinction will reappear in the elliptic curve.

We next determine the interaction with the adjoint chiral field. On each internal fundamental space introduce the antisymmetric form

$$E=\begin{pmatrix}0&1\\-1&0\end{pmatrix}, \qquad \Omega=E\otimes E\otimes E, \qquad \Omega^T=-\Omega, \qquad T_i^T\Omega+\Omega T_i=0. \tag{XVI.3.14}$$

These are internal representation indices, not Lorentz spinor indices. The last identity says that the gauged generators preserve the holomorphic symplectic form. It also implies that ΩT_i is symmetric, so it defines a nonzero quadratic expression in commuting chiral fields.

Write each trinion as a column, with its gauged index ordered last. Its holomorphic moment map is normalized by the action it generates:

$$\mu_i(Q)=\frac{1}{2}Q^T\Omega T_i Q, \qquad \frac{\partial\mu_i}{\partial Q}=\Omega T_i Q, \qquad \Omega^{-1}\frac{\partial\mu_i}{\partial Q}=T_i Q. \tag{XVI.3.15}$$

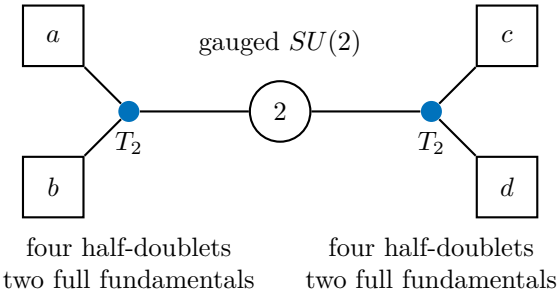


Figure XVI.3.2: The two-trinion construction. Blue vertices represent half-trifundamentals, the middle circle represents the gauged $SU(2)$, and the four squares label puncture flavor factors. Each vertex supplies two full fundamental hypermultiplets to the middle gauge group. Edges record representation factors; they are not additional matter multiplets.

The factor $1/2$ is fixed by differentiating a symmetric quadratic form. Halving it again would generate half the specified flavor transformation. For example, for lexicographically ordered components $Q_0, \dots, Q_7$,

$$\mu_3(Q) = \frac{1}{2}(-Q_0Q_7 - Q_1Q_6 + Q_2Q_5 + Q_3Q_4). \tag{XVI.3.16}$$

This explicit expression shows both the gauge weights and the contractions between the two spectator indices.

Let $\Phi = \Phi_i t_i$ denote the adjoint scalar matrix, in the standard $\mathcal{N} = 2$ holomorphic normalization. With the same gauge orientation on both sectors, the superpotential is

$$W = \sqrt{2}\sum_{i=1}^{3} \Phi_i\big(\mu_i(Q) + \mu_i(P)\big), \qquad \frac{\partial W}{\partial \Phi_i} = \sqrt{2}\big(\mu_i(Q) + \mu_i(P)\big). \tag{XVI.3.17}$$

The adjoint F equation sets the sum of the two moment maps to zero. This is an interaction between already existing matter sectors. A different consistent choice of field orientation can rewrite signs, but a sign change must be accompanied by the corresponding field convention.

There are two useful ways to verify the coupling. In the eight-dimensional trinion representation, the fundamental matrix acts as $\widehat{\Phi} = I_4 \otimes \Phi = \sum_i \Phi_i T_i$. Let T act in that same representation. An infinitesimal gauge transformation then gives $\delta Q = TQ$ and $\delta\widehat{\Phi} = [T, \widehat{\Phi}]$. The coefficient of its variation vanishes:

$$T^T\Omega\widehat{\Phi} + \Omega[T, \widehat{\Phi}] + \Omega\widehat{\Phi}T = -\Omega T\widehat{\Phi} + \Omega(T\widehat{\Phi} - \widehat{\Phi}T) + \Omega\widehat{\Phi}T = 0. \tag{XVI.3.18}$$

This checks covariance but does not determine an overall Yukawa coefficient. To fix that coefficient relative to ordinary hypers, group the eight chiral components into four gauge doublets $Q_{00}, Q_{01}, Q_{10}, Q_{11}$. Directly expanding the first two epsilon tensors gives

$$\frac{1}{2}Q^T\Omega(I_4 \otimes \Phi)Q = Q_{00}^T E\Phi Q_{11} - Q_{01}^T E\Phi Q_{10}. \tag{XVI.3.19}$$

The rows $Q_{00}^T E$ and $-Q_{01}^T E$ transform as antifundamentals. Calling them $\widetilde{q}_1, \widetilde{q}_2$, and calling Q_{11}, Q_{10} the corresponding fundamentals, turns this expression into two terms $\widetilde{q}\Phi q$. With the prefactor $\sqrt{2}$ in (XVI.3.17), these are precisely the standard $\mathcal{N} = 2$ Yukawas. Repeating the argument for P gives the four-flavor Lagrangian, including its interaction and not just its field count.

The three puncture factors of an isolated free T_2 are a distinguished $SU(2)^3$ subgroup of its larger free-field flavor symmetry $USp(8)$. Its three geometric puncture masses do not exhaust the free theory's mass deformations. After sewing, the four visible puncture factors sit inside the $\mathfrak{so}(8)$ flavor algebra of the four-flavor gauge theory. We will use that embedding when comparing different degeneration channels, while leaving global flavor quotients to Chapter 11.

XVI.3.3 Pants counts and a handle

The first construction extends to a connected surface of genus g with n full regular punctures. We restrict to the stable domain

$$g, n \in \mathbb{Z}_{\geq 0}, \qquad 2g - 2 + n > 0. \tag{XVI.3.20}$$

This is the domain in which the surface can be decomposed into three-holed spheres. It includes a three-punctured sphere and a once-punctured torus, but excludes the unpunctured torus discussed in Chapter 1. All the following counts are for untwisted A_1 constructions with maximal regular punctures.

Let P be the number of pairs of pants and I the number of sewn tubes. Each pair of pants has Euler characteristic -1. Sewing boundary circles changes neither the total Euler characteristic nor the number of external punctures. Therefore

$$-P = \chi(C) = 2 - 2g - n, \qquad P = 2g - 2 + n. \tag{XVI.3.21}$$

The $3P$ boundaries are exhausted by two ends for every internal tube and one end for every external puncture:

$$3P = 2I + n, \qquad I = 3g - 3 + n. \tag{XVI.3.22}$$

Equivalently, the connected trivalent graph has P vertices, I internal edges and g independent loops. This gives a separate way to read the genus:

$$g = I - P + 1. \tag{XVI.3.23}$$

A self-loop counts as one internal edge with two ends at the same vertex. Forgetting that double incidence would spoil both formulas.

Each trinion contributes four quaternionic matter components and each gauge tube contributes a three-dimensional vector algebra. The weak-frame component counts are consequently

$$n_h = 4P = 4(2g - 2 + n), \qquad n_v = 3I = 3(3g - 3 + n). \tag{XVI.3.24}$$

They are useful inputs for later anomaly calculations. They are not a general formula for a Higgs-branch dimension: subtracting n_v from n_h would additionally require a suitable freely acting, fully broken gauge group. We have made no such assertion for arbitrary graphs.

For a five-punctured sphere the calculation gives

$$(g,n)=(0,5): \qquad P=3, \qquad I=2, \qquad (n_h,n_v)=(12,6). \tag{XVI.3.25}$$

In its chain frame, each end trinion supplies two fundamentals to the neighboring gauge group. The middle trinion is a full bifundamental of the two gauge groups: the remaining spectator doublet pairs its half-hyper components. Thus each gauge node sees two fundamentals from the end plus two effective fundamentals from the bifundamental. The same local count that gave $b_0=0$ in the four-punctured example applies at both nodes.

The smallest handle gives a revealing second example. Sewing two legs of a single trinion leaves

$$(g,n)=(1,1): \qquad P=1, \qquad I=1, \qquad (n_h,n_v)=(4,3). \tag{XVI.3.26}$$

The gauged group now acts diagonally on two factors of the *same* tensor. It cannot be counted as two unrelated fundamental sectors. On their tensor product its generators are

$$J_i = t_i\otimes I_2 + I_2\otimes t_i. \tag{XVI.3.27}$$

The symmetric basis vectors $|00\rangle$, $(|01\rangle+|10\rangle)/\sqrt{2}$, $|11\rangle$ form a triplet. The antisymmetric vector $(|01\rangle-|10\rangle)/\sqrt{2}$ is annihilated by every J_i. If S exchanges the two tensor factors, the projectors and Casimir are

$$\begin{gathered} P_3=\frac{I+S}{2}, \qquad P_1=\frac{I-S}{2}, \qquad \sum_i J_i^2 = 2P_3, \\ \operatorname{rank}P_3=3, \qquad \operatorname{rank}P_1=1. \end{gathered} \tag{XVI.3.28}$$

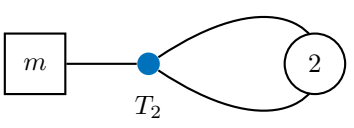
The spectator doublet has not been gauged. Including it and the original half-hyper condition gives

$$\begin{aligned} \frac{1}{2}(\mathbf{2},\mathbf{2},\mathbf{2}) &\longrightarrow \frac{1}{2}(\mathbf{3},\mathbf{2})\oplus\frac{1}{2}(\mathbf{1},\mathbf{2}) \\ &= \text{one adjoint full hyper} + \text{one neutral full hyper}. \end{aligned} \tag{XVI.3.29}$$

The triplet contributes six chiral components and the singlet two. The two spectator weights pair each real gauge representation into a full hyper. Erasing the neutral sector would leave six of the original eight components, even though it would leave the gauge beta coefficient unchanged.

The interaction also separates. Every J_i annihilates the singlet, so its contribution to the gauge moment map is zero. The adjoint has trace index 2; a full adjoint hyper gives screening 4 and hence

$$b_0 = 2h^\vee - 2T(\text{adj}) = 4-4=0, \qquad W_{\text{gauge}}\big|_{\text{singlet}}=0. \tag{XVI.3.30}$$



$\frac{1}{2}(\mathbf{2},\mathbf{2},\mathbf{2})$
$\longrightarrow\ \frac{1}{2}(\mathbf{3},\mathbf{2}) \oplus \frac{1}{2}(\mathbf{1},\mathbf{2})$
adjoint hyper + neutral hyper

Figure XVI.3.3: Self-gluing a trinion produces one handle and one remaining puncture. The gauge group acts on two tensor factors diagonally. The spectator doublet converts both the triplet and singlet summands into full hypermultiplets. The neutral hyper is present alongside the interacting adjoint sector.

Together with the canonical $\mathcal{N} = 2$ coupling, the vector and adjoint hyper form the interacting $\mathcal{N} = 4$ theory when their mass vanishes. The neutral hyper remains a separate free sector. This statement concerns the self-glued punctured torus; it does not add a free hyper to the unpunctured-torus construction of Chapter 1.

The remaining puncture provides a mass deformation. In the residue-eigenvalue convention of Chapter 2, its Cartan background is $m\,\mathrm{diag}(1,-1)$ on the spectator. For the trinion column V write the mass quadratic as

$$W_m = \frac{m}{2} V^T \Omega T_s V, \qquad T_s = I_4 \otimes \mathrm{diag}(1,-1). \tag{XVI.3.31}$$

The first-two-factor basis used above block-diagonalizes it. On the singlet doublet (s_+, s_-), the restricted antisymmetric form and mass matrix are

$$\begin{aligned} \Omega_1 &= \begin{pmatrix} 0 & 1 \\ -1 & 0 \end{pmatrix}, \qquad W_{m,1} = -m s_+ s_-, \\ K_1 &= \Omega_1 \begin{pmatrix} 1 & 0 \\ 0 & -1 \end{pmatrix} = \begin{pmatrix} 0 & -1 \\ -1 & 0 \end{pmatrix}, \end{aligned} \tag{XVI.3.32}$$

The singlet is gauge neutral but is not neutral under this flavor Cartan. On the ordered triplet basis above, restricting $E \otimes E$ gives the symmetric matrix B. The six-dimensional adjoint block therefore has

$$B = \begin{pmatrix} 0 & 0 & 1 \\ 0 & -1 & 0 \\ 1 & 0 & 0 \end{pmatrix}, \qquad \Omega_3 = B \otimes E, \qquad K_3 = B \otimes \begin{pmatrix} 0 & -1 \\ -1 & 0 \end{pmatrix}. \tag{XVI.3.33}$$

Both factors of K_3 are invertible. Multiplying by the inverse symplectic form recovers the spectator action on each of the three gauge components:

$$\Omega_3^{-1} K_3 = \mathrm{diag}(1,-1,1,-1,1,-1), \qquad \mathrm{rank}\, K_3 = 6, \qquad \mathrm{rank}\, K_1 = 2. \tag{XVI.3.34}$$

There is no mixed adjoint-singlet block. At nonzero m both hypers acquire a mass; at $m = 0$ both mass terms vanish. The interacting sector at nonzero mass is therefore $\mathcal{N} = 2^*$, accompanied by a free massive neutral hyper. This explicit decomposition will matter whenever protected quantities count all degrees of freedom of the sewn construction.

XVI.3.4 The sphere and its elliptic cover

Return to the two-trinion sphere. A Möbius transformation fixes three marked punctures at $0, 1, \infty$. The fourth position is a complex parameter q:

$$C = \mathbb{P}^1 \setminus \{0, 1, q, \infty\}, \qquad q \notin \{0, 1, \infty\}. \tag{XVI.3.35}$$

It is a cross-ratio coordinate on the space of marked surfaces. The three values excluded here are degeneration limits. They are three ends of one complex parameter space, not three independent gauge couplings.

At zero puncture masses the quadratic differential may have simple poles at the four punctures. Its line bundle has degree

$$\deg K_C^{\otimes 2}(D) = -4 + 4 = 0, \qquad D = 0 + 1 + q + \infty. \tag{XVI.3.36}$$

Here K_C denotes the canonical bundle of the compact sphere before punctures are removed. A degree-zero line bundle on the sphere has a one-dimensional section space. In the chosen coordinate a basis is $dz^2/[z(z-1)(z-q)]$. To check the pole at infinity, put $r = 1/z$:

$$\frac{dz^2}{z(z-1)(z-q)} = \frac{dr^2}{r(1-r)(1-qr)}. \tag{XVI.3.37}$$

It has a simple pole at $r = 0$, as required. The remaining coefficient u is the single Coulomb parameter in this spectral chart.

The class-S spectral dictionary assigns the double cover and differential

$$\Sigma: \quad x^2 = \frac{u}{z(z-1)(z-q)}, \qquad \lambda_{\mathrm{geom}} = x\, dz. \tag{XVI.3.38}$$

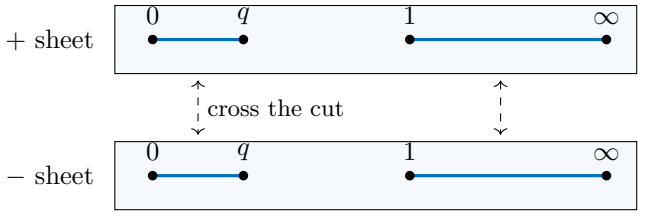
We keep the subscript because no absolute calibration to the physical BPS central charge or primitive charge lattice is performed in this chapter. The coefficient u has mass dimension two, while q, z are dimensionless. Its normalization need not equal a separately normalized microscopic $\mathrm{tr}\,\phi^2$ without a further matching calculation.

For $u \neq 0$, choose a local square root and set $y = \sqrt{u}/x$. Then

$$y^2 = z(z-1)(z-q), \qquad \lambda_{\mathrm{geom}} = \sqrt{u}\,\frac{dz}{y}. \tag{XVI.3.39}$$

The cover is branched at $0, 1, q, \infty$. Riemann–Hurwitz determines its genus:

$$2g_\Sigma - 2 = 2(2g_C - 2) + 4 = -4 + 4 = 0, \qquad g_\Sigma = 1. \tag{XVI.3.40}$$



Two copies of the punctured z sphere are sewn crosswise.

Figure XVI.3.4: A cut description of the elliptic cover of the four-punctured sphere. Each rectangle represents a copy of the z sphere opened along cuts joining 0 to q and 1 to ∞. Crossing a cut changes sheets. The branch points are points of the base; the two sheets together form Σ. Positions in the drawing are schematic.

The ultraviolet surface is a sphere; the Seiberg–Witten surface is an elliptic double cover of it. The genus counts the one low-energy abelian gauge field. Its modulus is independent of nonzero u in this massless conformal family because $\sqrt{u}$ multiplies both periods equally. At $u = 0$ the change of variables to y fails, so this observation does not make the Coulomb origin a smooth elliptic fiber.

We can calculate the complex structure directly from the cubic. Its root differences give the polynomial discriminant

$$\operatorname{disc}_z\big[z(z-1)(z-q)\big] = (0-1)^2(0-q)^2(1-q)^2 = q^2(1-q)^2. \tag{XVI.3.41}$$

To pass to Weierstrass form, translate $z = X + (1+q)/3$ and set $Y = 2y$. Expanding the cubic removes its quadratic term and gives

$$Y^2 = 4X^3 - g_2X - g_3, \qquad g_2 = \frac{4}{3}(1-q+q^2), \qquad g_3 = \frac{4}{27}(q-2)(q+1)(2q-1). \tag{XVI.3.42}$$

The Weierstrass discriminant in this normalization is $g_2^3 - 27g_3^2 = 16q^2(1-q)^2$. It differs from the polynomial discriminant by the displayed factor sixteen. Their zeros agree, while their normalizations serve different formulas. The invariant that forgets the marking is

$$j(q) = 1728\frac{g_2^3}{g_2^3 - 27g_3^2} = 256\frac{(1-q+q^2)^3}{q^2(1-q)^2}. \tag{XVI.3.43}$$

For example, $q = 1/2$ gives $j = 1728$, and $q = (1+i\sqrt{3})/2$ makes the numerator vanish and gives $j = 0$. These are the square and equianharmonic elliptic curves. They provide recognizable smooth examples as well as the singular limits detected by the discriminant.

Permuting four marked points produces the six rational cross-ratio transformations

$$q, \quad 1-q, \quad \frac{1}{q}, \quad \frac{1}{1-q}, \quad \frac{q-1}{q}, \quad \frac{q}{q-1}. \tag{XVI.3.44}$$

Substitution in (XVI.3.43) leaves j unchanged. At special values some transformed numbers coincide because the elliptic curve has extra automorphisms. These six

functions describe relabelings of the marked branch data; equality of j alone remembers only the unmarked elliptic curve.

The differential requires more information. For reflection, write $w = 1 - z$ and $q' = 1 - q$. Substitution in the quadratic differential gives

$$\frac{u\,dz^2}{z(z-1)(z-q)} = \frac{-u\,dw^2}{w(w-1)(w-q')}, \qquad u' = -u, \qquad x_w = -x_z. \tag{XVI.3.45}$$

The last sign is needed for the *one-form* identity $x_w dw = x_z dz$; it cannot be recovered by checking squares alone. Likewise, using $w = z/q$ moves the old puncture at q to 1 and gives

$$q' = \frac{1}{q}, \qquad u' = \frac{u}{q}, \qquad x_w = q x_z, \qquad \frac{u\,dz^2}{z(z-1)(z-q)} = \frac{(u/q)\,dw^2}{w(w-1)(w-1/q)}. \tag{XVI.3.46}$$

Thus a transformation of the coupling coordinate also changes the convenient Coulomb coordinate. At $q = 1/3$, this chart has $q' = 3$ and $u' = 3u$. Keeping u fixed would preserve the numerical j but would fail the displayed differential relation. The physical duality interpretation must therefore retain more than an elliptic invariant.

XVI.3.5 Degeneration channels and coupling coordinates

A degeneration should recover the weak gauge tube and its two matter sectors. Consider $q \to 0$ at fixed nonzero u. The punctures at $z = 0$ and $z = q$ collide in the original coordinate. Keeping z fixed away from their collision gives the right component

$$\phi_R(z)\,dz^2 = \lim_{q\to 0} \frac{u\,dz^2}{z(z-1)(z-q)} = \frac{u\,dz^2}{z^2(z-1)}. \tag{XVI.3.47}$$

This component retains the external punctures $1, \infty$ and develops a node at $z = 0$. The pole at the node is now double, with coefficient $-u$.

To retain the two colliding external punctures, zoom in with $z = qw$ before taking the limit. The Jacobian matters:

$$\phi_2(z)\,dz^2 = \frac{u\,dw^2}{w(w-1)(qw-1)} \longrightarrow -\frac{u\,dw^2}{w(w-1)} = \phi_L(w)\,dw^2. \tag{XVI.3.48}$$

The left component has external punctures at $w = 0, 1$ and its node at $w = \infty$. Set $\xi = 1/w$ near that node. Both branches have the same leading quadratic coefficient:

$$\lim_{z\to 0} z^2\phi_R(z) = -u, \qquad \phi_L(w)dw^2 = \frac{u\,d\xi^2}{\xi^2(\xi-1)}, \qquad \lim_{\xi\to 0} \xi^2\phi_L(\xi) = -u. \tag{XVI.3.49}$$

This equality allows the two puncture mass-squared data created by cutting the tube to be identified with the gauge Coulomb parameter. It does not fix the overall physical period normalization, which remains separate.

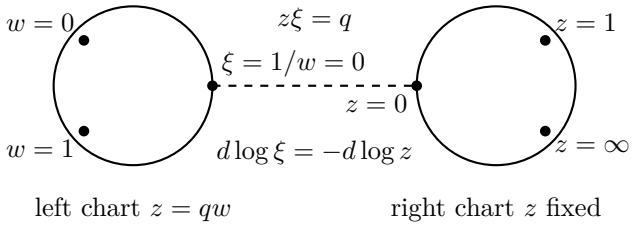


Figure XVI.3.5: The two normalization components in the fixed-u, $q \to 0$ limit. On the left, $w = z/q$ resolves the colliding punctures. On the right, z remains fixed. Their node coordinates obey $z\xi = q$, so logarithmic one-forms have opposite signs. Each component has two external punctures and one node.

The signs of the unsquared residues follow from sewing. Before the limit, $z = qw$ implies

$$z\xi = q, \qquad d\log\xi = -d\log z. \tag{XVI.3.50}$$

Choose $a_{\mathrm{geom}}^2 = -u$ on a local branch. A differential $a_{\mathrm{geom}} d\log z$ on the right is then $-a_{\mathrm{geom}} d\log\xi$ on the left. Its residues are opposite, as required for the local smoothing. Equality of their squares would not by itself select those signs.

In the overlap $|q| \ll |z| \ll 1$, the differential exhibits the tube explicitly:

$$\lambda_{\mathrm{geom}}^2 \simeq -u\frac{dz^2}{z^2}, \qquad \lambda_{\mathrm{geom}} \simeq a_{\mathrm{geom}}\frac{dz}{z}. \tag{XVI.3.51}$$

An A cycle circles the narrow neck. A complementary B cycle traverses it and returns on the other sheet. With compatible orientations, their leading periods are

$$\oint_A \lambda_{\mathrm{geom}} \simeq 2\pi i a_{\mathrm{geom}}, \qquad \oint_B \lambda_{\mathrm{geom}} \simeq 2a_{\mathrm{geom}}\log q + \text{finite multiple of } a_{\mathrm{geom}}. \tag{XVI.3.52}$$

The factor two in the second period comes from the two-sheeted return path. The ratio thus contains $(\log q)/(\pi i)$. The finite contribution requires the whole curve, not only the middle of the tube.

We can calculate that ratio on a definite smooth slice. For $0 < q < 1$, choose the cycle marking for which its imaginary part is positive. The complete elliptic integral and period ratio are

$$K(m) = \int_0^{\pi/2} \frac{d\theta}{\sqrt{1 - m\sin^2\theta}}, \qquad \tau_{\mathrm{geom}} = i\frac{K(1-q)}{K(q)}. \tag{XVI.3.53}$$

To obtain the first integral from the cubic, set $z = q\sin^2\theta$ on the cut from 0 to q:

$$\frac{dz}{\sqrt{z(1-z)(q-z)}} = \frac{2\,d\theta}{\sqrt{1 - q\sin^2\theta}}. \tag{XVI.3.54}$$

Closing the cut doubles this integral and gives $4K(q)$. The substitution $z = q/[1 - (1 - q)\sin^2\theta]$ on the complementary cut gives $4iK(1-q)$ with the chosen orientation. Their

common factor $\sqrt{u}$ cancels. Away from the real slice, the formula requires analytic continuation and transport of the cycles; it is not a globally single-valued function of the unmarked curve.

The elliptic nome is a third coordinate worth distinguishing:

$$Q = e^{\pi i \tau_{\mathrm{geom}}}, \qquad \theta_2(Q) = \sum_{n\in\mathbb{Z}} Q^{(n+1/2)^2}, \qquad \theta_3(Q) = \sum_{n\in\mathbb{Z}} Q^{n^2}. \tag{XVI.3.55}$$

In this convention the branch cross-ratio is the modular lambda function:

$$q = \frac{\theta_2(Q)^4}{\theta_3(Q)^4}. \tag{XVI.3.56}$$

The first terms follow from the sums themselves:

$$\theta_2(Q) = 2Q^{1/4}(1 + Q^2 + Q^6 + \cdots), \qquad \theta_3(Q) = 1 + 2Q + 2Q^4 + \cdots. \tag{XVI.3.57}$$

Taking their ratio to fourth power gives

$$\begin{aligned} q &= 16Q - 128Q^2 + 704Q^3 - 3072Q^4 + 11488Q^5 + O(Q^6), \\ \tau_{\mathrm{geom}} &= \frac{\log(q/16)}{\pi i} + O(q). \end{aligned} \tag{XVI.3.58}$$

The leading factor sixteen is already enough to distinguish q from Q. Higher terms show that the difference is not merely a constant convention for the scale of a coordinate.

A familiar point checks the distinction without a weak-limit approximation. At $q = 1/2$, the two elliptic integrals are equal, so

$$\tau_{\mathrm{geom}} = i, \qquad Q = e^{-\pi} \simeq 0.0432139, \qquad 16Q \simeq 0.691423, \qquad q = 0.5. \tag{XVI.3.59}$$

Keeping only $16Q$ is a cusp approximation, not the exact square-curve value. The convergent theta sums reconstruct $q = 1/2$; the successive series terms improve the estimate. Direct period integrals also reconstruct the cross-ratio at $q = 1/16$ and $q = 1/4$, providing checks with a changed complex structure.

There are now three distinct notions: the cross-ratio q of the punctured ultraviolet sphere, the microscopic coupling τ_{h} in a chosen renormalization scheme, and the modulus τ_{geom} of its spectral torus. The long-cylinder result fixes the leading logarithm of the microscopic coupling, while the double cover fixes the spectral period ratio. If a local plumbing coordinate is chosen proportional to q near zero, the coefficients obey

$$\operatorname{Im}\tau_{\mathrm{h}} \sim -\frac{\log|q|}{2\pi}, \qquad \operatorname{Im}\tau_{\mathrm{geom}} \sim -\frac{\log|q|}{\pi}. \tag{XVI.3.60}$$

The factor two reflects the specified normalization and cycle description. Finite shifts and holomorphic corrections still distinguish coupling schemes. The elliptic torus here is also different from the actual compactification torus that gave $\mathcal{N} = 4$ in Chapter 1. Identifying symbols called τ across those constructions would lose both the physical distinction and the normalization.

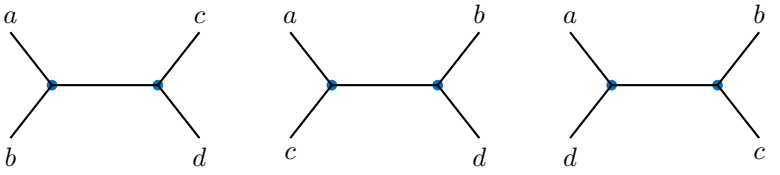


Figure XVI.3.6: The three pairings of four marked punctures into two trinions. Each middle edge is one gauge tube. The three graphs describe distinct weak channels of the same one-dimensional conformal parameter space, with different assignments of the puncture flavor factors to the two matter sectors.

Finally consider the other two channels. Their singular behavior follows directly from the invariant:

$$\begin{aligned} q^2 j(q) &\longrightarrow 256 \quad (q \to 0), \\ (1-q)^2 j(q) &\longrightarrow 256 \quad (q \to 1), \\ \frac{j(q)}{q^2} &\longrightarrow 256 \quad (q \to \infty). \end{aligned} \tag{XVI.3.61}$$

Each limit has a long tube in an appropriate coordinate. Four labeled punctures have exactly three unordered pairings into two pairs,

$$ab \,|\, cd, \qquad ac \,|\, bd, \qquad ad \,|\, bc. \tag{XVI.3.62}$$

The two halves of each pairing give the two T_2 sectors of its weak frame. The labels of the visible flavor factors change between frames, so we should compare their representations as well as the curves.

For a direct representation calculation, let $e_1, \ldots, e_4$ be the orthonormal weight coordinates of $\mathfrak{so}(8)$. Restrict a weight $w = (w_1, w_2, w_3, w_4)$ to four doubled $SU(2)$ Cartan coordinates by

$$w \longmapsto (w_1 + w_2,\ w_1 - w_2,\ w_3 + w_4,\ w_3 - w_4). \tag{XVI.3.63}$$

A fundamental of an $SU(2)$ factor has weights ± 1 in this doubled notation. The vector weights $\pm e_i$ consequently occupy the (a, b) or (c, d) pair of coordinates. Half-spin weights have the form $(\pm 1, \pm 1, \pm 1, \pm 1)/2$. Even parity of minus signs puts their supports in (a, c) or (b, d), while odd parity puts them in (a, d) or (b, c). Thus

$$\mathbf{8}_v = (\mathbf{2}_a, \mathbf{2}_b) \oplus (\mathbf{2}_c, \mathbf{2}_d), \tag{XVI.3.64}$$

$$\mathbf{8}_s = (\mathbf{2}_a, \mathbf{2}_c) \oplus (\mathbf{2}_b, \mathbf{2}_d), \tag{XVI.3.65}$$

$$\mathbf{8}_c = (\mathbf{2}_a, \mathbf{2}_d) \oplus (\mathbf{2}_b, \mathbf{2}_c). \tag{XVI.3.66}$$

Each summand has four weights, so all three branchings retain dimension eight. These are exactly the three pairings of puncture factors. They explain how the familiar triality action can permute the flavor interpretation of the weak matter without changing its local counting.

The physical statement is that these are S-dual weak descriptions of the four-flavor theory. The representation calculation, transformed spectral differentials and degeneration limits display compatible consequences of that statement. They do not constitute a proof of equality of all observables of the full quantum theories. The six-dimensional construction supplies a common origin together with its physical assumptions; the known four-dimensional duality supplies the full interpretation. Global choices of genuine line operators and flavor quotients require additional data and will be addressed in Chapter 11.

Take-home message

A sewn tube gauges two puncture symmetries and introduces an $\mathcal{N} = 2$ vector multiplet. Two T_2 half-trifundamentals then give the complete weak Lagrangian of $SU(2)$ with four full fundamental hypers. Self-gluing changes the representation problem and retains a neutral hyper alongside the adjoint sector. The punctured surface controls how these weak descriptions are organized; its spectral double cover supplies the low-energy period geometry. The next chapter develops that spectral description as a Hitchin system and extends it beyond this first rank-one example.

Exercises

1. For a connected genus-two surface with two maximal regular punctures, derive the numbers of trinions, tubes, hypermultiplet quaternionic components and vector components. Check both the incidence equation and the graph loop count. Explain why the same formula is not a decomposition of an unpunctured torus.

2. Redo the gauge trace calculation if the two T_2 blocks are each incorrectly treated as a full trifundamental hyper. Find the resulting beta coefficient. Explain separately why subtracting the $\mathcal{N} = 1$ adjoint inside the vector from (XVI.3.13) would also be an error.

3. Construct the symmetric and antisymmetric projectors on $\mathbf{2} \otimes \mathbf{2}$. Find their ranks and the number of neutral full hypers after self-gluing. For nonzero puncture mass, determine the ranks of the adjoint and singlet mass matrices. Explain why a vanishing gauge beta coefficient cannot detect omission of the singlet.

4. Set $q = 1/3$. Translate the Legendre cubic to the normalization (XVI.3.42) and compute g_2, g_3 and j. In the chart $w = z/q$, find the new cross-ratio and the coefficient u'/u. Compare the differential before and after the coordinate change.

5. At fixed nonzero u, derive both components of the $q \to 0$ limit and compute the two squared node residues divided by u. Determine the cotangent-coordinate multipliers for $w = 1 - z$ and for $w = z/q$ at $q = 1/3$. Explain which sign information would be lost if only quadratic differentials were compared.

6. For the square elliptic curve, compute Q and $16Q$, keeping at least eight decimal places. Compare them with the exact cross-ratio. Explain why defining a UV coupling through the cross-ratio is a choice of scheme and why the elliptic nome need not be that scheme's instanton parameter.

For benchmark submissions, see `benchmark/PROTOCOL.md`. Include the requested written derivations and explanations.

Sources and scope

Section 3.1. The zero-mode integral and cylinder modulus are explicit calculations. Their interpretation as gauging full-puncture flavor factors is a geometric construction input, [GEO-E], using the circle normalization of Chapter 1. Gaiotto (2012, arXiv v1, §2.3, printed pp. 22–23) states the required assumptions about the four-dimensional limit and cylinder/defect replacement. The calculation gives the leading weak-cylinder coupling; it supplies no finite UV matching scheme.

Section 3.2. The restriction of the two half-trifundamentals, their trace indices, the symplectic moment maps and the normalized Yukawa identity are finite representation and polynomial calculations, [MATH]. The T_2 and sewing interpretation is inherited from Chapter 2 and Gaiotto (2012, arXiv v1, §2.1, pp. 4, 8–10). The standard microscopic $\sqrt{2}\,\widetilde{q}\Phi q$ interaction is in Seiberg and Witten (1994, arXiv v1, eq. (3.1), p. 10). Exact marginality is sourced protected physics, [BPS:1/2|holo]; the computed $b_0 = 0$ alone does not prove it. Seiberg–Witten §4.1 gives the perturbative result and §10, pp. 33–34, explicitly assumes exact scale invariance in developing its solution; Gaiotto p. 4 treats the exactly marginal conformal theory. Finite changes of coupling coordinates remain allowed.

Section 3.3. The stable-surface counts, Casimir/projector decomposition and mass-block calculations are [MATH]. They apply to connected untwisted A_1 surfaces with maximal regular punctures and $2g-2+n>0$. The geometric self-gluing interpretation is [GEO-E], with the generalized sewing and genus-one construction in Gaiotto (2012, arXiv v1, pp. 10–11 and §2.2, pp. 18–19). The massless vector-plus-adjoint identification is recalled in Seiberg and Witten (1994, arXiv v1, p. 3). The neutral hyper and its mass have been retained. No global gauge form, absolute mass calibration or general Higgs-branch dimension is inferred.

Section 3.4. The massless spectral family is a sourced geometric dictionary, [GEO-E], from Gaiotto (2012, arXiv v1, eqs. (2.7)–(2.12), pp. 14–15). The degree count, double-cover genus, cubic invariants and full cotangent pullbacks are [MATH] with the stated smooth-fiber hypotheses. Their one-form normalization is geometric and has not been calibrated to the book's physical charge lattice. Equality of j is not a full-QFT equivalence criterion.

Section 3.5. The two-chart limit, node coefficients, period reduction, nome coefficients through fifth order, and the three flavor branchings are [MATH]. The numerical period/theta comparisons are finite samples, not a global analytic continuation prescription. The elliptic theta uniformization is anchored to Seiberg and Witten (1994,

arXiv v1, eqs. (16.11)–(16.13), p. 58), with the nome and theta notation defined explicitly here. The three-channel and triality interpretation is a sourced nonperturbative statement with compatible protected and representation checks, [CONJ+], from Gaiotto (2012, arXiv v1, §2.1, pp. 4–5) and Seiberg and Witten (1994, arXiv v1, eq. (10.4), printed p. 36). No proof of full duality, massive-family extension or global line-lattice equivalence follows. Gaiotto p. 15 explicitly distinguishes the spectral modulus from a conventional UV coupling.

References

Gaiotto, D. (2012). "N=2 dualities". In: *JHEP* 08, p. 034. DOI: 10.1007/JHEP08(2012)034. arXiv: 0904.2715 [hep-th].

Seiberg, N. and E. Witten (1994). "Monopoles, duality and chiral symmetry breaking in N=2 supersymmetric QCD". In: *Nucl. Phys. B* 431, pp. 484–550. DOI: 10.1016/0550-3213(94)90214-3. arXiv: hep-th/9408099.

Chapter XVI.4

Hitchin systems and Seiberg–Witten geometry

A vacuum of a four-dimensional $\mathcal{N} = 2$ theory can be described by an abelian low-energy gauge theory even when its microscopic construction is strongly coupled. In the class-S construction, the coefficients of that abelian theory are encoded by a differential on a covering surface. Chapter 3 exhibited its simplest example, a double cover of a four-punctured sphere. We now derive how the twisted gauge fields produce the cover, which of its coefficients can vary in a fixed theory, and how to integrate the differential.

The central distinction is between a puncture and a vacuum. A puncture fixes a boundary condition, including mass parameters. A Coulomb-branch displacement changes the vacuum while keeping those boundary conditions fixed. The differential responds differently to these two operations. Its mass residues stay constant along a Coulomb direction, and its derivative becomes a holomorphic one-form on the smooth spectral cover. That fact is what makes period coordinates useful.

We assume the circle reduction and twist of Chapters 1–2, elementary matrix invariants, and contour integration. We first derive the local Hitchin equations from reduced self-duality. We then compute their characteristic coefficients, impose fixed residues in both A_1 and A_2 examples, and evaluate actual cycles of the A_1 differential. A final comparison separates a weak-coupling degeneration of the punctured sphere from a nodal degeneration at fixed masses. The physical identification of the circle-reduced vacuum system with Hitchin geometry is an input from the class-S construction. The explicit work here determines spectral equations and their periods within that identification.

XVI.4.1 The BPS equations after the twist

The twist in Chapter 2 tells us that a complex adjoint scalar becomes a one-form on the compactification surface C. It does not by itself say which configurations are vacua. For that we need the BPS equations. Their local form can be understood through the

dimensional reduction of four-dimensional self-duality, a calculation that also fixes the relative signs in the real and complex equations.

Start with an anti-Hermitian connection on local Euclidean coordinates $x^1, \dots, x^4$, oriented by $dx^1 \wedge dx^2 \wedge dx^3 \wedge dx^4$. Assume translation invariance in x^3, x^4. The corresponding connection components become adjoint scalar fields.

$$B_3 = A_3, \qquad B_4 = A_4, \qquad \partial_3 = \partial_4 = 0, \qquad B_i^\dagger = -B_i. \tag{XVI.4.1}$$

The curvature contains both covariant derivatives and scalar commutators. In particular,

$$F_{34} = [B_3, B_4], \quad F_{13} = D_1 B_3, \quad F_{24} = D_2 B_4, \quad F_{14} = D_1 B_4, \quad F_{23} = D_2 B_3. \tag{XVI.4.2}$$

Self-duality $F = *F$ therefore reduces to three equations on the remaining surface.

$$F_{12} = [B_3, B_4], \qquad D_1 B_3 = -D_2 B_4, \qquad D_1 B_4 = D_2 B_3. \tag{XVI.4.3}$$

The minus sign in the middle equation follows from $*(dx^1 \wedge dx^3) = -dx^2 \wedge dx^4$. It will be essential for holomorphy.

Let $z = x^1 + i x^2$ and package the two scalars into the coefficient of a $(1,0)$-form.

$$D_{\bar z} = \frac{1}{2}(D_1 + i D_2), \qquad \Psi = \psi\, dz, \qquad \psi = \frac{1}{2}(B_3 - i B_4), \qquad \psi^\dagger = \frac{1}{2}(-B_3 - i B_4). \tag{XVI.4.4}$$

The dagger conjugates both the matrix and the form, so $\Psi^\dagger = \psi^\dagger d\bar z$. Expanding the complex equation before using self-duality gives

$$D_{\bar z}\psi = \frac{1}{4}\big(D_1 B_3 + D_2 B_4 + i D_2 B_3 - i D_1 B_4\big) = 0. \tag{XVI.4.5}$$

Both real combinations vanish separately by (XVI.4.3). Thus the holomorphic structure comes from the BPS equation as well as the bundle type selected by the twist.

To convert the remaining equation, use the orientation and the anti-Hermitian convention.

$$dz \wedge d\bar z = -2i\, dx^1 \wedge dx^2, \qquad F_{z\bar z} = \frac{i}{2} F_{12}, \qquad [\psi, \psi^\dagger] = -\frac{i}{2}[B_3, B_4]. \tag{XVI.4.6}$$

The two coefficients cancel. In the circle-reduced physical system a positive radius R multiplies the Higgs field. Writing $\Psi = R\Phi$, the equations take the form

$$F_A + R^2[\Phi, \Phi^\dagger] = 0, \qquad \bar\partial_A \Phi = 0, \qquad \Phi = \phi\, dz. \tag{XVI.4.7}$$

Here $[\Phi, \Phi^\dagger] = (\phi\phi^\dagger - \phi^\dagger\phi) dz \wedge d\bar z$. The first equation is often called the real or moment-map equation. The second is the complex equation. The sourced circle/BPS identification supplies their physical role; the reduction above explains their local algebra Hitchin 1987; Gaiotto et al. 2013.

Why retain both equations? Take a constant upper triangular matrix in a local trivialization, with the flat connection and Hermitian metric.

$$A = 0, \qquad \phi = N = \begin{pmatrix} 0 & 1 \\ 0 & 0 \end{pmatrix}, \qquad \bar\partial \phi = 0, \qquad [N, N^\dagger] = \begin{pmatrix} 1 & 0 \\ 0 & -1 \end{pmatrix}. \tag{XVI.4.8}$$

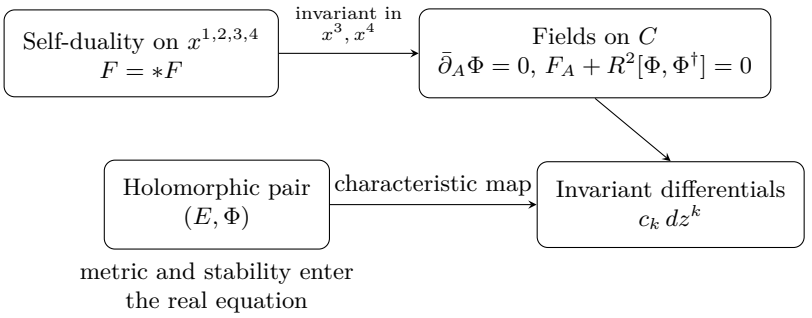


Figure XVI.4.1: Reduced self-duality gives a complex equation and a real equation on C. The characteristic map retains invariant differentials from the holomorphic pair. Recovering a real solution also requires a Hermitian metric and appropriate global and boundary conditions. The arrows indicate the operations used in this chapter, rather than inverse maps established by the polynomial calculation.

This is holomorphic, but it fails the real equation for every $R > 0$ in that metric. The example concerns a chosen representative and metric. It does not settle a global existence problem after changing the metric and imposing boundary conditions.

By contrast, a constant diagonal coefficient in the same local problem solves both equations.

$$\phi = \begin{pmatrix} a & 0 \\ 0 & -a \end{pmatrix}, \qquad [\phi, \phi^\dagger] = 0, \qquad F_A = 0. \tag{XVI.4.9}$$

Changing a changes the eigenvalue differential. Changing R at fixed Φ changes the coefficient of the real equation. Algebraically the substitution $\Psi = R\Phi$ removes the explicit R^2 because

$$[R\Phi, (R\Phi)^\dagger] = R^2[\Phi, \Phi^\dagger], \qquad \lambda_\Psi = R\lambda_\Phi, \qquad \oint \lambda_\Psi = R \oint \lambda_\Phi. \tag{XVI.4.10}$$

It also rescales the periods. It is therefore a change of field coordinates, not a reason to erase the compactification radius from the real metric of the vacuum space.

There is a global mathematical issue behind this local distinction. The connection defines a holomorphic bundle E through its $(0,1)$ part, and the complex equation says that Φ is a holomorphic section of $\mathrm{End}_0(E) \otimes K_C$ away from the punctures. Complex gauge transformations act on this pair. The real equation concerns a unitary representative and its Hermitian metric. Stability conditions control whether a suitable representative exists.

For example, Hitchin's compact rank-two result on a compact surface of genus greater than one relates stability, with its determinant and degree hypotheses, to solutions of these equations. Its hypotheses do not include the punctured sphere used below. A punctured problem requires prescribed singular behavior and further real boundary information; generic higher rank is another extension. We use the punctured class-S/Hitchin correspondence as the physical construction described in Gaiotto et al.

2013, rather than deducing that analytic correspondence from our matrices. The next operation needs only the holomorphic pair, so we can proceed while keeping the real problem distinct.

XVI.4.2 From a Higgs field to its spectral cover

The low-energy differential is obtained by following an eigenvalue of the Higgs field. Eigenvalues are multivalued on C because they exchange around branch points. The surface on which an eigenvalue becomes single-valued is the spectral cover. We will construct its equation and determine exactly which information the characteristic polynomial retains.

In a coordinate z, write an eigenvalue as $x = x_z$. The tautological one-form on the cotangent bundle and the characteristic polynomial are

$$\lambda = x_z\,dz, \qquad \det(x_z I - \phi) = x_z^N + \sum_{k=2}^{N} c_k(z) x_z^{N-k} = 0. \tag{XVI.4.11}$$

We impose $\operatorname{Tr}\phi = 0$. Under a coordinate change $w = w(z)$, the one-form is invariant, so

$$\phi_w = \phi_z \frac{dz}{dw}, \qquad x_w = x_z \frac{dz}{dw}, \qquad c_{k,w} = c_{k,z}\left(\frac{dz}{dw}\right)^k. \tag{XVI.4.12}$$

Consequently $c_k(z)dz^k$ is a meromorphic k-differential. A coefficient is not an ordinary scalar function globally. This is the cotangent transformation law already encountered in Chapter 3.

To calculate the first coefficients, denote the eigenvalues by r_i and their power sums by $p_j = \sum_i r_i^j = \operatorname{Tr}\phi^j$. The first elementary symmetric sums satisfy

$$e_1 = p_1 = 0, \qquad 2e_2 = e_1p_1 - p_2 = -p_2, \qquad 3e_3 = e_2p_1 - e_1p_2 + p_3 = p_3. \tag{XVI.4.13}$$

Since the characteristic polynomial has coefficients $(-1)^k e_k$, we obtain

$$c_2 = -\frac{1}{2}\operatorname{Tr}\phi^2, \qquad c_3 = -\frac{1}{3}\operatorname{Tr}\phi^3. \tag{XVI.4.14}$$

These polynomial identities hold even when the matrix is not diagonalizable. Diagonalization motivates them, while the identity on unrestricted matrices extends them through eigenvalue collisions.

For rank two, this can be checked without eigenvalues. Put

$$\phi = \begin{pmatrix} a & b \\ c & -a \end{pmatrix}, \qquad \det(xI-\phi) = (x-a)(x+a) - bc = x^2 - a^2 - bc, \qquad \frac{1}{2}\operatorname{Tr}\phi^2 = a^2 + bc. \tag{XVI.4.15}$$

We keep the positive quadratic differential of Chapter 3 by defining $\varphi_2 = -c_2\,dz^2$. The rank-two curve is therefore $\lambda^2 = \varphi_2$, rather than $\lambda^2 = c_2 dz^2$. A branch point occurs at a simple zero of φ_2.

Rank three brings a second independent invariant. For the unrestricted traceless matrix

$$\phi = \begin{pmatrix} a & b & c \\ d & e & f \\ g & h & -a-e \end{pmatrix}, \qquad \frac{1}{2}\operatorname{Tr}\phi^2 = a^2 + ae + e^2 + bd + cg + fh, \tag{XVI.4.16}$$

expanding the determinant gives

$$\det\phi = -ae(a+e) - afh + bd(a+e) + bfg + cdh - ceg, \qquad \frac{1}{3}\operatorname{Tr}\phi^3 = \det\phi. \tag{XVI.4.17}$$

Thus $\varphi_3 = -c_3 dz^3$ and the coordinate form of the spectral equation is

$$x^3 - \varphi_{2,z}x - \varphi_{3,z} = 0, \qquad \lambda^3 - \varphi_2\lambda - \varphi_3 = 0. \tag{XVI.4.18}$$

The products in the second equation all have type K_C^3. The sign convention matters for both the branch locus and residue eigenvalues.

We can locate a repeated eigenvalue directly. If r is a double root of $f(x) = x^3 - \varphi_{2,z}x - \varphi_{3,z}$, then $f(r) = f'(r) = 0$. These equations give

$$\varphi_{2,z} = 3r^2, \qquad \varphi_{3,z} = -2r^3, \qquad 4\varphi_{2,z}^3 - 27\varphi_{3,z}^2 = 0. \tag{XVI.4.19}$$

Eliminating r, or taking the resultant of f and f', yields the discriminant

$$\Delta = \prod_{i<j}(r_i - r_j)^2 = -4c_2^3 - 27c_3^2 = 4\varphi_{2,z}^3 - 27\varphi_{3,z}^2. \tag{XVI.4.20}$$

For distinct eigenvalues $1, 2, -3$, we have $\varphi_{2,z} = 7$, $\varphi_{3,z} = -6$ and $\Delta = 400$. The same answer follows from the squared gaps $1, 16, 25$. If instead the eigenvalues are $r, r, -2r$, the two terms in the discriminant cancel. At a generic simple zero of Δ on C, two sheets exchange while the third remains separate. When both invariants vanish, the local geometry needs a separate analysis.

The invariant differentials specify a point in the Hitchin base. They do not specify the full holomorphic pair. Already at one point there is a loss of information.

$$\det(xI - 0) = x^2 = \det(xI - N), \qquad \operatorname{rank}(0) = 0, \qquad \operatorname{rank}(N) = 1. \tag{XVI.4.21}$$

Zero and the nonzero nilpotent matrix are not conjugate. On a smooth spectral cover one also needs eigenline information, appropriate determinant conditions, and global gluing to reconstruct a Higgs pair. At singular fibers this is expressed using spectral sheaves. The real equation and metric add the analytic problem discussed in the previous section. Our next calculation determines the allowed invariant differentials before those additional steps.

XVI.4.3 Masses stay fixed while Coulomb parameters vary

A regular puncture permits a simple pole in the Higgs field. Its residue eigenvalues give mass parameters in the class-S dictionary. Varying those eigenvalues changes the

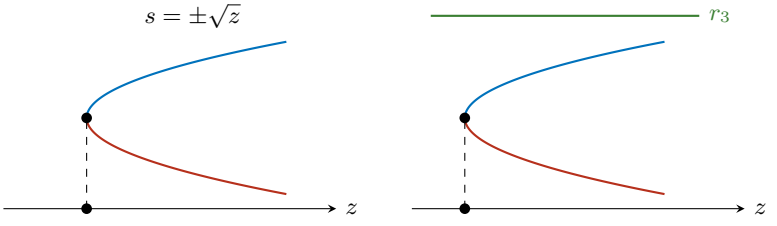


Figure XVI.4.2: Local sheet exchange. On the left, a simple zero of the quadratic differential interchanges the two A_1 eigenvalues. On the right, a generic discriminant zero of the cubic exchanges two A_2 eigenvalues and leaves a third sheet separate. The drawings concern local projection maps to C and do not specify a global spectral line bundle.

boundary problem. To vary the vacuum of a fixed theory, we must instead vary the spectral equation while preserving its leading pole coefficients. We will solve these constraints explicitly, including the puncture at infinity.

For A_1, take $C = \mathbb{P}^1$ with marked points $0, 1, q, \infty$, where $q \neq 0, 1$. The quadratic differential and its square root can be written

$$D(z) = z(z-1)(z-q), \qquad \varphi_2 = \frac{P_4(z)}{D(z)^2}dz^2, \qquad \lambda = \frac{\sqrt{P_4(z)}}{D(z)}dz, \qquad \deg P_4 \leq 4. \tag{XVI.4.22}$$

The degree bound follows from the allowed double pole at infinity. Near a finite puncture p, $D(z) = D'(p)(z-p) + O((z-p)^2)$, so

$$\lambda = \frac{\sqrt{P_4(p)}}{D'(p)}\frac{dz}{z-p} + O(dz), \qquad m_p^2 = \frac{P_4(p)}{D'(p)^2}. \tag{XVI.4.23}$$

The two sheets have opposite residues. Fixing m_p^2 fixes their unordered pair; a local choice of mass sign selects a mass sheet.

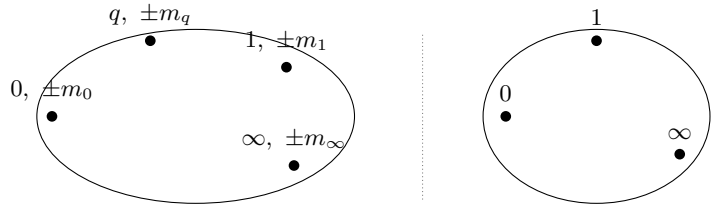
At infinity use $w = 1/z$. If a_4 is the coefficient of z^4, then $\sqrt{P_4}/D \sim \sqrt{a_4}/z$. The differential transforms as

$$\lambda \sim \sqrt{a_4}\frac{dz}{z} = -\sqrt{a_4}\frac{dw}{w}, \qquad m_\infty^2 = a_4. \tag{XVI.4.24}$$

The minus sign affects an unsquared residue, while its square gives the fourth independent constraint. Omitting infinity would retain a deformation that changes a mass.

Write $v_p = m_p^2 D'(p)^2$ for $p = 0, 1, q$. A particular solution is obtained by first fixing $a_4 = m_\infty^2$ and interpolating the remaining three values with a quadratic polynomial.

$$L_p(z) = \prod_{\substack{s\in\{0,1,q\}\\ s\neq p}} \frac{z-s}{p-s}, \qquad P_*(z) = m_\infty^2 z^4 + \sum_{p\in\{0,1,q\}} (v_p - m_\infty^2 p^4) L_p(z). \tag{XVI.4.25}$$



$\delta P_4 = \delta u D$ at fixed q, m_p $\qquad$ A_2 full trinion, $\delta P_3 = vz(z-1)$

Figure XVI.4.3: The four-punctured A_1 base carries the complex-structure parameter q and four residue pairs $\pm m_p$. A displacement δu changes the quartic by $\delta u D$ and leaves these boundary residues fixed. The three-punctured A_2 example has no complex-structure modulus but retains one cubic invariant after its three full residue conditions are fixed.

Each L_p is one at its own puncture and zero at the other two. Its degree is two, so it cannot change the leading coefficient. The general solution differs from P_* by a polynomial of degree at most three vanishing at all three finite punctures. It must therefore be divisible by D.

$$P_4 = P_* + uD, \qquad \delta P_4\big|_{q,m_p} = \delta u\, D, \qquad \partial_u \lambda = \frac{dz}{2\sqrt{P_4}}. \tag{XVI.4.26}$$

There is exactly one such direction, not just at most one. The five quartic coefficients obey four independent linear constraints, and D is their nonzero common kernel. The parameter u is a Coulomb coordinate; its additive origin depends on the chosen particular solution.

For a numerical algebraic example, choose $q = 2$ and the family

$$P_t = (z-3)^2(z-4)(z-5)+t\,z(z-1)(z-2) = z^4+(t-15)z^3+(83-3t)z^2+(2t-201)z+180. \tag{XVI.4.27}$$

Using $D'(0) = 2$, $D'(1) = -1$, $D'(2) = 2$ gives

$$\begin{aligned} P_t(0) = 180, \quad P_t(1) = 48, \quad P_t(2) = 6, \quad a_4 = 1, \\ (m_0^2, m_1^2, m_2^2, m_\infty^2) = (45, 48, 3/2, 1). \end{aligned} \tag{XVI.4.28}$$

All four masses remain fixed as t changes. Conversely, a general quartic with these residues has $a_0 = 180$, $a_4 = 1$, $a_1 + a_2 + a_3 = -133$, and $2a_1 + 4a_2 + 8a_3 = -190$. Solving leaves the tangent $(\delta a_1, \delta a_2, \delta a_3) = (2, -3, 1)\delta t$, precisely $\delta t D$. We have set a reference mass unit to one; restoring it multiplies the first term in P_t by that unit squared. Both t and u have mass dimension two, while z, q are dimensionless.

Now change the rank and number of punctures. Consider A_2 on a sphere with three full regular punctures at $0, 1, \infty$. The full-puncture assignment, including generic traceless semisimple residue matrices before taking a massless limit, is physical source input Gaiotto 2012. Given it, the coefficient count is elementary. For $k = 2, 3$, write

$$c_k\, dz^k = \frac{P_k(z)}{z^k(z-1)^k} dz^k, \qquad \deg P_k \le k. \tag{XVI.4.29}$$

The leading coefficients at the three punctures are $(-1)^k P_k(0)$, $P_k(1)$ and $(-1)^k \operatorname{lc}(P_k)$, respectively. The first sign comes from $(z-1)^{-k}$ near zero; the last comes from $dz^k = (-1)^k w^{-2k} dw^k$. Fixing them forces a homogeneous variation to satisfy

$$\delta P_k(0) = \delta P_k(1) = 0, \qquad [z^k]\delta P_k = 0, \qquad \dim\{\delta P_k\} = (k+1)-3 = k-2. \tag{XVI.4.30}$$

For $k = 2$, these conditions kill every coefficient. For $k = 3$, they leave $\delta P_3 = vz(z-1)$. The trinion has no gauge-tube complex modulus, but its fixed-mass spectral base has a cubic Coulomb direction. These are different types of parameter.

At zero masses, choose $v = -u_3$ to agree with $\varphi_3 = -c_3 dz^3$. Then

$$\varphi_2 = 0, \qquad \lambda^3 = \frac{u_3}{z^2(z-1)^2} dz^3, \qquad [u_3] = 3. \tag{XVI.4.31}$$

For $u_3 \neq 0$ its normalized spectral cover is a cyclic triple cover of genus one. To see this, temporarily use the coefficient $x^3 = u_3/[z^2(z-1)^2]$. Its rational right side has orders $-2, -2, 4$ at $0, 1, \infty$. Each is coprime to three, so each point has one preimage with ramification index three. The total ramification is six, and Riemann–Hurwitz gives

$$2g_\Sigma - 2 = 3(2g_C - 2) + \sum_P (e_P - 1) = -6 + 3 \cdot 2 = 0, \qquad g_\Sigma = 1. \tag{XVI.4.32}$$

Infinity contributes even though the rational coefficient has a zero there. In the cotangent chart $w = 1/z$, the cubic differential is $-u_3 dw^3/[w^2(1-w)^2]$, with a second-order pole. Changing trivialization changes that integer order by six and preserves its residue modulo three, hence preserves ramification. At $u_3 = 0$ the cover degenerates, so this smooth-genus calculation no longer applies. The example transfers the fixed-boundary method to higher rank without supplying a general classification of punctures, which is the subject of Chapter 5.

XVI.4.4 The differential and its actual periods

The spectral equation becomes a low-energy geometry through integrals of λ. Before computing them, we should establish why changing a Coulomb parameter produces the right kind of differential. In the massive quartic family, hold q and the mass eigenvalues fixed and transport cycles continuously in a smooth region of the parameter space. Equation (XVI.4.26) gives

$$\omega_u = \partial_u \lambda = \frac{dz}{2\sqrt{P_4(z)}}, \qquad \partial_u \oint_{\gamma(u)} \lambda = \oint_{\gamma(u)} \omega_u. \tag{XVI.4.33}$$

The derivative uses locally transported homology cycles, rather than a fixed contour that is allowed to cross a moving branch point. Exact changes associated with a local choice of trivialization do not change a closed-cycle integral.

This derivative is holomorphic on the smooth compact genus-one double cover. At a simple zero b of P_4, use $z = b + s^2$ and $P_4 = s^2 H(s^2)$, with $H(0) \neq 0$. Then

$$\omega_u = \frac{2s\, ds}{2s\sqrt{H(s^2)}} = \frac{ds}{\sqrt{H(s^2)}}. \tag{XVI.4.34}$$

The apparent singularity in the z chart is removed by the cover coordinate. At a finite puncture with nonzero mass, $P_4(p) \neq 0$, so ω_u is regular directly. At infinity, for nonzero leading coefficient,

$$w = 1/z, \qquad \widetilde{P}(w) = w^4 P_4(1/w), \qquad \omega_u = -\frac{dw}{2\sqrt{\widetilde{P}(w)}}, \qquad \widetilde{P}(0) = m_\infty^2 \neq 0. \tag{XVI.4.35}$$

The original λ has mass poles, but its fixed-mass derivative has lost their principal parts. Smooth limits with zero masses can be studied on the normalized cover, as in the massless example below.

A mass variation behaves differently. On a chosen mass sheet near a puncture,

$$\lambda = \pm m_p \frac{dz}{z-p} + O(dz), \qquad \partial_{m_p}\lambda = \pm \frac{dz}{z-p} + O(dz). \tag{XVI.4.36}$$

It has simple poles on the two preimages with opposite residues. Such a variation gives a third-kind differential rather than a holomorphic differential. Holding the boundary condition fixed is therefore an analytic requirement for the Coulomb-period calculation, not just a parameter-counting convention.

For actual integrals, return to Chapter 3's massless A_1 family in the real chart $0 < q < 1$, $u > 0$.

$$P_4 = uD, \qquad y^2 = z(z-1)(z-q), \qquad \lambda = \sqrt{u}\,\frac{dz}{y}. \tag{XVI.4.37}$$

The four branch points of the normalization are $0, q, 1, \infty$. Choose the A cycle by going from 0 to q on the sheet with $y > 0$ and returning on the opposite sheet. The reversal of path and sign of y cancel, so both halves contribute equally.

$$a_{\text{geom}} = \oint_A \lambda = 2\sqrt{u} \int_0^q \frac{dz}{\sqrt{z(q-z)(1-z)}}. \tag{XVI.4.38}$$

A path between branch points on one sheet alone is not closed. Omitting the return would lose a factor two.

The substitution $z = q\sin^2\theta$, $0 \leq \theta \leq \pi/2$, removes the endpoint square roots. Its numerator and denominator are

$$dz = 2q\sin\theta\cos\theta\,d\theta, \qquad y = q\sin\theta\cos\theta\sqrt{1 - q\sin^2\theta}, \qquad \frac{dz}{y} = \frac{2d\theta}{\sqrt{1 - q\sin^2\theta}}. \tag{XVI.4.39}$$

Define the complete elliptic integral with parameter m, not modulus $\sqrt{m}$, by

$$K(m) = \int_0^{\pi/2} \frac{d\theta}{\sqrt{1 - m\sin^2\theta}}, \qquad a_{\text{geom}} = 4\sqrt{u}\,K(q). \tag{XVI.4.40}$$

This convention is needed to compare either numerical values or weak-limit expansions.

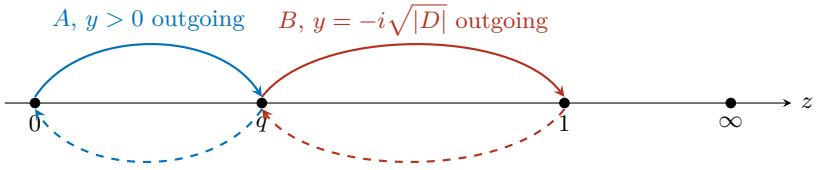


Figure XVI.4.4: Outgoing paths for the declared A and B cycles over the real z axis. Each path is completed by a return on the opposite sheet. The A outgoing sheet has $y > 0$ on $(0, q)$; the B outgoing sheet has $y = -i\sqrt{z(1-z)(z-q)}$ on $(q, 1)$. These choices give a real positive A period and an imaginary positive B period.

Choose B to go from q to 1 on the sheet $y = -i\sqrt{z(1-z)(z-q)}$, then return on the opposite sheet. We choose the intersection convention compatible with a positive imaginary period ratio. This gives

$$a_{D,\mathrm{geom}} = 2i\sqrt{u}\int_q^1 \frac{dz}{\sqrt{z(1-z)(z-q)}}. \tag{XVI.4.41}$$

For the endpoint-regularizing substitution set $h = 1 - (1-q)\sin^2\theta$ and $z = q/h$. Then

$$\begin{aligned} dz &= \frac{2q(1-q)\sin\theta\cos\theta}{h^2}d\theta, \\ \sqrt{z(1-z)(z-q)} &= \frac{q(1-q)\sin\theta\cos\theta}{h^{3/2}}, \\ \frac{dz}{\sqrt{z(1-z)(z-q)}} &= \frac{2d\theta}{\sqrt{h}}. \end{aligned} \tag{XVI.4.42}$$

It follows that

$$a_{D,\mathrm{geom}} = 4i\sqrt{u}\,K(1-q), \qquad \tau_{\mathrm{geom}} = \frac{\partial_u a_{D,\mathrm{geom}}}{\partial_u a_{\mathrm{geom}}} = i\frac{K(1-q)}{K(q)}, \qquad \operatorname{Im}\tau_{\mathrm{geom}} > 0. \tag{XVI.4.43}$$

Here the ratio of periods equals the ratio of their derivatives because both periods are proportional to $\sqrt{u}$. That equality is special to this massless family. The derivative ratio is the relevant expression in the more general family.

For a concrete check, take $u = 9/4$. At the symmetric value $q = 1/2$, the two integrals coincide in magnitude.

$$\begin{aligned} K(1/2) &\simeq 1.8540746773, \qquad \tau_{\mathrm{geom}} = i, \\ a_{\mathrm{geom}} &\simeq 11.1244480638, \qquad a_{D,\mathrm{geom}} \simeq 11.1244480638i. \end{aligned} \tag{XVI.4.44}$$

At the same u but $q = 1/8$, the actual integrals give $a_{\mathrm{geom}} \simeq 9.7420001557$ and $a_{D,\mathrm{geom}} \simeq 14.8415770425i$, hence $\tau_{\mathrm{geom}} \simeq 1.5234630266i$. The changed complex structure changes

the ratio. At fixed q, changing u from $9/4$ to 9 doubles both periods and leaves the ratio fixed. Their derivatives are

$$\partial_u a_{\mathrm{geom}} = \frac{2K(q)}{\sqrt{u}}, \qquad \partial_u a_{D,\mathrm{geom}} = \frac{2iK(1-q)}{\sqrt{u}}. \tag{XVI.4.45}$$

Thus $\partial_u a_{\mathrm{geom}} \simeq 2.4720995697$ at $q = 1/2, u = 9/4$.

The physical Seiberg–Witten identification uses a common normalization of the differential. In the conventions inherited here, it remains a fixed nonzero constant.

$$a_{\mathrm{phys}} = c_{\mathrm{SW}} a_{\mathrm{geom}}, \qquad a_{D,\mathrm{phys}} = c_{\mathrm{SW}} a_{D,\mathrm{geom}}, \qquad \frac{\partial_u a_{D,\mathrm{phys}}}{\partial_u a_{\mathrm{phys}}} = \tau_{\mathrm{geom}}. \tag{XVI.4.46}$$

The common constant cancels in the ratio, but matters for an absolute physical mass. It is not fixed by the polynomial or contour calculations. Neither is an integral physical charge lattice specified by calling the two geometric cycles A, B. These are distinct physical choices. As Chapter 3 emphasized, the cross-ratio q, the elliptic nome $e^{\pi i \tau_{\mathrm{geom}}}$, and a microscopic instanton coordinate also remain distinct.

XVI.4.5 A node and a weak-coupling cusp are different limits

A cycle can shrink in a family of surfaces without its chosen differential having a vanishing integral. The differential can become singular at the same time. We now compare two explicit paths through parameters. The first changes the ultraviolet punctured sphere at fixed u; the second changes a Coulomb coordinate at fixed punctures and masses. The period calculation identifies the difference.

For the massless family, take $q \to 0^+$ with $u > 0$ fixed. Expanding the integrand of $K(q)$ by the binomial series and integrating gives

$$K(q) = \frac{\pi}{2}\left(1 + \frac{q}{4} + \frac{9q^2}{64} + O(q^3)\right), \qquad a_{\mathrm{geom}} = 2\pi\sqrt{u}\left(1 + \frac{q}{4} + O(q^2)\right). \tag{XVI.4.47}$$

The coefficients use $\int_0^{\pi/2} \sin^2\theta\, d\theta = \pi/4$ and $\int_0^{\pi/2} \sin^4\theta\, d\theta = 3\pi/16$. The cycle over $[0, q]$ becomes small in the base, but its period tends to $2\pi\sqrt{u}$.

The complementary integral has a logarithm from its endpoint near $\theta = \pi/2$. Put $s = \pi/2 - \theta$ so the local denominator is $\sqrt{s^2 + q}$. The constant in the logarithm matters for comparison with the nome. To find it, set $v = \tan\theta$ in the whole integral and split it at T, with $1 \ll T \ll q^{-1/2}$. In the first region we can set $q = 0$ to leading order. In the second region $\sqrt{1+v^2}$ can be replaced by v. Rescaling the second region by $s = \sqrt{q}\, v$ gives

$$\begin{aligned} K(1-q) &= \int_0^\infty \frac{dv}{\sqrt{(1+v^2)(1+qv^2)}}, \\ \int_0^T \frac{dv}{\sqrt{1+v^2}} &= \operatorname{arsinh} T \sim \log(2T), \\ \int_{\sqrt{q}T}^\infty \frac{ds}{s\sqrt{1+s^2}} &= \log\frac{1+\sqrt{1+qT^2}}{\sqrt{q}T} \sim \log\frac{2}{\sqrt{q}T}. \end{aligned} \tag{XVI.4.48}$$

The T dependence cancels, leaving $\log(4/\sqrt{q})$. Choosing, for example, $T = q^{-1/4}$ makes both neglected regions small in the limit. Retaining the next terms in the matched expansion gives, with $L = \log(4/\sqrt{q})$,

$$K(1-q) = L + \frac{q}{4}(L-1) + O(q^2 \log(1/q)), \qquad a_{D,\mathrm{geom}} = 2i\sqrt{u}\log(16/q) + O(q\log(1/q)). \tag{XVI.4.49}$$

The logarithm can also be checked against the exact contour substitution in the preceding section. Its coefficient gives

$$\tau_{\mathrm{geom}} \sim \frac{i}{\pi}\log(16/q), \qquad a_{\mathrm{geom}} \longrightarrow 2\pi\sqrt{u} \neq 0. \tag{XVI.4.50}$$

This is the weak-coupling cusp of the ultraviolet surface discussed in Chapter 3, rather than a zero of the A period at fixed u.

To see the finite period locally, use the inner chart $z = q\xi$. Before taking the limit, the differential becomes

$$\lambda = \sqrt{u}\frac{d\xi}{\sqrt{\xi(\xi-1)(q\xi-1)}} \;\longrightarrow\; \sqrt{u}\frac{d\xi}{\sqrt{\xi(1-\xi)}}. \tag{XVI.4.51}$$

Its integral along $0 < \xi < 1$ and back is $2\pi\sqrt{u}$. In the outer chart at $q = 0$ one instead finds $\lambda = \sqrt{u}\,dz/[z\sqrt{z-1}]$. A simple pole develops at the limiting node. The two-chart description explains why a small geometric neck need not give a small period of this differential.

Now keep the base points fixed at $0, 1, 2, \infty$ and use P_t from (XVI.4.27). At $t = 0$, two zeros of the numerator coincide at $z = 3$, away from every puncture. With $Y^2 = P_t(z)$ and $w = z - 3$, the local equation is

$$Y^2 = w^2(2 - 3w + w^2) + tD(3 + w), \qquad D(3) = 6. \tag{XVI.4.52}$$

The quadratic part at $t = 0$ is $Y^2 - 2w^2$, a product of two distinct linear factors. This is an ordinary node. For small nonzero t the nearby branch points satisfy $w^2 \simeq -3t$, so the cut between them collapses as $t \to 0$. All mass residues remain those of (XVI.4.28).

The polynomial discriminant gives an independent measure of this singular fiber. Compute the resultant of P_t and its z derivative. Since P_t is monic of degree four, the resultant has the discriminant sign $(-1)^6 = 1$.

$$\operatorname{disc}_z P_t = t\big(4t^5 + 780t^4 - 58727t^3 + 930972t^2 - 128t - 192\big), \qquad \partial_t \operatorname{disc}_z P_t\big|_0 = -192. \tag{XVI.4.53}$$

The zero in t is simple, even though the two branch locations approach each other as $\sqrt{t}$. The discriminant measures their squared separation times nonzero gaps to the remaining roots. If the colliding roots are r_+, r_-, their leading squared gap is $-12t$. The other roots tend to $4, 5$, so the product of gaps also determines the linear coefficient without expanding a degree-six polynomial.

$$(r_+ - r_-)^2 \sim -12t, \qquad \operatorname{disc} P_t \sim (-12t)(3-4)^4(3-5)^4(4-5)^2 = -192t. \tag{XVI.4.54}$$

Choose the local analytic sheet at $t = 0$ by

$$\sqrt{P_0} = w\sqrt{2 - 3w + w^2}, \qquad \sqrt{2} > 0. \tag{XVI.4.55}$$

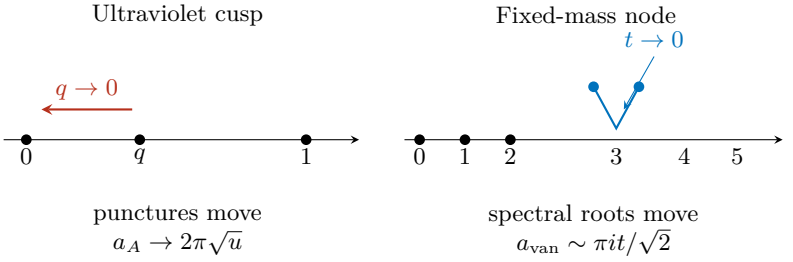


Figure XVI.4.5: Different parameter paths to a singular cover. Left, the ultraviolet punctures $0, q$ collide while u is fixed; the A period tends to $2\pi\sqrt{u}$. Right, with ultraviolet points $0, 1, 2, \infty$ fixed, two spectral roots collide near $z = 3$ as $t \to 0$; the cycle computed in the text has period $\pi i t/\sqrt{2} + O(t^2)$. The two moving points on the right are branch points, not new punctures.

Take a counterclockwise contour $|w| = 0.15$ on its continuation for sufficiently small t. It encloses the two nearby branch points and no puncture. It represents the cycle that collapses at the node. At $t = 0$ the differential itself is regular and vanishes at $w = 0$.

$$\lambda_0 = \frac{w\sqrt{2 - 3w + w^2}}{D(3 + w)}\,dw, \qquad \oint \lambda_0 = 0. \tag{XVI.4.56}$$

Its first variation is singular on the normalization of the nodal fiber. Differentiating at fixed masses gives

$$\partial_t \lambda_t|_0 = \frac{dw}{2w\sqrt{2 - 3w + w^2}}, \qquad \operatorname{Res}_{w=0} \partial_t \lambda_t|_0 = \frac{1}{2\sqrt{2}}. \tag{XVI.4.57}$$

The residue theorem now evaluates the leading period, including its sign and factor of two.

$$a_{\mathrm{van}}(t) = \oint \lambda_t = \frac{\pi i}{\sqrt{2}} t + O(t^2), \qquad a'_{\mathrm{van}}(0) = \frac{\pi i}{\sqrt{2}}. \tag{XVI.4.58}$$

The expansion is uniform on the fixed contour when t is sufficiently small, allowing differentiation under the integral. Reversing the contour or the sheet reverses its sign. The vanishing statement is unchanged.

For example, direct integration on that contour yields

$$\begin{aligned} \frac{a_{\mathrm{van}}(10^{-6})}{10^{-6}} &\simeq 2.2214271516i, \\ \frac{a_{\mathrm{van}}(10^{-8})}{10^{-8}} &\simeq 2.2214413259i, \qquad \frac{\pi i}{\sqrt{2}} \simeq 2.2214414691i. \end{aligned} \tag{XVI.4.59}$$

Reducing t by a factor one hundred reduces the leading slope error by approximately the same factor, as expected from an $O(t)$ correction to a_{van}/t.

The two limits teach complementary lessons. The cusp changes the ultraviolet complex structure and develops a pole in the limiting differential. The node lies on a

fixed-mass spectral family and has a differential whose collapsing-cycle period vanishes linearly. Neither conclusion alone determines a stable particle spectrum. To turn a vanishing geometric period into a physical central charge requires the Seiberg–Witten identification, the common normalization, and a physical charge assignment. Whether a BPS particle with that charge exists is a further stability question, taken up in Part B.

Take-home message

The Hitchin equations connect the twisted fields to a spectral cover through their characteristic invariants. Fixing puncture residues leaves the Coulomb directions, and varying along such a direction produces holomorphic differentials on a smooth cover. The A_1 example makes this sequence explicit from the quartic kernel to the two elliptic periods. The A_2 trinion changes the rank and coefficient count while retaining the same method. A period limit depends on both the path through parameters and the differential. The fixed-mass node has a vanishing period; the fixed-u ultraviolet cusp does not. A reader should now be able to distinguish a boundary mass, a Coulomb parameter, a complex-structure parameter, a spectral invariant and a full Higgs-bundle solution before studying general punctures in Chapter 5.

Exercises

1. Use the orientation and anti-Hermitian fields of Section XVI.4.1. Expand $D_{\bar z}\psi$ and $[\psi,\psi^\dagger]$ for $\psi=(B_3-iB_4)/2$. Determine the coefficients α,β in $F_{z\bar z}=\alpha F_{12}$ and $[\psi,\psi^\dagger]=\beta[B_3,B_4]$. For $N=\left(\begin{smallmatrix}0&2\\0&0\end{smallmatrix}\right)$ compute $[N,N^\dagger]$. Explain why holomorphy of this matrix does not solve the real equation in the flat metric, and what extra global question would remain after changing that metric.

2. For a rank-three Higgs coefficient with eigenvalues $1,2,-3$, compute $\operatorname{Tr}\phi^2$, $\operatorname{Tr}\phi^3$, c_2,c_3 and the discriminant. Recompute the discriminant as a product of squared eigenvalue gaps. Compare the zero rank-two matrix with a nonzero nilpotent matrix. State which information their common characteristic polynomial loses and which additional information a smooth spectral cover would need to recover a global Higgs pair.

3. Start with $P=\sum_{j=0}^{4}a_jz^j$ at $q=2$ and fix squared residues $(45,48,3/2,1)$. Derive the linear equations and the coefficients of the homogeneous tangent with its z^3 coefficient normalized to one. Compute the nullity if the infinity condition is dropped. Explain why the extra direction then changes the theory's boundary condition rather than adding a Coulomb modulus.

4. For the three-full-puncture A_2 sphere, compute the nullities of the fixed-leading-invariant constraints on P_2,P_3. For $u_3\neq0$ calculate the ramification contributions above $0,1,\infty$ in (XVI.4.31) and determine the genus. Explain why infinity contributes, why the full-puncture assignment is additional physical input, and why the answer cannot be extended to $u_3=0$ by the same smooth-cover argument.

5. Evaluate both closed-cycle periods at $q = 1/2, u = 9/4$ to eight significant figures, together with $\partial_u a_{\text{geom}}$ and $\operatorname{Im} \tau_{\text{geom}}$. Repeat the scaling argument when u increases to 9. Derive the two endpoint substitutions, explain the return-sheet factor, and show why one common nonzero c_{SW} cancels in the derivative ratio while leaving absolute periods unfixed.

6. For (XVI.4.27), determine the coefficients of $\operatorname{disc}_z P_t$ in ascending powers of t, its derivative at zero, and the imaginary coefficient of $a'_{\text{van}}(0)$ in the declared orientation. Compare the limiting A period at $q \to 0, u = 9/4$. Explain which parameters stay fixed along each path, why their period limits differ, and why a zero geometric period alone does not establish a stable BPS particle.

For benchmark submissions, see `benchmark/PROTOCOL.md`. Include the requested written derivations and explanations.

Sources and scope

Section 4.1. The reduced self-duality coefficients, nonnormal counterexample and radius rescaling are explicit calculations, [MATH]. The physical circle/BPS identification is [GEO-E], from Gaiotto et al. (2013, arXiv:0907.3987v2, §3.1.6, eqs. (51)–(54)). The local reduction is compared with Hitchin (1987, p. 64, eqs. (1.1)–(1.3)). The compact stability/existence discussion uses only its compact rank-two Theorem 4.3 on p. 80 with the original hypotheses. Its integrable-fibration comparison, Theorem 8.1 on p. 100, concerns rank two, odd degree, fixed determinant and simple-zero fibers. Neither theorem is promoted to a punctured higher-rank existence result. GMN's punctured boundary discussion remains a sourced physical/mathematical interface. The reduction uses anti-Hermitian gauge fields and the cotangent differential $\lambda = x\,dz$ of Chapters 2–3. The characteristic-coefficient and period conventions are specified in this chapter.

Section 4.2. The unrestricted rank-two and rank-three trace identities, discriminant elimination and loss of Jordan information are [MATH]. The characteristic-map construction is anchored to Gaiotto et al. (2013, arXiv v2, §4.2.2, eq. (166) and the following paragraph). The same source describes puncture boundary behavior in §4.1, eqs. (155)–(158). The sign convention retains $\varphi_2 = -c_2 dz^2$ from Chapter 3. Spectral-base coefficients, a holomorphic Higgs pair, and a real solution with metric are separate objects.

Section 4.3. Interpolation, the fixed-residue kernel and the A_2 coefficient nullities and ramification count are [MATH]. Mass/residue and full-puncture identifications are [GEO-E], using Gaiotto et al. (2013, arXiv v2, §4.2.2, eqs. (165)–(166)) and Gaiotto (2012, arXiv:0904.2715v1, pp. 33–35, eqs. (3.16), (3.21)–(3.25), full-residue paragraph p. 35). The latter's index typo in a counting formula is not used. The three full punctures are imposed explicitly. GMN's residue matrix $\rho/2$ is the matrix r with eigenvalues $\pm m$ here. No general puncture classification or stable punctured bundle is constructed.

Section 4.4. Holomorphy in local cover charts and the endpoint-substituted integrals are [MATH]. Numerical values test finitely many parameters. The physical period

interpretation is [GEO-E], using Gaiotto et al. (2013, arXiv v2, §3.1.5, eqs. (48)–(50), and §4.1). Its physical period normalization is not imported. The inherited geometric chart is $0 < q < 1, u > 0$ with the stated outgoing sheets and positive imaginary ratio. The common c_{SW} stays unspecified. No absolute physical period, global physical charge lattice or full hyperkähler metric is determined.

Section 4.5. The elliptic expansions, fixed-mass resultant, ordinary-node calculation and oriented residue slope are [MATH]. The node at $q = 2$ is a separate family from the real elliptic-period chart. The finite numerical contour samples support the explicitly derived slope, not a global continuation or particle-stability theorem. Characteristic coefficients and periods do not establish full QFT duality or a BPS spectrum. The physical inputs remain those cited above.

References

Gaiotto, D. (2012). "N=2 dualities". In: *JHEP* 08, p. 034. DOI: 10.1007/JHEP08(2012)034. arXiv: 0904.2715 [hep-th].

Gaiotto, D., G. W. Moore, and A. Neitzke (2013). "Wall-crossing, Hitchin Systems, and the WKB Approximation". In: *Advances in Mathematics* 234, pp. 239–403. DOI: 10.1016/j.aim.2012.09.027. arXiv: 0907.3987 [hep-th].

Hitchin, N. J. (1987). "The self-duality equations on a Riemann surface". In: *Proceedings of the London Mathematical Society* s3-55.1, pp. 59–126. DOI: 10.1112/plms/s3-55.1.59.

Chapter XVI.5

Regular punctures and partial closure

A puncture is part of the definition of a compactification. Its local boundary condition determines which singular differentials are allowed and which flavor symmetry a four-dimensional observer can couple to background fields. In the A_1 examples, all nontrivial regular punctures looked alike. Beginning with A_2, different boundary conditions give different matter sectors on the same three-punctured sphere. We need a way to calculate that difference.

The useful label is an embedding of $SU(2)$ in $SU(N)$. We will turn this label into matrices, calculate the poles of their invariant polynomials, and count the resulting parameters on a sphere. We will then change the puncture by a Higgs-branch expectation value. The same example will distinguish the matter that remains from the Goldstone modes released by the flow. Finally, sewing two examples will recover the screening calculation of an $SU(3)$ gauge theory with six full fundamental hypermultiplets.

The prerequisites are the twist and sewing operation of Chapters 2 and 3, $\mathcal{N} = 2$ multiplets from Volume I, and the Hermitian Nahm convention of Volume VII-A. We define the local spectral coefficients here, so the calculation does not require an implicit choice of characteristic-polynomial sign. Our central example has $N = 3$. The $N = 4$ examples change a feature that $N = 3$ alone cannot expose. The two partitions attached to a puncture need not coincide.

XVI.5.1 From a boundary condition to a partition

How can a boundary condition have a finite label? An embedding $\rho : SU(2) \to SU(N)$ makes the defining representation of $SU(N)$ a representation of $SU(2)$. Decompose it into irreducibles. Their dimensions sum to N.

$$\mathbb{C}^N = \bigoplus_{d\geq 1} V_d \otimes \mathbb{C}^{m_d}, \qquad \sum_d d m_d = N, \qquad \lambda_N = [d^{m_d}]_{d \text{ decreasing}}. \tag{XVI.5.1}$$

Here V_d is the d-dimensional irreducible representation and m_d its multiplicity. The subscript N means Nahm, rather than the integer N specifying the rank. A partition in this chapter is written as row lengths. These choices matter because a second partition will describe the Hitchin residue.

First construct the embedding explicitly. In the complexified algebra, use one block of dimension d with matrices

$$e_d = \sum_{i=1}^{d-1} E_{i,i+1}, \qquad f_d = \sum_{i=1}^{d-1} i(d-i) E_{i+1,i}, \qquad h_d = \operatorname{diag}(d-1, d-3, \ldots, 1-d). \tag{XVI.5.2}$$

E_{ij} has one unit entry in row i, column j. The difference of adjacent entries of h_d is two, so multiplying each nonzero entry of e_d gives

$$[h_d, e_d] = 2e_d, \qquad [h_d, f_d] = -2f_d, \qquad (e_d f_d - f_d e_d)_{ii} = d + 1 - 2i. \tag{XVI.5.3}$$

The last expression includes the end entries by setting the missing off-diagonal terms to zero. It is exactly the ith diagonal entry of h_d. Thus $[e_d, f_d] = h_d$. Taking direct sums constructs the triple (e_N, f_N, h_N) for the whole partition.

For $\lambda_N = [2,1]$, all matrices fit on one line.

$$e_N = \begin{pmatrix} 0 & 1 & 0 \\ 0 & 0 & 0 \\ 0 & 0 & 0 \end{pmatrix}, \qquad f_N = \begin{pmatrix} 0 & 0 & 0 \\ 1 & 0 & 0 \\ 0 & 0 & 0 \end{pmatrix}, \qquad h_N = \operatorname{diag}(1, -1, 0). \tag{XVI.5.4}$$

The doublet occupies the first two coordinates; the third is a singlet. For the other two partitions of three, $[1,1,1]_N$ gives the zero triple, while $[3]_N$ gives

$$e_N = E_{12} + E_{23}, \qquad f_N = 2E_{21} + 2E_{32}, \qquad h_N = \operatorname{diag}(2, 0, -2). \tag{XVI.5.5}$$

The nilpotency orders are respectively one, two and three, with the convention that the zero matrix has order one. They distinguish the three Jordan decompositions directly.

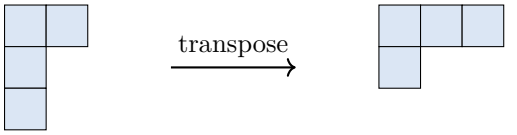
These complex matrices are convenient for polynomial calculations. They need not satisfy $f_N = e_N^\dagger$. To recover the compact embedding, start instead with Hermitian angular momentum matrices. On the d-dimensional block, their raising operator has entries $\sqrt{i(d-i)}$. A diagonal similarity transformation with diagonal entries s_i sends them to unit entries if

$$\frac{s_i}{s_{i+1}} \sqrt{i(d-i)} = 1, \qquad s_{i+1} = s_i \sqrt{i(d-i)}. \tag{XVI.5.6}$$

It simultaneously sends the lowering operator to f_d. This explains why the complex triple and the compact embedding describe the same representation while their displayed adjoint conventions differ.

The associated Hermitian Nahm pole uses $[J_i, J_j] = i\epsilon_{ijk} J_k$ and $X_i = J_i / s$. In a gauge with no connection along s, substitution checks the orientation.

$$\frac{dX_i}{ds} - \frac{i}{2} \epsilon_{ijk} [X_j, X_k] = -\frac{J_i}{s^2} + \frac{\epsilon_{ijk} \epsilon_{jk\ell} J_\ell}{2s^2} = 0. \tag{XVI.5.7}$$



$[2,1,1]_N$ $[3,1]_H$

Figure XVI.5.1: Row diagrams for the Nahm partition $[2,1,1]_N$ and its transpose Hitchin partition $[3,1]_H$. The arrows specify the dictionary between boundary-condition labels, not transposition of a matrix. The corresponding nilpotent matrices have blocks $J_2 \oplus 0 \oplus 0$ and $J_3 \oplus 0$.

The identity $\epsilon_{ijk}\epsilon_{jk\ell} = 2\delta_{i\ell}$ makes the cancellation explicit. Changing the sign of the commutator term would require changing the pole convention as well.

For an untwisted regular A-type puncture, the massless Hitchin residue has the transpose partition. This is the physical dictionary relating the two local descriptions.

$$\lambda_H = \lambda_N^t, \qquad (\lambda_N^t)_j = \#\{i : (\lambda_N)_i \geq j\}, \qquad \Phi = \left(\frac{e_H}{z} + A + O(z)\right) dz. \quad \text{(XVI.5.8)}$$

e_H is the direct sum of unit Jordan blocks of sizes λ_H; A is a generic traceless regular matrix. The Higgs field Φ is a meromorphic one-form. The transpose is not a matrix transpose of e_N. It changes the Jordan block sizes.

The full puncture has a trivial Nahm embedding and a principal massless Hitchin residue. At the other end, the principal Nahm embedding describes a closed point.

λ_N	λ_H	e_H
$[1,1,1]_N$	$[3]_H$	$E_{12} + E_{23}$
$[2,1]_N$	$[2,1]_H$	E_{12}
$[3]_N$	$[1,1,1]_H$	0

. (XVI.5.9)

The middle partition happens to be self-transpose. It therefore gives no test of whether we have used the correct side of the dictionary.

Change the defining representation to dimension four, $N = 4$. A doublet and two singlets give a different massless residue.

$$[2,1,1]_N \longmapsto [3,1]_H, \qquad e_N = E_{12}, \qquad e_H = E_{12} + E_{23} \quad \text{in } \mathfrak{sl}_4. \qquad \text{(XVI.5.10)}$$

Conversely $[3,1]_N$ maps to $[2,1,1]_H$ and has $e_H = E_{12}$. This reversal will change the cubic pole in the next section. It provides a concrete reason to attach the labels N and H even when a diagram looks familiar.

XVI.5.2 Invariant poles and puncture flavor

A simple pole of a matrix does not mean every invariant has a simple pole. Nilpotency cancels many of the most singular terms. We can calculate the surviving orders using

the determinant, without assigning a pole independently to every eigenvalue. Define the coefficient functions $c_k(z)$ by

$$\det(xI - \Phi_z) = x^N + \sum_{k=2}^{N} c_k(z) x^{N-k}, \qquad \lambda_{\mathrm{geom}} = x\,dz, \qquad \mathcal{C}_k = c_k(z)(dz)^k. \tag{XVI.5.11}$$

Tracelessness removes the degree-one term. Under a change of coordinate x transforms as a cotangent coordinate, making $\mathcal{C}_k$ a k-differential. With dimensionless z, x has mass dimension one and c_k has dimension k. We keep the determinant sign. A convention writing $\lambda^N = \sum_k \phi_k \lambda^{N-k}$ has $\phi_k = -\mathcal{C}_k$.

For $N = 3$, Newton identities reduce the determinant to two traces.

$$c_2 = -\frac{1}{2}\operatorname{tr}\Phi_z^2, \qquad c_3 = -\frac{1}{3}\operatorname{tr}\Phi_z^3. \tag{XVI.5.12}$$

Set $t = 1/z$ and initially keep only $\Phi_z = te_H + A$. Since e_H is nilpotent, its positive powers have zero trace. Cyclicity of trace then gives

$$c_2 = -t\operatorname{tr}(e_H A) - \frac{1}{2}\operatorname{tr} A^2, \tag{XVI.5.13}$$

$$c_3 = -t^2\operatorname{tr}(e_H^2 A) - t\operatorname{tr}(e_H A^2) - \frac{1}{3}\operatorname{tr} A^3. \tag{XVI.5.14}$$

These equations show which matrix entries make the orders generic, rather than merely upper bounds. For the full residue $e_H = E_{12} + E_{23}$, its square is E_{13}, so

$$\operatorname{tr}(e_H A) = A_{21} + A_{32}, \qquad \operatorname{tr}(e_H^2 A) = A_{31}, \qquad (p_2, p_3)_F = (1, 2). \tag{XVI.5.15}$$

The independent regular entries can make both coefficients nonzero. For the simple residue $e_H = E_{12}$, its square vanishes. Instead the coefficient of t in c_3 contains $(A^2)_{21}$.

$$\operatorname{tr}(e_H A) = A_{21}, \qquad \operatorname{tr}(e_H A^2) = (A^2)_{21}, \qquad (p_2, p_3)_S = (1, 1). \tag{XVI.5.16}$$

For example $A_{23}A_{31}$ is one contribution to $(A^2)_{21}$ and is not forced to vanish by tracelessness. The principal Nahm embedding has $e_H = 0$, so both coefficients are holomorphic. Terms of positive order in z in the regular part cannot raise a negative power. Each replaces a constant matrix entry by a term containing extra powers of z. Thus the generic constant matrix already detects the maximum pole.

The row rule packages this determinant result. Number the boxes of the Hitchin diagram along successive rows, starting at one, and let $r(k)$ be the row containing box k. Then the allowed massless poles are

$$p_k = k - r(k), \qquad k = 2, \ldots, N. \tag{XVI.5.17}$$

For $[3, 1]_H$ the row indices are $(1, 1, 1, 2)$, giving $(1, 2, 2)$. For $[2, 1, 1]_H$ they are $(1, 1, 2, 3)$, giving $(1, 1, 1)$. This is precisely the changed cubic order predicted by (XVI.5.10). The

determinant calculation extends to every partition at $N = 4$.

λ_N	λ_H	(p_2, p_3, p_4)	$\mathfrak{f}$	$\dim_{\mathbb{C}} \mathcal{O}_{e_N}$
$[1,1,1,1]_N$	$[4]_H$	$(1,2,3)$	$\mathfrak{su}(4)$	0
$[2,1,1]_N$	$[3,1]_H$	$(1,2,2)$	$\mathfrak{su}(2) \oplus \mathfrak{u}(1)$	6
$[2,2]_N$	$[2,2]_H$	$(1,1,2)$	$\mathfrak{su}(2)$	8
$[3,1]_N$	$[2,1,1]_H$	$(1,1,1)$	$\mathfrak{u}(1)$	10
$[4]_N$	$[1,1,1,1]_H$	$(0,0,0)$	0	12

. (XVI.5.18)

The last row is a closed point. To understand the flavor column, we must return to the Nahm embedding rather than commute with e_H.

A transformation commuting with the whole $SU(2)$ representation acts on the multiplicity spaces in (XVI.5.1). Unitarity and the $SU(N)$ determinant condition give the compact matrix centralizer.

$$\begin{aligned} F_\rho &= \left\{ (g_d) \in \prod_d U(m_d) : \prod_d \det(g_d)^d = 1 \right\}, \\ \operatorname{Lie} F_\rho &= \bigoplus_d \mathfrak{su}(m_d) \oplus \mathfrak{u}(1)^{\#\{d : m_d > 0\} - 1}. \end{aligned} \tag{XVI.5.19}$$

Its connected Lie algebra is the puncture flavor algebra; masses lie in a Cartan. We will not determine global quotients from this Lie algebra. For $[2,1,1]_N$, the singlets have multiplicity two and the doublet multiplicity one. They give $\mathfrak{su}(2) \oplus \mathfrak{u}(1)$. For $[2,2]_N$ only the doublet multiplicity space remains and the determinant condition removes its continuous scalar generator, leaving $\mathfrak{su}(2)$.

There is a second centralizer relevant to orbit dimensions. It commutes only with e_N and is generally larger. Solving $[B, E_{12}] = 0$ for a traceless 3×3 matrix gives

$$B = \begin{pmatrix} a & b & c \\ 0 & a & 0 \\ 0 & d & -2a \end{pmatrix}, \qquad \dim_{\mathbb{C}} Z_{\mathfrak{sl}_3}(e_N) = 4. \tag{XVI.5.20}$$

Commuting also with h_N kills b, c, d, and the remaining diagonal matrix commutes with f_N. Thus the triple centralizer has complex dimension one. Its compact form is the $U(1)$ flavor algebra of the simple puncture. Confusing these two linear systems would incorrectly assign four flavor generators to this example.

Finally introduce a mass background for that $U(1)$. Its eigenvalue pattern may be represented by $M = \operatorname{diag}(m, m, -2m)$. Its leading characteristic polynomial is

$$\det(xI - M/z) = (x - m/z)^2 (x + 2m/z) = x^3 - \frac{3m^2}{z^2} x + \frac{2m^3}{z^3}. \tag{XVI.5.21}$$

Writing the leading coefficients as $a_2 = -3m^2$ and $a_3 = 2m^3$ eliminates the one mass parameter.

$$4a_2^3 + 27a_3^2 = 0. \tag{XVI.5.22}$$

The second- and third-order poles are fixed background terms. They do not replace the massless Coulomb pole orders $(1,1)$ by two freely varying coefficients. This calculation

determines leading invariants, not every subleading constraint of a massive puncture. Moreover, taking this diagonal representative to zero is not a derivation of the massless nilpotent representative in a fixed holomorphic frame.

XVI.5.3 Counting parameters on a trinion

Local poles become four-dimensional parameters only when they fit into global differentials. Consider a sphere with marked points z_i and massless pole bounds $p_k^{(i)}$. The coefficient differential belongs to the line bundle

$$\mathcal{C}_k \in H^0(\mathbb{P}^1, L_k), \qquad L_k = K^k \left(\sum_i p_k^{(i)} [z_i] \right), \qquad \deg L_k = -2k + \sum_i p_k^{(i)}. \tag{XVI.5.23}$$

The $-2k$ comes from the degree of the canonical bundle of the sphere. We can obtain its section count without an abstract Riemann–Roch computation. Put all finite marked points at distinct z_i and write a differential with their maximum allowed denominators.

$$\mathcal{C}_k = \frac{P(z)(dz)^k}{\prod_{i \neq \infty} (z - z_i)^{p_k^{(i)}}}. \tag{XVI.5.24}$$

Let $s = \sum_{i \neq \infty} p_k^{(i)}$ and $n = \deg P$. Under $z = 1/w$, the largest numerator power contributes

$$z^{n-s}(dz)^k = (-1)^k w^{s-n-2k}(dw)^k. \tag{XVI.5.25}$$

The order at infinity must be at most $p_k^{(\infty)}$. Therefore $n \leq s + p_k^{(\infty)} - 2k = \deg L_k$. A polynomial of maximum degree $\ell \geq 0$ has $\ell + 1$ coefficients. If $\ell < 0$ there is no nonzero polynomial. Consequently

$$d_k^{\mathrm{virt}} = 1 - 2k + \sum_i p_k^{(i)}, \qquad h^0(L_k) = \max(0, d_k^{\mathrm{virt}}). \tag{XVI.5.26}$$

The first is the virtual count. The second is an actual vector-space dimension. The distinction will diagnose an inadmissible ordinary fixture below.

For three A_2 punctures, use $F = (1, 2)$ for full and $S = (1, 1)$ for simple. Their virtual counts are

punctures	$\sum p_2$	$\sum p_3$	$(d_2^{\mathrm{virt}}, d_3^{\mathrm{virt}})$
FFF	3	6	$(0, 1)$
FFS	3	5	$(0, 0)$
FSS	3	4	$(0, -1)$

. (XVI.5.27)

The FFF trinion is denoted T_3. It has one degree-three parameter in this massless count. The absence of a degree-two parameter is already forced by the global degree. Three simple quadratic poles cannot compensate the degree -4 of K^2.

Place the FFF punctures at $0, 1, \infty$. For the cubic differential, the finite denominator is $z^2(z-1)^2$, and (XVI.5.25) allows only a constant numerator. The unique basis differential is

$$\mathcal{C}_3 = \frac{u_3(dz)^3}{z^2(z-1)^2}, \qquad [u_3] = 3. \tag{XVI.5.28}$$

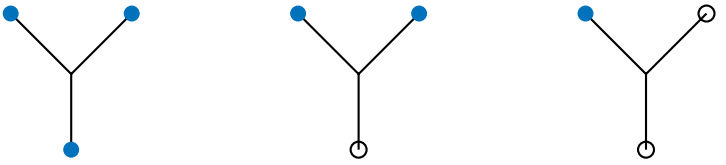


Figure XVI.5.2: Three massless A_2 puncture sets on a sphere. Full punctures are filled blue circles, and simple punctures are open circles. The displayed pair is the virtual degree-two and degree-three count. The double cubic pole at infinity of the FFF differential is disallowed in FFS. The negative virtual entry for FSS signals failure of the ordinary fixture test, even though its section spaces have dimension zero.

Check infinity directly, retaining the odd Jacobian sign.

$$\frac{(dz)^3}{z^2(z-1)^2} = -\frac{(dw)^3}{w^2(1-w)^2}, \qquad w = 1/z. \tag{XVI.5.29}$$

The pole is double at each of the three full punctures. It is precisely the double pole at infinity that a closure will remove.

Change only the puncture at infinity to simple. Its cubic bound becomes one. The same local expression would retain a double pole unless

$$\lim_{w\to 0} w^2 \mathcal{C}_{3,w} = -u_3 = 0. \tag{XVI.5.30}$$

Thus the single cubic mode disappears. The quadratic mode was absent already. This realizes the FFS count by an actual section calculation, rather than just subtracting entries of a table. It also makes clear that partial closure changes the boundary condition of the compactification, not the position of a marked point.

For FSS the cubic bundle has degree -2 and the quadratic bundle degree -1.

$$L_3 = \mathcal{O}(-2), \quad L_2 = \mathcal{O}(-1), \qquad (h^0(L_2), h^0(L_3)) = (0,0), \quad (d_2^{\mathrm{virt}}, d_3^{\mathrm{virt}}) = (0,-1). \tag{XVI.5.31}$$

There is no negative-dimensional physical vector space. Nevertheless the negative virtual entry means this puncture set fails the ordinary fixture test requiring nonnegative virtual counts at every degree. Replacing -1 by zero in a dimension formula cannot turn it into a free matter fixture.

Even for FFS, where both virtual counts vanish, the calculation only says that these Coulomb differentials have no variable coefficients. The identification of this fixture as free matter uses additional physical information. We will use that identification in the next section, with its representation stated explicitly. The global differential calculation supplies an independent consequence of the proposed closure, not the dynamical reason for freeness.

XVI.5.4 A nilpotent moment-map expectation value

The pole calculation describes the Coulomb-sector data of a puncture. Partial closure is implemented physically on the Higgs branch. A full puncture has an $SU(3)$ flavor moment map, whose holomorphic component is a traceless matrix operator μ_+. Give it the expectation value

$$\langle \mu_+ \rangle = vE_{12}, \qquad v \neq 0, \qquad [v] = 2. \tag{XVI.5.32}$$

The dimension follows from the dimension-two moment-map operator. This matrix is labeled by $[2,1]_N$. It is not the Hitchin field of dimension one in (XVI.5.8). The two matrices enter different branches of the four-dimensional construction, even when their Jordan types coincide in this example.

A nonzero scalar multiple of E_{12} lies on the same complex orbit. For example a diagonal element of $SL(3,\mathbb{C})$ gives

$$g = \mathrm{diag}(v, 1, v^{-1}), \qquad gE_{12}g^{-1} = vE_{12}. \tag{XVI.5.33}$$

Here the displayed group identity is an algebraic statement after choosing a nonzero numerical value for v in fixed units. It does not remove the physical scale of symmetry breaking. That scale controls when the infrared description is appropriate.

The complex orbit through $e = E_{12}$ is generated by conjugation. Expanding $\exp(\varepsilon B)e\exp(-\varepsilon B)$ gives its tangent map.

$$e \longmapsto e + \varepsilon[B,e] + O(\varepsilon^2), \qquad T_e\mathcal{O}_e = \mathrm{im}(\mathrm{ad}_e), \qquad \ker(\mathrm{ad}_e) = Z_{\mathfrak{sl}_3}(e). \tag{XVI.5.34}$$

The sign of the map is immaterial for its rank. To see every constraint, write B as an arbitrary traceless matrix. Matrix multiplication gives

$$[B, E_{12}] = \begin{pmatrix} -B_{21} & B_{11} - B_{22} & -B_{23} \\ 0 & B_{21} & 0 \\ 0 & B_{31} & 0 \end{pmatrix}. \tag{XVI.5.35}$$

The four independent combinations are B_{21}, $B_{11} - B_{22}$, B_{23} and B_{31}. They span four tangent directions. Setting them to zero recovers (XVI.5.20). Since $\dim \mathfrak{sl}_3 = 8$, rank-nullity yields

$$\dim_{\mathbb{C}} \mathcal{O}_{[2,1]_N} = 8 - 4 = 4. \tag{XVI.5.36}$$

The full embedding centralizer has dimension one, but subtracting one from eight would count the wrong space. It is the centralizer of e alone that appears as the kernel of this tangent map.

For a good $\mathcal{N} = 2$ nilpotent closure, the orbit directions give a Goldstone sector. A hypermultiplet has two complex scalar coordinates in one complex structure. The resulting local count is therefore

$$n_h^{\mathrm{NG}} = \frac{1}{2}\dim_{\mathbb{C}} \mathcal{O}_{[2,1]_N} = 2. \tag{XVI.5.37}$$

This interpretation assumes that the chosen expectation value lies in the physical Higgs branch and realizes the good closure. The matrix rank establishes the number once those physical hypotheses hold; it does not establish the vacuum by itself.

The infrared identification for closing one full puncture of T_3 is a residual FFS fixture together with this separate Goldstone sector. The residual fixture is one full hypermultiplet in a bifundamental representation.

$$R = (\mathbf{3}, \overline{\mathbf{3}}), \qquad Q \in R, \quad \widetilde{Q} \in \overline{R}, \qquad n_h^{\text{res}} = \dim_{\mathbb{C}} R = 3 \cdot 3 = 9. \tag{XVI.5.38}$$

Changing the orientation of one flavor group can conjugate the displayed second factor. The counting is unaffected. This is a full hyper in a complex representation, not a half-hyper. It has eighteen complex scalars, or nine quaternionic components. There is one bifundamental representation, not nine separate bifundamentals.

In a local infrared neighborhood of the specified closure vacuum, we consequently keep two contributions.

$$\text{residual } FFS: \ n_h = 9, \qquad \text{Goldstone sector}: \ n_h = 2. \tag{XVI.5.39}$$

The free residual identification is physical input from the class-S fixture and closure construction. The calculation $d_2 = d_3 = 0$ in the preceding section did not derive it. Nor does (XVI.5.39) assert a global product decomposition of the entire ultraviolet Higgs branch. It describes the local low-energy sectors relevant to this flow.

The closed puncture leaves $\mathfrak{u}(1)$, and the other two punctures retain their $\mathfrak{su}(3)$ factors. They form the manifest puncture subalgebra

$$\mathfrak{f}_{\text{punctures}} = \mathfrak{su}(3) \oplus \mathfrak{su}(3) \oplus \mathfrak{u}(1). \tag{XVI.5.40}$$

The free fields can have additional symmetry; this expression keeps only the factors tracked by the punctures. Their survival is crucial when one of the unchanged full legs is later gauged.

Changing N tests the orbit calculation independently of the self-transpose example. For $[2,1,1]_N$ in $\mathfrak{sl}_4$, the nilpotent is still E_{12}. Its commutator with a general matrix has the constraints

$$B_{21} = B_{23} = B_{24} = B_{31} = B_{41} = 0, \qquad B_{11} = B_{22}. \tag{XVI.5.41}$$

These are six independent linear conditions on fifteen traceless entries. Thus its nilpotent centralizer has dimension nine and its orbit has dimension six.

$$\dim_{\mathbb{C}} \mathcal{O}_{[2,1,1]_N} = 15 - 9 = 6, \qquad \frac{1}{2} \dim_{\mathbb{C}} \mathcal{O}_{[2,1,1]_N} = 3. \tag{XVI.5.42}$$

The second number would count Goldstone hypers for a good closure realizing this orbit. We have not specified a residual A_3 fixture or established its vacuum here. The changed example teaches the reusable linear-algebra method while keeping the physical assumptions distinct.

XVI.5.5 Closure and gauging in a complete example

We can now ask whether a closure leaves a familiar weak gauge description. Take two T_3 blocks, called L and R, and gauge one full puncture of each with the same $SU(3)$

vector multiplet. There are four full external punctures. On each block close a different external full puncture to simple, leaving the gauged leg untouched. Use the good closure vacuum that preserves the spectator full-puncture factors.

The spectator condition determines the gauge charges of the orbit sector. Let $\mathfrak{g}_c$ be the flavor algebra of the closed leg and $\mathfrak{g}_s$ that of an unchanged spectator leg. They are commuting factors. Let x_0 denote the chosen Higgs-branch vacuum point. The unbroken spectator fixes x_0. For $s \in \mathfrak{g}_s$ and $b \in \mathfrak{g}_c$, their infinitesimal actions on the Goldstone tangent obey

$$[s,b] = 0, \qquad s \cdot x_0 = 0 \quad \Longrightarrow \quad s \cdot (b \cdot x_0) = [s,b] \cdot x_0 + b \cdot (s \cdot x_0) = 0. \tag{XVI.5.43}$$

Thus this spectator acts trivially on the local Goldstone tangents. Gauging that unchanged factor leaves the two Goldstone hypers from each block gauge neutral. Both the commuting-factor statement and preservation of the spectator at the vacuum enter the argument; assigning an arbitrary vev on a gauged leg would not meet these conditions.

Each residual FFS fixture is a full bifundamental under the gauged $SU(3)$ and the remaining external $SU(3)$. We obtain the matter representations

$$R_L = (\mathbf{3}_g, \overline{\mathbf{3}}_L), \qquad R_R = (\overline{\mathbf{3}}_g, \mathbf{3}_R), \qquad n_h^{\mathrm{NG,total}} = 2 + 2 = 4. \tag{XVI.5.44}$$

A full hyper contains both its displayed representation and its complex conjugate, so reversing the gauge orientation on R_R does not change its contribution. Each external triplet index supplies three full fundamental flavors for the gauge group.

The screening can be calculated as an actual trace. Normalize the generators by $\mathrm{tr}_{\mathbf{3}}\, T_a T_b = \delta_{ab}/2$. On the left bifundamental the gauge generator is $T_a \otimes I_3$. Consequently

$$\mathrm{tr}_{R_L}\big[(T_a \otimes I_3)(T_b \otimes I_3)\big] = \mathrm{tr}_{\mathbf{3}}(T_a T_b)\, \mathrm{tr}_{\mathbf{3}}\, I_3 = \frac{3}{2}\delta_{ab}. \tag{XVI.5.45}$$

The right bifundamental has the same index. In the $\mathcal{N} = 2$ convention in which a full fundamental contributes one to screening, a full hyper in R contributes $2T(R)$. Therefore

$$\sum_{\text{full hypers}} 2T(R) = 2\left(\frac{3}{2} + \frac{3}{2}\right) = 6, \qquad b_0 = 2h^\vee_{SU(3)} - 6 = 6 - 6 = 0. \tag{XVI.5.46}$$

This is $N_f = 6$ in a weak $SU(3)$ frame. A mistaken half-hyper assignment would halve the screening and give $b_0 = 3$. The complex representation forbids that assignment independently of the beta calculation. Zero one-loop beta coefficient is the result being computed; exact marginality and the existence of the infrared frame require the physical construction.

There is also a global parameter check. For a sphere with four full punctures, (XVI.5.26) gives

$$(d_2, d_3)_{FFFF} = (1 - 4 + 4,\ 1 - 6 + 8) = (1, 3). \tag{XVI.5.47}$$

After the two external closures there are two full and two simple punctures. Thus

$$(d_2, d_3)_{FFSS} = (1 - 4 + 4,\ 1 - 6 + 2 + 2 + 1 + 1) = (1, 1). \tag{XVI.5.48}$$

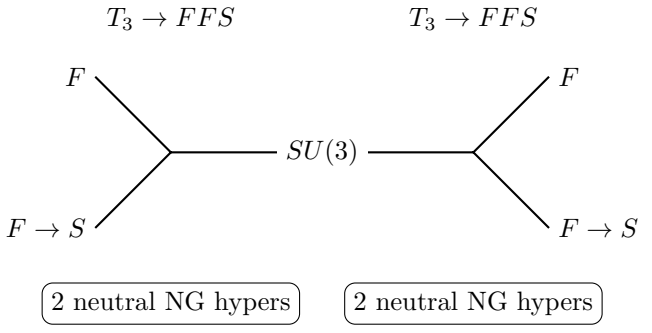


Figure XVI.5.3: Two T_3 blocks joined at unchanged full legs. The horizontal edge is the $SU(3)$ gauge tube. Each downward external full leg is closed to simple, yielding an FFS bifundamental on each side and two gauge-neutral Goldstone hypers per block. The diagram applies at the spectator-preserving good closure vacuum. It records these external closures, not a rule for closing the gauged leg.

The two lost degree-three parameters are the cubic parameters of the two original T_3 fixtures. The gauge tube retains one degree-two and one degree-three parameter, the degrees of the $SU(3)$ Casimirs. In the weak frame these are represented by

$$u_2^g \;\propto\; \operatorname{tr}\varphi_g^2, \qquad u_3^g \;\propto\; \operatorname{tr}\varphi_g^3. \tag{XVI.5.49}$$

The proportionalities leave the coordinate normalization unspecified. The degrees and number of independent parameters already agree between the differential count and the matter construction. The ungauged puncture algebra is $\mathfrak{su}(3)_L \oplus \mathfrak{su}(3)_R \oplus \mathfrak{u}(1)^2$, and the four neutral Goldstone hypers remain separate from the gauge screening.

To see why the untouched leg matters, examine the gauge moment-map equation. In a common orientation the adjoint chiral φ_g in the $\mathcal{N} = 2$ vector couples through

$$W = \sqrt{2}\operatorname{tr}\varphi_g(\mu_L + \mu_R), \qquad \frac{\partial W}{\partial \varphi_g} = 0 \quad\Longrightarrow\quad \mu_L + \mu_R = 0. \tag{XVI.5.50}$$

These are moment maps for the gauged punctures. Inserting a vev on only one of them fails the equation.

$$(\langle\mu_L\rangle, \langle\mu_R\rangle) = (vE_{12}, 0) \quad\Longrightarrow\quad \langle\mu_L + \mu_R\rangle = vE_{12} \neq 0. \tag{XVI.5.51}$$

The balanced pair $(vE_{12}, -vE_{12})$ solves this particular complex equation. It does not by itself solve the real moment-map equations or prove that either block realizes the necessary Higgs vacuum. Existence of a compatible physical vacuum remains a separate question. Our complete example compares external closures at a sourced spectator-preserving vacuum; it establishes no universal interchange law for closure and gauging.

Take-home message

The Nahm partition determines an embedding, its transpose determines the massless Hitchin residue, and the generic determinant determines the invariant poles. The embedding commutant gives the manifest puncture flavor algebra. A global section calculation then turns the local poles into allowed Coulomb parameters. A good nilpotent Higgs closure adds physical information. Its residual fixture must be identified and its Goldstone sector retained. For the external closures studied here, these steps give two bifundamentals coupled to $SU(3)$, with six fundamental flavors and four neutral Goldstone hypers. The next step in using the construction is to keep these puncture data alongside the spectral geometry and the gauge-tube data, rather than compress them into an unlabeled partition.

Exercises

1. Construct (e_N, f_N, h_N) for $[2,1,1]_N$ in $\mathfrak{sl}_4$ and check all three commutators. Find λ_H, the nilpotency orders of e_N, e_H, and (p_2, p_3, p_4). Submit the Hitchin partition, the two orders and the pole tuple. Explain why the A_2 simple puncture alone cannot test the transpose rule.

2. For $[2,2]_N$, calculate the degree-two through degree-four poles from a generic traceless regular matrix. Solve the traceless nilpotent centralizer and the triple centralizer. Submit the poles and both dimensions. Derive the connected compact flavor algebra and explain why its Lie algebra does not determine all global quotient data.

3. For the simple $SU(3)$ mass residue, expand the determinant and compute the leading quadratic and cubic coefficients at $m = 2$. Submit both coefficients and $4a_2^3 + 27a_3^2$. Derive the relation for general m and explain why the two massive leading terms are not two Coulomb parameters.

4. Derive the cubic differential on the FFF sphere at $0, 1, \infty$ and transform it to $w = 1/z$. Submit its pole order at infinity and the ratio of its leading coefficient there to u_3. Submit the virtual and actual section-dimension pairs for FSS. Explain why making infinity simple removes the cubic, and why neither clipping a negative virtual count nor a vanishing Coulomb count proves a free fixture.

5. Compute the rank and kernel dimension of $\mathrm{ad}_{E_{12}}$ on $\mathfrak{sl}_3$. For a good T_3 closure, submit the Goldstone hyper count and the residual bifundamental quaternionic dimension separately. Derive a basis of tangent directions. Identify the physical input needed in addition to this orbit calculation.

6. Gauge two residual FFS fixtures at unchanged full legs. Submit the total full-hyper screening, b_0, the total number of neutral Goldstone hypers, and the final sphere's (d_2, d_3). For the gauged-leg pair $(E_{12}, 0)$ submit the $(1,2)$ entry of the complex F-term. Derive the spectator-neutrality argument and state the vacuum

condition it uses. Explain why $(E_{12}, -E_{12})$ solving the complex equation is not a proof of a physical vacuum.

For benchmark submissions, see `benchmark/PROTOCOL.md`. Include the requested written derivations and explanations.

Sources and scope

Section 5.1. The regular-defect assignment and Nahm/Hitchin transpose dictionary are [GEO-E]. The primary transpose anchor is Xie and Yonekura (2014, arXiv v1, §3.3.2, eqs. (3.26)–(3.29)); the representation setup is also discussed in its §2.1. The finite triples, their similarity transformation, nilpotency orders and Nahm-sign substitution are [MATH], with the explicit block convention in Nanopoulos and Xie (2009, arXiv v2, §5.2, eqs. (5.9)–(5.13)). The Hermitian orientation agrees with Volume VII-A. No general existence theorem for boundary conditions is derived.

Section 5.2. The exact $N = 3, 4$ determinant coefficients, pole orders, centralizer dimensions and leading mass relation are [MATH]. Sources are Nanopoulos and Xie (2009, arXiv v2, eqs. (5.14)–(5.16), Fig. 16, and §5.4, eq. (5.32)). The identification of the compact embedding commutant with puncture flavor, and masses with its Cartan, is [GEO-E], from Chacaltana and Distler (2010, arXiv v2, §2.1, pp. 3–5). That source draws its diagrams in a different convention; here every partition is a row partition and the two labels are explicit. Full massive normal forms, global flavor quotients and symmetry enhancement are outside the calculation.

Section 5.3. The sphere bundle dimensions, explicit cubic section and its removal are [MATH]. The ordinary fixture criterion and degree count are anchored to Chacaltana and Distler (2010, arXiv v2, eqs. (1), (3), §2.3, p. 6). The criterion is necessary, not a sufficient physical classification. In particular no freeness claim follows from $d_k = 0$.

Section 5.4. The tangent-map ranks and complex orbit dimensions are [MATH], with the orbit convention in Nanopoulos and Xie (2009, arXiv v2, eq. (5.8)). The good closure and residual/Goldstone interpretation are [GEO-E], from Xie and Yonekura (2014, arXiv v1, §5.1, eq. (5.2), p. 23 and following paragraph). The residual FFS full bifundamental is independently stated in the free fixture table of Chacaltana and Distler (2010, arXiv v2, §5.2, p. 15). The half-orbit Goldstone count is conditional on this good physical closure. No global Higgs-branch product or vacuum-existence proof is inferred.

Section 5.5. The endpoint weak $SU(3)$ frame uses Gaiotto (2012, arXiv v1, §4.2, pp. 42–44, especially p. 43 near Fig. 38), together with the closure sources of Section 5.4, as [GEO-E]. Gauge neutrality of the local orbit sector is an inference from commuting flavor factors at the sourced spectator-preserving vacuum, not a direct quotation or a general gauged-leg statement. The trace screening, parameter counts and displayed complex F-term test are [MATH]. The vector trace and moment-map conventions are inherited from Chapter 3. The one-loop coefficient alone proves neither exact marginality nor a physical vacuum; the balanced complex equation supplies no D-flatness proof.

References

Chacaltana, O. and J. Distler (2010). "Tinkertoys for Gaiotto Duality". In: arXiv: 1008.5203 [hep-th].

Gaiotto, D. (2012). "N=2 dualities". In: *JHEP* 08, p. 034. DOI: 10.1007/JHEP08(2012)034. arXiv: 0904.2715 [hep-th].

Nanopoulos, D. and D. Xie (2009). "Hitchin Equation, Singularity, and N=2 Superconformal Field Theories". In: arXiv: 0911.1990 [hep-th].

Xie, D. and K. Yonekura (2014). "The moduli space of vacua of N=2 class S theories". In: arXiv: 1404.7521 [hep-th].

Chapter XVI.6

The T_N theories and non-Lagrangian fixtures

A gauge tube needs matter at its ends. For the A_1 compactification that matter was a free trifundamental. The same three-punctured sphere at higher rank supplies an interacting sector. How can we calculate with such a sector before knowing a vector and hypermultiplet action for it? The punctures still specify Coulomb differentials, background masses and flavor currents. These quantities let us construct a block, gauge a flavor subgroup, and compare the resulting description with a familiar gauge theory.

We begin with three full punctures and derive the Coulomb spectrum of T_N. Protected Higgs operators then explain why T_3 is special. We construct the relevant exceptional root system explicitly, while taking its physical current interpretation from the class-S construction. Finally we study the Argyres–Seiberg frame of $SU(3)$ with six flavors and sew two T_4 blocks. The calculations use the spectral curve of Chapter 4, full punctures from Chapter 5, and the $\mathcal{N}=2$ multiplets and gauge screening recalled in Chapter 3. The aim is to use a strongly coupled block with the same care about charges and parameters as an elementary hypermultiplet.

XVI.6.1 Three full punctures

The first question is how many Coulomb coordinates a trinion actually carries. Put the punctures at $0, 1, \infty$ on $\mathbb{P}^1$. Fix their masses to zero. A full puncture then permits a pole of order $k-1$ for the degree-k invariant differential. With K the canonical bundle, the coefficient is a section of

$$c_k \in H^0\big(\mathbb{P}^1, K^k((k-1)(0+1+\infty))\big), \qquad 2 \le k \le N. \tag{XVI.6.1}$$

We use c_k as the coefficient of $\det(x-\Phi)$, so that the spectral convention of Chapter 4 is $\phi_k = -c_k$. This sign does not change the section count. Since $\lambda = x\,dz$ has mass dimension one and z is dimensionless, a variable coefficient of c_k has dimension k.

The allowed poles at the two finite punctures can be removed by multiplying by $[z(z-1)]^{k-1}$. The resulting coefficient has no finite pole, hence is a polynomial P_k.

Thus

$$c_k = \frac{P_k(z)}{[z(z-1)]^{k-1}}(dz)^k, \qquad P_k(z) = \sum_{j\geq 0} u_{k,j} z^j. \tag{XVI.6.2}$$

The infinity puncture limits this polynomial. Set $w = 1/z$, including the Jacobian of the differential rather than transforming its coefficient alone. Each monomial becomes

$$\frac{z^j (dz)^k}{[z(z-1)]^{k-1}} = (-1)^k \frac{w^{-j-2}}{(1-w)^{k-1}}(dw)^k. \tag{XVI.6.3}$$

Its pole has order $j+2$. The full-puncture condition gives the decisive degree bound

$$j+2 \leq k-1 \quad \Longleftrightarrow \quad 0 \leq j \leq k-3, \qquad d_k = k-2. \tag{XVI.6.4}$$

For $k = 2$ the interval is empty, so $d_2 = 0$. Distinct monomials have distinct leading pole orders at infinity. Their independence also follows by multiplying any proposed linear relation by the common denominator. We have therefore obtained a basis, rather than just an upper bound on its size.

The bundle degree reproduces the answer and explains why the count grows linearly with k.

$$\deg K^k((k-1)\textstyle\sum p_i) = -2k+3(k-1) = k-3, \qquad h^0(\mathbb{P}^1, \mathcal{O}(k-3)) = k-2. \tag{XVI.6.5}$$

The last formula includes $k = 2$, since $\mathcal{O}(-1)$ has no section. Summing the graded multiplicities gives the Coulomb rank

$$r(T_N) = \sum_{k=2}^{N} (k-2) = \frac{(N-1)(N-2)}{2}. \tag{XVI.6.6}$$

The first examples teach more than the total rank alone. T_2 has no Coulomb coordinate, T_3 has one coordinate of dimension three, and T_4 has one of dimension three and two of dimension four. Explicitly,

$$c_2 = 0, \qquad c_3 = \frac{u_{3,0}(dz)^3}{z^2(z-1)^2}, \qquad c_4 = \frac{(u_{4,0}+u_{4,1}z)(dz)^4}{z^3(z-1)^3}. \tag{XVI.6.7}$$

The last expression exists only when $N \geq 4$. In its infinity chart the two terms have orders two and three, both permitted for $k = 4$. A quadratic numerator would give order four and fail. For T_5 the changed degree adds

$$c_5 = \frac{(u_{5,0}+u_{5,1}z+u_{5,2}z^2)(dz)^5}{z^4(z-1)^4}, \qquad (d_2, d_3, d_4, d_5) = (0, 1, 2, 3). \tag{XVI.6.8}$$

This is the calculation a reader can repeat for any N.

Masses are different parameters. Each full puncture has a traceless Cartan residue with $N-1$ independent eigenvalues. For three punctures,

$$M_i = \operatorname{diag}(m_{i,1}, \ldots, m_{i,N}), \qquad \sum_{a=1}^{N} m_{i,a} = 0, \qquad r_{\text{mass}} = 3(N-1). \tag{XVI.6.9}$$

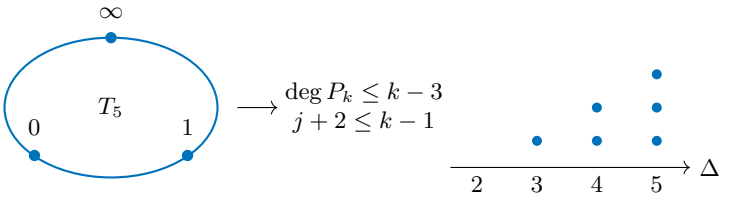


Figure XVI.6.1: A three-full-puncture sphere and its rational differential. The finite charts remove the denominator, while the infinity chart restricts its numerator. Each dot in the right panel is one independent Coulomb coordinate of the indicated dimension for T_5. The absence of a dimension-two dot is common to all T_N.

These are dimension-one backgrounds, not the variable $u_{k,j}$. Replacing the massless poles by poles of order k would count the larger bundle $K^k(k\sum p_i)$ as if every leading coefficient were free.

$$d_k^{\text{unfixed}} = h^0(\mathcal{O}(k)) = k+1, \qquad d_k^{\text{unfixed}} - d_k = 3. \tag{XVI.6.10}$$

At each degree the three extra leading coefficients are fixed by the three mass residues. Across degrees they are functions of the same mass eigenvalues. This explains why the larger section space cannot be called the Coulomb branch at fixed masses. The absence of Coulomb coordinates for T_2 likewise says nothing by itself about whether its matter is free; that identification requires the physical fixture construction.

XVI.6.2 Protected operators and the exceptional T_3 symmetry

Which operators couple a block to background flavor fields? Each full leg has a dimension-two moment map μ_i in its $SU(N)$ adjoint. The protected operators conventionally called $Q_{(k)}$ have the sourced assignments

$$Q_{(k)} \in (\wedge^k\mathbf{N}, \wedge^k\mathbf{N}, \wedge^k\mathbf{N}), \qquad \Delta(Q_{(k)}) = k(N-k), \qquad 1 \le k \le N-1. \tag{XVI.6.11}$$

All three fundamental orientations are chosen together; $Q_{(N-k)}$ is conjugate to $Q_{(k)}$. These assignments specify named operators, not a presentation of their full chiral ring.

For $N = 2$, the representation $(\mathbf{2},\mathbf{2},\mathbf{2})$ is pseudoreal. The physical T_2 fixture is a free half-hypermultiplet in this representation. Its eight complex representation components give four full-hyper equivalents for anomaly counting.

$$\Delta(Q_{(1)}) = 1, \qquad \dim(\mathbf{2},\mathbf{2},\mathbf{2}) = 8, \qquad n_h(T_2) = \tfrac{1}{2}\,8 = 4. \tag{XVI.6.12}$$

Its moment maps are quadratic composites of these fields. Counting them as additional independent free hypers would double count operators. Freeness here is the fixture identification, consistent with the spectrum derived above.

For $N = 3$, both Q representations instead have dimension two. Together with the three moment maps they fit the decomposition

$$\mathbf{78} = (\mathbf{8},\mathbf{1},\mathbf{1}) \oplus (\mathbf{1},\mathbf{8},\mathbf{1}) \oplus (\mathbf{1},\mathbf{1},\mathbf{8}) \oplus (\mathbf{3},\mathbf{3},\mathbf{3}) \oplus (\overline{\mathbf{3}},\overline{\mathbf{3}},\overline{\mathbf{3}}), \qquad 24 + 27 + 27 = 78. \tag{XVI.6.13}$$

The physical T_3 identification assigns these operators to the moment maps of an enhanced $\mathfrak{e}_6$ flavor algebra. Counting 78 components is not enough to establish that assignment. We can, however, derive the associated root algebra and expose what the dimension count leaves out.

Take three orthogonal copies of the plane in $\mathbb{R}^3$ whose coordinates sum to zero. In each copy, let e_a be the orthonormal coordinate vectors and define the weights of the fundamental representation

$$w_a = e_a - \tfrac{1}{3}(e_1 + e_2 + e_3), \qquad w_a \cdot w_b = \delta_{ab} - \tfrac{1}{3}, \qquad \sum_a w_a = 0. \tag{XVI.6.14}$$

The six $SU(3)$ roots in a given plane are $w_a - w_b$ with $a \neq b$. Adding the trifundamental weights and their negatives produces the set

$$\mathcal{R} = \bigcup_{i=1}^{3} \{(w_a - w_b)_i \mid a \neq b\} \;\cup\; \{\; \pm(w_a, w_b, w_c) \mid a, b, c = 1, 2, 3 \;\}. \tag{XVI.6.15}$$

There are $18 + 54 = 72$ distinct vectors. Each has squared length two, since a triple weight has length $3(2/3) = 2$. They span six dimensions, the sum of the three planes.

The nontrivial test is reflection closure. For roots of length two the reflection is

$$s_\alpha(v) = v - (v \cdot \alpha)\alpha. \tag{XVI.6.16}$$

Reflections in roots of one $SU(3)$ permute its three weights, preserving the displayed set. It remains to check a triple-weight root $\alpha = (w_a, w_b, w_c)$. For another positive triple $v = (w_d, w_e, w_f)$, let m be the number of equal indices in corresponding positions. Then

$$v \cdot \alpha = m - 1, \qquad m = 0, 1, 2, 3. \tag{XVI.6.17}$$

For $m = 0$, $v + \alpha$ is a negative triple, using $w_1 + w_2 + w_3 = 0$ in each plane. For $m = 1$ the reflection fixes v. For $m = 2$, $v - \alpha$ is a root in the remaining plane. For $m = 3$ it gives $-\alpha$. A root β in one plane has $\beta \cdot \alpha = 0, \pm 1$; a nonzero value sends it to a triple or its negative by the same weight-sum identity. Negating v completes the cases. Thus the whole set is reflection closed.

A simple system makes the Dynkin type explicit. Let $r_1 = e_2 - e_1$, $r_2 = e_3 - e_2$ in one plane, with subscripts indicating the plane, and choose

$$(\alpha_1, \ldots, \alpha_6) = \big((r_1)_1, (r_2)_1, (r_1)_2, (r_2)_2, (r_1)_3, (-w_3, -w_3, -w_2)\big). \tag{XVI.6.18}$$

The inner products give the Cartan matrix

$$A_{ij} = \alpha_i \cdot \alpha_j = \begin{pmatrix} 2 & -1 & 0 & 0 & 0 & 0 \\ -1 & 2 & 0 & 0 & 0 & -1 \\ 0 & 0 & 2 & -1 & 0 & 0 \\ 0 & 0 & -1 & 2 & 0 & -1 \\ 0 & 0 & 0 & 0 & 2 & -1 \\ 0 & -1 & 0 & -1 & -1 & 2 \end{pmatrix}, \qquad \det A = 3. \tag{XVI.6.19}$$

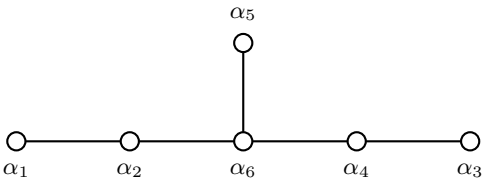


Figure XVI.6.2: The E_6 simple roots of (XVI.6.18). An edge denotes inner product -1, and absent edges denote zero inner product. The three $SU(3)$ weight planes supply 18 roots; the triple weights and their negatives supply 54 more. The graph identifies a root algebra, while the physical flavor-current assignment uses the T_3 construction.

Its three arms have lengths two, two and one. This is the E_6 diagram shown in Figure XVI.6.2. Removing a positive triple while retaining its negative immediately destroys reflection closure, since reflecting the negative in itself requires the missing positive vector. A dimension count would not detect this failure of algebraic structure.

Changing N shows why this enhancement argument is special. For T_4 the three Q dimensions and representation sizes are

$$\begin{aligned}(\Delta Q_{(1)}, \Delta Q_{(2)}, \Delta Q_{(3)}) &= (3,4,3),\\ (\dim R_1, \dim R_2, \dim R_3) &= (4^3, 6^3, 4^3) = (64, 216, 64).\end{aligned} \tag{XVI.6.20}$$

They are not dimension-two moment maps. The T_3 root calculation therefore cannot simply be repeated as a current enhancement argument for T_4. For T_3 the three puncture Cartans give six independent masses, in agreement with the rank-six enhanced algebra; the global form of its flavor group requires further information.

XVI.6.3 Gauging a flavor subgroup

To attach a vector multiplet we need the current two-point normalization, not a list of elementary fields inside the block. Normalize $SU(n)$ generators in the fundamental by

$$\mathrm{tr}_{\mathbf{n}}(T_a T_b) = \tfrac{1}{2}\delta_{ab}, \qquad T(\mathbf{n}) = \tfrac{1}{2}, \qquad T(\mathrm{adj}) = n. \tag{XVI.6.21}$$

Here $h^\vee$ is the dual Coxeter number, with $h^\vee_{SU(n)} = n$ and $h^\vee_{E_6} = 12$. The normalized invariant form is $\mathrm{Tr}_{\mathrm{adj}}/(2h^\vee)$. Write k for the flavor level in which a full fundamental hyper has $k = 2$. An interacting sector at level k contributes $k/2$ to screening. For independent sectors and ordinary full hypers the one-loop coefficient is

$$b_0 = 2h^\vee - \sum_{\text{sectors}} \frac{k_i}{2} - \sum_{\text{full hypers}} 2T(R), \qquad \beta(g) = -\frac{b_0}{16\pi^2} g^3 + \cdots . \tag{XVI.6.22}$$

The level already includes all current-carrying degrees of freedom of the specified sector. Adding the block's protected operators as extra matter would count its screening twice. A full T_N leg has the sourced level

$$k_{SU(N)}(T_N) = 2N, \qquad \frac{k_{SU(N)}}{2} = N. \tag{XVI.6.23}$$

Thus its contribution is equivalent to N full fundamental flavors for this purpose. It need not consist of N free hypers.

For T_3 we will gauge a different subgroup, a root $SU(2) \subset E_6$. The roots perpendicular to its root α form an A_5 root system. For $\alpha^2 = 2$, the coroot H_α acts on a root vector of root β with eigenvalue $\beta \cdot \alpha$. The physical $SU(2)$ generator is $H_\alpha/2$. One way to see the commutant size is to count its charges $q = \beta \cdot \alpha/2$ on the 72 roots in (XVI.6.15).

q	-1	$-\frac{1}{2}$	0	$\frac{1}{2}$	1
# roots	1	20	30	20	1

$$\mathfrak{e}_6 \supset \mathfrak{su}(2) \oplus \mathfrak{su}(6). \tag{XVI.6.24}$$

Of the six Cartan generators, one completes the $SU(2)$ triplet, and five complete the $SU(6)$ adjoint from its 30 roots. Consequently

$$\mathbf{78} = (\mathbf{3}, \mathbf{1}) \oplus (\mathbf{1}, \mathbf{35}) \oplus (\mathbf{2}, \mathbf{20}) \tag{XVI.6.25}$$

under $SU(2) \times SU(6)$. To verify the commutant type directly, choose $\alpha = (e_3 - e_1)_1$. A triple root is perpendicular precisely when its first weight is $\pm w_2$. Together with the roots in planes two and three, these give $18 + 12 = 30$ perpendicular roots. In the notation of Section XVI.6.2, set

$$\begin{gathered} \gamma_1 = (w_2, w_1, w_3), \quad \gamma_2 = (r_1)_2, \quad \gamma_3 = (r_2)_2, \\ \gamma_4 = (-w_2, -w_3, -w_2), \quad \gamma_5 = (r_1)_3. \end{gathered} \tag{XVI.6.26}$$

Their only off-diagonal nonzero inner products are $\gamma_i \cdot \gamma_{i+1} = -1$, giving the five-node A_5 chain. Their span is the rank-five perpendicular Cartan. The embedding has index one because the subgroup roots retain squared length two. For the $SU(2)$ generator $H_\alpha/2$, the same normalization can be read from the charge trace,

$$\mathrm{tr}_{\mathbf{78}}(H_\alpha/2)^2 = 2 + 40\left(\tfrac{1}{2}\right)^2 = 12, \qquad \frac{12}{2h^\vee_{E_6}} = \frac{12}{24} = \frac{1}{2}. \tag{XVI.6.27}$$

This equals the normalized $SU(2)$ fundamental trace. The sourced E_6 level six therefore restricts to the same numerical level on this $SU(2)$ and on the index-one commuting $SU(6)$.

Now couple that $SU(2)$ current to an $\mathcal{N} = 2$ vector and one full hypermultiplet in its fundamental. Let $q^a, \widetilde{q}_a$, $a = 1, 2$, be the two complex scalars in conjugate representations. The matter content and its contributions are

$$q \in \mathbf{2}_g, \quad \widetilde{q} \in \overline{\mathbf{2}}_g, \qquad n_h(q, \widetilde{q}) = 2, \qquad 2T(\mathbf{2}) = 1. \tag{XVI.6.28}$$

Although $\mathbf{2}$ is pseudoreal, the specified matter is a full hyper, not a half-hyper. It is charged at nonzero gauge coupling. Calling it a neutral free hyper would give both the wrong screening and the wrong anomaly contribution. Its coupling to the adjoint chiral φ_g illustrates the charge explicitly,

$$W = \sqrt{2}\, \widetilde{q}_a (\varphi_g)^a{}_b q^b + \sqrt{2}\, \varphi_g^A \mu^A_{T_3}, \qquad b_0 = 4 - \frac{6}{2} - 1 = 0. \tag{XVI.6.29}$$

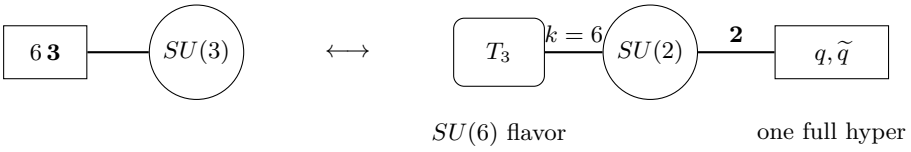


Figure XVI.6.3: The two proposed frames. The left circle is an $SU(3)$ vector coupled to six full fundamental hypers. The right circle gauges the root $SU(2)$ of the T_3 block and also couples to a full fundamental hyper $q, \widetilde{q}$. The latter is charged under the displayed gauge group. The commuting $SU(6)$ flavor currents lie in T_3.

The second term denotes the coupling to the block's moment map in the same generator convention. Its existence is part of the proposed gauging, not a constituent-field action for T_3.

Changing the added matter makes the cancellation discriminating. If n is the number of full-doublet equivalents, then

$$b_0(n) = 1 - n, \qquad b_0(0) = 1, \quad b_0(\tfrac{1}{2}) = \tfrac{1}{2}, \quad b_0(1) = 0. \tag{XVI.6.30}$$

Only the full doublet supplies the missing unit. The Argyres–Seiberg trace convention has $T_{\rm AS}(\mathbf{2}) = 1 = 2T(\mathbf{2})$. Its displayed current-algebra coefficient, denoted here by $B_{\rm AS}$, obeys

$$B_{\rm AS} = -4h^\vee + \sum_i k_i + \sum_R 4T(R) = -2b_0. \tag{XVI.6.31}$$

The sign and factor cannot be fixed by a zero alone. Pure $SU(2)$ has $(b_0, B_{\rm AS}) = (4, -8)$, while the T_3 gauging without the doublet has $(1, -2)$. These nonzero examples fix the conversion. The source extracts $k_{E_6} = 6$ by assuming the proposed conformal frame, so reinserting that level into (XVI.6.29) is a conditional consistency calculation, not independent evidence for the duality. Vanishing b_0 alone also does not establish existence of an arbitrary proposed gauging.

XVI.6.4 The Argyres–Seiberg comparison

Can the charged T_3 construction describe a familiar gauge theory? The Argyres–Seiberg proposal relates $SU(3)$ with six full fundamental hypers to $SU(2)$ gauging the root subgroup of T_3, together with precisely the full doublet just described. Figure XVI.6.3 keeps this doublet visible. We compare Coulomb degrees, anomalies and continuous flavor data. A matching list constrains the proposal but does not determine the entire infrared theory or its coupling map.

First count ordinary multiplets in the weak frame. For a full hyper, n_h is the complex dimension of its gauge representation, not just the number of flavor labels. Hence

$$(n_v, n_h)_{SU(3), N_f=6} = (3^2 - 1, 6 \cdot 3) = (8, 18). \tag{XVI.6.32}$$

The interacting T_3 sector has effective anomaly coordinates $(5, 16)$. These coordinates are defined by its two conformal anomalies,

$$a = \frac{5n_v + n_h}{24}, \qquad c = \frac{2n_v + n_h}{12}, \qquad (n_v, n_h)_{T_3} = (5, 16). \tag{XVI.6.33}$$

They do not assert that T_3 contains five elementary vectors and sixteen elementary hypers. For this frame the same numbers follow by source-based subtraction of the ordinary gauge and doublet contributions,

$$(n_v, n_h)_{T_3} = (8, 18) - (3, 0) - (0, 2) = (5, 16). \tag{XVI.6.34}$$

The spectral relation $n_v = \sum_k (2k-1)d_k$ also gives $5 \cdot 1 = 5$ for its single cubic coordinate. That relation supplies a protected anomaly comparison; it does not provide constituent fields for the sector.

Adding the gauging back gives the two independent anomaly coefficients of the full system,

$$(n_v, n_h)_{\text{gauged}} = (5 + 3, 16 + 2) = (8, 18), \qquad a = \frac{40 + 18}{24} = \frac{29}{12}, \quad c = \frac{16 + 18}{12} = \frac{17}{6}. \tag{XVI.6.35}$$

The doublet alone has $a = 1/12$ and $c = 1/6$. Replacing it with one gauge-neutral full hyper would change n_h by -1 and fail both the anomaly and screening calculations.

A different erroneous addition is suggested by the preceding chapter. Its two external nilpotent closures gave four neutral Goldstone hypers, alongside an $SU(3)$ six-flavor residual frame. Those hypers belong to that Higgs-flow endpoint. The present comparison concerns the six-flavor theory itself. Adding them on only one side would give

$$(n_v, n_h)_{\text{wrong}} = (8, 22), \qquad a_{\text{wrong}} = \frac{31}{12}, \qquad c_{\text{wrong}} = \frac{19}{6}. \tag{XVI.6.36}$$

The shifts are $4/24$ and $4/12$, respectively. Keeping separate infrared sectors visible prevents this mistaken use of the earlier closure example.

The Coulomb degrees also agree without identifying coordinates absolutely. The weak $SU(3)$ vector supplies its quadratic and cubic Casimirs. In the proposed frame the $SU(2)$ vector supplies degree two and the T_3 block supplies degree three.

$$\{\Delta u\}_{SU(3)} = \{2, 3\} = \{2\}_{SU(2)} \cup \{3\}_{T_3}. \tag{XVI.6.37}$$

This comparison fixes graded dimensions. It does not fix a multiplicative normalization of Seiberg–Witten periods or a map between the two gauge couplings.

In the weak frame the six flavor labels give $\mathfrak{su}(6) \oplus \mathfrak{u}(1)$. In the proposed frame the root $SU(2)$ leaves the $\mathfrak{su}(6)$ commutant of Section XVI.6.3. The full pseudoreal doublet has continuous flavor algebra $\mathfrak{so}(2) \simeq \mathfrak{u}(1)$. Thus

$$\mathfrak{f}_{\text{weak}} = \mathfrak{su}(6) \oplus \mathfrak{u}(1), \qquad \mathfrak{f}_{\text{gauged}} = \mathfrak{su}(6) \oplus \mathfrak{so}(2), \qquad \operatorname{rank} \mathfrak{f} = 5 + 1 = 6. \tag{XVI.6.38}$$

The nonabelian level has a simple weak-frame trace calculation. Regarding the hypers as a bifundamental of gauge $SU(3)$ and flavor $SU(6)$, the flavor generator is $I_3 \otimes t_A$. Its index is

$$\operatorname{tr}_{\mathbf{3}\otimes\mathbf{6}}[(I_3 \otimes t_A)(I_3 \otimes t_B)] = 3 \operatorname{tr}_{\mathbf{6}}(t_A t_B) = \tfrac{3}{2}\delta_{AB}, \qquad k_{SU(6)} = 4 \cdot \tfrac{3}{2} = 6. \tag{XVI.6.39}$$

The index-one commutant in T_3 has the same sourced level. This is a third anomaly coefficient, distinct from a, c. Its extraction and the effective anomaly subtraction nevertheless share the proposed dual-frame premises. These agreements check the charge assignments and normalization consistently; they do not constitute an independent derivation of the Argyres–Seiberg duality. We have compared continuous algebras and local protected quantities, leaving global flavor quotients, line operators and the full BPS spectrum unspecified.

XVI.6.5 Two T_4 blocks and a complete gluing

We can now use a higher-rank block in a full construction. Take two T_4 fixtures and gauge one full leg from each diagonally by $SU(4)$. Four external full punctures remain. The two trinions and the tube form a four-punctured sphere, as in Figure XVI.6.4. Both blocks contribute level eight to the gauge current, so

$$b_0 = 2h^\vee_{SU(4)} - \tfrac{1}{2}(k_L + k_R) = 8 - 4 - 4 = 0. \tag{XVI.6.40}$$

The physical class-S sewing supplies the candidate gauging. This cancellation is its screening check.

Each T_4 has $(d_2, d_3, d_4) = (0, 1, 2)$. The vector on the tube adds one Casimir at each of degrees two, three and four. Consequently

$$(d_2, d_3, d_4)_{\text{sewn}} = 2(0, 1, 2) + (1, 1, 1) = (1, 3, 5), \qquad r = 1 + 3 + 5 = 9. \tag{XVI.6.41}$$

The same result follows directly on the four-full-puncture sphere. The degree-k bundle has four pole divisors instead of three,

$$\deg L_k = -2k + 4(k - 1) = 2k - 4, \qquad d_k = h^0(\mathcal{O}(2k - 4)) = 2k - 3. \tag{XVI.6.42}$$

At $k = 2, 3, 4$ this is precisely $(1, 3, 5)$. Omitting the gauge Casimirs would give $(0, 2, 4)$ and rank six. The tube therefore carries Coulomb information as well as the coupling used to join the blocks.

For an explicit changed surface calculation, put the four punctures at $0, 1, t, \infty$ with $t \neq 0, 1$. Removing the three finite denominators gives

$$c_k = \frac{P_k(z)(dz)^k}{[z(z - 1)(z - t)]^{k-1}}, \qquad \deg P_k \leq 2k - 4. \tag{XVI.6.43}$$

Indeed a monomial z^j transforms at infinity into a coefficient proportional to w^{k-3-j}, and the pole bound is $j - (k - 3) \leq k - 1$. Thus there are $2k - 3$ monomials. This verifies each graded multiplicity rather than only the total rank.

The effective anomalies can also be assembled without introducing fictitious elementary fields. The source-based trinion anomaly subtraction uses an ordinary comparison quiver and its tail. For T_4, the original $SU(4)^3$ quiver has two adjacent bifundamentals and four fundamentals at each end. The $SU(2)$–$SU(3)$–$SU(4)$ tail has adjacent bifundamentals and one fundamental at each end. These are comparison-frame matter assignments, not constituents of T_4. Their finite counts are

$$n_v^{\text{original}} = 3(4^2 - 1) = 45, \qquad n_h^{\text{original}} = (4 - 2)4^2 + 2 \cdot 4^2 = 64, \tag{XVI.6.44}$$

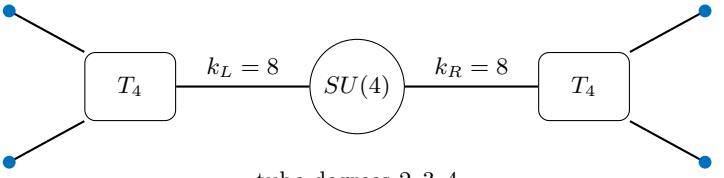


Figure XVI.6.4: Two T_4 blocks joined by an $SU(4)$ tube. Filled ends are full punctures, and four external legs remain after gluing. The tube adds one gauge Casimir in each degree $2, 3, 4$ and one dimensionless plumbing parameter. Each external full puncture retains three mass directions.

$$n_v^{\text{tail}} = (2^2-1)+(3^2-1)+(4^2-1) = 26, \qquad n_h^{\text{tail}} = 2+4+(2\cdot3+3\cdot4) = 24. \tag{XVI.6.45}$$

Subtracting the tail gives the sourced block coordinates and their spectral consistency relation,

$$(n_v, n_h)_{T_4} = (45-26, 64-24) = (19, 40), \qquad \sum_{k=2}^{4}(2k-1)d_k = 5+2\cdot7 = 19. \tag{XVI.6.46}$$

The quiver subtraction assumes the corresponding source frames. The finite sums explain the numerical values used here; their agreement is conditional on those identifications. General anomaly integration will be developed in the next chapter.

The sewn theory contains two such blocks and one fifteen-dimensional vector multiplet. Its anomalies are therefore

$$\begin{gathered}(n_v, n_h) = (2\cdot19+15, 2\cdot40) = (53, 80),\\ a = \frac{5\cdot53+80}{24} = \frac{115}{8}, \qquad c = \frac{2\cdot53+80}{12} = \frac{31}{2}.\end{gathered} \tag{XVI.6.47}$$

The spectral calculation checks $n_v = 3\cdot1+5\cdot3+7\cdot5 = 53$. Four remaining full Cartans contribute masses, while the complex structure of the sphere contributes a coupling,

$$r_{\text{mass}} = 4(4-1) = 12, \qquad \dim_{\mathbb{C}} \mathcal{M}_{0,4} = 4-3 = 1. \tag{XVI.6.48}$$

The cross ratio t is one coordinate on that complex-structure space. A plumbing parameter near a degeneration gives a weak gauge-coupling coordinate, without an absolute normalization of periods being implied. Twelve masses, nine Coulomb coordinates and one marginal parameter have different physical roles.

Finally, why do we need blocks beyond ordinary $\mathcal{N} = 2$ gauge matter? Any ordinary nonabelian gauge factor has a quadratic adjoint Casimir; an abelian factor has a dimension-one scalar coordinate. The isolated T_N spectrum instead satisfies

$$d_1(T_N) = d_2(T_N) = 0, \qquad r(T_N) > 0 \quad (N \geq 3). \tag{XVI.6.49}$$

Thus an ordinary weak vector/hyper frame cannot reproduce this Coulomb spectrum. With no vector factors, such an ordinary frame would consist of free hypers, incompatible

with the sourced interacting T_N sector. This is an obstruction within that specific class of manifest $\mathcal{N} = 2$ descriptions. It does not exclude other ultraviolet constructions, including flows with less manifest supersymmetry. The two-T_4 example shows the practical consequence. A usable generalized quiver is built from flavor currents, protected spectra and anomaly coefficients even when its vertices are interacting sectors.

Take-home message

Three full massless punctures give $d_k = k - 2$ by the infinity-chart bound. The resulting block has neither dimension-one nor dimension-two Coulomb generators. T_2 is sourced free matter, while T_3 is the sourced interacting E_6 fixture. Its explicit roots explain the exceptional algebra available to the protected operators. Gauging uses a current level and actual charged matter. The Argyres–Seiberg comparison needs one full $SU(2)$ doublet; two T_4 blocks instead supply all screening of an $SU(4)$ tube. In both examples a complete construction retains block spectra, tube Casimirs, masses and anomaly contributions separately.

Exercises

1. Derive the complete T_5 differential basis and transform every monomial to $w = 1/z$. Submit (d_2, d_3, d_4, d_5), the rank, and the infinity pole orders of the three degree-five basis terms in increasing numerator degree. Explain in writing why allowing pole order k would add fixed mass terms rather than new Coulomb coordinates.

2. Construct the 72 vectors in (XVI.6.15) and the simple roots in (XVI.6.18). Submit their Cartan matrix, determinant, rank, and root count. Show the reflection cases classified by m and exhibit a failed reflection after removing just one positive triple. Explain why even a correct root calculation does not prove the physical current enhancement.

3. Gauge the root $SU(2)$ of T_3 with zero, half, and one full fundamental hyper. Submit the three house b_0 values, the corresponding B_{AS} values, and the pure-$SU(2)$ pair. Derive the trace conversion including its factor of two. State why the source extraction of the level prevents treating the cancellation as independent duality evidence.

4. Reconstruct the anomaly subtraction in (XVI.6.34). Submit the T_3 effective coordinates, the full gauged (a, c) pair and its pair after wrongly adding four neutral Goldstone hypers. Derive the charged-doublet contribution. Explain which physical flow actually contains those four Goldstones and why replacing the full doublet by one neutral hyper fails.

5. Sew two T_4 fixtures. Submit the graded Coulomb multiplicities, rank, b_0, effective (n_v, n_h), (a, c), external mass rank and number of complex couplings. Derive the numerator bound in (XVI.6.43) in the infinity chart. Explain why the vector Casimirs and the plumbing parameter are different entries in this calculation.

6. For $N = 2, 3, 4$, submit the ordered lists of dimensions and representation-component counts of $Q_{(k)}$. Derive the exterior-power component counts and distinguish composite moment maps in T_2 from independent free fields. Give the obstruction to an ordinary weak $\mathcal{N} = 2$ vector/hyper frame for isolated interacting T_N, addressing both abelian and nonabelian factors and stating what other ultraviolet possibilities it leaves open.

For benchmark submissions, see `benchmark/PROTOCOL.md`. Include the requested written derivations and explanations.

Exit checklist

The reader should be able to recover a differential basis including its infinity bound, distinguish fixed masses from Coulomb coordinates, and identify exactly which physical statements turn a fixture spectrum into free matter or an enhanced current algebra. For a gauging, the reader should specify the subgroup, level and charged hypers before calculating screening. For a comparison of frames, the reader should track a, c, graded Coulomb dimensions and continuous flavor data without promoting their agreement to a proof of all infrared observables. These operations prepare the anomaly calculation of the next chapter.

Sources and scope

Section 6.1. The full-puncture compactification and massless pole input are [GEO-E], using Gaiotto (2012, arXiv v1, pp. 41–42, Fig. 37e), the puncture dictionary of Chapter 5, and Gaiotto and Maldacena (2009, arXiv v4, p. 5). The rational bases, infinity transformation, graded counts and mass-rank arithmetic are [MATH]. The spectrum agrees with Maruyoshi et al. (2013, arXiv v2, eq. (2.1)). No physical existence or freeness theorem follows from the section count.

Section 6.2. The physical T_2 and rank-one T_3 identifications are [GEO-E], from Chacaltana and Distler (2010, arXiv v2, §5.2, pp. 15–16) and Gaiotto (2012, arXiv v1, §3.1, pp. 23–24). The named Higgs operators and their protected dimensions are [BPS], with protection by half-BPS shortening, from Maruyoshi et al. (2013, arXiv v2, §2.1, eqs. (2.1), (2.3)–(2.4)). The 72 roots, reflections, Cartan matrix and representation counts are [MATH]. Their assignment to physical E_6 moment maps remains the sourced fixture identification. No complete Higgs ring or global flavor quotient is determined.

Section 6.3. The flavor-level inputs are [ANOM], from Gaiotto and Maldacena (2009, arXiv v4, p. 5) and Argyres and Seiberg (2007, arXiv v3, eqs. (3.1)–(3.8), pp. 10–12). Their power here is one E_6 level and its index-one subgroup restrictions. The charge decomposition and trace conversion are [MATH]. The beta cancellation is [ANOM], conditional on the level and actual full-doublet content of Argyres and Seiberg (2007, arXiv v3, eq. (2.1), p. 5). In that source the displayed coefficient is $-2b_0$. Level extraction assumes the conformal frame and supplies no independent proof of it.

Section 6.4. The Argyres–Seiberg dual-frame proposal is retained as [CONJ+], using Argyres and Seiberg (2007, arXiv v3, §2, eqs. (2.1)–(2.2)), Gaiotto (2012, arXiv v1, pp. 23–25), and Chacaltana and Distler (2010, arXiv v2, p. 16). It is used as a sourced proposal with bounded comparisons, not as a newly derived duality. Effective anomaly subtraction uses Gaiotto and Maldacena (2009, arXiv v4, eqs. (2.1)–(2.4), pp. 5–6). The [ANOM] comparisons have power two independent conformal anomaly coefficients a, c and one flavor level. Their source premises overlap the dual-frame premise. Graded spectra and flavor-rank arithmetic are [MATH]. No absolute period normalization, coupling map or full infrared equivalence is derived.

Section 6.5. The gluing uses the [GEO-E] full-leg construction of Gaiotto and Maldacena (2009, arXiv v4, p. 5 and Fig. 2). The T_4 anomaly input is also tabulated in Chacaltana and Distler (2010, arXiv v2, §5.3, p. 19). Rational section dimensions are [MATH]; the additive anomaly and beta calculations are [ANOM], with power two anomaly coordinates and one beta coefficient. The ordinary weak $\mathcal{N} = 2$ obstruction combines the derived spectrum with the sourced interacting nature of T_N for $N \geq 3$. It is restricted to vector/hyper frames and does not exclude other ultraviolet realizations. General anomaly integration is deferred to Chapter 7.

References

Argyres, P. C. and N. Seiberg (2007). "S-duality in N=2 supersymmetric gauge theories". In: arXiv: 0711.0054 [hep-th].

Chacaltana, O. and J. Distler (2010). "Tinkertoys for Gaiotto Duality". In: arXiv: 1008.5203 [hep-th].

Gaiotto, D. (2012). "N=2 dualities". In: *JHEP* 08, p. 034. DOI: 10.1007/JHEP08(2012)034. arXiv: 0904.2715 [hep-th].

Gaiotto, D. and J. Maldacena (2009). "The Gravity duals of N=2 superconformal field theories". In: arXiv: 0904.4466 [hep-th].

Maruyoshi, K. et al. (2013). "N=1 dynamics with T_N theory". In: arXiv: 1305.5250 [hep-th].

Chapter XVI.7

From six-dimensional to four-dimensional anomalies

A four-dimensional class-S theory can have a weakly coupled gauge description in one region of its coupling space and an interacting trinion in another. An anomaly can be followed through that change without following the coupling. This makes anomalies useful observables of the construction itself. We will compute them by integrating the six-dimensional anomaly polynomial over the compactification curve, then adding the local contributions of its punctures.

The twist determines which background fields enter that integral. It does not determine the anomaly of a defect placed at a marked point. Keeping these operations distinct lets us compare a closed curve, a punctured sphere and a gauged trinion with one set of four-dimensional conventions. Our main example is the A_2 three-full-puncture sphere, whose effective anomaly coordinates are $(n_v, n_h) = (5, 16)$. Gauging a particular subgroup and adding a charged doublet produces the same anomaly polynomial as $SU(3)$ theory with six flavors.

We assume the twist of Chapter 2, the gluing operation of Chapter 3 and the full and simple punctures of Chapter 5. We recall characteristic roots where they enter the integral and derive the Weyl-fermion anomaly map before using flavor levels. The six-dimensional polynomial, the identification of the infrared R symmetry and the physical identity of each defect are inputs. Within those inputs we derive the coefficients, including finite-rank corrections. Equality of these coefficients tests a proposed frame change but does not establish an equivalence of its complete QFTs.

XVI.7.1 Insert the twist into I8

The question is how curvature of the compactification curve becomes an anomaly of the surviving R symmetry. The twist couples rotations on the curve to an R-symmetry connection. Consequently the R bundle acquires a root containing the curve curvature, and every term of the parent polynomial can contribute to the integral. We must expand before integrating.

Let the six-manifold be $M_4 \times C$, with the complex orientation on C. Write the four-dimensional background classes as

$$\begin{gathered} u = c_1(U(1)_r), \qquad c = c_2(SU(2)_R), \qquad p = p_1(TM_4), \\ t = c_1(TC), \qquad \int_C t = 2 - 2g. \end{gathered} \tag{XVI.7.1}$$

Here u, t have degree two and c, p degree four. For a fixed curve, a product containing t^2 vanishes upon restriction to its cohomology. We are integrating over a fixed compactification surface, rather than over a family of varying curves.

To fix the factors of two, choose $SU(2)_R$ fundamental roots $\pm y$. The second Chern class is $c = -y^2$, while its real three-dimensional adjoint bundle has roots $0, \pm 2y$. With the twist branch of Chapter 2, the rank-five R bundle $\mathcal{R}$ therefore has roots

$$\mathcal{R} \longleftrightarrow \{\pm(2u - t),\ \pm 2y,\ 0\}, \qquad c = -y^2. \tag{XVI.7.2}$$

The positive-r preserved supercharge has curve spin $+1/2$. Its R weight supplies $-t/2$, canceling that spin. The vector root contains $-t$, since a spinor weight is half the vector root. Replacing $2u - t$ with $u - t$ would change both the charge normalization and the polynomial.

For a real bundle with two nonzero root pairs $\pm n_1, \pm n_2$, the Pontryagin classes are $p_1 = n_1^2 + n_2^2$ and $p_2 = n_1^2 n_2^2$. Applying this rule gives

$$p_1(\mathcal{R}) = (2u - t)^2 - 4c, \qquad p_2(\mathcal{R}) = -4c(2u - t)^2. \tag{XVI.7.3}$$

The tangent bundle instead splits into the spacetime and curve tangent bundles. The Whitney formula gives

$$p_1(T_6) = p + t^2, \qquad p_2(T_6) = p_2(TM_4) + pt^2. \tag{XVI.7.4}$$

In particular the tangent classes themselves have no term linear in t. The mixed R background will supply that term.

For a six-dimensional interacting theory of ADE type G, use rank r_G, dimension d_G and dual Coxeter number $h_G^\vee$, and set $H = d_G h_G^\vee$. The parent anomaly input is

$$I_8[G] = r_G I_8[1] + \frac{H}{24} p_2(\mathcal{R}), \qquad I_8[1] = \frac{1}{48}\left[p_2(\mathcal{R}) - p_2(T_6) + \frac{1}{4}\big(p_1(T_6) - p_1(\mathcal{R})\big)^2\right]. \tag{XVI.7.5}$$

The symbol $I_8[1]$ denotes a free tensor multiplet polynomial. We take this six-dimensional expression as an anomaly input, rather than deriving the interacting theory from local tensor fields.

We can now isolate the terms which survive integration. Introduce $D_0 = p - 4u^2 + 4c$. Expanding the ingredients first gives

$$\begin{aligned} p_1(T_6) - p_1(\mathcal{R}) &= D_0 + 4ut, \\ p_2(\mathcal{R}) &= -16u^2 c + 16uct - 4ct^2, \\ [t]\big(p_1(T_6) - p_1(\mathcal{R})\big)^2 &= 8uD_0. \end{aligned} \tag{XVI.7.6}$$

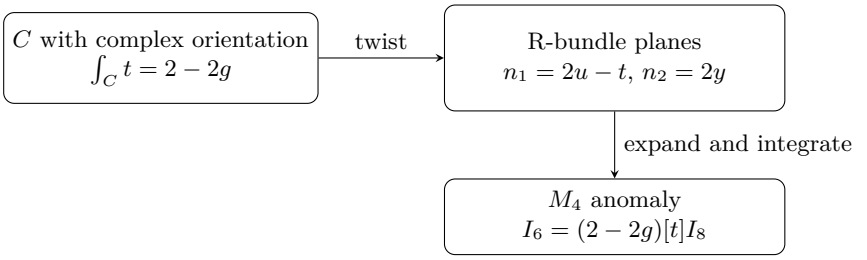


Figure XVI.7.1: The twist inserts the curve root into one plane of the rank-five R bundle. The second plane is the $SU(2)_R$ adjoint plane, with root $2y$. Only a term with one t is integrated over the oriented curve. The remaining classes live on M_4.

The cancellation of the two t^2 terms in the first line is exact. The notation $[t]$ extracts the coefficient of one power of t. Inserting the last line into the free-tensor polynomial displays the cubic and gravitational terms separately.

$$[t]I_8[1] = \frac{16uc + 2u(p - 4u^2 + 4c)}{48} = -\frac{u^3}{6} + \frac{up}{24} + \frac{uc}{2}. \tag{XVI.7.7}$$

The interacting contribution changes only the uc coefficient at this stage. Thus the complete linear term is

$$[t]I_8[G] = -\frac{r_G}{6}u^3 + \frac{r_G}{24}up + \left(\frac{r_G}{2} + \frac{2H}{3}\right)uc. \tag{XVI.7.8}$$

The term proportional to H will be responsible for cubic rank growth. Neither the tangent contribution nor r_G alone can reproduce it.

Multiplying by the Euler integral in (XVI.7.1) completes the pushforward.

$$I_6^{\text{closed}} = \int_C I_8[G] = (g-1)\left[r_G\left(\frac{u^3}{3} - \frac{up}{12}\right) - \left(r_G + \frac{4H}{3}\right)uc\right]. \tag{XVI.7.9}$$

The sign of $g - 1$ follows jointly from the oriented Euler class and the chosen twist. Flipping only the sign of t in (XVI.7.2), while keeping the orientation fixed, reverses this result. A change of convention must transform the preserved-charge identification as well.

For N M5-branes the interacting A_{N-1} theory has $r_G = N - 1$ and $H = N(N^2 - 1)$. Keeping the center tensor would instead use $r_G = N$ in the first term. Their four-dimensional difference is fixed, rather than chosen as a free four-dimensional hypermultiplet.

$$I_6^{\text{stack}} - I_6^{\text{interacting}} = (g-1)\left(\frac{u^3}{3} - \frac{up}{12} - uc\right). \tag{XVI.7.10}$$

For example at $N = 3, g = 2$ this adds one vector anomaly coordinate and no hyper coordinate in the map below. It is a subtraction of the parent center tensor, before adding any punctures. We will encounter a neutral hyper from self-gluing later; its origin and polynomial are different.

XVI.7.2 The bulk result on closed curves

The pushforward becomes a four-dimensional observable once its background fields are identified with the infrared $\mathcal{N}=2$ R symmetry. We use that physical identification for the closed class-S compactifications of genus at least two. To read the answer, introduce effective coordinates n_v, n_h by the polynomial

$$I_6^{R,\mathrm{grav}} = (n_v - n_h)\left(\frac{u^3}{3} - \frac{up}{12}\right) - n_v uc. \tag{XVI.7.11}$$

A vector multiplet component contributes $(1,0)$ and a full hypermultiplet component contributes $(0,1)$. This makes the coordinates convenient in a gauge frame. For an interacting trinion they remain anomaly coordinates, with no implication that elementary vectors or hypers exist.

Matching the two independent combinations in (XVI.7.9) and (XVI.7.11) yields

$$n_v = (g-1)A, \qquad n_h = (g-1)B, \qquad A = r_G + \frac{4H}{3}, \qquad B = \frac{4H}{3}. \tag{XVI.7.12}$$

In particular $n_v - n_h = (g-1)r_G$. The cubic rank term cancels in this difference but remains in the mixed R anomaly. Two coefficients therefore test different pieces of the six-dimensional input.

The standard $\mathcal{N}=2$ anomaly map gives the conformal central charges

$$a = \frac{5n_v + n_h}{24} = (g-1)\left(\frac{5r_G}{24} + \frac{H}{3}\right), \qquad c_{4d} = \frac{2n_v + n_h}{12} = (g-1)\left(\frac{r_G}{6} + \frac{H}{3}\right). \tag{XVI.7.13}$$

We write c_{4d} to distinguish the central charge from the background class $c = c_2(SU(2)_R)$. Section XVI.7.4 derives the fermionic conventions which enter this map.

Take the first nonabelian example, A_1 on a genus-two curve. Here $r_G = 1$ and $H = 3 \cdot 2 = 6$, so the integral gives

$$(A,B) = (9,8), \qquad (n_v, n_h) = (9,8), \qquad I_6 = \frac{u^3}{3} - \frac{up}{12} - 9uc. \tag{XVI.7.14}$$

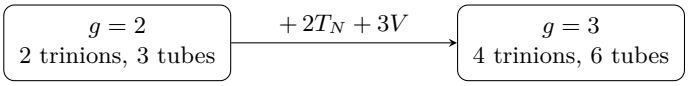
The associated charges are $a = 53/24$ and $c_{4d} = 13/6$. Increasing the genus by one doubles both coordinates in this example, because the Euler integral doubles.

$$A_1,\ g=3 \quad \Longrightarrow \quad (n_v, n_h) = (18,16), \qquad (a, c_{4d}) = \left(\frac{53}{12}, \frac{13}{3}\right). \tag{XVI.7.15}$$

This change can also be seen by cutting the surface into trinions. A closed genus-g surface contains $2g-2$ trinions and $3g-3$ internal tubes. For the A_1 construction a trinion is the half-trifundamental T_2, with $(0,4)$, and each tube gauges $SU(2)$ and adds three vector components. Hence

$$n_v = (3g-3)\cdot 3 = 9(g-1), \qquad n_h = (2g-2)\cdot 4 = 8(g-1). \tag{XVI.7.16}$$

The trinion identity is a physical input of the construction. This agreement tests additivity within it. We derive its puncture count in the next section rather than assuming that every trinion is free.



	$g=2$	$g=3$
A_1	$(9,8)$	$(18,16)$
A_2	$(34,32)$	$(68,64)$

Figure XVI.7.2: Changing genus adds two trinions and three gauge tubes. The finite-rank table distinguishes this linear topological change from a change in rank. Each pair denotes (n_v, n_h). The trinion and tube interpretation uses the class-S construction, while the same totals follow from the smooth-curve integral.

Changing the rank at fixed genus gives a less uniform change. For A_2 at genus two, $r_G = 2$ and $H = 8 \cdot 3 = 24$. Then

$$(n_v, n_h) = (34, 32), \qquad I_6 = 2\left(\frac{u^3}{3} - \frac{up}{12}\right) - 34uc, \qquad (a, c_{4d}) = \left(\frac{101}{12}, \frac{25}{3}\right). \tag{XVI.7.17}$$

Two T_3 blocks and three $SU(3)$ tubes give $2(5,16) + 3(8,0) = (34,32)$. The replacement of a free trinion by the interacting T_3 preserves the additive rule while changing the physical constituents.

For general A_{N-1}, insert $r_G = N - 1$ and $H = N^3 - N$ before taking any limit.

$$n_v = (g-1)\frac{4N^3 - N - 3}{3}, \qquad n_h = (g-1)\frac{4N^3 - 4N}{3}. \tag{XVI.7.18}$$

The exact central charges follow by one substitution.

$$\begin{aligned} a &= (g-1)\left(\frac{N^3}{3} - \frac{N}{8} - \frac{5}{24}\right), \\ c_{4d} &= (g-1)\left(\frac{N^3}{3} - \frac{N}{6} - \frac{1}{6}\right), \qquad a - c_{4d} = \frac{(g-1)(N-1)}{24}. \end{aligned} \tag{XVI.7.19}$$

At large N and fixed genus both charges start with $(g-1)N^3/3$. Their difference is only linear in N. The common cubic growth comes from the $Hp_2(\mathcal{R})$ term; dropping it would leave an answer linear in rank.

There is a necessary exception to direct substitution. For the unpunctured torus the formal integral has Euler number zero. The compactification is separately identified with enhanced $\mathcal{N} = 4$ Yang–Mills, whose superconformal R symmetry requires additional zero-mode and R-symmetry information. For $SU(2)$, its $\mathcal{N} = 2$ vector and adjoint hyper give

$$\int_C I_8\Big|_{g=1} = 0, \qquad I_6^{\mathcal{N}=4\ SU(2)} = I_6(3,3) = -3uc. \tag{XVI.7.20}$$

Thus a vanishing formal integral is not the full enhanced infrared anomaly. Our physical closed examples use integer $N \geq 2$ and $g \geq 2$. With punctures the necessary stability

condition will be $2g-2+n>0$. This condition selects a geometric domain; it is not an existence criterion for arbitrary proposed defect assignments.

XVI.7.3 Anomalies of punctures

A smooth bulk integral knows the genus and the parent theory but cannot distinguish two defect boundary conditions at the same marked point. We therefore supply local regular-defect anomalies in addition to the bulk answer. The first task is to make the separation unambiguous, since one can assign part of the Euler contribution either to the puncture or to the surface with a small disk removed.

In the closed-curve prescription, retain (XVI.7.12) and add corrections $\delta_v(P),\delta_h(P)$ for each puncture P.

$$n_v=(g-1)A+\sum_{i=1}^{n}\delta_v(P_i),\qquad n_h=(g-1)B+\sum_{i=1}^{n}\delta_h(P_i). \tag{XVI.7.21}$$

For the full and simple regular A_{N-1} punctures, let p_k be the allowed pole order of the degree-k differential and let ℓ_j be the rows of the diagram transposed from the Nahm block partition. The local anomaly input is

$$\delta_v(P)=\sum_{k=2}^{N}(2k-1)p_k,\qquad \delta_h(P)-\delta_v(P)=\frac{1}{2}\left(\sum_j \ell_j^2-N\right). \tag{XVI.7.22}$$

The first sum weights degree-k Coulomb parameters by $2k-1$. The second term depends on the defect label even after the bulk is fixed. These rules are additional defect information, rather than a consequence of integrating the smooth polynomial.

A full puncture has Nahm partition $[1^N]$, transposed rows $[N]$ and pole orders $p_k=k-1$. Performing the finite sum gives

$$\begin{aligned}\delta_v(F)&=\sum_{k=2}^{N}(2k-1)(k-1)=\frac{N(N-1)(4N+1)}{6},\\ \delta_h(F)&=\delta_v(F)+\frac{N^2-N}{2}=\frac{2N(N^2-1)}{3}.\end{aligned} \tag{XVI.7.23}$$

A simple puncture instead has Nahm partition $[N-1,1]$, rows $[2,1^{N-2}]$ and $p_k=1$. Therefore

$$\delta_v(S)=\sum_{k=2}^{N}(2k-1)=N^2-1,\qquad \delta_h(S)=\delta_v(S)+\frac{4+(N-2)-N}{2}=N^2. \tag{XVI.7.24}$$

At $N=2$ the two partitions coincide, as do these formulas. At $N=3$ they differ, so replacing one full puncture changes the answer without changing the genus.

To derive the alternative allocation, remove one disk around each puncture. The resulting Euler characteristic is $2-2g-n$. Its bulk contribution is proportional to

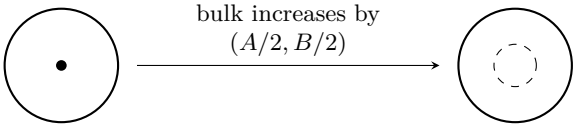


Figure XVI.7.3: The same marked surface in two prescriptions. Keeping a marked disk assigns $(A/2, B/2)$ less to the bulk and that much more to its local correction. Removing the disk shifts the bulk and the local term oppositely. Physical totals agree only when the two prescriptions are used consistently.

$g - 1 + n/2$. Equality of the total anomalies requires

$$n_v(P) = \delta_v(P) - \frac{A}{2}, \qquad n_h(P) = \delta_h(P) - \frac{B}{2}. \tag{XVI.7.25}$$

Indeed the two halves cancel separately for every puncture, giving

$$\begin{aligned} n_v &= \left(g - 1 + \frac{n}{2}\right) A + \sum_i n_v(P_i) = (g-1)A + \sum_i \delta_v(P_i), \\ n_h &= \left(g - 1 + \frac{n}{2}\right) B + \sum_i n_h(P_i) = (g-1)B + \sum_i \delta_h(P_i). \end{aligned} \tag{XVI.7.26}$$

Local numbers in the excised prescription need not be positive. They measure a difference relative to the excised bulk and do not count physical negative multiplets.

For A_2, the bulk pair is $(A, B) = (34, 32)$. The local terms are particularly transparent.

	δ_v	δ_h	$n_v(P)$	$n_h(P)$
F	13	16	-4	0
S	8	9	-9	-7

(XVI.7.27)

A sphere with three full punctures can now be calculated in either prescription, including every term.

$$\begin{aligned} (n_v, n_h)_{FFF} &= -(34, 32) + 3(13, 16) = (5, 16), \\ (n_v, n_h)_{FFF} &= \tfrac{1}{2}(34, 32) + 3(-4, 0) = (5, 16). \end{aligned} \tag{XVI.7.28}$$

Using the closed bulk together with the excised corrections would give $(-46, -32)$. The problem would be the mixed allocation, not a failure of anomaly additivity.

Replace the third puncture by a simple one. Its closed correction decreases by $(5, 7)$, so the same sphere becomes

$$\begin{aligned} (n_v, n_h)_{FFS} &= -(34, 32) + 2(13, 16) + (8, 9) = (0, 9), \\ (n_v, n_h)_{FFS} &= \tfrac{1}{2}(34, 32) + 2(-4, 0) + (-9, -7) = (0, 9). \end{aligned} \tag{XVI.7.29}$$

The sourced physical fixture is a full bifundamental hypermultiplet of two $SU(3)$ groups, with nine hyper components. The anomaly coordinates agree with this description. The fact that $n_v = 0$ alone would not establish that the fixture is free.

The algebra also explains why the full-full-simple fixture has the same simple count at higher rank. Since $2\delta_h(F) = B$ and $2\delta_v(F) = A - (N^2 - 1)$, one obtains

$$(n_v, n_h)_{FFS} = (-A + 2\delta_v(F) + \delta_v(S),\, -B + 2\delta_h(F) + \delta_h(S)) = (0, N^2). \quad \text{(XVI.7.30)}$$

The simple-puncture vector correction completes the cancellation of the bulk vector coordinate. For example A_3 has $(A, B) = (83, 80)$ and local full/simple pairs $(34, 40)$ and $(15, 16)$, giving $(-83, -80) + 2(34, 40) + (15, 16) = (0, 16)$.

For three full punctures the same finite sums instead yield

$$n_v(T_N) = \frac{2N^3}{3} - \frac{3N^2}{2} - \frac{N}{6} + 1, \qquad n_h(T_N) = \frac{2}{3}(N^3 - N). \quad \text{(XVI.7.31)}$$

At $N = 2$ this gives $T_2 = (0, 4)$. Its physical description is a half hyper in $(\mathbf{2}, \mathbf{2}, \mathbf{2})$, whose representation has complex dimension eight and hence four full-hyper anomaly units. At $N = 3$ it gives the interacting T_3 in (XVI.7.28). These identities let us use the trinion contributions in a gluing calculation while keeping their physical source separate from the local arithmetic.

XVI.7.4 Central charges and flavor levels

We now fix the four-dimensional normalization directly from left-handed Weyl fermions. This step matters twice. It determines how to read a, c_{4d} from the integrated polynomial, and it prevents a factor of two in a flavor coefficient from being confused with the factor used in a gauge beta function.

For a Weyl fermion with total background root x, the index density is the degree-six part of $\widehat{A}(T)\,\mathrm{ch}$.

$$\widehat{A}(T) = 1 - \frac{p}{24} + \cdots, \qquad e^x = 1 + x + \frac{x^2}{2} + \frac{x^3}{6} + \cdots, \qquad I_6^{\mathrm{Weyl}} = \frac{x^3}{6} - \frac{xp}{24}. \quad \text{(XVI.7.32)}$$

A vector multiplet has two gauginos of $r = +1$, forming an $SU(2)_R$ doublet. Their roots are $u + y$ and $u - y$. Summing their characters before replacing $y^2 = -c$ gives

$$\begin{aligned} I_6^v &= \frac{(u+y)^3 + (u-y)^3}{6} - \frac{2up}{24} \\ &= \frac{u^3}{3} + uy^2 - \frac{up}{12} = \frac{u^3}{3} - \frac{up}{12} - uc. \end{aligned} \quad \text{(XVI.7.33)}$$

A full hyper component has two $SU(2)_R$ singlet Weyl fermions of $r = -1$. It contributes

$$I_6^h = 2\left(\frac{(-u)^3}{6} - \frac{(-u)p}{24}\right) = -\frac{u^3}{3} + \frac{up}{12}. \quad \text{(XVI.7.34)}$$

Adding n_v vector and n_h hyper contributions reproduces (XVI.7.11). Taking traces over the same fermions gives a second useful form. Here I_3 is the Cartan generator of $SU(2)_R$, with doublet eigenvalues $+1/2$ and $-1/2$.

$$\operatorname{Tr} r^3 = \operatorname{Tr} r = 2(n_v - n_h), \qquad \operatorname{Tr} r I_3^2 = n_v \left[\left(\tfrac{1}{2}\right)^2 + \left(-\tfrac{1}{2}\right)^2 \right] = \frac{n_v}{2}. \tag{XVI.7.35}$$

The mixed R coefficient is consequently $-2 \operatorname{Tr} r I_3^2$. Equality of $\operatorname{Tr} r$ and $\operatorname{Tr} r^3$ means that the two displayed trace tests are linked, rather than independent measurements.

One can obtain the conformal map by choosing an $\mathcal{N} = 1$ subalgebra with $R_1 = r/3 + 4I_3/3$. Inserting the $\mathcal{N} = 2$ traces into the $\mathcal{N} = 1$ Weyl-anomaly formulas gives

$$\begin{aligned} \operatorname{Tr} R_1 &= \tfrac{1}{3} \operatorname{Tr} r, \qquad \operatorname{Tr} R_1^3 = \tfrac{1}{27} \operatorname{Tr} r^3 + \tfrac{16}{9} \operatorname{Tr} r I_3^2, \\ a &= \tfrac{3}{32}(3 \operatorname{Tr} R_1^3 - \operatorname{Tr} R_1) = \frac{5n_v + n_h}{24}, \\ c_{4d} &= \tfrac{1}{32}(9 \operatorname{Tr} R_1^3 - 5 \operatorname{Tr} R_1) = \frac{2n_v + n_h}{12}. \end{aligned} \tag{XVI.7.36}$$

The background must be the superconformal R symmetry for these to be the conformal central charges. This is the physical identification used for the class-S examples, including their interacting trinions.

For a nonabelian flavor group F, set $\operatorname{tr}_{\mathrm{f}} T^a T^b = \delta^{ab}/2$ and define

$$k_F \delta^{ab} = -2 \operatorname{Tr}(r T^a T^b), \qquad c_2(F) \text{ in fundamental unit-instanton normalization.} \tag{XVI.7.37}$$

A full fundamental hyper contains fermions in the fundamental and its conjugate. Each has $r = -1$ and quadratic index $1/2$, so $k_F = 2$. The Chern-character calculation fixes its polynomial coefficient without using a beta function. Write d_{f} for the dimension of the fundamental representation.

$$\operatorname{ch}_{\mathrm{f}}(F) = d_{\mathrm{f}} - c_2(F) + \cdots, \qquad \left[e^{-u} \left(\operatorname{ch}_{\mathrm{f}} + \operatorname{ch}_{\bar{\mathrm{f}}} \right) \right]_6 \supset 2u c_2(F). \tag{XVI.7.38}$$

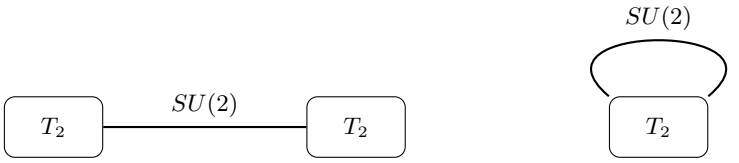
Thus the complete selected polynomial and the one-loop gauging test use different appearances of the same level.

$$I_6 = I_6^{R,\mathrm{grav}} + \sum_F k_F u c_2(F), \qquad b_0 = 2h^\vee - \frac{1}{2} \sum_i k_i. \tag{XVI.7.39}$$

The polynomial coefficient is k_F, while the matter contribution to b_0 is $k_F/2$. An embedding of a subgroup multiplies the level by its embedding index before either formula is applied.

As a complete weakly coupled example, glue two T_2 blocks along one $SU(2)$ leg. Each supplies four hyper units and the tube adds three vector units. Independently, $SU(2)$ with four full fundamental hypers contains four times two hyper components and three adjoint vector components. Both counts give

$$(n_v, n_h) = (3, 8), \qquad I_6 = 3I_6^v + 8I_6^h = -\frac{5}{3}u^3 + \frac{5}{12}up - 3uc. \tag{XVI.7.40}$$



two blocks and one tube
$(0,4)+(0,4)+(3,0)=(3,8)$

one block and one tube
$\mathbf{2}\otimes\mathbf{2}=\mathbf{3}\oplus\mathbf{1}$
$(n_v,n_h)=(3,4)$

Figure XVI.7.4: Two different operations on T_2. Gluing two trinions adds an $SU(2)$ vector and gives four-flavor SQCD. Gluing two legs of the same trinion instead restricts $\mathbf{2}\otimes\mathbf{2}$ to $\mathbf{3}\oplus\mathbf{1}$. The resulting adjoint hyper is accompanied by a neutral hyper. Both operations add the gauge vector, but only the second produces this representation decomposition.

The central charges are therefore

$$a=\frac{15+8}{24}=\frac{23}{24},\qquad c_{4d}=\frac{6+8}{12}=\frac{7}{6}. \tag{XVI.7.41}$$

The puncture prescription gives the same result directly on the four-full-puncture sphere, $-(9,8)+4(3,4)=(3,8)$. Omitting the tube would leave $(0,8)$ and erase the entire uc coefficient.

For a leg of T_2, the half-trifundamental supplies four Weyl doublets under that $SU(2)$. Their $r=-1$ trace yields $k=4$. Gluing the two legs therefore gives

$$k_{T_2\text{ leg}}=-2\left(-4\cdot\frac{1}{2}\right)=4,\qquad b_0=4-\frac{4+4}{2}=0. \tag{XVI.7.42}$$

This is a direct free-fermion normalization check. At higher rank the full regular leg has sourced level $2N$; two such legs cancel $2h^\vee=2N$ when gauged diagonally.

Self-gluing makes a once-punctured torus. The anomaly sum uses just one T_2 and one tube, so it gives $(3,4)$. The singlet in Figure XVI.7.4 explains why it differs from a vector plus only an adjoint hyper. Under the diagonal gauge group,

$$(\mathbf{2}\otimes\mathbf{2},\mathbf{2}_F)=(\mathbf{3},\mathbf{2}_F)\oplus(\mathbf{1},\mathbf{2}_F),\qquad \tfrac{1}{2}(6+2)=3+1. \tag{XVI.7.43}$$

The half hyper in the first summand is one adjoint full-hyper equivalent; the second is one neutral full-hyper equivalent. Consequently

$$I_6^{\text{once punctured}}=3I_6^v+4I_6^h=-\frac{u^3}{3}+\frac{up}{12}-3uc,\qquad (a,c_{4d})=\left(\frac{19}{24},\frac{5}{6}\right). \tag{XVI.7.44}$$

Removing the neutral hyper gives $-3uc$, changing the cubic and gravitational terms. This neutral sector comes from a representation under self-gluing. It is distinct from the center tensor removed in (XVI.7.10), and the once-punctured torus obeys the stable-curve condition that the unpunctured torus fails.

XVI.7.5 Comparing a non-Lagrangian frame

The A_2 three-full-puncture sphere is the first example where the trinion anomaly is not that of a collection of free hypers. Its physical identification is the T_3 theory with E_6 flavor symmetry. We use that sourced identification to compare the proposed Argyres–Seiberg frames. The local anomaly calculation by itself does not establish the symmetry enhancement or the frame equivalence.

Begin with the pair already derived in (XVI.7.28). Its four-dimensional observables are

$$\begin{aligned} I_6(T_3) &= -\frac{11}{3}u^3 + \frac{11}{12}up - 5uc, \\ a(T_3) &= \frac{25+16}{24} = \frac{41}{24}, \qquad c_{4d}(T_3) = \frac{10+16}{12} = \frac{13}{6}. \end{aligned} \tag{XVI.7.45}$$

The negative $n_v - n_h = -11$ is consistent with positive central charges. An individual anomaly coefficient is a signed fermion trace, not a count of all states.

For the weak frame, take $SU(3)$ gauge theory with six full fundamental hypers. The adjoint has dimension eight and each fundamental has dimension three. The multiplicity factors give

$$n_v^{\mathrm{w}} = 3^2 - 1 = 8, \qquad n_h^{\mathrm{w}} = 6 \cdot 3 = 18, \qquad I_6^{\mathrm{w}} = -\frac{10}{3}u^3 + \frac{5}{6}up - 8uc. \tag{XVI.7.46}$$

The proposed strong frame gauges an index-one $SU(2)$ subgroup of the E_6 symmetry of T_3 and contains one additional full gauge doublet. That doublet is charged at finite gauge coupling. Its two representation components supply $n_h = 2$, rather than one neutral hyper unit. Adding each contribution yields

$$\begin{aligned} (n_v, n_h)^{\mathrm{s}} &= (5,16) + (3,0) + (0,2) = (8,18), \\ I_6^{\mathrm{s}} &= I_6(T_3) + 3I_6^v + 2I_6^h = -\frac{10}{3}u^3 + \frac{5}{6}up - 8uc. \end{aligned} \tag{XVI.7.47}$$

This is equality of the whole selected R/gravity polynomial. In conformal coordinates it gives

$$a^{\mathrm{w}} = a^{\mathrm{s}} = \frac{40+18}{24} = \frac{29}{12}, \qquad c_{4d}^{\mathrm{w}} = c_{4d}^{\mathrm{s}} = \frac{16+18}{12} = \frac{17}{6}. \tag{XVI.7.48}$$

The source proposal supplies the identification of the two frames. The sum shows how the proposed interacting constituent participates in anomaly matching without an elementary-field description of T_3.

The charged doublet is required by the gauge anomaly normalization as well. Use the sourced E_6 level $k_{E_6} = 6$ and embedding indices one for $SU(2)$ and $SU(6)$. Restriction gives

$$k_{SU(2)\subset E_6} = 1 \cdot 6 = 6, \qquad k_{\text{full doublet}} = 2, \qquad b_0^{SU(2)} = 4 - \frac{6}{2} - \frac{2}{2} = 0. \tag{XVI.7.49}$$

At zero gauge coupling the doublet is free as a field theory sector, but at finite coupling it interacts with the gauge vector. Calling it a neutral free hyper would lose its beta-function contribution and its representation dimension. The source determination of

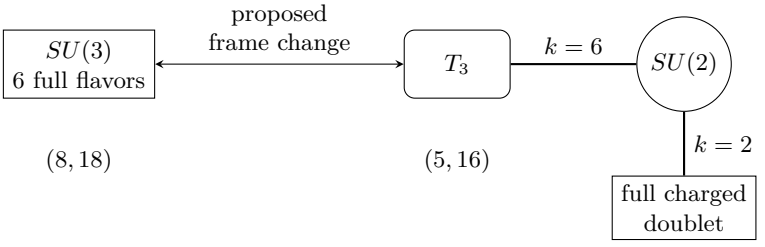


Figure XVI.7.5: The proposed Argyres–Seiberg frames. The weak frame has six full $SU(3)$ fundamentals. The other frame gauges an index-one $SU(2)$ subgroup of T_3 and includes a full charged doublet. Both have $(n_v, n_h) = (8, 18)$. Restricting the sourced E_6 level to the commuting $SU(6)$ gives one additional specified flavor coefficient.

$k_{E_6} = 6$ itself uses conformality of this proposed gauging. Replaying (XVI.7.49) with that value is a consistency check of conventions, rather than independent evidence for conformality.

There is a further flavor comparison which is not obtained just by rewriting a and c_{4d}. In the weak frame, the two conjugate hyper fermion representations each contain three color copies of an $SU(6)$ fundamental or antifundamental. Their trace is

$$k^{\mathrm{w}}_{SU(6)} = -2\left[(-1)\cdot 2\cdot 3\cdot\frac{1}{2}\right] = 6, \qquad k^{\mathrm{s}}_{SU(6)} = 1\cdot k_{E_6} = 6. \tag{XVI.7.50}$$

The extra gauge doublet is an $SU(6)$ singlet. Including this flavor background, the compared part of the polynomial is therefore

$$I_6^{\mathrm{w}} = I_6^{\mathrm{s}} = -\frac{10}{3}u^3 + \frac{5}{6}up - 8uc + 6uc_2(SU(6)). \tag{XVI.7.51}$$

Abelian puncture levels and global group quotients are outside this calculation. The displayed nonabelian flavor class has the same unit-instanton convention as (XVI.7.38).

Changing one constituent explains the force of the comparison. If the charged full doublet is omitted, the strong pair becomes $(8, 16)$. If it is replaced by one neutral hyper, the pair becomes $(8, 17)$ and the $SU(2)$ beta coefficient is one. The respective polynomial errors relative to the proposed frame are

$$\Delta I_6^{\mathrm{omit}} = -2I_6^h = \frac{2}{3}u^3 - \frac{1}{6}up, \qquad \Delta I_6^{\mathrm{neutral}} = -I_6^h = \frac{1}{3}u^3 - \frac{1}{12}up. \tag{XVI.7.52}$$

Neither error changes the uc term, so checking that term alone would miss both mistakes. Adding four neutral Goldstone hypers from the different puncture-closure flow of Chapter 5 would instead shift I_6 by $4I_6^h$. Those fields belong to that flow, not to either frame here.

The number of independent conditions also matters. In an $\mathcal{N} = 2$ R background, the u^3 and up coefficients are tied by $\mathrm{Tr}\, r^3 = \mathrm{Tr}\, r$. The R/gravity part has two independent coordinates, equivalently (n_v, n_h) or (a, c_{4d}). The specified $SU(6)$ term supplies one more flavor coefficient. The defect formulas and T_N anomaly formulas

use overlapping class-S and generalized-duality inputs, so their agreement with this proposed frame cannot be counted as an independent proof of the duality. What the calculation establishes is that the sourced local assignments, the smooth integral and the four-dimensional fermion conventions give the same selected observables.

Take-home message

The twist turns the six-dimensional characteristic polynomial into a four-dimensional one by inserting the curve root in the R bundle and retaining the term linear in that root. Defects supply separate local contributions. Moving a half-Euler contribution between a puncture and the bulk changes the allocation but leaves the total fixed. The resulting n_v, n_h determine two independent R/gravity anomaly coordinates, while a specified flavor level adds a further coefficient. A reader should now be able to reproduce the smooth integral, change a full puncture to a simple one, add a gauge tube, retain the singlet of self-gluing and compare the proposed Argyres–Seiberg frames with the charged doublet present. These operations compute anomalies within the physical compactification and defect identifications; they do not replace those identifications.

Exercises

1. Expand the parent polynomial using (XVI.7.2). Submit the coefficients of u^3, up, uc in $[t]I_8[G]$, as expressions in r, H, and the coefficients of these monomials in the genus-two free-center difference. Derive the intermediate square explicitly in a written answer. Explain why only a single t survives on a fixed curve and which physical assumptions are needed to interpret its integral.

2. Compute (n_v, n_h, a, c_{4d}) for A_3 at genus three. Submit also the coefficients of N^3 in a and c_{4d} at general genus g, and the formal genus-one integral. Explain why that zero does not compute the enhanced unpunctured-torus anomaly, using the $SU(2)$ example.

3. For A_3, compute the full and simple local pairs in both prescriptions, then the FFS total. Submit all ten numbers. Derive the conversion from the Euler characteristic of the excised surface. Explain which defect information the smooth integral lacks and why $(n_v, n_h) = (0, 16)$ alone would not identify a free fixture.

4. Starting with the Weyl roots, derive the $SU(2)$ four-flavor polynomial and submit its u^3, up, uc coefficients, a, c_{4d}, the level of one full fundamental hyper and the gluing beta coefficient. Explain in writing why the polynomial uses k and the beta function uses $k/2$. Include a trace or character calculation rather than quoting those factors.

5. Self-glue two legs of T_2. Submit the total pair, the pair after discarding the neutral singlet, and the three polynomial coefficients of the total. Explain the representation decomposition and distinguish this singlet from the six-dimensional center tensor and the charged doublet in the next exercise.

6. Compute the two AS-frame pairs, a, c_{4d} and $k_{SU(6)}$. Submit the strong-frame cubic coefficient with the full doublet, after omitting it and after replacing it by one neutral hyper, together with the three corresponding gauge beta coefficients. Explain which displayed conditions are independent, where conformality entered the source level, and why matching these anomalies does not prove the proposed duality.

For benchmark submissions, see `benchmark/PROTOCOL.md`. Equivalent rational and symbolic expressions are accepted. Include the derivations, physical interpretations and source-dependence arguments.

Sources and scope

Section 7.1. The ADE polynomial and center tensor are sourced [ANOM] inputs from Bah and Nardoni (2018, arXiv:1803.00136v2, pp. 7–8, eqs. (2.6)–(2.7), Table 1). The R-root convention is the twist of Chapter 2. The expansion, linear coefficient and pushforward are explicit [ANOM] calculations conditional on that input and on the preserved-background identification. The free-center difference is a parent-tensor subtraction. It is not a choice of absolute theory or a puncture contribution.

Section 7.2. The finite-rank formulas and leading cubic coefficients are computed [ANOM]. The bulk expression and anomaly map are anchored to Bah and Nardoni (2018, arXiv v2, eqs. (2.10), (2.13)–(2.15), Appendix A). The physical class-S/R identification and the trinion construction are [GEO-E] inputs. The unpunctured-torus caveat is explicit in that source, p. 6, footnote 3, and in Chapter 1. Formal genus-one zero does not give the full enhanced R anomaly. Integer rank and stable topology are necessary domain conditions, not SCFT existence tests.

Section 7.3. The closed local rule is sourced [ANOM] from Chacaltana and Distler (2010, arXiv:1008.5203v2, printed pp. 8–10, eqs. (9)–(11)); the excised prescription is compared with Bah and Nardoni (2018, arXiv v2, Appendix C, eqs. (C.3)–(C.7)). Transposition from Nahm blocks to the rows used here is explicit. The conversion and FFF/FFS sums are calculated [ANOM]. Physical fixture identities are [GEO-E], from Chacaltana–Distler, printed p. 14 for T_2, p. 15 for the A_2 bifundamental and E_6 fixture, and p. 18 for the A_3 bifundamental. See also Gaiotto and Maldacena (2009, arXiv:0904.4466v4, p. 7). No general irregular or twisted puncture construction is inferred.

Section 7.4. The degree-six Weyl expansions, gluing sums and self-gluing comparison are calculated [ANOM]. Characteristic-class conventions and anomaly maps are anchored to Bah and Nardoni (2018, arXiv v2, eqs. (A.5)–(A.8), (B.3)–(B.13)) and Gaiotto and Maldacena (2009, arXiv v4, eq. (2.1)). The $\mathcal{N} = 1$ Weyl-anomaly formulas used to recover a, c_{4d} are general formalism. The T_2 and gluing identifications are the sourced physical inputs of Chapters 2–3. The flavor polynomial coefficient is k, while beta uses $k/2$ in the stated fundamental trace convention. No abelian level or global group quotient is claimed.

Section 7.5. The AS proposal remains [CONJ+], using Argyres and Seiberg (2007, arXiv:0711.0054v3, p. 5, eq. (2.1)). Its index-one embeddings, $k_{E_6} = 6$ and flavor

comparison use pp. 11–12, eqs. (3.6)–(3.8). The two R/gravity coordinates and the specified $SU(6)$ coefficient are calculated [ANOM]. The level extraction shares the conformal-gauging premise. The T_N anomaly assignments also share generalized-duality inputs, as in Gaiotto and Maldacena (2009, arXiv v4, eqs. (2.2)–(2.4)). Agreement is conditional consistency, not independent proof of duality.

References

Argyres, P. C. and N. Seiberg (2007). "S-duality in N=2 supersymmetric gauge theories". In: arXiv: 0711.0054 [hep-th].

Bah, I. and E. Nardoni (2018). "Structure of Anomalies of 4d SCFTs from M5-branes, and Anomaly Inflow". In: arXiv: 1803.00136 [hep-th].

Chacaltana, O. and J. Distler (2010). "Tinkertoys for Gaiotto Duality". In: arXiv: 1008.5203 [hep-th].

Gaiotto, D. and J. Maldacena (2009). "The Gravity duals of N=2 superconformal field theories". In: arXiv: 0904.4466 [hep-th].

Chapter XVI.8

Higgs branches and three-dimensional mirrors

A strongly coupled trinion need not have an elementary-field Lagrangian, yet its Higgs branch can sometimes be calculated using a different gauge theory. Circle reduction provides the bridge. In three dimensions a mirror exchanges Higgs and Coulomb branches, so monopole operators of a star-shaped quiver can describe Higgs operators of the original four-dimensional theory. The punctures determine its legs. The choice of gauge group determines which magnetic charges are allowed.

We construct the stars for T_2, T_3 and the four-punctured A_1 sphere. Their first protected coefficients will expose free fields, the E_6 root system and the D_4 root system, respectively. A separate Higgs quotient calculation for $SU(2)$ with four full flavors supplies a comparison on the original side. The mirror assignment and Higgs-branch protection are physical inputs. We calculate dimensions, charge sums and selected representation dimensions within those inputs.

The reader should know the full and simple punctures of Chapter 5, the trinion and gauging constructions of Chapters 3 and 6, and the hyperkähler quotient from the supersymmetric gauge-theory foundations. We recall the moment maps explicitly in the smallest tail. All masses and FI parameters vanish. We keep the singular affine varieties, choose one complex structure, and count holomorphic operators rather than all states.

XVI.8.1 Circle reduction and the branches being compared

The first task is to identify which branch survives the comparison. Compactification on a supersymmetric circle of radius R gives a three-dimensional theory at energies $E \ll R^{-1}$. Its Higgs branch is protected under this reduction. The proposed mirror $\mathcal{Q}$ exchanges the two branches in the infrared. In the chosen complex structure the

comparison is

$$\mathcal{H}_{4d} \simeq \mathcal{H}_{3d} \simeq \mathcal{C}(\mathcal{Q}), \qquad E \ll R^{-1}, \qquad m = \zeta = 0. \tag{XVI.8.1}$$

The second identification uses the mirror proposal. Equality of dimensions below is a necessary check on it, rather than a construction of the identification itself.

A quaternionic coordinate contains two complex or four real coordinates. Thus every branch dimension must be converted with the same convention.

$$d_{\mathbb{C}} = 2d_{\mathbb{H}}, \qquad d_{\mathbb{R}} = 4d_{\mathbb{H}}. \tag{XVI.8.2}$$

For a gauge theory with effective compact group G, the Coulomb branch has quaternionic dimension $\operatorname{rank} G$. At a generic point, its vector multiplet supplies one triplet of real scalars and one dual photon for each Cartan generator. Quantum effects change the geometry and singularities but preserve this dimension.

$$\dim_{\mathbb{H}} \mathcal{C} = \operatorname{rank} G, \qquad \dim_{\mathbb{R}} \mathcal{C} = 4 \operatorname{rank} G. \tag{XVI.8.3}$$

A Higgs quotient uses a different subtraction. If the hypermultiplet space has quaternionic dimension n and the effective group acts freely on the regular zero level of its moment maps, the three real equations and the gauge orbit remove four real dimensions per generator.

$$\dim_{\mathbb{R}}(V/\!/\!/G) = 4n - 3\dim G - \dim G, \qquad \dim_{\mathbb{H}}(V/\!/\!/G) = n - \dim G. \tag{XVI.8.4}$$

This counts a regular, fully broken principal component. A stabilizer or an excess component invalidates that direct subtraction. A singular tangent space can also have dimension larger than its component.

For T_3 the star will have central $U(3)$, three $U(2)$ nodes and three $U(1)$ nodes. One diagonal $U(1)$ acts on no hypermultiplet. Removing it gives

$$d_{\mathbb{H}}\mathcal{C}(T_3^{\text{mir}}) = 3 + 3(2+1) - 1 = 11, \qquad (d_{\mathbb{C}}, d_{\mathbb{R}}) = (22, 44). \tag{XVI.8.5}$$

The same quiver has hypermultiplet representation dimension 24 and effective group dimension 23. Its own regular Higgs quotient therefore has quaternionic dimension one. This branch belongs to the other side of the mirror exchange.

$$\dim_{\mathbb{H}} \mathcal{H}(T_3^{\text{mir}}) = 24 - 23 = 1 \quad \text{on the regular fully broken locus.} \tag{XVI.8.6}$$

Confusing these two subtractions would assign one instead of eleven to the Higgs branch of the four-dimensional trinion.

There are two examples with elementary four-dimensional fields. The T_2 half hyper in the trifundamental has eight complex scalar coordinates. Four full $SU(2)$ flavors instead have quaternionic matter dimension eight and a gauge group of dimension three.

	$d_{\mathbb{H}}$	$d_{\mathbb{C}}$	$d_{\mathbb{R}}$
T_2	4	8	16
$SU(2),\ N_f = 4$	$8 - 3 = 5$	10	20

(XVI.8.7)

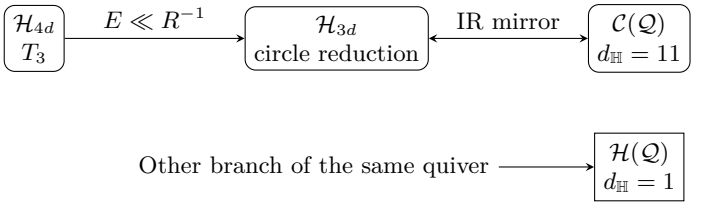


Figure XVI.8.1: The compared holomorphic symplectic branches. Circle reduction preserves the Higgs branch, and the sourced infrared mirror exchanges it with the star Coulomb branch. The lower branch is the mirror's own Higgs quotient and has a different dimension. These arrows do not assert equality of finite-radius metrics.

The $SU(2)$ subtraction will be justified directly by its moment-map shell in Section 4. The stars give ranks $2+3-1=4$ and $2+4-1=5$, respectively, agreeing with these dimensions.

The purpose of the star is now precise. It replaces an inaccessible Higgs-operator calculation by a magnetic-charge sum. Neither a finite-radius metric nor an unprotected spectrum is part of this comparison. We next construct the legs before counting their charges.

XVI.8.2 From a partition to a tail

A puncture determines a descending Nahm partition $\rho = (h_1, \dots, h_J)$ of N. The tail remembers the parts which remain after successive blocks have been removed. An isolated tail starts with a square flavor node $[N]$, followed by round gauge nodes with suffix ranks

$$\sum_{a=1}^{J} h_a = N, \qquad r_a = N - \sum_{b=1}^{a} h_b = \sum_{b>a} h_b, \qquad 1 \le a < J. \tag{XVI.8.8}$$

Every link is a full bifundamental hypermultiplet. The square node is a background flavor symmetry and contributes no magnetic sum. It becomes dynamical only when the tails are joined into a star.

For a full puncture every block has size one. For a simple puncture only the last size-one block remains after removing the first block. Consequently

$$\begin{aligned} [1^N]_{\text{Nahm}} &\longmapsto [N] - (N-1) - \cdots - (1), \\ [N-1, 1]_{\text{Nahm}} &\longmapsto [N] - (1). \end{aligned} \tag{XVI.8.9}$$

Parentheses here denote $U(r)$ gauge nodes. The partition is the Nahm partition of Chapter 5. Transposing it before applying the suffix rule would turn the full partition into $[N]$ and incorrectly erase the entire tail.

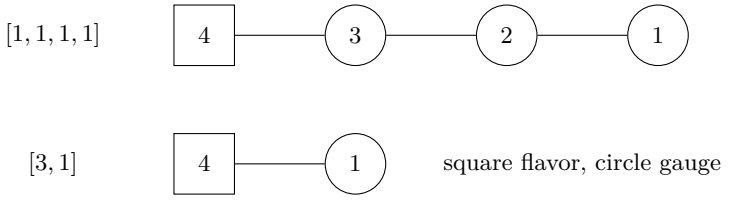


Figure XVI.8.2: Isolated tails generated by two Nahm partitions of four. Squares are flavor nodes and circles are dynamical unitary gauge nodes. The upper tail contains three full bifundamental hypers, whereas the lower tail contains one. The node labels are group ranks, not Young-diagram row lengths.

A changed partition makes each subtraction visible.

N	ρ_{Nahm}	$(r_1, r_2, \ldots)$
4	$[1,1,1,1]$	$(3,2,1)$
4	$[3,1]$	(1)
4	$[2,2]$	(2)
8	$[3,2,2,1]$	$(8-3, 8-3-2, 8-3-2-2) = (5,3,1)$

(XVI.8.10)

In particular the $N = 8$ example has neither consecutive ranks nor the ranks obtained from the transpose. It is a useful way to distinguish the rule from a guess based on the full tail.

The smallest full tail is $[2] - (1)$, the theory $T[SU(2)]$. It gives a complete quotient calculation to compare with a later monopole sum. Write its two charged chirals as a column $q = (q_1, q_2)^T$ and two oppositely charged chirals as a row $\widetilde{q}$. In one complex structure the zero-FI moment maps are

$$\mu_{\mathbb{C}} = \widetilde{q}q = 0, \qquad \mu_{\mathbb{R}} = |q|^2 - |\widetilde{q}|^2 = 0, \qquad (q, \widetilde{q}) \mapsto (\lambda q, \lambda^{-1}\widetilde{q}). \tag{XVI.8.11}$$

For the affine complex quotient $\lambda \in \mathbb{C}^\times$. Every invariant monomial pairs a positive-charge field with a negative-charge field, so the four mesons $M_{ij} = q_i \widetilde{q}_j$ generate the invariant algebra. The moment map removes the trace, while the outer-product form gives rank at most one.

$$\operatorname{tr} M = 0, \qquad \det M = 0, \qquad M = \begin{pmatrix} C & A \\ B & -C \end{pmatrix}, \qquad AB + C^2 = 0. \tag{XVI.8.12}$$

There are no further relations. Before imposing the trace, the invariant algebra of one column and one row is the rank-one matrix algebra; its only 2×2 minor is the determinant. Taking the invariant complex moment-map equation then gives the displayed hypersurface. Its matrix also satisfies $M^2 = 0$.

A dense parametrization checks the signs without pretending to cover the origin by a single chart.

$$q = (a, b)^T, \qquad \widetilde{q} = (-bc, ac), \qquad (A, B, C) = (a^2 c, -b^2 c, -abc). \tag{XVI.8.13}$$

Substitution gives $AB + C^2 = -a^2b^2c^2 + a^2b^2c^2 = 0$. Each meson has degree two when each chiral scalar has degree one. Removing one degree-four relation from three degree-two generators yields

$$\mathbb{C}[\mathcal{H}] = \mathbb{C}[A, B, C]/(AB + C^2), \qquad H(x) = \frac{1 - x^4}{(1 - x^2)^3} = 1 + 3x^2 + 5x^4 + 7x^6 + O(x^8). \tag{XVI.8.14}$$

This is the A_1 singularity, including its singular origin. Its tangent space there has three complex generators, whereas the variety has complex dimension two.

The real moment map explains which complex orbits represent the hyperkähler quotient. If $M \neq 0$, both norms $a_0 = |q|^2$ and $b_0 = |\widetilde{q}|^2$ are positive. The positive real part of a complex gauge transformation balances them at a finite value.

$$k = (b_0/a_0)^{1/4}, \qquad |kq|^2 - |k^{-1}\widetilde{q}|^2 = k^2 a_0 - k^{-2} b_0 = 0. \tag{XVI.8.15}$$

A nonzero zero-meson configuration need not admit such a representative. For $q = (1, 0)^T$ and $\widetilde{q} = 0$, the complex equation holds but the real equation is $k^2 = 0$, with no finite positive solution. Its complex orbit is nonclosed and its closure contains the origin. The affine quotient identifies it with that closed orbit. This distinction is essential when translating a holomorphic quotient into a real zero-level quotient.

XVI.8.3 Gluing the star and removing its ineffective U1

To construct the genus-zero mirror, identify the square $[N]$ nodes of the puncture tails and gauge the resulting central $U(N)$. Each tail keeps its own smaller gauge nodes. For three full A_2 punctures, label the central node c and the nodes of leg ℓ by a_ℓ, b_ℓ of ranks two and one. The hypermultiplet representation is

$$R = \bigoplus_{\ell=1}^{3} \left[(\mathbf{3}, \overline{\mathbf{2}}_\ell) \oplus (\mathbf{2}_\ell, \overline{\mathbf{1}}_\ell) \right], \qquad \dim_{\mathbb{C}} R = 3(3 \cdot 2 + 2 \cdot 1) = 24. \tag{XVI.8.16}$$

Each summand denotes a full hyper in the stated complex representation, with its conjugate chiral also present. Counting both chirals as two quaternionic copies would double the answer.

On every edge the same scalar gauge transformation at its two ends cancels. Thus a common phase acts trivially on all matter and must be divided out.

$$G = \frac{U(3) \times U(2)^3 \times U(1)^3}{U(1)_{\mathrm{diag}}}, \qquad \dim G = 9 + 3(4 + 1) - 1 = 23. \tag{XVI.8.17}$$

The quotient removes a rank-one gauge direction as well as one group generator. It does not discard a charged free hypermultiplet. Free twisted hypers in an ugly theory will instead appear as genuine positive-degree operators.

The global quotient matters when assigning magnetic charges. Before division, a unitary node of rank r_i has integers $m_{i,1} \geq \cdots \geq m_{i,r_i}$, modulo permutations. The

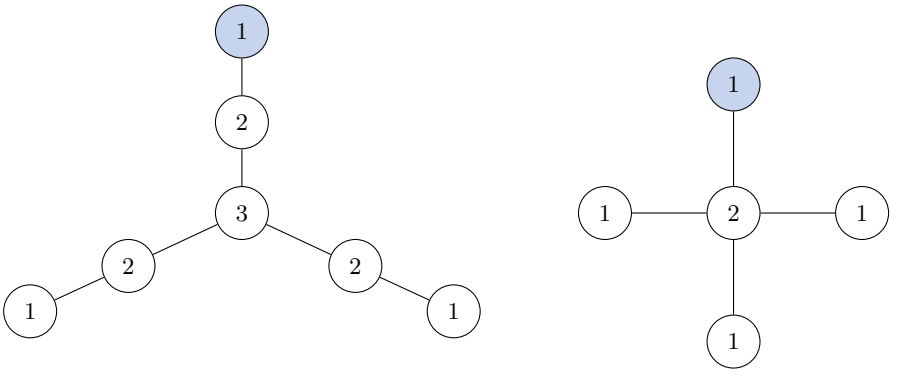


Figure XVI.8.3: The T_3 mirror and the four-punctured A_1 mirror. All displayed nodes are gauge nodes and every edge is a full bifundamental hyper. The filled outer node is the chosen magnetic anchor. Its charge and its degree-one Casimir are omitted after dividing by the ineffective diagonal $U(1)$. The remaining graph specifies the effective magnetic sum.

diagonal cocharacter translates every entry by a common integer. The effective lattice is therefore

$$\Gamma_G = \left(\bigoplus_i \mathbb{Z}^{r_i} \right) / \mathbb{Z}(1, \dots, 1), \qquad m_{i,a} \sim m_{i,a} + k \quad (k \in \mathbb{Z}). \tag{XVI.8.18}$$

Choose the outer $U(1)$ node b_1 as anchor. Each class has a unique representative with its charge zero, obtained by subtracting that integer from all entries.

$$m'_{i,a} = m_{i,a} - m_{b_1}, \qquad m'_{b_1} = 0. \tag{XVI.8.19}$$

This integral slice is more specific than writing only a central $SU(3)$. A trace-zero integral central tuple alone need not realize all classes of the quotient lattice. The allowed charges belong to the declared global gauge group, not just its Lie algebra.

Why does retaining the ineffective direction cause a problem? Every hyper contribution and vector root depends on a charge difference. A common shift leaves all these differences fixed, and in particular a constant charge configuration has zero dimension.

$$|(m_{i,a} + k) - (m_{j,b} + k)| = |m_{i,a} - m_{j,b}|, \qquad \Delta(k\mathbf{1}) = 0. \tag{XVI.8.20}$$

Summing this ray before division would give infinitely many operators at degree zero. Removing only a rank from the dimension count would leave that divergence in the actual series. The magnetic sum must use the quotient from the start.

The anchor also has a scalar Casimir of degree one. Since its vector multiplet is removed, its dressing factor must be removed with it. At zero charge the T_3 dressing is

consequently

$$P_G(x;0)=\frac{1}{(1-x^2)(1-x^4)(1-x^6)}\left[\frac{1}{(1-x^2)(1-x^4)}\right]^3\frac{1}{(1-x^2)^2}. \tag{XVI.8.21}$$

There are six degree-one Casimirs here, one for each unanchored node. Keeping the seventh would change the coefficient of x^2 from 78 to 79.

The same construction gives the companion ranks directly.

star	central rank	leg ranks	rank G
T_2	2	$(1),(1),(1)$	$2+3-1=4$
T_3	3	$(2,1),(2,1),(2,1)$	$3+9-1=11$
A_1 four punctures	2	$(1),(1),(1),(1)$	$2+4-1=5$

(XVI.8.22)

Their quotient lattices are fixed by anchoring one of the displayed outer $U(1)$ nodes. We now have enough information to calculate, rather than infer, their first protected coefficients.

XVI.8.4 Monopoles and a finite Hilbert series

A bare monopole inserts a magnetic charge m. Charged fermion zero modes determine its canonical R charge, while scalars of the unbroken gauge group dress it. Use $x^{2\Delta}$ for its degree. For full bifundamental edges in a unitary quiver the source prescription is

$$\Delta(m)=\frac{1}{2}\sum_{(i,j)\in E}\sum_{a=1}^{r_i}\sum_{b=1}^{r_j}|m_{i,a}-m_{j,b}|-\sum_i\sum_{a<b}|m_{i,a}-m_{i,b}|. \tag{XVI.8.23}$$

The negative vector term subtracts positive roots once. Its sign is consequential. The magnetic charges are the ordered representatives of (XVI.8.18) with the anchor fixed, so no additional division by the order of a Weyl group is made.

If a node has equal-charge blocks of sizes $k_1,k_2,\ldots$, its residual group is $\prod_\alpha U(k_\alpha)$. The scalar Casimirs of $U(k)$ have degrees $1,\ldots,k$ and contribute

$$P_i(x;m_i)=\prod_\alpha\prod_{j=1}^{k_\alpha}\frac{1}{1-x^{2j}},\qquad H_C(x)=\sum_{m\in\Gamma_G/W}x^{2\Delta(m)}P_G(x;m). \tag{XVI.8.24}$$

The product P_G omits the anchor. For example, equal $U(2)$ charges leave $U(2)$ unbroken, whereas distinct charges leave $U(1)^2$.

$$P_{U(2)}(x;(0,0))=\frac{1}{(1-x^2)(1-x^4)},\qquad P_{U(2)}(x;(1,0))=\frac{1}{(1-x^2)^2}. \tag{XVI.8.25}$$

The first bare monopole of the four-legged rank-two star can be seen without a large sum. Set the central tuple to $(1,0)$ and every outer charge to zero. Each edge contributes $1/2$, and the central positive root subtracts one.

$$\Delta_{D_4}((1,0);0,0,0,0)=4\cdot\frac{1}{2}-1=1. \tag{XVI.8.26}$$



Figure XVI.8.4: Two charge sectors of a rank-two node. Equal charges leave a $U(2)$ block with Casimir degrees one and two. Split charges leave two $U(1)$ blocks, each with a degree-one Casimir. The picture depicts residual gauge groups in a magnetic background, not different puncture tails.

With only three outer nodes the same calculation gives $\Delta = 1/2$. These degree-one operators will explain why T_2 contains free fields rather than beginning at x^2.

An infinite magnetic sum requires a reason why a finite charge range suffices through a given power. For integer a, b decompose their difference into positive and negative threshold indicators.

$$|a-b| = \sum_{s\geq 1} |\mathbf{1}_{a\geq s} - \mathbf{1}_{b\geq s}| + \sum_{s\geq 1} |\mathbf{1}_{a\leq -s} - \mathbf{1}_{b\leq -s}|\,. \tag{XVI.8.27}$$

For charges of the same sign this counts the thresholds between their magnitudes. For opposite signs the two sums count their magnitudes separately. Applying the identity to every edge and every root in (XVI.8.23) preserves the negative vector terms as well. The dimension is additive over signed binary layers.

$$2\Delta(m) = \sum_{s\geq 1} 2\Delta(b_s^+) + \sum_{s\geq 1} 2\Delta(b_s^-), \qquad b_s^+ = \mathbf{1}_{m\geq s}, \quad b_s^- = \mathbf{1}_{m\leq -s}. \tag{XVI.8.28}$$

At the anchor all these indicators vanish. Within each node only the number n_i of entries equal to one matters. A binary orbit therefore has $0 \leq n_i \leq r_i$, with $n_{\text{anchor}} = 0$, and its dimension can be evaluated without choosing individual entries.

$$2\Delta(b) = \sum_{(i,j)\in E} \big[n_i(r_j - n_j) + n_j(r_i - n_i)\big] - 2\sum_i n_i(r_i - n_i). \tag{XVI.8.29}$$

Enumerating these small finite sets, excluding the empty orbit, gives eleven orbits for T_2, 431 for T_3 and 23 for the four-punctured A_1 star. Their minimum values $c = \min 2\Delta(b)$ are

$$c_{T_2} = 1, \qquad c_{T_3} = c_{D_4} = 2, \qquad L \leq \lfloor K/c \rfloor, \quad |m_{i,a}| \leq \lfloor K/c \rfloor \quad \text{through } x^K. \tag{XVI.8.30}$$

Here L is the number of nonempty signed layers. The first bound follows from additivity and positivity; the second follows because a charge of magnitude q occupies q layers. Scalar dressings only increase degree. Thus through x^4 the complete intervals are $[-4, 4]$ for T_2 and $[-2, 2]$ for the other two stars. This is a completeness argument, rather than observed agreement between two cutoffs.

The resulting sums, including all residual-group dressings, are

$$\begin{aligned} H_{T_2^{\mathrm{mir}}}(x) &= 1 + 8x + 36x^2 + 120x^3 + 330x^4 + O(x^5), \\ H_{T_3^{\mathrm{mir}}}(x) &= 1 + 78x^2 + 2430x^4 + O(x^5), \\ H_{D_4^{\mathrm{mir}}}(x) &= 1 + 28x^2 + 300x^4 + O(x^5). \end{aligned} \tag{XVI.8.31}$$

For the single $U(1)$ two-flavor tail, $\Delta(m) = |m|$. Summing the positive and negative integers gives an exact elementary comparison with (XVI.8.14).

$$\frac{1}{1-x^2} \sum_{m \in \mathbb{Z}} x^{2|m|} = \frac{1+x^2}{(1-x^2)^2} = \frac{1-x^4}{(1-x^2)^3}. \tag{XVI.8.32}$$

For T_2, the sourced free trifundamental half hyper instead has eight independent complex scalars. Its polynomial algebra has

$$H_{\mathcal{H}(T_2)}(x) = (1-x)^{-8} = \sum_{k \geq 0} \binom{k+7}{7} x^k, \qquad \binom{8}{7} = 8, \quad \binom{11}{7} = 330. \tag{XVI.8.33}$$

The selected coefficients match the star sum. Removing its degree-one operators as if they were the ineffective gauge direction would destroy this agreement.

The four-punctured sphere permits a different Higgs calculation. Its $SU(2)$ theory has eight chiral doublets, arranged as a 2×8 matrix Q with rows $u, v \in \mathbb{C}^8$. In a flavor basis with standard symmetric pairing the complex moment map is $QQ^T = 0$, giving

$$u \cdot u = u \cdot v = v \cdot v = 0. \tag{XVI.8.34}$$

To use three equations in a Hilbert numerator we must justify a regular sequence, and to describe a reduced shell we need more than a smooth example. For $u \neq 0$ the null cone for u has dimension seven. For each such u, v lies in $u^\perp$ and obeys a nonzero quadratic equation. The rank-two locus consequently has dimension $7 + 6 = 13$. The rank-at-most-one locus consists of a null vector and its proportional row, or a zero row. Its dimension is at most eight. Thus

$$\dim\{QQ^T = 0\} = 13, \qquad \operatorname{codim}_{\mathbb{C}^{16}}\{QQ^T = 0\} = 3, \qquad \dim\{\operatorname{rank} Q \leq 1\} \leq 8. \tag{XVI.8.35}$$

Three equations of height three in a polynomial ring form a complete intersection. The full-rank locus consists of bases of isotropic two-planes in $\mathbb{C}^8$. Its base is the irreducible orthogonal isotropic Grassmannian of two-planes, and its frame fibers are connected $GL(2)$ varieties, so this locus is irreducible. It is smooth because the differential of QQ^T surjects onto symmetric 2×2 matrices when Q has row rank two. No separate component can fit in the rank-one locus, since complete intersections are unmixed and all components have dimension thirteen. Smoothness on this dense irreducible locus gives generic reducedness; complete-intersection Cohen–Macaulayness excludes embedded components and promotes generic reducedness to reducedness of the shell.

The full-rank stabilizer in $SL(2)$ is trivial. The principal quotient therefore has complex dimension $13 - 3 = 10$, confirming quaternionic dimension five. For the graded

calculation a doublet has weights z, z^{-1}, and the moment map is an adjoint with weights $z^2, 1, z^{-2}$. Define the plethystic exponential by

$$\mathrm{PE}[f(x,z)] = \exp\left(\sum_{k\geq 1} \frac{f(x^k, z^k)}{k}\right). \tag{XVI.8.36}$$

The regular sequence supplies the negative adjoint term, and the $SU(2)$ Haar constant term projects invariants.

$$\begin{aligned} H_{\mathcal{H}}(x) &= \mathrm{CT}_z\left[(1-z^2)\,\mathrm{PE}\big(8x(z+z^{-1}) - x^2(z^2+1+z^{-2})\big)\right] \\ &= 1 + 28x^2 + 300x^4 + O(x^6). \end{aligned} \tag{XVI.8.37}$$

The degree-two invariants are antisymmetric flavor mesons, giving $\binom{8}{2} = 28$. Without the moment-map numerator the degree-four answer would be 336; the three covariant equations and gauge projection reduce it to 300. Omitting Haar projection instead gives 63 at degree two. These are different operations, both needed for the quotient. Agreement with the magnetic sum compares two selected protected coefficients under the sourced infrared assignments. It does not determine all products in either ring.

XVI.8.5 Enhancement and the domain of the calculation

The coefficient 78 has more information than an integer. Record each $\Delta = 1$ monopole by its topological charges, the sums of the flux entries at the unanchored nodes. After deleting the anchor from the T_3 graph, use the order $(c, a_1, a_2, b_2, a_3, b_3)$. The associated finite Cartan matrix is

$$C_{E_6} = \begin{pmatrix} 2 & -1 & -1 & 0 & -1 & 0 \\ -1 & 2 & 0 & 0 & 0 & 0 \\ -1 & 0 & 2 & -1 & 0 & 0 \\ 0 & 0 & -1 & 2 & 0 & 0 \\ -1 & 0 & 0 & 0 & 2 & -1 \\ 0 & 0 & 0 & 0 & -1 & 2 \end{pmatrix}, \qquad \det C_{E_6} = 3. \tag{XVI.8.38}$$

For example a central tuple $(1,0,0)$ with all leg charges zero gives 3 from the edges and subtracts 2 from the central roots. It has $\Delta = 1$ and topological vector $(1,0,0,0,0,0)$. The full charge enumeration supplies 72 distinct vectors. In simple-root coordinates they have length squared two and are closed under all six simple reflections.

$$v^T C_{E_6} v = 2, \qquad s_i(v) = v - (C_{E_6} v)_i e_i, \qquad |\Phi_{E_6}| = 72, \qquad 72 + 6 = 78. \tag{XVI.8.39}$$

The last six are the neutral degree-one Casimirs already counted in (XVI.8.21). Charged and neutral operators thus have the multiplicities of the E_6 adjoint. A count of 72 alone would not establish a root system; the lengths and reflection closure use the actual charge vectors.

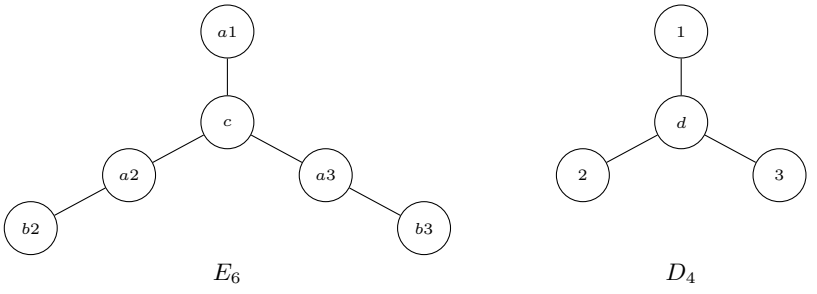


Figure XVI.8.5: Finite Dynkin graphs on the unanchored nodes. Deleting the marked outer node in the star leaves E_6 or D_4. The graphs specify the Cartan matrices used to test the actual topological-charge vectors. They depict root inner products, whereas Figure XVI.8.3 depicts bifundamental matter.

For the four-punctured A_1 star, delete one outer anchor and order the remaining nodes as center and three outer nodes. This gives

$$C_{D_4} = \begin{pmatrix} 2 & -1 & -1 & -1 \\ -1 & 2 & 0 & 0 \\ -1 & 0 & 2 & 0 \\ -1 & 0 & 0 & 2 \end{pmatrix}, \qquad \det C_{D_4} = 4, \qquad |\Phi_{D_4}| + 4 = 24 + 4 = 28. \tag{XVI.8.40}$$

Its enumerated charged vectors again have squared length two and close under the simple reflections. These finite Lie-algebra checks identify the representation organization compatible with the proposed enhancement. They do not determine the global flavor-group quotient or a current operator-product algebra.

One more coefficient can be tested using representation theory without assuming a complete ring. Let θ be the highest root and ρ_W the Weyl vector. The Weyl dimension product gives

$$\dim V_{2\theta} = \prod_{\alpha>0} \frac{(2\theta + \rho_W, \alpha)}{(\rho_W, \alpha)}, \qquad \dim V_{2\theta}^{E_6} = 2430, \qquad \dim V_{2\theta}^{D_4} = 300. \tag{XVI.8.41}$$

These values agree with x^4 in (XVI.8.31). The all-order interpretation in terms of the minimal nilpotent orbit is supplied by the sources. Our finite dimensions and reflection checks establish compatibility at the computed orders. They neither derive Joseph relations nor fix multiplication maps or metrics.

The domain of the canonical grading can also be tested by changing the punctures. For a node of rank r_i, define its excess by the sum of adjacent ranks minus twice its rank.

$$e_i = \sum_{j \sim i} r_j - 2r_i. \tag{XVI.8.42}$$

Balanced means $e_i = 0$. In these unitary examples a central excess -1 signals ugly behavior with dimension-half monopoles, while more negative excess can invalidate the

ultraviolet R grading. The source prescription requires good or ugly theories with the stated protected grading; it is not an arbitrary nonnegative formal sum.

Change the third full puncture of T_3 to the simple Nahm partition $[2,1]$. Its leg becomes a single $U(1)$, so the rank and central excess change by actual tail arithmetic.

$$\begin{aligned} \operatorname{rank} G_{\mathrm{FFS}} &= 3 + (2+1) + (2+1) + 1 - 1 = 9, \\ e_c^{\mathrm{FFS}} &= 2 + 2 + 1 - 2 \cdot 3 = -1. \end{aligned} \tag{XVI.8.43}$$

This is compatible with the sourced free bifundamental residual fixture of Chapter 5. Its separate closure Goldstone sector is not part of this rank sum. No Hilbert series for this changed fixture has been computed here.

Changing N instead retains three full legs. For T_4 each leg is $(3,2,1)$ and the central rank is four.

$$\operatorname{rank} G_{T_4} = 4 + 3(3+2+1) - 1 = 21, \qquad e_c^{T_4} = 3 + 3 + 3 - 2 \cdot 4 = 1. \tag{XVI.8.44}$$

These are rank and excess calculations. The T_3 root result does not turn them into a T_4 protected series or a ring identification.

Finally let p be the number of full A_1 legs. The center has rank two and every leg rank one. On the central charge $(1,0)$ with all outer charges zero,

$$\operatorname{rank} G = p + 1, \qquad e_c = p - 4, \qquad \Delta((1,0);0,\dots,0) = \frac{p}{2} - 1. \tag{XVI.8.45}$$

Four legs give $(5,0,1)$ for these three quantities. Three legs give $(4,-1,1/2)$ and recover T_2 with its physical free fields. Two legs give $(3,-2,0)$. In that last diagnostic the binary minimum is zero, so the positive-layer bound of Section 4 fails and arbitrarily many such layers can contribute at degree zero. The ultraviolet graded sum is rejected. The two-punctured sphere is also outside the ordinary stable fixture domain. This calculation diagnoses the failure of this grading, rather than proving absence of every possible infrared description.

Take-home message

The Nahm partition generates a tail by suffix sums. Gauging the common flavor node makes a star, and dividing by its ineffective diagonal $U(1)$ fixes both the magnetic lattice and the scalar dressing. In the stated good and ugly examples, signed binary layers give a complete finite charge interval for each requested order. The sums recover the first coefficients of eight free scalars, the E_6 adjoint and the D_4 adjoint, with an independent $SU(2)$ Higgs quotient comparison. A reader should be able to change a puncture, choose an integral anchor, evaluate a monopole sector and distinguish an actual free operator from an ineffective gauge direction. Mirror protection and infrared assignments remain physical source inputs. Finite coefficients and root compatibility do not establish a full mirror equivalence, its ring multiplication, a metric or a global flavor group.

Exercises

1. For the T_3 mirror submit its Coulomb quaternionic, complex and real dimensions, its hypermultiplet representation dimension, its effective group dimension and its regular Higgs quotient quaternionic dimension. Derive the subtraction from real moment maps and gauge orbits. Explain why the tangent space at the $T[SU(2)]$ singular origin has a different dimension from the variety.

2. Apply the suffix rule to $[1,1,1,1]$, $[3,1]$, $[2,2]$ and $[3,2,2,1]$. Submit the ranks in their order from the flavor node. Draw at least one changed tail with square and round nodes and explain why transposing the Nahm partition before this operation changes the construction.

3. Submit the meson relation as a polynomial in A, B, C, the exact hypersurface Hilbert series in x, and its coefficients at degrees zero through six. Derive invariant generation and the determinant relation. Explain finite real-moment-map balancing on nonzero-meson closed orbits and give a nonzero complex solution which reaches the origin only in its orbit closure. Discuss why nonzero FI changes the geometric quotient.

4. Submit the equal-charge and split-charge $U(2)$ dressing functions, the binary minimum for the four-legged A_1 star and the complete absolute charge bound through x^4. Prove the signed-layer identity including the vector subtraction. Explain why a common-shift quotient requires removal of the anchor dressing and why a different cocharacter lattice could change the sum.

5. Submit the coefficients at degrees zero through four of the $SU(2)$ four-flavor Molien series. Derive the moment-shell codimension and justify the regular sequence. Explain why reducedness needs the irreducible smooth rank-two locus and complete-intersection unmixedness, rather than one smooth example. Identify which physical premises remain after the finite Higgs and Coulomb coefficients agree.

6. Submit the ranks and central excesses for FFF and FFS A_2, for T_4, and for A_1 with four, three and two full legs. For the last three stars also submit the dimension of the central $(1,0)$ monopole. Explain the difference between a free twisted hyper, the ineffective diagonal vector and the bad ultraviolet grading. State what the E_6/D_4 root and Weyl-dimension checks do and do not establish.

For benchmark submissions, see `benchmark/PROTOCOL.md`. Equivalent rational expressions are accepted. Include the derivations, orbit arguments and physical interpretations.

Sources and scope

Section 8.1. Higgs-branch protection and the star-shaped infrared mirror assignment are sourced [CONJ+] premises from Benini et al. (2010, arXiv:1007.0992v1, p. 5 and

pp. 7–10) and Cremonesi, Hanany, Mekareeya, et al. (2014, arXiv:1403.2384v2, pp. 1–2, 10). The selected branch dimensions are calculated [MATH]. The physical T_2/T_3 assignments are those of Chapter 6. The anomaly coordinates of Chapter 7 are not independent Higgs-ring evidence. No finite-radius metric comparison is made.

Section 8.2. The sourced tail assignment uses Benini et al. (2010, arXiv v1, eqs. (3.1), (3.3)–(3.5), Figs. 6–7). The Nahm suffix ranks and the $U(1)$ invariant hypersurface are calculated [MATH]. The abelian comparison uses Cremonesi, Hanany, and Zaffaroni (2014, arXiv:1309.2657v3, pp. 8–9, eqs. (3.3)–(3.4)). The affine quotient includes nonclosed zero-meson orbits through their closed-orbit limits. Only nonzero-meson closed orbits are asserted to balance at finite positive gauge scale.

Section 8.3. The quotient lattice, integral anchor, ineffective-direction subtraction and representation counts are calculated [MATH], using Cremonesi, Hanany, and Zaffaroni (2014, arXiv v3, eq. (3.1), p. 13, eq. (3.22)) and Cremonesi, Hanany, Mekareeya, et al. (2014, arXiv v2, eqs. (3.3)–(3.7)). Central special-unitary notation without its global-form qualification does not replace this cocharacter lattice.

Section 8.4. The protected monopole prescription is a sourced [BPS:1/2|short] input from Cremonesi, Hanany, and Zaffaroni (2014, arXiv v3, eqs. (2.2), (2.4)–(2.7)). The signed-layer cutoff is calculated [MATH] for these integral anchored graphs. The three finite series and the separate Molien/free-scalar comparisons are calculated [BPS:1/2|short], compared with Cremonesi, Hanany, Mekareeya, et al. (2014, arXiv v2, eq. (3.16)). The $SU(2)$ moment shell is a reduced complete intersection by the rank-two-locus and unmixedness argument in the text. The orbit calculation checks finite balancing and the nonclosed counterexample. No all-order equality follows from the selected coefficients.

Section 8.5. The actual charge-root sets, reflection closure and Weyl dimensions are calculated [MATH], compared with Cremonesi, Hanany, and Zaffaroni (2014, arXiv v3, eqs. (3.21)–(3.25)). The sourced E_6 minimal-orbit infrared interpretation remains [CONJ+]. The changed FFS and T_4 results are rank/excess arithmetic only, using the tails of Benini et al. (2010, arXiv v1, eqs. (3.3)–(3.4)) and the residual FFS fixture of Chapter 5. The good/ugly/bad domain follows Cremonesi, Hanany, and Zaffaroni (2014, arXiv v3, pp. 4–7). The zero binary minimum in the two-leg diagnostic prevents the stated cutoff proof. Masses, FI resolutions, higher genus, twisted tails, accidental R mixing in bad theories, global line lattices, Joseph relations and full metric matching are outside the calculation.

References

Benini, F., Y. Tachikawa, and D. Xie (2010). "Mirrors of 3d Sicilian theories". In: arXiv: 1007.0992 [hep-th].

Cremonesi, S., A. Hanany, N. Mekareeya, et al. (2014). "Coulomb branch Hilbert series and Three Dimensional Sicilian Theories". In: arXiv: 1403.2384 [hep-th].

Cremonesi, S., A. Hanany, and A. Zaffaroni (2014). "Monopole operators and Hilbert series of Coulomb branches of 3d N=4 gauge theories". In: arXiv: 1309.2657 [hep-th].

Chapter XVI.9

Irregular ends and Argyres–Douglas theories

A massive flavor can disappear from the low-energy spectrum while leaving a finite scale behind. In the spectral description this process collides two regular ends. Their separate residues grow, but a correlated change of the Coulomb coordinate leaves a finite quadratic differential with a higher-order pole. We will follow that cancellation before asking what data must be fixed at the new end.

An irregular end also describes the cubic model encountered in Chapter 5. There the useful question is different. Which coefficients change the theory, and which select a vacuum of one theory? The differential answers through its polar part and its scaling weight. A comparison with an isolated IIB hypersurface then gives the same deformation directions by a second calculation. Finally, actual periods distinguish approaching a node at fixed coupling from approaching the scale-invariant cubic.

The reader needs the cotangent transformation law and compact periods of Chapter 4, the cubic period orientations of Chapter 5, and the Jacobi quotient of the IIB construction in Section XII.3.3. We use $Q = \lambda^2 = \phi(z)dz^2$ and $\lambda = x\,dz$. Physical central charges equal geometric periods times one common nonzero constant c_{SW} whose absolute normalization is left unspecified. The class-S, SCFT and IIB decoupling interpretations are physical inputs. The calculations below establish their stated local curve and parameter comparisons.

XVI.9.1 Colliding regular ends and decoupling a flavor

The first task is to remove one full flavor rather than two independent residues. Put four regular ends at $0, q, 1, \infty$ on a sphere. Their eigenvalue residues are $\pm m_0, \pm m_q, \pm b, \pm c$. A convenient quadratic differential is

$$\phi_4 = \frac{m_0^2}{z^2} + \frac{m_q^2}{(z-q)^2} + \frac{b^2}{(z-1)^2} + \frac{c^2 - m_0^2 - m_q^2 - b^2}{z(z-1)} + \frac{U_{\mathrm{parent}}}{z(z-q)(z-1)}. \quad \text{(XVI.9.1)}$$

The coefficient at infinity is c^2 after applying the quadratic-differential Jacobian. In the selected weakly coupled $SU(2)$ frame, the four fundamental masses are $m_0+m_q, m_0-m_q, b+c, b-c$. This identification comes from the regular-puncture construction. It tells us which residue motion removes one flavor.

$$m_0=\frac{H+m}{2},\qquad m_q=\frac{m-H}{2},\qquad m_0+m_q=m,\qquad m_0-m_q=H. \tag{XVI.9.2}$$

Only H becomes heavy. The three finite masses are $m, b+c, b-c$. Merely taking m_0 large at fixed m_q would make both combinations large. Simultaneously bring the ends together and retain a dimension-one scale $L_{\rm AF}$.

$$q=\frac{L_{\rm AF}}{H},\qquad S=m_0^2+m_q^2=\frac{H^2+m^2}{2},\qquad U_{\rm parent}=(1-q)S-\widehat{U}. \tag{XVI.9.3}$$

Here z,q are dimensionless and $\widehat{U}$ has mass dimension two. The last equation includes both a quadratic and a linear subtraction in H. We now see why both are needed.

Separate off the terms involving only b,c. Over the common denominator $D=z^2(z-q)^2(z-1)$ the remaining numerator is

$$\begin{aligned} N=&\,m_0^2(z-q)^2(z-1)+m_q^2z^2(z-1)\\ &-Sz(z-q)^2+[(1-q)S-\widehat{U}]z(z-q). \end{aligned} \tag{XVI.9.4}$$

Introduce two polynomials F,G only to collect the powers of the heavy mass. Their elementary expansions give the entire cancellation.

$$\begin{aligned} F&=(z-q)^2(z-1)+z^2(z-1)-2z(z-q)^2,\\ F+2(1-q)z(z-q)&=q^2(z-1),\\ G&=(z-q)^2(z-1)-z^2(z-1)=(q^2-2qz)(z-1). \end{aligned} \tag{XVI.9.5}$$

Indeed the coefficients of H^2+m^2 and Hm in N are respectively one quarter of the second line and one half of G. Consequently

$$\begin{aligned} N&=(z-1)\left[\frac{q^2(H+m)^2}{4}-qHmz\right]-\widehat{U}z(z-q),\\ q^2(H+m)^2&=L_{\rm AF}^2(1+m/H)^2,\qquad qHm=L_{\rm AF}m. \end{aligned} \tag{XVI.9.6}$$

The apparent H^2 and H growth has become finite. Restoring the separated terms gives an exact expression at finite H, rather than a truncated expansion.

$$\begin{aligned} \phi_H=&\frac{L_{\rm AF}^2(1+m/H)^2/4-L_{\rm AF}mz}{z^2(z-L_{\rm AF}/H)^2}+\frac{b^2}{(z-1)^2}+\frac{c^2-b^2}{z(z-1)}\\ &-\frac{\widehat{U}}{z(z-L_{\rm AF}/H)(z-1)}. \end{aligned} \tag{XVI.9.7}$$

At fixed z separated from the marked ends its limit can first be read with the last term uncombined. Splitting that term supplies the standard three-flavor chart.

$$\phi_3=\frac{L_{\rm AF}^2}{4z^4}-\frac{L_{\rm AF}m}{z^3}+\frac{\widehat{U}}{z^2}+\frac{b^2}{(z-1)^2}-\frac{b^2-c^2+\widehat{U}}{z(z-1)}. \tag{XVI.9.8}$$

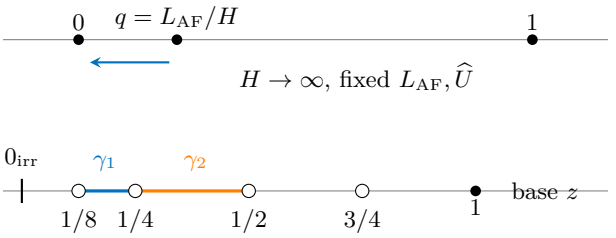


Figure XVI.9.1: Marked ends and interior branch points are different objects on the base. The upper row depicts the two regular ends at $0, q$ approaching an irregular end at zero. The lower row marks the limiting four simple zeros of the worked example. Its two retained lifted arcs join adjacent zeros; neither arc ends on the colliding punctures. Positions along the lower row are the actual limiting rational positions.

This is an order-four quadratic pole at the collided end. If we subtract only the quadratic divergence, taking $U_{\mathrm{wrong}} = S - \widehat{U}$, then $U_{\mathrm{wrong}} - U_{\mathrm{parent}} = qS$. The residual term exposes the failure.

$$\lim_{H\to\infty} \frac{\phi_{\mathrm{wrong}} - \phi_H}{H} = \lim_{H\to\infty} \frac{qS/H}{z(z-q)(z-1)} = \frac{L_{\mathrm{AF}}}{2z^2(z-1)} \neq 0. \tag{XVI.9.9}$$

Holding U_{parent} fixed is another path through the original parameter space. It does not keep $\widehat{U}$ finite and does not produce the family in (XVI.9.8).

To compare complete differentials, use $t = 1/z$. The cotangent law transforms both the coordinate and its coefficient.

$$x_t = -t^{-2} x_z(1/t), \qquad \phi_t = t^{-4}\phi_3(1/t), \qquad x_t\, dt = x_z\, dz. \tag{XVI.9.10}$$

Substitution and partial fractions give the source chart without dropping its finite parameters.

$$\begin{aligned} \phi_t &= \frac{c^2}{t^2} + \frac{b^2}{(t-1)^2} + \frac{2\Lambda_G m_G + u_G}{2t} + \frac{2\Lambda_G m_G - u_G}{2(t-1)} + \Lambda_G^2, \\ \Lambda_G &= \frac{L_{\mathrm{AF}}}{2}, \qquad m_G = -m, \qquad u_G = 2(b^2 + c^2 - \widehat{U}) - L_{\mathrm{AF}} m. \end{aligned} \tag{XVI.9.11}$$

The two remaining source masses are $m_+ = c, m_- = b$. This agrees with the full three-flavor differential of Gaiotto et al. 2013. Treating ϕ as a scalar would miss t^{-4} and fail this comparison.

Figure XVI.9.1 separates colliding marked ends from the interior branch points used for compact cycles. There is also a shorter statement about subsequent heavy thresholds. In a fixed holomorphic scheme define $b_{N_f} = 4 - N_f$ and $Q_{N_f} = \Lambda_{N_f}^{b_{N_f}}$ for $N_f < 4$. Matching inverse couplings at a heavy full-hyper mass M gives

$$\begin{aligned} b_{N_f} \log M - \log Q_{N_f} &= b_{N_f - 1} \log M - \log Q_{N_f - 1}, \\ Q_{N_f - 1} &= M Q_{N_f}, \qquad (b_4, b_3, b_2, b_1, b_0) = (0, 1, 2, 3, 4). \end{aligned} \tag{XVI.9.12}$$

Thus $\Lambda_2^2 = M_3\Lambda_3$, $\Lambda_1^3 = M_2\Lambda_2^2$ and $\Lambda_0^4 = M_1\Lambda_1^3$. These products are threshold arithmetic, with finite normalization depending on the scheme. Only the four-to-three-flavor step has a complete curve construction here. Also, q is the geometric cusp coordinate used in this limit; an exact all-orders identification with a microscopic exponential coupling has not been imposed.

A nonzero retained period tests more than convergence of coefficients. Choose

$$\begin{gathered} L_{\mathrm{AF}} = 1, \quad m = \frac{10}{3}, \quad \widehat{U} = \frac{47}{4}, \quad b^2 = \frac{7}{4}, \quad c^2 = \frac{64}{3}, \\ N_\infty = \frac{64}{3}(z - \tfrac{1}{8})(z - \tfrac{1}{4})(z - \tfrac{1}{2})(z - \tfrac{3}{4}). \end{gathered} \tag{XVI.9.13}$$

Here $N_\infty = z^4(z-1)^2\phi_3$. At finite H define $N_H = z^2(z-1/H)^2(z-1)^2\phi_H$ and solve for its roots again. For the first two adjacent intervals $[r_k(H), r_{k+1}(H)]$ the lifted periods are

$$\Pi_k(H) = 2\int_{r_k(H)}^{r_{k+1}(H)} \frac{\sqrt{N_H(z)}}{z(z-1/H)(z-1)}\, dz, \qquad k = 1, 2. \tag{XVI.9.14}$$

Choose the numerator square root positive imaginary on the first interval and positive real on the second. The denominator is negative on both intervals. The factor two includes the return sheet, so the limiting signs are fixed.

$$\Pi_1(\infty) \simeq -0.918959585270\, i, \qquad \Pi_2(\infty) \simeq -0.812776006324. \tag{XVI.9.15}$$

The errors at three finite masses make the rate visible.

H	$\lvert\Pi_1(H) - \Pi_1(\infty)\rvert$	$\lvert\Pi_2(H) - \Pi_2(\infty)\rvert$
1000	0.0242988	0.0329030
2000	0.0121665	0.0164248
4000	0.00608760	0.00820575

(XVI.9.16)

Each approximate halving is a numerical witness, rather than a certified error enclosure.

The estimate itself comes from a compact-contour argument. Let K be the fixed enclosing contour. Enclose each pair of limiting simple roots by a contour separated from every root and marked end. It lifts to a closed contour representing the corresponding arc cycle. The rational coefficients converge uniformly there at order H^{-1}. Because ϕ_3 is nonzero along this fixed contour, the continued square root has the same estimate.

$$\begin{gathered} \sup_K |\phi_H - \phi_3| = O(H^{-1}), \qquad \sup_K |\sqrt{\phi_H} - \sqrt{\phi_3}| = O(H^{-1}), \\ |\Pi_k(H) - \Pi_k(\infty)| = O(H^{-1}). \end{gathered} \tag{XVI.9.17}$$

This reasoning needs smooth fibers, transported sheets and separated compact contours. It says nothing about cycles entering the irregular end, flavor loops, or transport through a discriminant. The two periods require no common rescaling, but their convergence does not establish convergence of the full punctured charge lattice.

XVI.9.2 Boundary data at infinity

The higher pole produced by confluence has fixed data as well as variable data. To distinguish them, take a square root before naming its coefficients. At zero in the three-flavor chart write $\lambda = (a_{-2}z^{-2} + a_{-1}z^{-1} + a_0 + \cdots)dz$. Squaring and matching the first three coefficients gives

$$a_{-2}^2 = \frac{L_{\mathrm{AF}}^2}{4}, \qquad 2a_{-2}a_{-1} = -L_{\mathrm{AF}}m, \qquad a_{-1}^2 + 2a_{-2}a_0 = \widehat{U}. \tag{XVI.9.18}$$

On the sheet $a_{-2} = L_{\mathrm{AF}}/2$, this determines

$$\lambda = \left(\frac{L_{\mathrm{AF}}}{2z^2} - \frac{m}{z} + \frac{\widehat{U} - m^2}{L_{\mathrm{AF}}} + O(z)\right)dz, \qquad \partial_{\widehat{U}}\lambda = \left(\frac{1}{L_{\mathrm{AF}}} + O(z)\right)dz. \tag{XVI.9.19}$$

Fixing L_{AF}, m fixes its polar part. A variation of $\widehat{U}$ is regular there. At a regular end with nonzero mass instead $\lambda \sim \pm m_p\, dz/z$. A vanishing residue can reduce the quadratic pole to a simple pole without removing the defect. The pole order of Q alone is therefore incomplete boundary information.

Now consider the cubic of Chapter 5 in its scaling chart.

$$x^2 = z^3 + gz + u, \qquad \lambda = x\, dz, \qquad Q = (z^3 + gz + u)dz^2. \tag{XVI.9.20}$$

At infinity $w = 1/z$ and $dz = -w^{-2}dw$. The full Jacobian increases the pole order by four.

$$Q = (w^{-7} + gw^{-5} + uw^{-4})dw^2, \qquad \lambda = -w^{-7/2}\sqrt{1 + gw^2 + uw^3}\, dw. \tag{XVI.9.21}$$

The half-integer eigenvalue expansion calls for a double cover of the local coordinate. On $w = t^2$, including $dw = 2t\, dt$, it becomes an ordinary Laurent expansion.

$$\begin{aligned} \lambda &= -2t^{-6}\sqrt{1 + gt^4 + ut^6}\, dt \\ &= \left(-2t^{-6} - gt^{-2} - u + \frac{g^2}{4}t^2 + O(t^4)\right)dt. \end{aligned} \tag{XVI.9.22}$$

Thus the order-seven quadratic pole has an order-six eigenvalue one-form on the resolving cover. In particular g changes the polar jet and u changes its regular term.

$$\partial_g\lambda = (-t^{-2} + O(t^2))dt, \qquad \partial_u\lambda = (-1 + O(t^4))dt. \tag{XVI.9.23}$$

A loop around $w = 0$ exchanges the two eigenvalue sheets. This ramified formal description does not require a meromorphic matrix representative to have fractional-power entries. The leading eigenvalue orbit, the polar coefficients, the ramification and compatible monodromy data belong to the boundary prescription.

Figure XVI.9.2 compares the three local one-form descriptions, specifying the coordinate for each pole order. There is a second way to see why g and u have different

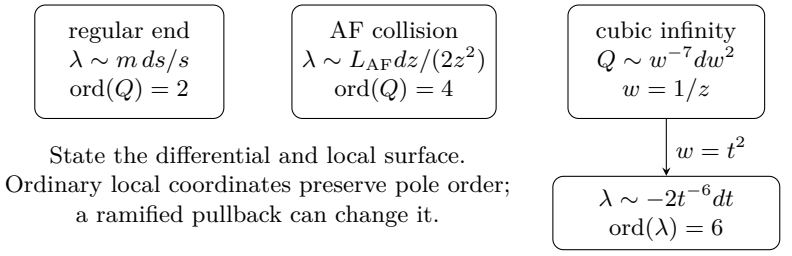


Figure XVI.9.2: Local eigenvalue one-forms, all expressed at an end in the indicated coordinate. A nonzero regular residue has order one. The confluence gives an order-two one-form in z. The cubic infinity has an order-seven quadratic differential in w, resolved to an order-six eigenvalue one-form on $w = t^2$. The branch arrow records a local coordinate cover, not a physical renormalization-group flow.

roles. On a smooth spectral curve $x^2 = P_N(z)$ a monomial variation of its polynomial gives

$$\delta\lambda = \frac{\delta v_j z^j}{2\sqrt{P_N(z)}}\, dz, \qquad |\delta\lambda|^2 \sim \frac{|\delta v_j|^2}{4} r^{2j-N} |dz|^2. \tag{XVI.9.24}$$

The asymptotic spectral norm includes the plane measure $r\,dr\,d\theta$. Up to a positive angular factor its convergence is determined by

$$\|\delta\lambda\|^2_{r>R} \;\propto\; |\delta v_j|^2 \int_R^\infty r^{2j-N+1} dr, \qquad \text{finite precisely when } j < \frac{N-2}{2}. \tag{XVI.9.25}$$

At equality the divergence is logarithmic. For $N = 3$, u has $j = 0$ and radial exponent -2, whereas g has $j = 1$ and exponent zero. A simple finite root is locally integrable in this norm, since the square-root denominator gives $|\delta\lambda|^2 \sim |z - r|^{-1} |dz|^2$. A multiple root requires separate local analysis.

$N = 3$	u	g
j	0	1
$2j - N + 1$	-2	0
asymptotic norm	finite	power divergent

(XVI.9.26)

The sourced Hitchin prescription keeps the polar boundary fixed when varying a vacuum. It therefore treats u as a Coulomb coordinate and g as an external theory parameter. The norm calculation supports this separation on the smooth spectral locus. It is not a theorem about the full noncompact Calabi–Yau metric or its complete L^2 cohomology.

Formal boundary data also differs from Stokes data. After choosing a flat connection associated to a real Hitchin solution, sectorial asymptotic solutions are related across rays by Stokes factors. A polynomial characteristic equation fixes neither those matrices nor a harmonic metric. Here we compute the eigenvalue polar jets and their allowed finite variations. Solving the real equations and finding the analytic Stokes factors would be further tasks, even when the formal type has already been specified.

XVI.9.3 Scaling from the Seiberg–Witten differential

The cubic can now be scaled without confusing a vacuum coordinate with a fixed boundary coefficient. At the monomial point $x^2 = z^3$, require the Seiberg–Witten differential to have weight one. If $d_x = [x]$ and $d_z = [z]$, the two linear equations are

$$2d_x = 3d_z, \qquad d_x + d_z = 1, \qquad d_z = \frac{2}{5}, \quad d_x = \frac{3}{5}. \tag{XVI.9.27}$$

Every term in the polynomial must then have weight $6/5$. The coefficient of z^j carries the missing weight.

$$[v_j] = \frac{6}{5} - \frac{2j}{5}, \qquad [u] = \frac{6}{5}, \qquad [g] = \frac{4}{5}, \qquad [u] + [g] = 2. \tag{XVI.9.28}$$

The source/vev interpretation is an input from the four-dimensional supersymmetric construction. With that interpretation, u is a rank-one Coulomb vev and g a relevant coupling. Fractional weights alone would not prove that an interacting SCFT exists. The class-S and IIB constructions identify this cubic with the (A_1, A_2) Argyres–Douglas theory.

Why is there no independent z^2 coefficient? Begin with a general monic cubic $z^3 + Az^2 + gz + u$ and translate $z = \zeta - A/3$. Translation leaves $dz = d\zeta$, so it preserves the form of λ.

$$\begin{aligned} z^3 + Az^2 + gz + u &= \zeta^3 + g'\zeta + u', \\ g' = g - \frac{A^2}{3}, &\qquad u' = u - \frac{Ag}{3} + \frac{2A^3}{27}. \end{aligned} \tag{XVI.9.29}$$

The quadratic term describes a coordinate choice; eliminating it changes the other coefficients. Reading three independent physical parameters from a monic cubic would count that coordinate freedom as a deformation.

Chapter 5 used $g = -3\Lambda_{\mathrm{AD}}^2$. Its scale symbol consequently has the fractional weight

$$g = -3\Lambda_{\mathrm{AD}}^2, \qquad [\Lambda_{\mathrm{AD}}] = \frac{2}{5}, \qquad [L_{\mathrm{AF}}]_{\mathrm{UV}} = 1. \tag{XVI.9.30}$$

These belong to different charts. The first is an infrared scaling parameter; the second is the ultraviolet asymptotically-free scale in the heavy-flavor limit. No equality between them, or between u and $\widehat{U}$, has been made. An infrared scaling chart can mix ultraviolet masses and Coulomb parameters.

Changing the polynomial degree gives a useful test of the method. For $x^2 = z^N + \sum_{j=0}^{N-2} v_j z^j$, after removing the degree-$N-1$ term, solve the same two equations.

$$2[x] = N[z], \qquad [x] + [z] = 1, \qquad [z] = \frac{2}{N+2}, \quad [x] = \frac{N}{N+2}, \quad [v_j] = \frac{2(N-j)}{N+2}. \tag{XVI.9.31}$$

For the quartic write its three coefficients in descending physical weight.

$$x^2 = z^4 + hz^2 + m_4 z + u_4, \qquad ([u_4], [m_4], [h]) = \left(\frac{4}{3}, 1, \frac{2}{3}\right). \tag{XVI.9.32}$$

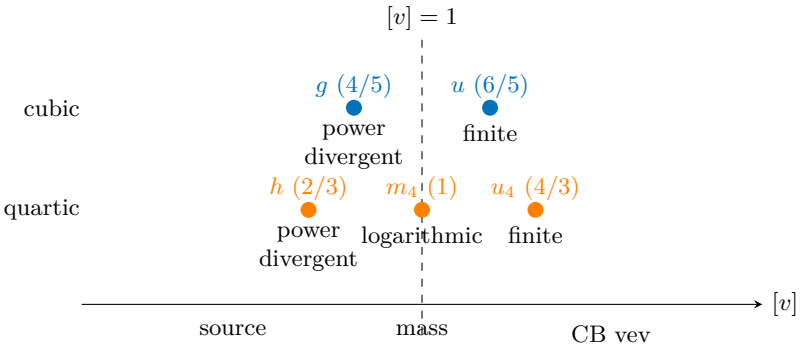


Figure XVI.9.3: Dimensions of the independent polynomial coefficients. A dot to the right of the weight-one line is a Coulomb vev, a dot on the line is a mass background, and a dot to its left is a relevant source in the sourced dictionary. The labels below the dots give the separately computed asymptotic spectral norm classes. The quartic adds a mass direction; its residue on the chosen sheet is $-m_4/2$.

The dimension-one direction is new. Its asymptotic norm is logarithmic, while the constant direction is finite and the quadratic direction power divergent.

	u_4	m_4	h
j	0	1	2
$2j-4+1$	-3	-1	1
role	CB vev	mass	relevant coupling

(XVI.9.33)

The names in the last row use the sourced parameter dictionary, in addition to the weight and norm calculations. A logarithmically divergent background is held fixed when varying a vacuum. It does not become an extra Coulomb modulus.

The mass can also be seen as an actual eigenvalue residue. At infinity take $w = 1/z$ on the sheet $x \sim z^2$. The binomial expansion is

$$\begin{aligned} \lambda &= -w^{-4}\sqrt{1 + hw^2 + m_4 w^3 + u_4 w^4}\, dw \\ &= -\left(w^{-4} + \frac{h}{2}w^{-2} + \frac{m_4}{2}w^{-1} + O(1)\right) dw, \\ \operatorname*{Res}_{w=0} \lambda &= -\frac{m_4}{2}. \end{aligned} \tag{XVI.9.34}$$

The other sheet reverses the sign. The raw polynomial coefficient m_4 is therefore not numerically equal to this eigenvalue residue. For the cubic, the ramified series in (XVI.9.22) contains no t^{-1} term and the independent deformation list contains no weight-one coefficient.

Figure XVI.9.3 places the coefficient weights beside their norm classes. A reader can now change the degree and repeat three independent operations. Remove the translation direction, normalize weights using $[\lambda] = 1$, and test each variation at infinity. Agreement among those operations explains the parameter separation. None specifies a

flavor Lie algebra merely from counting one mass. The IIB comparison will recover the same list without starting from $\lambda = x\,dz$.

XVI.9.4 Matching the IIB singularity direction by direction

The IIB construction replaces the double cover by an isolated hypersurface in four complex variables. The two extra quadratic directions are essential. Consider the suspended polynomial and its small deformations

$$F_N = a_0^2 + a_1^2 + x^2 - z^N - \sum_{j=0}^{N-2} v_j z^j = 0. \tag{XVI.9.35}$$

Setting the two suspension coordinates to zero leaves the same spectral polynomial. The physical IIB interpretation uses the string and gravity decoupling limit of the isolated-singularity construction. It is a physical premise, rather than a consequence of this restriction of equations.

Infinitesimal coordinate changes remove polynomials in the gradient ideal. At the undeformed point the derivatives are

$$(\partial_{a_0}F, \partial_{a_1}F, \partial_x F, \partial_z F) = (2a_0, 2a_1, 2x, -Nz^{N-1}). \tag{XVI.9.36}$$

Over $\mathbb{C}$ the nonzero constants can be divided out. The quotient therefore reduces every polynomial to a unique polynomial in z of degree at most $N-2$.

$$\mathcal{J}_N = \frac{\mathbb{C}[a_0, a_1, x, z]}{(a_0, a_1, x, z^{N-1})} \simeq \frac{\mathbb{C}[z]}{(z^{N-1})}, \qquad \mathcal{B}_N = \{1, z, \ldots, z^{N-2}\}, \quad \mu = N-1. \tag{XVI.9.37}$$

For example the cubic has basis $1, z$ and relation $z^2 = 0$, while the quartic has basis $1, z, z^2$ and relation $z^3 = 0$. These nilpotent relations describe the quotient for deformation counting. They are not equations for the physical position coordinate on every deformed fiber.

$$\delta F_3 = -u - gz, \qquad \delta F_4 = -u_4 - m_4 z - hz^2. \tag{XVI.9.38}$$

This gives a term-by-term map before assigning any dimensions. In particular the Milnor number counts all deformation directions. For the cubic $\mu = 2$, while the sourced Coulomb rank is one.

The weight normalization is different from the SW calculation. First give F homogeneous degree one, so the four coordinate weights are

$$(q_{a_0}, q_{a_1}, q_x, q_z) = \left(\frac{1}{2}, \frac{1}{2}, \frac{1}{2}, \frac{1}{N}\right), \qquad q(v_j) = 1 - \frac{j}{N}. \tag{XVI.9.39}$$

The holomorphic three-form is a residue. Its denominator removes one unit of polynomial weight from the numerator's coordinate-weight sum.

$$\Omega = \operatorname*{Res}_{F=0} \frac{da_0 \wedge da_1 \wedge dx \wedge dz}{F}, \qquad q_\Omega = \sum_i q_i - 1 = \frac{1}{2} + \frac{1}{N}. \tag{XVI.9.40}$$

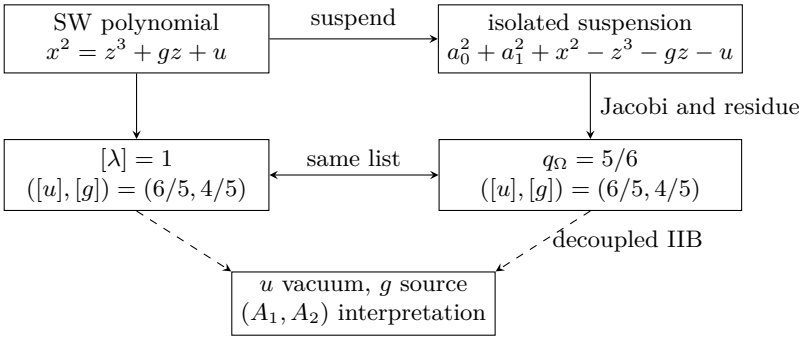


Figure XVI.9.4: The local parameter comparison. Solid arrows are the explicit polynomial and weight maps in the text. Dashed arrows use the physical class-S and decoupled IIB interpretation to name a vacuum or a source. The lower equality compares the two coefficient lists, with $g = -3\Lambda_{\rm AD}^2$. It does not identify global charge lattices or all physical observables.

Requiring periods of Ω to have physical weight one gives

$$[v_j]_{\rm IIB} = \frac{1 - j/N}{1/2 + 1/N} = \frac{2(N-j)}{N+2} = [v_j]_{\rm SW}. \tag{XVI.9.41}$$

Dropping the minus one in q_Ω would change every dimension. The equality here is a comparison of local deformation spectra using two normalization formulas. The source/vev rule identifies dimensions above one as Coulomb vevs, dimension one as mass backgrounds, and the present dimensions below one as relevant sources.

N	Jacobi basis	coefficient dimensions in that order	$(n_{\rm CB}, n_{\rm mass}, n_{\rm source})$
3	$1, z$	$6/5, 4/5$	$(1, 0, 1)$
4	$1, z, z^2$	$4/3, 1, 2/3$	$(1, 1, 1)$

(XVI.9.42)

In the all-plus cubic convention of Section XII.3.3, the same equation is obtained by $z_{\rm IX} = -z$, $g_{\rm IX} = g$, $u_{\rm IX} = -u$ and $x_i = (a_0, a_1, x)$. Thus the sign of a named constant deformation changes with the coordinate convention.

$$a_0^2 + a_1^2 + x^2 - z^3 - gz - u = \sum_{i=1}^{3} x_i^2 + z_{\rm IX}^3 + g_{\rm IX} z_{\rm IX} + u_{\rm IX}. \tag{XVI.9.43}$$

This coordinate equality does not equate absolute numerical periods in independently calibrated conventions. The common $c_{\rm SW}$ from the chapter opening is still uncalibrated.

Figure XVI.9.4 separates the algebraic coefficient maps from the physical interpretation. Isolation is part of this physical use of the hypersurface. If one deletes x^2 while keeping the ambient variable x, the derivatives no longer constrain it.

$$\widetilde{F} = a_0^2 + a_1^2 - z^N, \qquad {\rm Crit}(\widetilde{F}) = \{a_0 = a_1 = z = 0,\ x \in \mathbb{C}\}. \tag{XVI.9.44}$$

The resulting critical line has an infinite Jacobi quotient. It is outside the isolated problem just solved. Removing the variable itself instead changes the ambient dimension and the residue form, so it also cannot preserve the preceding calculation. Exercise 5 changes N to five while retaining the isolated suspension. That is a controlled transfer of the algebra; establishing a complete physical duality would additionally require global information and a comparison of the relevant protected structures.

XVI.9.5 Deformations and singular fibers

Once g and u have distinct roles, there are two different questions about degeneration. At a fixed nonzero coupling, which vacua make the cubic nodal? At the scale-invariant coupling, how do all periods scale toward the origin? The discriminant locates the first question. A double root r obeys $P(r) = P'(r) = 0$.

$$P = z^3 + gz + u, \qquad 3r^2 + g = 0, \qquad r^3 + gr + u = 0, \qquad (g, u) = (-3r^2, 2r^3). \tag{XVI.9.45}$$

Eliminating r gives the discriminant cusp, with the sign fixed by the standard cubic discriminant.

$$\Delta = -4g^3 - 27u^2, \qquad g = -3\Lambda_{\mathrm{AD}}^2 \implies \Delta = 27(4\Lambda_{\mathrm{AD}}^6 - u^2). \tag{XVI.9.46}$$

For nonzero Λ_{AD} the two singular values are distinct and have different double roots.

$$\begin{aligned} u = 2\Lambda_{\mathrm{AD}}^3 \quad &\implies \quad P = (z - \Lambda_{\mathrm{AD}})^2(z + 2\Lambda_{\mathrm{AD}}), \\ u = -2\Lambda_{\mathrm{AD}}^3 \quad &\implies \quad P = (z + \Lambda_{\mathrm{AD}})^2(z - 2\Lambda_{\mathrm{AD}}). \end{aligned} \tag{XVI.9.47}$$

Only at $g = u = 0$ do all three roots collide. Figure XVI.9.5 shows both a fixed-g path into an ordinary node and a $g = 0$ scaling path into this cusp.

A familiar period at $g = -3, u = 0$ fixes the size of the geometric normalization. Between zero and $\sqrt{3}$, $z^3 - 3z$ is negative. With the right arc orientation of Chapter 5 let

$$I = 2\int_0^{\sqrt{3}} \sqrt{3z - z^3}\, dz, \qquad \Pi_R = iI, \qquad \Pi_L = I. \tag{XVI.9.48}$$

Put $z = \sqrt{3}\, s$ and then $v = s^2$. The endpoint factor and the return sheet factor yield

$$\begin{aligned} I &= 2\, 3^{5/4} \int_0^1 s^{1/2}(1 - s^2)^{1/2} ds \\ &= 3^{5/4} \int_0^1 v^{-1/4}(1 - v)^{1/2} dv = 3^{5/4} B(\tfrac{3}{4}, \tfrac{3}{2}) \simeq 3.78441894434. \end{aligned} \tag{XVI.9.49}$$

This provides a nonzero comparison point. It is not the nodal period which we compute next. Set $\Lambda_{\mathrm{AD}} = 1$, $u = 2 + \delta$, and introduce $z = 1 + w$. Then

$$P = w^2(w + 3) + \delta, \qquad \lambda = w\sqrt{3 + w}\sqrt{1 + \frac{\delta}{w^2(3 + w)}}\, dw. \tag{XVI.9.50}$$

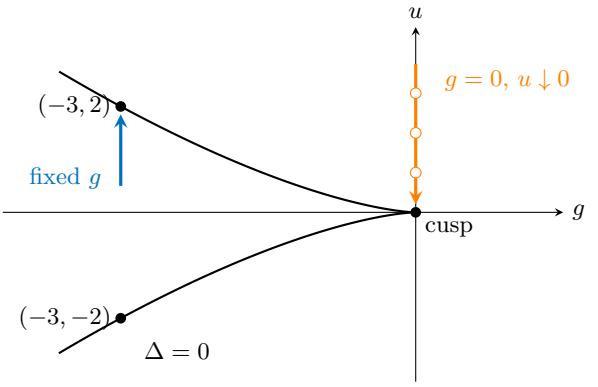


Figure XVI.9.5: The real slice of $\Delta = 0$, parametrized exactly by $(g, u) = (-3r^2, 2r^3)$. The blue vertical path keeps $g = -3$ and approaches the node $u = 2$. The orange path keeps $g = 0$ and approaches the cusp at the origin. The open points on the latter path are smooth fibers. The cusp geometry concerns parameter space, whereas the double and triple roots discussed in the text lie in the separate spectral z plane.

Use a counterclockwise contour $|w| = 0.1$, with the branches displayed in this equation. If $|\delta| < 0.01 \cdot 2.9$, the second square root has a uniformly convergent binomial expansion on the contour. At $\delta = 0$ the integrand is holomorphic inside, and its integral vanishes.

$$\lambda = \left[w\sqrt{3+w} + \frac{\delta}{2w\sqrt{3+w}} + O(\delta^2) \right] dw, \qquad \oint \lambda\big|_{\delta=0} = 0. \tag{XVI.9.51}$$

The linear coefficient has a simple pole at $w = 0$. Its residue, with the chosen orientation, gives the actual slope.

$$\Pi_{\text{node}}(\delta) = \frac{\delta}{2} \oint \frac{dw}{w\sqrt{3+w}} + O(\delta^2) = \frac{\pi i}{\sqrt{3}}\delta + O(\delta^2). \tag{XVI.9.52}$$

At $\delta = 10^{-6}$ the geometric quadrature gives $\Pi_{\text{node}} \simeq 1.813799332\,74\,10^{-6} i$, compared with slope $\pi i/\sqrt{3} \simeq 1.81379936423i$. Reversing the contour changes the sign. This is a local vanishing cycle; its orientation has not been identified with a globally transported charge from Chapter 5.

For the second path set $g = 0$ and take $u > 0$ toward zero. All three roots shrink together. Rescale $z = u^{1/3}t$ and $x = u^{1/2}\xi$, choosing the branches continuously along this positive ray.

$$\xi^2 = t^3 + 1, \qquad \lambda = u^{5/6}\xi\, dt, \qquad \Pi_\gamma(u) = u^{5/6}\Pi_\gamma(1). \tag{XVI.9.53}$$

The same transported lifted contour in the t curve supplies the last equality. The exponent is forced by $[u] = 6/5$, since a period has weight one. It differs from the linear nodal law because a triple collision changes the local scaling problem.

$$\frac{\Pi_\gamma(8)}{\Pi_\gamma(1)} = 8^{5/6}, \qquad \text{whereas} \qquad \lim_{\delta\to 0} \frac{\Pi_{\text{node}}(\delta)}{\delta} = \frac{\pi i}{\sqrt{3}}. \tag{XVI.9.54}$$

A zero geometric period is a necessary ingredient for a massless state of that charge if such a state is present. Occupancy and stability require a physical charge assignment and BPS information. Neither follows from the vanishing integral. Likewise the source identification of the cusp as an AD fixed point uses the physical constructions, beyond the discriminant calculation. This distinction will matter when irregular defects are used as building blocks rather than only as polynomial models.

Take-home message

A heavy-flavor collision has a finite spectral limit only after the Coulomb coordinate follows the required path. The explicit four-to-three-flavor cancellation retains two compact periods and produces an irregular polar jet. In the cubic, fixing that jet fixes g while u varies a vacuum. SW scaling and the IIB residue form independently give dimensions $4/5$ and $6/5$ for those directions. The quartic adds a dimension-one mass with a logarithmic spectral norm and an actual eigenvalue residue. Finally a fixed-coupling node has a linear vanishing period, while the homogeneous cubic path scales as $u^{5/6}$. The reader should be able to reproduce these cancellations, coordinate changes and parameter distinctions before using a local curve to discuss a physical theory.

Exercises

1. Reconstruct the finite-H numerator in (XVI.9.4). Submit the finite limiting rational function and the coefficient of the residual H divergence when $U_{\text{wrong}} = S - \widehat{U}$. Use L for L_{AF} and U for $\widehat{U}$ in your submission. Derive both cancellations. Explain why making one residue large at fixed partner removes two fundamental mass combinations.

2. Starting from equality of inverse holomorphic couplings at a heavy full-hyper mass M, submit $(b_4, b_3, b_2, b_1, b_0)$ and the multiplier Q_{N_f-1}/Q_{N_f} for $N_f = 3, 2, 1$. Derive the threshold products and discuss their scheme dependence. Explain why these products do not give the missing lower-flavor curve maps.

3. Invert the cubic differential and pass to $w = t^2$. Submit its quadratic pole order in w, its resolved one-form pole order in t, the jet through the constant term, and the radial norm exponents for u and g. Explain which data fix a formal boundary type and what additional work would determine Stokes matrices and a real Hitchin solution.

4. For the quartic submit the dimensions of u_4, m_4, h, their radial exponents, and the residue at infinity on the sheet $x \sim z^2$. Derive the square-root expansion and explain why the logarithmic direction is a fixed mass background rather than another vacuum coordinate.

5. For the suspended cubic and the changed-input degree-five suspension, submit the highest Jacobi basis exponent, the residue-form weight, every coefficient dimension

in ascending monomial order, and the numbers of Coulomb, mass and source directions. Derive the quotient and the normalization. Explain the IIB decoupling premise and exhibit the critical line obtained by omitting x^2 while retaining x.

6. Submit the cubic discriminant, the two factorizations at $g = -3A^2, u = \pm 2A^3$, the coefficient of δ in the positively oriented nodal period at $A = 1$, and the homogeneous scaling exponent at $g = 0$. Derive the residue slope and explain why these limits differ. State what further physical information is needed before declaring a stable massless BPS state.

7. Recompute the first retained compact period in (XVI.9.13), solving the finite-H branch roots anew. Submit the negative imaginary part's magnitude at infinity and its three absolute errors for $H = 1000, 2000, 4000$. Explain the return-sheet factor and sign. Give the compact-contour argument for $O(H^{-1})$ and identify the failure when a contour meets an end or a discriminant.

For benchmark submissions, see `benchmark/PROTOCOL.md`. Numerical comparisons use finite tolerances and supply no rigorous integral error bounds. Include the requested written derivations and explanations.

Sources and scope

Section 9.1. The finite-H identity, comparison with linear subtraction, absolute threshold powers and retained compact periods are calculated [MATH]. The class-S and heavy-flavor interpretation is a physical input [GEO-E]. The complete target differential is Gaiotto et al. (2013, arXiv:0907.3987v2, p. 134, eq. (10.19), and p. 136, eqs. (10.21), (10.23)); the heavy-flavor and $4 - N_f$ interpretation uses Gaiotto (2009, arXiv:0908.0307v1, pp. 1–2, p. 5, Sections 4 and 6). Lower-flavor steps are threshold products only. The compact-contour estimate assumes separated smooth contours and continued sheets. The quadrature values are not certified enclosures or full-lattice convergence.

Section 9.2. The cotangent and polar-jet comparison is calculated [MATH]. The boundary prescription and vacuum interpretation are physical inputs [GEO-E] from Gaiotto et al. (2013, arXiv v2, p. 100, Section 8, pp. 105–106, eqs. (9.7)–(9.12)) and Gaiotto (2009, arXiv:0908.0307v1, p. 6, Section 7). The ramified examples also use Xie (2013, arXiv:1204.2270v2, pp. 13–15, Section 4.1.1). Spectral asymptotic normalizability is evaluated on the smooth locus; no real metric, full noncompact metric L^2 theorem or Stokes multiplier is calculated.

Section 9.3. The scaling, removal of the translation parameter, asymptotic exponents and quartic residue are calculated [MATH]. The AD interpretation and physical parameter dictionary [GEO-E] come from Xie (2013, arXiv v2, pp. 13–15, eqs. (4.1)–(4.5) and Table 1) and Xie and Yau (2015, arXiv:1510.01324v1, pp. 7–8, eqs. (2.14)–(2.17)). A dimension-one coefficient does not by itself determine a flavor Lie algebra. The dimension-one UV scale L_{AF} is distinct from the weight-2/5 infrared parameter Λ_{AD}.

Section 9.4. The Jacobi quotient, residue weight and local coefficient map are calculated [MATH]. The physical roles of the parameters use the AD dictionary above [GEO-E]. The decoupling premise [DEC] comes from Xie and Yau (2015, arXiv v1, p. 5, Section 2.1, discussion following eq. (2.3)); the deformation and scaling formulas use pp. 6–8, eqs. (2.4)–(2.8), (2.12). The isolated suspension and its decoupling interpretation are assumed. There is no global compact embedding or complete global duality conclusion from the polynomial comparison.

Section 9.5. The discriminants, factorizations and explicitly oriented geometric periods are calculated [MATH]. The comparison anchors are Gaiotto et al. (2013, arXiv v2, p. 112, eq. (9.29), and p. 116, paragraph before eq. (9.35)). Chapter 5 supplies the beta-period orientation and cubic convention. The local nodal cycle is not identified with a globally transported charge. Vanishing does not establish occupancy, stability or an absolute BPS mass.

The geometric differential is $\lambda = x\,dz$ as in Chapter 4. Physical periods use one common uncalibrated c_{SW}. The degree-five exercise is a bounded algebra and weight calculation. No general classification of irregular defects is inferred.

References

Gaiotto, D. (2009). "Asymptotically free N=2 theories and irregular conformal blocks". In: arXiv: 0908.0307 [hep-th].

Gaiotto, D., G. W. Moore, and A. Neitzke (2013). "Wall-crossing, Hitchin Systems, and the WKB Approximation". In: *Adv. Math.* 234, pp. 239–403. DOI: 10.1016/j.aim.2012.09.027. arXiv: 0907.3987 [hep-th].

Xie, D. (2013). "General Argyres-Douglas Theory". In: *JHEP* 01, p. 100. DOI: 10.1007/JHEP01(2013)100. arXiv: 1204.2270 [hep-th].

Xie, D. and S.-T. Yau (2015). "4d N=2 SCFT and singularity theory Part I". In: arXiv: 1510.01324 [hep-th].

Chapter XVI.10

Outer twists and orthogonal–symplectic constructions

A field on the compactification surface need not return to itself after circling a puncture. It can return after an outer automorphism of the six-dimensional theory. This possibility changes both the allowed differentials and the types of ends that can be sewn together. We study one order-two twist of D_4, following it from roots to a spectral curve and then to two complete gauge theories.

The reader needs the cotangent spectral curve of Chapter 4, the distinction between Nahm and Hitchin labels in Chapter 5, and the half-hyper and current-level conventions of Chapter 6. We will calculate monodromy, local pole witnesses, global sections and gauge screening. The physical identification of a three-punctured sphere as matter is an additional ingredient of the compactification. Keeping that ingredient visible lets us use one free fixture to construct an orthogonal theory and a symplectic theory without confusing their differently decorated surfaces. A final pair of exceptional punctures shows why pole orders alone cannot replace the full boundary condition.

XVI.10.1 Why a twist line is needed

Which fields can pass through an outer-twisted cylinder? Begin with an orthonormal basis e_i for the D_4 root space. The roots and a convenient simple system are

$$R(D_4) = \{\pm e_i \pm e_j \mid i < j\}, \qquad (\alpha_1, \alpha_2, \alpha_3, \alpha_4) = (e_1 - e_2, e_2 - e_3, e_3 - e_4, e_3 + e_4). \tag{XVI.10.1}$$

There are six pairs of positions and four choices of signs, hence 24 roots. Choose the involution that reverses the last coordinate. Its action on the simple roots makes the

outer action explicit,

$$\sigma(e_4) = -e_4, \qquad \sigma(e_i) = e_i \ (i < 4), \qquad (\sigma\alpha_1, \sigma\alpha_2, \sigma\alpha_3, \sigma\alpha_4) = (\alpha_1, \alpha_2, \alpha_4, \alpha_3). \tag{XVI.10.2}$$

It preserves the vector weights $\{\pm e_i\}$ as a set. To see what it does to spinors, write their weights rather than identifying their equal dimensions,

$$\begin{aligned} W_s &= \left\{ \tfrac{1}{2}(\epsilon_1, \epsilon_2, \epsilon_3, \epsilon_4) \mid \epsilon_i = \pm 1, \ \prod_i \epsilon_i = 1 \right\}, \\ W_c &= \left\{ \tfrac{1}{2}(\epsilon_1, \epsilon_2, \epsilon_3, \epsilon_4) \mid \epsilon_i = \pm 1, \ \prod_i \epsilon_i = -1 \right\}. \end{aligned} \tag{XVI.10.3}$$

Reversing one sign changes the product. Thus $\sigma W_s = W_c$, whereas $\sigma W_v = W_v$. The selected twist exchanges 8_s and 8_c and fixes the vector representation. It is one chosen $\mathbb{Z}_2$ inside the triality group, rather than the full set of S_3 twists.

The invariant Cartan subspace is $e_4 = 0$. Project each root with $\pi = (1 + \sigma)/2$, retaining each resulting vector once. Roots involving e_4 project to the short vectors $\pm e_i$, while the others remain unchanged,

$$\pi R(D_4) = \{\pm e_i \pm e_j \mid 1 \le i < j \le 3\} \cup \{\pm e_i \mid 1 \le i \le 3\}. \tag{XVI.10.4}$$

The twelve long roots have squared length two and the six short roots squared length one. These are B_3 roots. Boundary labels will also require the coroots,

$$\beta^\vee = \frac{2\beta}{(\beta, \beta)}, \qquad R^\vee = \{\pm e_i \pm e_j\} \cup \{\pm 2e_i\}, \qquad (N_{\ell^2=2}, N_{\ell^2=4}) = (12, 6). \tag{XVI.10.5}$$

They form C_3. In the twisted construction the invariant Hitchin algebra is $\mathfrak{so}(7)$, and its Langlands-dual Nahm algebra is $\mathfrak{usp}(6)$. The interchange of root lengths matters. Rank three avoids the accidental $B_2 = C_2$ identification, which would conceal this distinction. The folding calculation supplies these root systems; the assignment of their roles in the defect boundary condition comes from the compactification dictionary.

A twist line records transport rather than a new local interaction. On a punctured sphere let g_i denote small positively oriented loops. The fundamental-group relation and its image in the selected $\mathbb{Z}_2$ give

$$\prod_i g_i = 1, \qquad \prod_i \sigma^{\varepsilon_i} = 1, \qquad \sum_i \varepsilon_i = 0 \pmod 2. \tag{XVI.10.6}$$

A trinion can therefore have one untwisted end U and two twisted ends T, M. Changing U to a third twisted end would give $\sigma^3 = \sigma$, inconsistent with this relation. The names T and M will distinguish their boundary conditions, although both have the same outer holonomy.

This picture also determines the holonomy of a future tube. A separating circle enclosing T and M has holonomy $\sigma\sigma = 1$, so sewing at the remaining U end gives an untwisted tube. Sewing a twisted full end instead gives a twisted tube. We now carry that transport rule into the invariant differentials that measure Coulomb parameters.

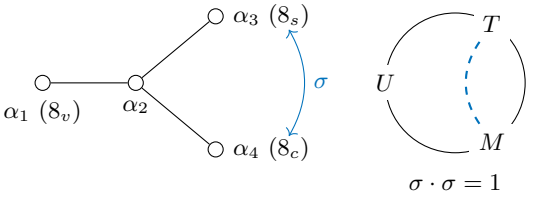


Figure XVI.10.1: The selected D_4 involution and a permitted twisted trinion. In the left panel the two spinor nodes are exchanged, while the vector node is fixed. In the right panel the dashed arc joins the two twisted ends T, M; the untwisted end U has no twist endpoint. The arc represents outer-automorphism transport.

XVI.10.2 Twisted differentials and their spectral curve

The determinant is insensitive to the exchange of spinors, but the Pfaffian detects it. Let B be a symmetric nondegenerate form with determinant one, and let Φ_z satisfy $\Phi_z^T B + B\Phi_z = 0$. Then $A = B\Phi_z$ is skew. In a coordinate z, define the scalar coefficients by

$$\det(x - \Phi_z) = x^8 + c_2 x^6 + c_4 x^4 + c_6 x^2 + p_4^2, \qquad p_4 = \operatorname{Pf}(B\Phi_z). \tag{XVI.10.7}$$

Here $c_k (dz)^k$ and $p_4 (dz)^4$ are the differentials. These characteristic coefficients use the D_4 convention directly. There is no extra minus sign inherited from an alternative A-type rearrangement of the curve.

Choose an orthogonal matrix O of determinant -1. Conjugation leaves the characteristic polynomial fixed. Since $BO = O^T B$ for the involution used below, Pfaffian covariance gives

$$\operatorname{Pf}(O^T A O) = \det(O)\operatorname{Pf}(A) = -\operatorname{Pf}(A), \qquad \sigma(c_2, c_4, c_6, p_4) = (c_2, c_4, c_6, -p_4). \tag{XVI.10.8}$$

One way to derive the covariance is to regard A as a two-form on an eight-dimensional vector space. Its fourth exterior power is $4!\operatorname{Pf}(A)$ times the volume form. A change of basis multiplies that volume form by its determinant. Thus the sign follows from orientation, rather than from a choice of square-root branch after computing the determinant.

Near a twisted end use the cover $z = t^2$. The coefficient matrix obeys the outer-equivariance condition

$$\Phi_z(-t) = O\Phi_z(t)O, \qquad c_{2j}(-t) = c_{2j}(t), \qquad p_4(-t) = -p_4(t). \tag{XVI.10.9}$$

Even powers of t become integer powers of z. Odd powers become half-integer powers. The latter describe a differential valued in a sign local system, not an ordinary single-valued meromorphic function on the punctured z-sphere.

The one-form itself includes a Jacobian. Writing its pullback coefficient as Ψ_t gives

$$\Phi = \Phi_z(t)\, dz = 2t\Phi_z(t)\, dt = \Psi_t(t)\, dt, \qquad -\Psi_t(-t) = O\Psi_t(t)O. \tag{XVI.10.10}$$

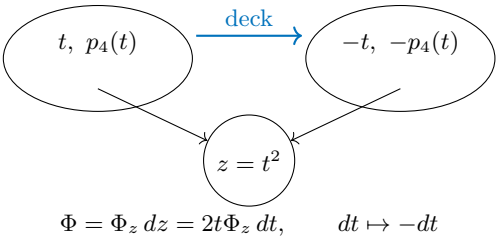


Figure XVI.10.2: A local double cover $z = t^2$ of a twisted puncture. The two marked preimages of a nonzero z are exchanged by the deck transformation. The Pfaffian coefficient changes sign, whereas its square does not. The lower relation records the one-form Jacobian that must accompany this exchange.

The minus sign on the left comes from $dt \mapsto -dt$. Dropping it would impose a different transformation on the one-form. Figure XVI.10.2 separates the coefficient parity from the differential transformation.

Why does p_4 remain an independent coordinate if only its square occurs in the curve? On a block-skew Cartan take four independent parameters a_i. The polynomial and Pfaffian are

$$\det(x - \Phi) = \prod_{i=1}^{4}(x^2 + a_i^2), \qquad (c_2, c_4, c_6, p_4) = \big(e_1(a^2), e_2(a^2), e_3(a^2), \prod_i a_i\big). \tag{XVI.10.11}$$

The elementary symmetric functions e_j are evaluated on $a_1^2, \dots, a_4^2$. Their fourth member is p_4^2. To test independence before squaring, put $y_i = a_i^2$. The Jacobian of all four elementary functions is a Vandermonde determinant. Applying the chain rule and then replacing e_4 by p_4 yields

$$\left|\det \frac{\partial(c_2, c_4, c_6, p_4)}{\partial(a_1, a_2, a_3, a_4)}\right| = 8\left|\prod_{i<j}(a_i^2 - a_j^2)\right| \neq 0 \tag{XVI.10.12}$$

when all squared eigenvalues differ and the displayed coordinate chart is nonsingular. For example $(1, 2, 3, 5)$ works. Deleting p_4 leaves only three functions, hence loses rank. With $\lambda = x\, dz$ of dimension one and dimensionless z, the four generator degrees are

$$[c_2, c_4, p_4, c_6] = (2, 4, 4, 6), \qquad [p_4^2] = 8. \tag{XVI.10.13}$$

Replacing a coordinate by its square changes the grading and loses its sign information, although every complex number still has a complex square root. A change in generator grading must not be confused with a restriction on attainable complex values. The same distinction will explain an exceptional puncture constraint at the end of the chapter.

XVI.10.3 Twisted puncture labels and boundary data

A twist holonomy alone does not choose a puncture. We must specify the Nahm embedding and translate it to a Hitchin residue. For our three selected ends the massless data are

	Nahm partition	Hitchin partition	$(p_2, p_4, p_6; p_{\mathrm{Pf}})$	$\mathfrak{f}$
U	$[1^8]$	$[7,1]$	$(1,3,5;3)$	$\mathfrak{so}(8)$
T	$[1^6]$	$[7]$	$(1,3,5;7/2)$	$\mathfrak{usp}(6)$
M	$[6]$	$[1^7]$	$(1,1,1;1/2)$	0

(XVI.10.14)

These are written row partitions. The twisted Nahm partitions belong to C_3 and the twisted Hitchin partitions to B_3. The selected rows carry no further coefficient constraints. The boundary dictionary and its general allowed-pole bounds are physical inputs. We can calculate their centralizers and construct explicit matrices attaining these bounds.

First distinguish full from principal Nahm data. On a basis indexed by $i = 0, \dots, 5$, construct the irreducible $\mathfrak{sl}_2$ triple and its alternating invariant form,

$$h_{ii} = 5 - 2i, \quad e_{i,i+1} = 1, \quad f_{i+1,i} = (i+1)(5-i), \quad S_{ij} = (-1)^i \delta_{i+j,5}. \tag{XVI.10.15}$$

All other entries vanish. The successive nonzero entries of f are $5, 8, 9, 8, 5$. Multiplying adjacent entries verifies

$$[h,e] = 2e, \qquad [h,f] = -2f, \qquad [e,f] = h, \qquad e^T S + Se = f^T S + Sf = h^T S + Sh = 0. \tag{XVI.10.16}$$

A matrix commuting with h is diagonal, since its six eigenvalues differ. Commuting also with e forces every diagonal entry to be the same. The symplectic Lie condition then removes that scalar,

$$[Z,h] = [Z,e] = [Z,f] = 0 \implies Z = aI_6, \qquad Z^T S + SZ = 2aS = 0 \implies Z = 0. \tag{XVI.10.17}$$

Thus the principal Nahm label [6] has trivial connected flavor algebra. For the zero embedding, $[1^6]$, only the symplectic equation remains. In a Darboux basis it has the block solution

$$Z = \begin{pmatrix} A & B_0 \\ C_0 & -A^T \end{pmatrix}, \qquad B_0 = B_0^T, \quad C_0 = C_0^T, \qquad \dim \mathfrak{usp}(6) = 9 + 6 + 6 = 21. \tag{XVI.10.18}$$

Full therefore means zero Nahm embedding here. Commuting with the nilpotent e alone would give a different, larger commutant and would not calculate the flavor algebra of this boundary condition.

For a local pole witness let S_7 be the symmetric matrix $(S_7)_{ij} = (-1)^i \delta_{i+j,6}$ for $0 \le i, j \le 6$. The following explicit block matrices define an orthogonal family,

$$\begin{aligned} B &= \mathrm{diag}(S_7, 1), \quad O = \mathrm{diag}(I_7, -1), \quad X = \mathrm{diag}(J_7, 0), \\ A &= \mathrm{diag}(S_7^{-1} K, 0), \qquad Y = \begin{pmatrix} 0 & v \\ -v^T S_7 & 0 \end{pmatrix}. \end{aligned} \tag{XVI.10.19}$$

Here $(J_7)_{i,i+1}=1$, $v=(1,2,3,5,7,11,13)^T$, and K is skew with upper entries $K_{ij}=((i+2)(j+3)\bmod 11)-5$, now indexed by $0\le i<j\le 6$. These entry formulas specify every matrix. They give $X^7=0$, $X^6\neq 0$, $OXO=X$, $OAO=A$ and $OYO=-Y$. The Jordan type of X is $[7,1]$, with its 7 block the principal B_3 residue.

Use $\Phi_z=X/t^2+Y/t+A$ on $z=t^2$. The first coefficient can be checked without expanding an eight-by-eight determinant. The specified matrices give

$$\begin{gathered}\operatorname{Tr}X^2=0,\quad \operatorname{Tr}A^2=-80,\quad \operatorname{Tr}Y^2=2,\quad \operatorname{Tr}(XA)=-16,\\ \operatorname{Tr}(XY)=\operatorname{Tr}(AY)=0,\qquad c_2=-\tfrac12\operatorname{Tr}\Phi_z^2=-\tfrac12\left[-80+\frac{2-32}{t^2}\right]=40+\frac{15}{t^2}.\end{gathered}\tag{XVI.10.20}$$

Deleting X removes the cross term $2\operatorname{Tr}(XA)/t^2$ and gives $c_2=40-t^{-2}$. To obtain the higher coefficients, write $T_j=\operatorname{Tr}\Phi_z^j$ and $\det(I-s\Phi_z)=\sum_m c_m s^m$. Expanding its logarithm yields the recurrence

$$mc_m=-\sum_{j=1}^{m}c_{m-j}T_j,\qquad c_0=1,\qquad c_4=\frac{T_2^2-2T_4}{8},\qquad c_6=-\frac{T_2^3}{48}+\frac{T_2T_4}{8}-\frac{T_6}{6}.\tag{XVI.10.21}$$

Here odd traces vanish by orthogonality. For the Pfaffian, pair the first index with each remaining index of the skew matrix $B\Phi_z$ in turn. The signed matching expansion is

$$\operatorname{Pf}(M)=\sum_{j=2}^{2n}(-1)^jM_{1j}\operatorname{Pf}(M_{\widehat{1j}}),\qquad \operatorname{Pf}(\varnothing)=1.\tag{XVI.10.22}$$

These recurrences give the full Laurent expressions

$$\begin{aligned}c_2&=40+15t^{-2},\\ c_4&=1545+2222t^{-2}-1509t^{-4}+23t^{-6},\\ c_6&=-113762+260545t^{-2}-4328t^{-4}-13871t^{-6}+1408t^{-8}+55t^{-10},\\ p_4&=-1931t^{-1}+72t^{-3}+91t^{-5}+13t^{-7}.\end{aligned}\tag{XVI.10.23}$$

The nonzero leading coefficients attain $(1,3,5;7/2)$ in the z coordinate. Removing precisely the residue X changes the boundary to a minimal witness,

$$\begin{aligned}&\Phi_z=Y/t+A,\qquad && c_2=40-t^{-2},\qquad && c_4=1545+1104t^{-2},\\ &c_6=-113762+280983t^{-2},\qquad && p_4=-1931t^{-1}.\end{aligned}\tag{XVI.10.24}$$

The resulting orders are $(1,1,1;1/2)$. Each determinant term uses the eighth row and column at most once, so it contains at most two entries from the odd block Y/t. Each Pfaffian matching pairs the eighth index exactly once, giving at most one such entry. This explains the small orders after X is removed. In an ordinary untwisted coordinate z, the family $X/z+A+Y$ instead gives

$$(p_2,p_4,p_6;p_{\mathrm{Pf}})=(1,3,5;3).\tag{XVI.10.25}$$

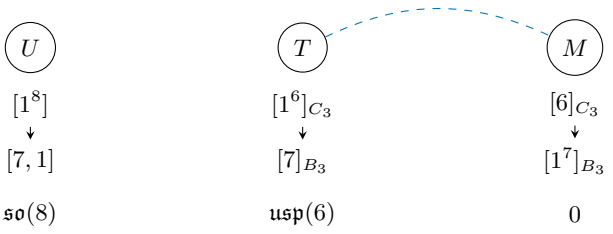


Figure XVI.10.3: The three puncture records used in the construction. Each column gives its written Nahm label, Hitchin label and flavor algebra. The dashed arc marks the two outer-twisted records. The arrows translate boundary labels between the appropriate algebras; they do not identify the Nahm and Hitchin partitions. Pole tuples are given in (XVI.10.14).

These examples demonstrate attainment of the selected sourced bounds. Their finite number does not establish the generic defect classification or exclude other constraints for other rows.

We can now assemble a surface using actual boundary conditions. The full flavor algebra at an end specifies the candidate gauging, but it still does not identify the matter residing on a trinion. That identification is the next physical input.

XVI.10.4 Gluing two fixtures into a complete theory

The trinion $F = (U, T, M)$ is identified by the twisted D construction as one half-hypermultiplet in $(8_v, 6)$ of $\mathfrak{so}(8) \oplus \mathfrak{usp}(6)$. This physical statement supplies more information than its vanishing Coulomb rank. It is compatible with the real vector metric I_8 and alternating fundamental metric J_6,

$$\Omega = I_8 \otimes J_6, \qquad \Omega^T = -\Omega, \qquad \det \Omega \neq 0, \qquad n_h(F) = \tfrac{1}{2} \dim(8_v \otimes 6) = 24. \tag{XVI.10.26}$$

The product representation is pseudoreal and admits the half-hyper reality condition. This calculation checks the representation's reality; it does not derive the existence of the physical fixture.

Let us first calculate its Coulomb sections and then sew it. A degree-k differential with finite pole orders p_i can be written as $P(z) \prod_{i<\infty} (z - z_i)^{-p_i} (dz)^k$. A numerator monomial of degree j has infinity order

$$p_\infty^{\text{term}} = 2k + j - \sum_{i<\infty} p_i, \qquad 0 \leq j \leq \sum_i p_i - 2k, \qquad h^0 = \max(0, 1 - 2k + \sum_i p_i). \tag{XVI.10.27}$$

For the Pfaffian, extract the square-root factors at the twisted ends before treating P as an ordinary polynomial. The even number of sign holonomies makes the total exponent integral. The same infinity argument then applies to its half-integer pole orders. For (U, T, M) the three even sums are $3, 7, 11$, and the Pfaffian sum is $3 + 7/2 + 1/2 = 7$.

Consequently

$$(d_2, d_4, d_6; d_{\mathrm{Pf}})(F) = (1{-}4{+}3, 1{-}8{+}7, 1{-}12{+}11; 1{-}8{+}7) = (0,0,0;0). \quad \text{(XVI.10.28)}$$

This is consistent with the supplied free matter, while not identifying that matter by itself.

Sew two U ends. The external ends are (T, M, T, M) and the cylinder is untwisted. Place T at $0, \infty$ and M at $1, q$, with $q \neq 0, 1, \infty$. The pole sums become $4, 8, 12; 8$, so each of the four generators has one coefficient. The explicit massless basis is

$$\begin{aligned} c_2 &= \frac{u_2}{z(z-1)(z-q)}, \qquad c_4 = \frac{u_4}{z^3(z-1)(z-q)}, \\ c_6 &= \frac{u_6}{z^5(z-1)(z-q)}, \quad p_4 = \frac{v_4}{z^{7/2}(z-1)^{1/2}(z-q)^{1/2}}. \end{aligned} \qquad \text{(XVI.10.29)}$$

The corresponding powers of dz are understood as in Section 10.2. A loop around each external end reverses p_4; its square is single valued. To check the omitted infinity end, put $w = 1/z$. For the even forms the denominator degree is $k+1$, and hence

$$\frac{(dz)^k}{z^{k-1}(z-1)(z-q)} = \frac{(-1)^k w^{-(k-1)}(dw)^k}{(1-w)(1-qw)}, \qquad k = 2, 4, 6. \qquad \text{(XVI.10.30)}$$

For the Pfaffian the total finite exponent is $9/2$, while the Jacobian has exponent eight. Its infinity order is $8 - 9/2 = 7/2$, exactly the second T pole. Adding a linear numerator to any displayed form would increase its infinity order by one and violate that bound.

Substitution into (XVI.10.7) gives a complete massless base family,

$$\begin{aligned} &x^8 + \frac{u_2 x^6}{z(z-1)(z-q)} + \frac{u_4 x^4}{z^3(z-1)(z-q)} \\ &+ \frac{u_6 x^2}{z^5(z-1)(z-q)} + \frac{v_4^2}{z^7(z-1)(z-q)} = 0, \qquad \lambda = x\,dz. \end{aligned} \qquad \text{(XVI.10.31)}$$

Thus the Coulomb degrees are $2, 4, 4, 6$, and the four-puncture complex structure supplies one dimensionless marginal parameter q. This is a massless family of coefficients, without a choice of absolute period normalization or a construction of the massive family.

As $\mathfrak{so}(8)$ matter, each half-bifundamental is six vector half-hypers. Two copies are therefore six full vector hypers. With $h^\vee_{\mathfrak{so}(8)} = 6$ and vector index one, the screening and anomaly calculation is

$$\begin{aligned} b_0 = 2h^\vee - 2N_f = 12 - 12 = 0, \qquad n_v = 28, \quad n_h = 2 \cdot 24 = 48, \\ (a, c) = \left(\frac{5n_v + n_h}{24}, \frac{2n_v + n_h}{12} \right) = \left(\frac{47}{6}, \frac{26}{3} \right). \end{aligned} \qquad \text{(XVI.10.32)}$$

The sourced real-matter flavor rule gives the full massless flavor algebra $\mathfrak{usp}(12)$, of dimension $6(13) = 78$. The visible $\mathfrak{usp}(6) \oplus \mathfrak{usp}(6)$ from the two T ends is a subgroup. Counting only the puncture currents would miss transformations mixing the two collections of vectors. The graded spectrum also gives $\sum(2\Delta - 1) = 3 + 7 + 7 + 11 = 28 = 4(2a - c)$.

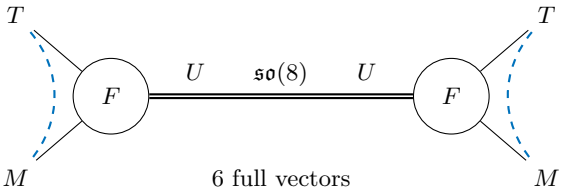


Figure XVI.10.4: Sewing the untwisted full ends U of two copies of F. The central cylinder carries $\mathfrak{so}(8)$. Each dashed arc joins T to M on its own trinion, so the cylinder has trivial outer holonomy. The four external ends are T, M, T, M, the decoration used in (XVI.10.29).

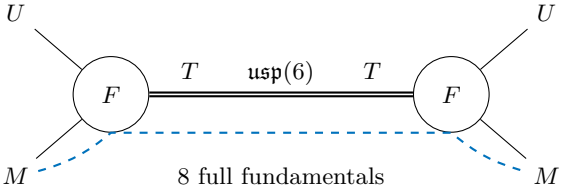


Figure XVI.10.5: Sewing the twisted full ends T. The dashed line crosses the $\mathfrak{usp}(6)$ cylinder and joins the remaining twisted minimal ends M. The external full ends are now untwisted U ends. This surface differs from Figure XVI.10.4 in its external decorations and gives a different gauge theory.

Now change which full ends are sewn. Gluing T to T gives a twisted $\mathfrak{usp}(6)$ cylinder and external decoration (U, M, U, M). Its even pole sums are unchanged. Its Pfaffian sum is instead $3 + 1/2 + 3 + 1/2 = 7$, leaving no Pfaffian section,

$$(d_2, d_4, d_6; d_{\mathrm{Pf}}) = (1, 1, 1; 0), \qquad \{\Delta\}_{\mathfrak{usp}(6)} = \{2, 4, 6\}. \tag{XVI.10.33}$$

For example place U at $0, \infty$ and M at $1, q$. The same three rational even coefficients work, whereas a putative Pfaffian constant numerator would have finite exponents $3, 1/2, 1/2$ and infinity order four, exceeding the allowed order three. Its numerator degree bound is -1.

Each fixture contributes eight fundamental half-hypers to this gauging. Thus there are sixteen half-hypers, or eight full fundamentals, and $h^\vee = 4$. With the fundamental screening contribution of one full symplectic hyper equal to one,

$$\begin{aligned} b_0 &= 2 \cdot 4 - 8 = 0, \qquad n_v = 21, \quad n_h = 48, \\ (a, c) &= \left(\frac{51}{8}, \frac{15}{2}\right), \qquad N_{\mathrm{half}} = 16 = 0 \pmod 2. \end{aligned} \tag{XVI.10.34}$$

The last condition is the fundamental Witten parity test. Removing just one half-hyper makes that parity odd and gives $b_0 = 1/2$. Treating each original fixture as a full bifundamental instead doubles screening, giving $b_0 = -12$ for the orthogonal gauging

and -8 for the symplectic gauging. The half factor therefore affects both local anomalies and global consistency of the symplectic matter representation.

The sourced pseudoreal-matter flavor rule gives $\mathfrak{so}(16)$ of dimension $16 \cdot 15/2 = 120$, containing the visible $\mathfrak{so}(8) \oplus \mathfrak{so}(8)$. The local full-leg levels $k_{\mathfrak{so}(8)} = 12$ and $k_{\mathfrak{usp}(6)} = 8$ are consistent with this same half-bifundamental count. Their agreement uses the matter premise, so it is not an independent identification of that matter. The two gluings have different ranks, anomalies and external ends. They are two constructions using one fixture, with no duality between them asserted. Absolute gauge and flavor groups and line operators require the additional choices treated in Chapter 11.

XVI.10.5 Reading D- and E-type fixture tables

What information must be retained when the twisted algebra is exceptional? Root folding still determines an invariant root system, but it does not determine the defect. We can isolate that distinction with two twisted E_6 punctures.

Take the E_6 diagram to have chain $1-2-3-4-5$ and an extra node 6 attached to 3. Its Gram matrix and involution are

$$G = \begin{pmatrix} 2 & -1 & 0 & 0 & 0 & 0 \\ -1 & 2 & -1 & 0 & 0 & 0 \\ 0 & -1 & 2 & -1 & 0 & -1 \\ 0 & 0 & -1 & 2 & -1 & 0 \\ 0 & 0 & 0 & -1 & 2 & 0 \\ 0 & 0 & -1 & 0 & 0 & 2 \end{pmatrix}, \qquad \sigma = (1\ 5)(2\ 4). \tag{XVI.10.35}$$

In simple-root coordinates a reflection changes only its ith coefficient,

$$s_i(v) = v - \left(\sum_j G_{ij} v_j \right) e_i, \qquad \pi(v) = \tfrac{1}{2}(v + \sigma v). \tag{XVI.10.36}$$

Starting with the six simple roots, this operation and sign reversal generate the 72 E_6 roots. For example $s_2(e_1) = e_1 + e_2$ and $s_3(e_1 + e_2) = e_1 + e_2 + e_3$. Their projections include $\beta_1 + \beta_2$ and $\beta_1 + \beta_2 + \beta_3$, where

$$\begin{aligned} (\beta_1, \beta_2, \beta_3, \beta_4) &= \left(\frac{\alpha_1 + \alpha_5}{2}, \frac{\alpha_2 + \alpha_4}{2}, \alpha_3, \alpha_6 \right), \\ ((\beta_i, \beta_j)) &= \begin{pmatrix} 1 & -1/2 & 0 & 0 \\ -1/2 & 1 & -1 & 0 \\ 0 & -1 & 2 & -1 \\ 0 & 0 & -1 & 2 \end{pmatrix}. \end{aligned} \tag{XVI.10.37}$$

The double link between the second and third roots identifies F_4. Projecting the generated root set gives 48 distinct vectors, 24 with squared length one and 24 with squared length two. The familiar realization makes these multiplicities transparent,

$$R(F_4) = \{\pm e_i \pm e_j\} \cup \{\pm e_i\} \cup \left\{ \tfrac{1}{2}(\pm e_1 \pm e_2 \pm e_3 \pm e_4) \right\}, \qquad 24 + 8 + 16 = 48. \tag{XVI.10.38}$$

The folding is a calculation about roots. The signs on invariant polynomials require a further source input. In the twisted E_6 construction the invariant degrees and their outer eigenvalues are

$$k = (2, 5, 6, 8, 9, 12), \qquad \sigma_k = (+1, -1, +1, +1, -1, +1). \tag{XVI.10.39}$$

Thus degrees five and nine have half-integral local pole orders at a twisted end. This is a translation of the sourced invariant action, rather than a derivation of it from the root count.

The two selected records have the same pole tuple,

$$(p_2, p_5, p_6, p_8, p_9, p_{12}) = (1, 9/2, 5, 7, 15/2, 11), \tag{XVI.10.40}$$

but retain different Nahm names and additional data. In these F_4 Bala–Carter labels, a tilde marks a short-root Levi component. It distinguishes $\widetilde{A}_1$ from the long-root A_1 component. The A_1 row has Hitchin record $(F_4(a_1), \mathbb{Z}_2)$, flavor $Sp(3)_{13}$ and $(\delta n_h, \delta n_v) = (599, 584)$. The $\widetilde{A}_1$ row has underlying orbit $F_4(a_1)$, flavor $SU(4)_{12}$ and $(584, 572)$. The attached $\mathbb{Z}_2$ is Sommers–Achar information, an additional discrete orbit and boundary label. It is distinct from the $\mathbb{Z}_2$ outer holonomy that transports fields around the puncture. These orbit, flavor-level and δn_h assignments come from the boundary tables, not from folding the diagram. Here $Sp(3)$ means $USp(6)$.

The difference that we can calculate is the effect of the sourced constraint for $\widetilde{A}_1$. Introduce a local degree-six coefficient $a^{(6)}_{11/2}$ and require

$$h_6 = \frac{a^{(6)}_{11/2}}{z^{11/2}}, \qquad \phi_{12} - h_6^2 = O(z^{-10}), \qquad c^{(12)}_{11} = (a^{(6)}_{11/2})^2. \tag{XVI.10.41}$$

The subscript describes pole order; the superscript describes scaling degree. In particular the half-integral pole order $11/2$ does not make this a Coulomb operator of dimension $11/2$. The leading degree-twelve coefficient is replaced by a new independent degree-six coordinate. Its square still attains every complex value. What changes is the graded coordinate algebra and the identification under its discrete action.

Write the local contributions in degree order $(2, 3, 4, 5, 6, 8, 9, 12)$. The two profiles are

$$\begin{aligned} d^{A_1} &= (1, 0, 0, 9/2, 5, 7, 15/2, 11), \\ d^{\widetilde{A}_1} &= (1, 0, 0, 9/2, 6, 7, 15/2, 10), \qquad \Delta d_6 = 1, \quad \Delta d_{12} = -1. \end{aligned} \tag{XVI.10.42}$$

These are local contributions, which may be half-integral; they are not the spectrum of a complete physical theory. Using the weighted sum for the local vector contribution we obtain

$$\begin{aligned} \delta n_v(A_1) &= 3 + 9(9/2) + 11(5) + 15(7) + 17(15/2) + 23(11) = 584, \\ \delta n_v(\widetilde{A}_1) &= 584 + (2 \cdot 6 - 1) - (2 \cdot 12 - 1) = 572. \end{aligned} \tag{XVI.10.43}$$

The twelve-unit shift follows from the actual constraint. Keeping only the common pole tuple would incorrectly retain 584 in both rows. Conversely, this sum does not calculate the listed δn_h or flavor levels.

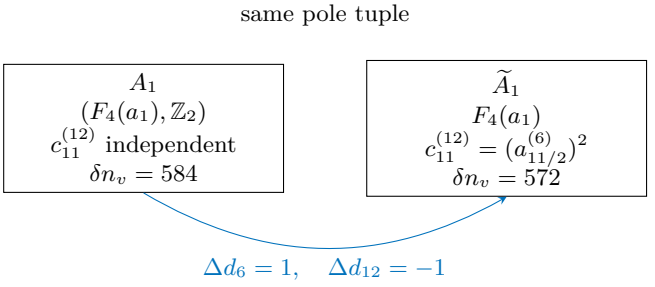


Figure XVI.10.6: The two twisted E_6 records share an underlying Hitchin orbit and pole tuple. The A_1 record also carries the displayed discrete label. For $\widetilde{A}_1$, the constraint replaces a degree-twelve generator by a degree-six generator whose square is the leading degree-twelve coefficient. The lower arrow tracks the resulting weighted vector contribution.

This two-row comparison supplies a practical reading method. Determine the outer action, keep Nahm and Hitchin labels separate, retain discrete information, and impose coefficient constraints before counting graded parameters. Only then combine local records with a full surface and its permitted cylinders. The method uses both algebra and physical boundary data. It does not construct a general exceptional fixture or classify all twisted defects.

Take-home message

The selected D_4 twist exchanges the spinors and makes the Pfaffian a sign-valued degree-four differential. Its invariant B_3 root system and dual C_3 Nahm system have different roles. With the supplied (U, T, M) half-bifundamental, sewing the untwisted full ends constructs $\mathfrak{so}(8)$ with six vectors, while sewing the twisted full ends constructs $\mathfrak{usp}(6)$ with eight fundamentals. The external decorations change with the sewing. The exceptional example shows why identical pole bounds do not determine the grading or the physical puncture.

Exercises

1. Generate the D_4 root set and apply the chosen reflection to its vector and spinor weights. Submit the original and projected root counts, the B_3 squared-length multiplicities at lengths squared $(2, 1)$ and the coroot multiplicities at $(2, 4)$, the spinor-exchange indicator, and the product holonomy for three twisted ends, with σ represented by -1. In writing derive the coroot lengths and explain why neither a physical gauge group nor a defect label follows from projection alone.

2. Use (XVI.10.11) at $(a_1, a_2, a_3, a_4) = (1, 2, 3, 5)$. Submit (c_2, c_4, c_6, p_4), their Jacobian rank, the rank after deleting p_4, their parity signs in that order, and the

pullback Jacobian exponent in $2t\,dt$. Derive Pfaffian covariance using the determinant line. Explain why a squared coefficient of degree eight does not replace the independent degree-four generator without changing the graded description.

3. Construct (XVI.10.15) and its invariant form. Submit the nullities of the full-triple centralizer and the zero-embedding centralizer, and the ordered pole tuples of T, M, U, each in $(2, 4, 6; \mathrm{Pf})$ order. In writing show the diagonal commutant argument, distinguish it from commuting with e alone, and identify which steps in the Nahm-to-Hitchin conversion use the physical boundary dictionary.

4. Reconstruct all four forms in (XVI.10.29). Submit the infinity orders in (c_2, c_4, c_6, p_4) order, the constant-numerator multiplicities for (T, M, T, M) and (U, M, U, M) in that order, and the number of complex marginal parameters. Show the square-root extraction and infinity calculation in writing. Explain why the spectrum identification uses the compactification dictionary in addition to this section calculation.

5. Gauge either full leg of two copies of the half-hyper $(8_v, 6)$. For each gauging submit (b_0, n_v, n_h, a, c) and the full flavor-algebra dimension. Submit the symplectic half-hyper count, the beta coefficient after removing one fundamental half-hyper, and the two beta coefficients after incorrectly replacing each fixture by a full bifundamental. In writing derive all representation multiplicities, give the Witten parity diagnosis, and explain why the visible puncture algebra need not exhaust the flavor algebra. State why these two surfaces do not establish a duality.

6. Fold the E_6 diagram with (XVI.10.36) and read the two exceptional puncture records. Submit the original and folded root counts, the two root-length multiplicities, the odd invariant degrees, $(\Delta d_6, \Delta d_{12})$, and the two δn_v values. Derive the weighted shift in writing. Explain the distinct meanings of pole order, scaling degree and Sommers–Achar information, and why the square relation changes grading while leaving all complex leading-coefficient values attainable.

For benchmark submissions, see `benchmark/PROTOCOL.md`. Use exact rational answers and preserve the specified array orders. Include all six written arguments.

Exit checklist

The reader should be able to carry an outer action from weights to invariant differentials, include the pullback Jacobian, and recover both the finite and infinity pole bounds of a massless family. A complete gauging should specify the actual fixture matter, its half factor, the sewn end and the remaining ends before screening or anomaly arithmetic. A table comparison should retain the orbit, discrete information and coefficient constraints before translating poles into graded contributions. Chapter 11 adds the global-form and line-operator information absent from these Lie-algebra constructions.

Sources and scope

Section 10.1. The root, weight, coroot and fundamental-group calculations are [MATH]. The physical D_4 involution, invariant Hitchin algebra and dual Nahm-label dictionary are [GEO-E], using Chacaltana et al. (2013, arXiv v1, pp. 1–3, eq. (2.2), footnotes 5–7). Only the selected order-two subgroup is treated, without a full triality-defect construction.

Section 10.2. The determinant, Pfaffian covariance, deck-equivariance and Cartan independence calculations are [MATH]. The physical invariant-differential assignment uses Chacaltana et al. (2013, arXiv v1, pp. 2–3, eqs. (2.1)–(2.2)), graded [GEO-E]. The characteristic-coefficient and cotangent conventions are those of Chapter 4, with the D-type sign translation stated in the text. No global moduli-space existence theorem or absolute period normalization is inferred from the local calculation.

Section 10.3. The chosen boundary records and generic allowed-pole bounds are [GEO-E], from Chacaltana et al. (2013, arXiv v1, §2, pp. 2–5, §3.1.1, pp. 33–34, §4.1, p. 60). The centralizer and explicit Laurent calculations are [MATH]. They attain these sourced bounds and do not establish a general classification. The flavor centralizer is that of the full Nahm triple. Chapter 5 supplies the Nahm/Hitchin naming convention, without transferring its A-type physical defect dictionary to this construction.

Section 10.4. The actual half-bifundamental fixture and permissible cylinders are [GEO-E], from Chacaltana et al. (2013, arXiv v1, §4.1, pp. 59–60). Reality and full matter-flavor rules use Tachikawa (2009, arXiv v2, §3.1, pp. 9–10, eq. (3.2), opening of §3.2, p. 11), also [GEO-E]. The representation and rational-section calculations are [MATH]; identifying their degrees with physical Coulomb generators uses the sourced Hitchin dictionary. Screening and additive anomaly arithmetic are [ANOM], conditional on that matter premise and the Chapter 6 normalization, with power one beta coefficient and two conformal anomaly coefficients per model, plus the symplectic fundamental parity test. The dimensions 78 and 120 translate the sourced flavor identifications; they are not independent derivations of physical current algebras. Local levels 12 and 8 share the matter premise. No duality between these differently decorated surfaces, absolute group, line lattice or massive period normalization is asserted.

Section 10.5. The root folding and conditional regrading are [MATH]. The invariant signs, exceptional boundary labels, orbit/discrete information, constraint, levels and δn_h entries are [GEO-E], from Chacaltana et al. (2015, arXiv v1, §2.2, p. 2, §3.1, p. 3, the $A_1, \widetilde{A}_1$ rows, Appendix A, p. 46, first constraint row). Reading degrees five and nine from the sourced signs is a translation, not an independent automorphism calculation. The weighted sum recomputes only δn_v from the sourced constraint. Local half-integral contributions are not a full SCFT spectrum. This bounded comparison supplies no general exceptional fixture construction.

References

Chacaltana, O., J. Distler, and A. Trimm (2013). “Tinkertoys for the Twisted D-Series”. In: arXiv: `1309.2299 [hep-th]`.

Chacaltana, O., J. Distler, and A. Trimm (2015). "Tinkertoys for the Twisted E6 Theory". In: arXiv: 1501.00357 [hep-th].
Tachikawa, Y. (2009). "Six-dimensional D N theory and four-dimensional SO-USp quivers". In: arXiv: 0905.4074 [hep-th].

Chapter XVI.11

Global forms and genuine line operators

A gauge algebra determines infinitesimal gauge transformations. It does not tell us which Wilson and magnetic lines can be inserted without an attached surface. That choice changes the global gauge group and the allowed bundles, even when every local field transforms in the adjoint. We will extract this extra information from wrapped six-dimensional surface defects, then see how dynamical matter changes the answer.

The prerequisites are the A_1 compactification of Chapter 1, the half-trifundamental T_2 of Chapter 3 and the distinction between the ultraviolet curve and spectral cover in Chapter 4. Our first example is the unpunctured flat compactification torus with periodic fermions and trivial R holonomy. After removing the free center tensor, it gives the interacting $\mathcal{N} = 4$ theory with algebra $\mathfrak{su}(2)$. This enhancement is a separate physical premise. The stable pants formula does not apply to this torus. Throughout, spacetime is oriented and spin. The explicit flux example has torsion-free cohomology, and the fundamental-matter example initially has trivial, liftable flavor backgrounds.

XVI.11.1 From wrapped surfaces to lines

How can a surface defect produce a line? Take its worldvolume to be a four-dimensional path ℓ times a closed one-cycle γ in the compactification curve C. At distances larger than the size of C, the wrapped direction is invisible. The center charge of the A_1 surface is valued in $\mathbb{Z}_2$, so the resulting finite candidate line charges are

$$\ell \times \gamma \longmapsto \ell, \qquad D = H_1(C, \mathbb{Z}_2), \qquad D(T^2) = \mathbb{Z}_2 A \oplus \mathbb{Z}_2 B. \tag{XVI.11.1}$$

Figure XVI.11.1 depicts the wrapping operation. This is the mod-center charge module. It records neither the spectrum of BPS particles nor all labels and degeneracies of line defects. The physical surface-to-line identification is an ingredient of the compactification. Once supplied, the cycle arithmetic is explicit.

Orient the marked torus by $A \cdot B = +1$. In integral homology, intersections are antisymmetric. Writing a charge as a column fixes our subsequent matrix convention,

$$A \cdot A = B \cdot B = 0, \quad B \cdot A = -1, \qquad q = eA + mB \longleftrightarrow \begin{pmatrix} e \\ m \end{pmatrix}. \tag{XVI.11.2}$$

Poincare duality identifies homology with cohomology on the closed oriented curve. It does not identify a cycle with a cochain without a map. If α, β evaluate on A, B respectively, the convention $\int_C \alpha \smile \beta = 1$ gives

$$\mathrm{PD}(A) = \beta, \qquad \mathrm{PD}(B) = -\alpha, \qquad \int_C \mathrm{PD}(q) \smile \mathrm{PD}(q') = em' - me'. \tag{XVI.11.3}$$

The minus sign disappears only after reduction modulo two. Thus the sourced description using $H^1(C, \mathbb{Z}_2)$ and our wrapped-cycle description using H_1 have the same pairing. For a genus-g closed curve the rank is $2g$, whereas $H^2(C, \mathbb{Z}_2)$ has rank one. Replacing H^1 by H^2 would already fail on this torus.

The center pairing divides the intersection by two. Its exponential is the mutual nonlocality phase,

$$b(q, q') = \frac{em' - me'}{2} \pmod 1, \qquad \exp(2\pi i b(q, q')) = (-1)^{em' - me'}. \tag{XVI.11.4}$$

For $W = (1, 0)$ and $H = (0, 1)$ this phase is -1. They therefore cannot both belong to one mutually local set of genuine lines. A genuine line needs no attached topological surface. This property says nothing yet about whether charged matter can screen it.

We can calculate every phase using only four representatives. In the order $0, H, W, D_0$, where $D_0 = W + H$, the numerator modulo two is

$$(0, H, W, D_0) = ((0,0), (0,1), (1,0), (1,1)), \qquad 2b = \begin{pmatrix} 0 & 0 & 0 & 0 \\ 0 & 0 & 1 & 1 \\ 0 & 1 & 0 & 1 \\ 0 & 1 & 1 & 0 \end{pmatrix} \pmod 2. \tag{XVI.11.5}$$

Every nonzero vector pairs trivially with itself and nontrivially with the other two. Exercise 1 asks the reader to reconstruct this matrix from intersections, rather than memorize it.

This distinction prevents a tempting shortcut from Chapter 4. For the four-punctured ultraviolet sphere, the spectral cover can have genus one. The periods on that cover describe a different construction from the wrapped center charges on an unpunctured ultraviolet torus. Even the topological premises differ,

$$2g - 2 + n\big|_{(1,0)} = 0, \qquad \dim H_1(T^2, \mathbb{Z}_2) = 2, \qquad \dim H_1(\mathbb{P}^1 \setminus \{4 \text{ points}\}, \mathbb{Z}_2) = 3. \tag{XVI.11.6}$$

The punctured sphere has a degenerate intersection form on these boundary cycles. It cannot be substituted into the nondegenerate torus calculation. We will return to its actual matter realization in the last section.

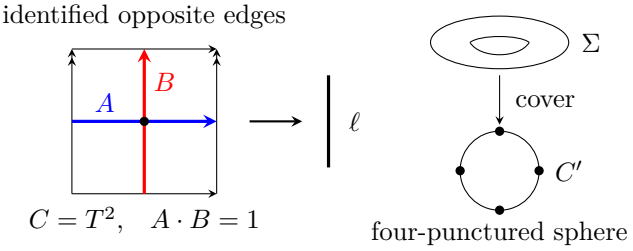


Figure XVI.11.1: A center-valued surface wraps A or B of the compactification torus C and leaves a path ℓ in spacetime. Opposite edges of the square are identified with matching arrows, so both colored paths close and meet at the marked point once. The right panel distinguishes this ultraviolet curve from an elliptic spectral cover $\Sigma \to C'$ over a four-punctured sphere. That cover does not turn C' into the compactification torus of the left panel.

XVI.11.2 Mutual locality and a choice of genuine lines

Which candidate charges can be declared genuine together? Fusion requires a subgroup $L \subset D$. Mutual locality requires isotropy. Completeness in this closed-surface example requires a maximal such subgroup. Define its orthogonal complement by

$$L^{\perp} = \{q \in D \mid b(q, l) = 0 \text{ for all } l \in L\},$$

$$L \subset L^{\perp}, \qquad L = L^{\perp} \text{ for a complete choice.} \tag{XVI.11.7}$$

The trivial subgroup is isotropic but incomplete. Each order-two subgroup is generated by one of the three nonzero vectors. Equation (XVI.11.5) shows that either additional nonzero vector would spoil locality,

$$L_W = \{0, W\}, \qquad L_H = \{0, H\}, \qquad L_D = \{0, W + H\}, \qquad L_i^{\perp} = L_i. \tag{XVI.11.8}$$

The full group is not isotropic since $b(W, H) = 1/2$. These exhaust all subgroups, so the three choices are maximal. Here maximal means that no further independent charge can be added while retaining isotropy. It does not mean that a larger subgroup exists with the same locality property.

To see how this method survives actual matter screening, change the compactification to the closed genus-two surface. A pants decomposition gives two T_2 blocks joined by three gauge cylinders, as in Figure XVI.11.2. Each block is a half-hyper in $(\mathbf{2}, \mathbf{2}, \mathbf{2})$. A center transformation (z_1, z_2, z_3) acts by the product of its three signs. Both blocks consequently carry the same electric center vector,

$$s = (1, 1, 1), \qquad S_{\text{mat}} = \langle s \rangle = \{000, 111\}, \qquad E = \mathbb{F}_2^3 / S_{\text{mat}}. \tag{XVI.11.9}$$

The two blocks do not provide two independent screening directions. They provide two

copies of the same direction. Listing the quotient cosets makes this visible,

$$\begin{aligned}[000] &= \{000, 111\}, \quad [100] = \{100, 011\},\\ [010] &= \{010, 101\}, \quad [110] = \{110, 001\}.\end{aligned} \tag{XVI.11.10}$$

A magnetic center charge must pair integrally with the dynamical matter. Thus the allowed magnetic charges form the annihilator of S_{mat},

$$M = \{m \in \mathbb{F}_2^3 \mid m \cdot 111 = 0\} = \{000, 101, 011, 110\}. \tag{XVI.11.11}$$

Changing e to $e + 111$ shifts $e \cdot m$ by zero, so the electric-magnetic pairing is well defined on the quotient. This is the reason to impose the magnetic constraint before treating the electric cosets as charges.

Choose electric coset representatives $u_1 = 100, u_2 = 010$ and magnetic vectors $v_1 = 101, v_2 = 011$. Their actual dot products are

$$\big(u_i \cdot v_j\big)_{ij} = \begin{pmatrix} 1 & 0 \\ 0 & 1 \end{pmatrix}, \qquad q = (x_1, x_2; y_1, y_2), \quad 2b(q, q') = x \cdot y' - y \cdot x' \pmod 2. \tag{XVI.11.12}$$

We have obtained a perfect pairing on $E \oplus M$ of order sixteen from a particular matter representation. We have not inferred the existence of a gauge theory from an arbitrary four-coordinate binary vector space.

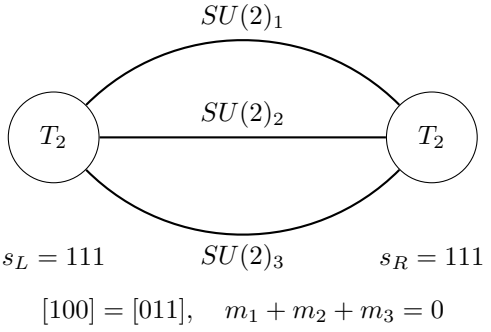


Figure XVI.11.2: Two T_2 half-trifundamentals joined by the three gauge cylinders of a genus-two theta graph. Each vertex carries electric center charge 111. The common screening subgroup identifies the displayed pairs of electric representatives, and magnetic locality imposes $m_1 + m_2 + m_3 = 0$.

A concrete maximal isotropic plane is generated by $(u_1, 0)$ and $(0, v_2)$. Its four charges and self-orthogonality can be checked directly,

$$L_* = \{(0,0), (u_1, 0), (0, v_2), (u_1, v_2)\}, \qquad u_1 \cdot v_2 = 0, \qquad |L_*| = 4. \tag{XVI.11.13}$$

For completeness, count all planes without guessing representatives. Choose the first nonzero vector in fifteen ways. Its orthogonal space has eight elements; exclude zero

and the first vector, leaving six possible independent second vectors. Each plane has three choices of first basis vector and two of second,

$$N_{\text{planes}} = \frac{15(8-2)}{3\cdot 2} = 15, \qquad |L| = 4 = \sqrt{|E \oplus M|}. \tag{XVI.11.14}$$

A maximal isotropic subgroup has this size because the nondegenerate pairing gives $|L||L^{\perp}| = 16$. Exercises 2 and 3 transfer the locality method from one handle to this sourced two-handle example. Mapping-class orbits and global flavor gauging are additional questions, beyond this enumeration.

XVI.11.3 SU(2), SO(3) and the discrete theta choice

How do the finite choices distinguish familiar gauge theories? Restore integral electric weights and magnetic coweights. We set the fundamental electric weight to $e = 1$ and the minimal magnetic coweight to $m = 1$; electric roots and coroots carry charge two. The Dirac pairing is

$$\langle (e,m),(e',m')\rangle = \frac{em' - me'}{2}, \qquad (e,m) \sim (e+2r, m+2s), \quad r,s \in \mathbb{Z}. \tag{XVI.11.15}$$

The finite classification is reduction modulo roots and coroots. Lift each subgroup in (XVI.11.8) by taking its full inverse image under this reduction. The result is three integral lattices,

$$\begin{aligned} \Lambda_W &= \{(e,m) \in \mathbb{Z}^2 \mid m = 0 \pmod 2\} = \langle (1,0),(0,2)\rangle, \\ \Lambda_H &= \{(e,m) \in \mathbb{Z}^2 \mid e = 0 \pmod 2\} = \langle (2,0),(0,1)\rangle, \\ \Lambda_D &= \{(e,m) \in \mathbb{Z}^2 \mid e+m = 0 \pmod 2\} = \langle (2,0),(1,1)\rangle. \end{aligned} \tag{XVI.11.16}$$

Figure XVI.11.3 displays these inverse images as subsets of the integral charge plane. The pairing of the two generators in each row is one. Any two integer combinations therefore pair integrally. Allowing both $(1,0)$ and $(0,1)$ would instead give a half-integer pairing. These are lattices of allowed charges before Weyl identification and finer line labels.

With adjoint dynamical matter, the physical global-form dictionary identifies Λ_W with $SU(2)$, Λ_H with $SO(3)_+$ and Λ_D with $SO(3)_-$. In the simply connected group the fundamental Wilson line is genuine. In the quotient group an isolated fundamental representation does not descend, and the allowed magnetic or dyonic line distinguishes the two completions. Local adjoint transformations see the same Lie algebra,

$$SU(2)/\{\pm 1\} = SO(3), \qquad (-1)|_{\mathbf{2}} = -1, \qquad (-1)|_{\mathbf{3}} = +1. \tag{XVI.11.17}$$

This equality on the adjoint explains why local Lagrangian terms do not select among the line choices. It does not imply equality of all bundle sums or observables.

An $SO(3)$ gauge bundle P carries the second Stiefel–Whitney class $w_2(P) \in H^2(X,\mathbb{Z}_2)$. It obstructs lifting P to an $SU(2)$ bundle. This gauge class can be nonzero even when the tangent-bundle class $w_2(TX)$ vanishes because spacetime is

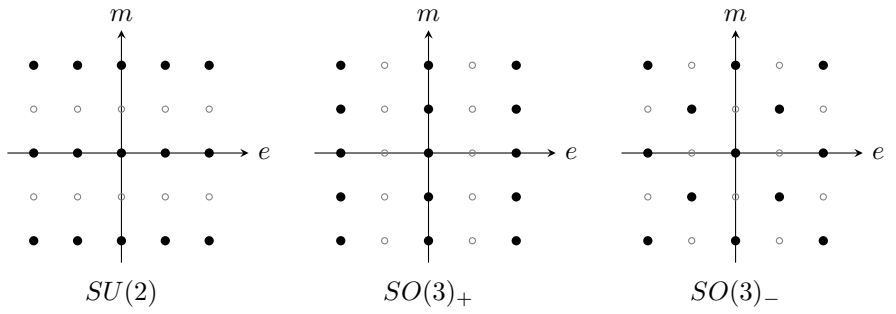


Figure XVI.11.3: Integral charge lattices for the three torus choices. Filled points have m even, e even or $e+m$ even, respectively. Horizontal and vertical coordinates are integral electric weight e and magnetic coweight m. The primitive generators in (XVI.11.16) have integral Dirac pairing even though the ambient unit square would have pairing $1/2$.

spin. We abbreviate $w_2(P)$ by w_2 below. Its discrete theta phase can be followed on a concrete spin spacetime. Let $X = S^2 \times S^2$, with integral generators x, y pulled back from the two factors. Their intersection form is

$$\int_X x^2 = \int_X y^2 = 0, \qquad \int_X xy = 1, \qquad w_2 = ax + by \pmod 2, \quad a, b \in \{0, 1\}. \tag{XVI.11.18}$$

For these liftable classes the Pontryagin square is the square of an integral lift modulo four. The cross term survives although the two squares vanish,

$$\int_X \mathcal{P}(w_2) = \int_X (ax + by)^2 = 2ab \pmod 4, \qquad q(w_2) = \frac{1}{2}\int_X \mathcal{P}(w_2) = ab \pmod 2. \tag{XVI.11.19}$$

The division by two here uses the even spin intersection form. It is not a prescription for arbitrary non-spin backgrounds. For example, a generator on $\mathbb{CP}^2$ has odd square and lies outside this calculation.

The function q is quadratic rather than linear. For $v = ax + by$ and $w = cx + dy$ modulo two, direct expansion gives

$$q(v + w) - q(v) - q(w) = (a + c)(b + d) - ab - cd = ad + bc = \int_X v \smile w \pmod 2. \tag{XVI.11.20}$$

Thus its polar form is the spacetime cup pairing. This pairing belongs to $H^2(X, \mathbb{Z}_2)$; it is distinct from the cycle pairing on the compactification curve.

Label the two completions at a reference theta angle by $n = 0, 1$. Their flux-sector coefficients and the fractional instanton number k obey

$$\epsilon_n(a, b) = (-1)^{nab}, \qquad k = \frac{ab}{2} \pmod 1, \qquad \big(\epsilon_n(0,0), \epsilon_n(0,1), \epsilon_n(1,0), \epsilon_n(1,1)\big) = (1, 1, 1, (-1)^n). \tag{XVI.11.21}$$

These four signs are weights multiplying flux sectors. They are not four partition-function values. Computing the sector amplitudes requires further dynamics and normalization.

A 2π shift of the continuous theta angle multiplies each sector by $\exp(2\pi ik)$. Hence

$$e^{2\pi ik} = (-1)^{ab}, \qquad (\theta + 2\pi, n) \sim (\theta, n+1), \qquad (\theta + 4\pi, n) \sim (\theta, n). \quad \text{(XVI.11.22)}$$

One may use theta modulo 2π together with n, or use a single theta coordinate modulo 4π for the $SO(3)$ family. Retaining both an extended 4π coordinate and an independent two-valued label would count the same completion twice. Exercise 4 ties this theta shift to the lattice shift of the next section. The flux and cycle pairings have different domains, $H^2(X, \mathbb{Z}_2)$ and $H_1(C, \mathbb{Z}_2)$, despite their hyperbolic matrices in these examples.

XVI.11.4 Mapping classes and the line-preserving subgroup

A torus mapping class can move the chosen genuine-line set to another one. Which transformations preserve one fixed absolute theory's line charges? We use active column transformations, rather than passive changes of cycle basis,

$$S = \begin{pmatrix} 0 & -1 \\ 1 & 0 \end{pmatrix}, \qquad T = \begin{pmatrix} 1 & 1 \\ 0 & 1 \end{pmatrix}, \qquad S(e,m) = (-m, e), \quad T(e,m) = (e+m, m). \quad \text{(XVI.11.23)}$$

Before reducing modulo two, multiply the matrices. This retains the charge-reversal sign,

$$ST = \begin{pmatrix} 0 & -1 \\ 1 & 1 \end{pmatrix}, \quad (ST)^2 = \begin{pmatrix} -1 & -1 \\ 1 & 0 \end{pmatrix}, \quad S^2 = (ST)^3 = \begin{pmatrix} -1 & 0 \\ 0 & -1 \end{pmatrix}. \quad \text{(XVI.11.24)}$$

The opposite convention $S_{\text{opp}} = -S$ sends (e, m) to $(m, -e)$. It gives the same permutation of unoriented mod-center line subgroups. It is a different signed integral matrix, so a modulo-two check alone cannot verify the convention.

Apply our matrices to the three generators. Reduction modulo two yields

	W	H	$W+H$
S	H	W	$W+H$
T	W	$W+H$	H

, $\qquad S\colon L_W \leftrightarrow L_H, \qquad T\colon L_H \leftrightarrow L_D.$ (XVI.11.25)

S fixes L_D, as shown in Figure XVI.11.4, and T fixes L_W. On integral lifts T sends an e-even lattice to the $e+m$-even lattice, reproducing the exchange of $SO(3)$ completions under the theta shift.

To obtain the stabilizers, enumerate the possible reduced matrices. There are three choices for a nonzero first column and two choices of independent second column,

$$SL(2, \mathbb{F}_2) = \left\{ I, \begin{pmatrix} 0 & 1 \\ 1 & 0 \end{pmatrix}, \begin{pmatrix} 1 & 1 \\ 0 & 1 \end{pmatrix}, \begin{pmatrix} 1 & 0 \\ 1 & 1 \end{pmatrix}, \begin{pmatrix} 0 & 1 \\ 1 & 1 \end{pmatrix}, \begin{pmatrix} 1 & 1 \\ 1 & 0 \end{pmatrix} \right\}. \quad \text{(XVI.11.26)}$$

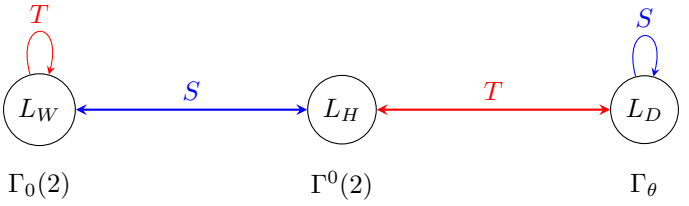


Figure XVI.11.4: Action on the three genuine-line choices. The S edge exchanges L_W, L_H and its loop fixes L_D. The T edge exchanges L_H, L_D and its loop fixes L_W. Stabilizer names refer to the active charge columns of (XVI.11.23).

Over this field, every nonzero determinant is one. The action on the three nonzero vectors is faithful, so this group has the full six permutations. For an integral matrix G, its determinant equation remains an integer equation,

$$G = \begin{pmatrix} a & b \\ c & d \end{pmatrix}, \quad ad - bc = 1, \qquad GW = \begin{pmatrix} a \\ c \end{pmatrix}, \quad GH = \begin{pmatrix} b \\ d \end{pmatrix}, \quad G(W+H) = \begin{pmatrix} a+b \\ c+d \end{pmatrix}. \tag{XVI.11.27}$$

Preserving an order-two subgroup means fixing its unique nonzero reduced vector. The first column must equal W modulo two for L_W. Its lower entry must therefore be even, while the determinant then forces a, d odd. The same argument with the second column gives

$$\begin{aligned} \mathrm{Stab}(L_W) &= \Gamma_0(2) = \{G \in SL(2,\mathbb{Z}) \mid c = 0 \pmod 2\}, \\ \mathrm{Stab}(L_H) &= \Gamma^0(2) = \{G \in SL(2,\mathbb{Z}) \mid b = 0 \pmod 2\}. \end{aligned} \tag{XVI.11.28}$$

For the dyonic line both row sums must be odd. Among the six reduced matrices only I and S satisfy this,

$$\Gamma_\theta = \mathrm{Stab}(L_D) = \{G \in SL(2,\mathbb{Z}) \mid a + b = c + d = 1 \pmod 2\}, \qquad \overline{\Gamma_\theta} = \{I, \overline{S}\}. \tag{XVI.11.29}$$

Each reduced stabilizer has order two. The reduction is surjective because S, T generate the six matrices, and its kernel $\Gamma(2)$ belongs to all three stabilizers. Consequently

$$[SL(2,\mathbb{Z}) : \Gamma_0(2)] = [SL(2,\mathbb{Z}) : \Gamma^0(2)] = [SL(2,\mathbb{Z}) : \Gamma_\theta] = 6/2 = 3. \tag{XVI.11.30}$$

For example T^2 preserves every reduced line set, whereas T exchanges two. These are exact line-preserving congruence groups. The physical interpretation uses the $\mathcal{N} = 4$ duality and six-dimensional covariance premises of the torus construction. Arithmetic alone establishes neither a full transformation law for an absolute partition function nor the absence of mapping-class anomalies. Exercise 5 separates the integral relations from these finite permutations.

XVI.11.5 Punctures, screening and flavor backgrounds

Does the torus list survive after adding fundamental matter? Use the actual four-punctured-sphere construction of Chapter 3. Glue one leg of each of two T_2 blocks to one $SU(2)$ gauge cylinder. Each block is a half-hyper in a tensor product of the gauge doublet and two flavor doublets,

$$Q_L \in (\mathbf{2}_g, \mathbf{2}_a, \mathbf{2}_b), \qquad Q_R \in (\mathbf{2}_g, \mathbf{2}_c, \mathbf{2}_d), \qquad n_{\text{half-doublets}} = 4 + 4 = 8. \quad \text{(XVI.11.31)}$$

This is four full fundamental hypers. It is a different compactification from the unpunctured $\mathcal{N} = 4$ torus, regardless of the genus of its spectral cover.

A fundamental carries the nonzero electric center charge. It can end a Wilson line, so the screening subgroup is the entire electric center group. Magnetic charges must still be local with that matter,

$$S_{\text{mat}} = \langle 1 \rangle = \mathbb{F}_2, \qquad E = \mathbb{F}_2/\langle 1 \rangle = 0, \qquad M = \{m \in \mathbb{F}_2 \mid m \cdot 1 = 0\} = 0. \quad \text{(XVI.11.32)}$$

The unscreened finite gauge defect module is therefore trivial. This conclusion concerns equivalence classes modulo dynamical screening. A fundamental Wilson line is still genuine in the $SU(2)$ theory, and a closed Wilson loop is still an observable. Its ability to terminate on charged matter removes an unscreened charge, not the observable itself.

Can one replace the gauge group by $SO(3)$ while keeping these fields? A representation descends to a quotient only if the quotient kernel acts trivially. Here it does not,

$$\rho_{\mathbf{2}}(-I) = -I_{\mathbf{2}} \neq I_{\mathbf{2}}, \qquad \rho_{\mathbf{3}}(-I) = I_{\mathbf{3}}. \quad \text{(XVI.11.33)}$$

With ordinary liftable flavor backgrounds this prevents an ordinary $SO(3)$ replacement retaining the fundamental matter. Deleting the fundamental center charge by hand would falsely restore the torus's three choices.

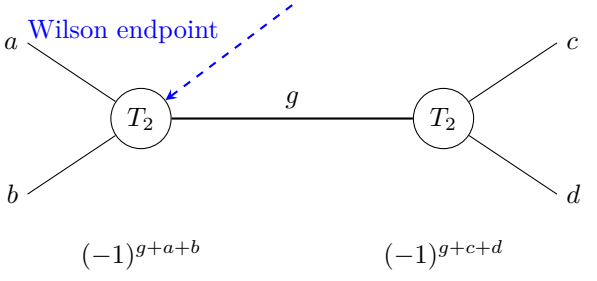


Figure XVI.11.5: Two T_2 blocks glued on the gauge leg g, with four external flavor legs. The left and right matter signs are $(-1)^{g+a+b}$ and $(-1)^{g+c+d}$. A fundamental Wilson line can end on either block. Canceling a gauge center sign by flavor signs changes the quotient-bundle problem.

The manifest flavor factors make a more general possibility visible. Write the five center bits in the order (g, a, b, c, d). Trivial action on both matter blocks imposes two

linear equations,

$$\begin{aligned} \chi_L(g,a,b,c,d) &= (-1)^{g+a+b}, \\ \chi_R(g,a,b,c,d) &= (-1)^{g+c+d}, \\ K &= \ker \begin{pmatrix} 1 & 1 & 1 & 0 & 0 \\ 1 & 0 & 0 & 1 & 1 \end{pmatrix}. \end{aligned} \tag{XVI.11.34}$$

Solve for b and d, leaving g, a, c free. This displays all eight elements without relying on a count alone,

$$\begin{aligned} K = \{(g,a,g+a,c,g+c) \mid g,a,c \in \mathbb{F}_2\}, \quad |K| = 8, \\ (1,1,0,1,0) \in K, \quad (1,0,0,0,0) \notin K. \end{aligned} \tag{XVI.11.35}$$

For the first example, the two signs are $(-1)^{1+1+0} = +1$ and $(-1)^{1+1+0} = +1$. For the second they are both -1. Thus the representation permits cancellation by correlated gauge and flavor centers but does not permit quotienting the gauge center alone.

Figure XVI.11.5 shows the two signs on the actual matter blocks. A diagonal gauge/flavor quotient would require correlated transition functions and specified background bundles. The kernel just calculated does not determine those bundles, the faithful global form of the enhanced Spin(8) flavor symmetry, its triality action, or its anomalies. This is where representation arithmetic stops and a new global construction would begin.

There is also a useful anomaly diagnosis within the ordinary spin $SU(2)$ setup. For a left-handed Weyl fermion of isospin j, use the old Witten-anomaly index

$$2T(j) = \frac{2}{3} j(j+1)(2j+1), \qquad 2T(\tfrac{1}{2}) = 1, \qquad 2T(1) = 4. \tag{XVI.11.36}$$

The two T_2 blocks give eight half-doublets, and the $\mathcal{N} = 2$ gauge multiplet gives two adjoint Weyl fermions. Their sum and its parity are

$$I_{\text{old}} = 8 \cdot 1 + 2 \cdot 4 = 16, \qquad I_{\text{old}} = 0 \pmod 2. \tag{XVI.11.37}$$

Removing one half-doublet would give fifteen and odd parity. This is a diagnostic of the ordinary spin $SU(2)$ anomaly, conditional on the stated matter content. It does not certify all anomalies of correlated gauge/flavor bundles or any non-spin extension.

The method of this chapter is now usable in both directions. A closed-surface defect module needs a maximal mutually local choice; a punctured matter construction first needs its screening charges and magnetic locality conditions. Spectral equations and local Lie algebras alone supply neither operation. Exercise 6 asks the reader to perform both the representation and anomaly tests before considering an alternative global form.

Exercises

1. Reconstruct the four torus charge classes and submit the numerator matrix $2b$ modulo two in charge order $(0,0), (0,1), (1,0), (1,1)$. Derive the surface-wrapping interpretation and explain the Poincare-duality map. Explain why an elliptic spectral cover of a punctured sphere cannot replace the ultraviolet torus here.

2. Submit the three maximal isotropic subgroups as full sets of torus charges. Prove that each equals its orthogonal complement and that adjoining either remaining charge spoils locality. Explain why the trivial subgroup is incomplete in this example.

3. For the genus-two theta graph submit the screening subgroup, one representative per electric coset, the magnetic annihilator, and all maximal isotropic planes in coordinates (x_1, x_2, y_1, y_2) of (XVI.11.12). Equivalent electric representatives and plane orderings are permitted. Derive the pairing from the actual two half-trifundamentals and recover $15 \cdot 6/6$. Exhibit the four charges of (XVI.11.13) in these coordinates.

4. Submit the primitive integral generator pairs of all three torus lattices and the four theta weights for each n in the flux order $(a, b) = (0, 0), (0, 1), (1, 0), (1, 1)$. Derive integrality of the Dirac pairing and the Pontryagin square. Explain why the signs are not partition functions and why an extended 4π theta period leaves no additional independent binary label.

5. Submit the S, T permutations, all reduced stabilizer matrices and both signed integral products $S^2, (ST)^3$. In writing derive the three congruence conditions for active column charges. Explain which conclusions survive reduction modulo two and which require the signed integral matrices. Distinguish line preservation from an anomaly-free physical duality action.

6. Submit the screened electric representatives and magnetic charges for $N_f = 4$, all five-center kernel elements, and the old anomaly indices before and after removing one half-doublet. Derive representation descent and explain why a screenable Wilson line remains genuine. State which correlated bundle information would be needed for a flavor-assisted quotient and why the kernel alone does not determine enhanced flavor triality or anomalies.

For benchmark submissions, see `benchmark/PROTOCOL.md`. The indicated reorderings and coset representatives are equivalent. Include the written arguments.

Sources and scope

Section 11.1. The wrapped-surface and closed untwisted defect-module premises are [GEO-E], using Tachikawa (2013, arXiv v2, pp. 1–3, §4, pp. 6–8). The enhanced unpunctured torus premise is that of Chapter 1, independently of any pants construction. Intersections, Poincare duality and the finite pairing table are [MATH]. The H^2 occurrences in the source's torus discussion are read as typographical errors, consistently with its eqs. (4.2) and (5.8) using H^1 of rank $2g$.

Section 11.2. Maximal isotropy and the genus-two electric quotient, magnetic annihilator and fifteen planes are [MATH], conditional on the physical line-choice dictionary and actual two-T_2 theta graph in Tachikawa (2013, arXiv v2, §4, pp. 6–8, §5.1–5.2, pp. 9–11, Fig. 1), graded [GEO-E]. Maximality means that another charge cannot be

added while preserving isotropy, correcting the source's contradictory wording. No general puncture formula or mapping-class orbit classification is asserted.

Section 11.3. The global-form assignment and spin discrete-theta premise are [GEO-E], from Aharony et al. (2013, arXiv v3, §1.1–1.2, pp. 2–5, §6.1, pp. 37–38). Lattice inverse images and the $S^2 \times S^2$ coefficients are [MATH]. The coefficients are formal flux weights. An absolute partition function, a torsion refinement and a non-spin extension are not constructed. Theta modulo 2π plus n and theta modulo 4π describe the same label space.

Section 11.4. The signed matrices, permutations and congruence stabilizers are [MATH]. The physical torus duality interpretation uses Aharony et al. (2013, arXiv v3, §2.4, pp. 17–18, eqs. (2.11)–(2.15)) and Tachikawa (2013, arXiv v2, §3–4, pp. 5–8), graded [GEO-E]. The opposite S sign in the first source is translated explicitly. These stabilizers do not establish a complete anomaly-free duality group.

Section 11.5. The actual four-fundamental theory is [GEO-E], using Gaiotto (2009, arXiv v1, §2.1, pp. 4–5, Figs. 2–3) and the Chapter 3 half-trifundamental convention. Screening and the manifest center kernel are [MATH]. The old spin $SU(2)$ anomaly criterion is [ANOM], using Wang et al. (2018, arXiv v1, §1, pp. 2–3, §2.2–2.3, pp. 6–9, eq. (2.9)). Only its index for the supplied matter is evaluated. Liftable flavor backgrounds are assumed; neither a faithful enhanced flavor quotient nor general gauge/flavor-bundle anomalies are determined.

References

Aharony, O., N. Seiberg, and Y. Tachikawa (2013). "Reading between the lines of four-dimensional gauge theories". In: arXiv: `1305.0318 [hep-th]`.

Gaiotto, D. (2009). "N=2 dualities". In: arXiv: `0904.2715 [hep-th]`.

Tachikawa, Y. (2013). "On the 6d origin of discrete additional data of 4d gauge theories". In: arXiv: `1309.0697 [hep-th]`.

Wang, J., X.-G. Wen, and E. Witten (2018). "A New SU(2) Anomaly". In: arXiv: `1810.00844 [hep-th]`.

Chapter XVI.12

A class-S construction atlas

A four-dimensional theory can be approached through a surface, a spectral curve, a weakly coupled gauge description or a protected observable. Moving between these descriptions requires us to remember which information each one retains. A Coulomb rank does not specify a spectrum of scaling dimensions. A spectrum does not determine a flavor algebra. Even a complete local gauge algebra leaves a choice of genuine line operators.

This chapter turns the constructions of Chapters 1 through 11 into a finite collection that the reader can use in both directions. Starting from a decorated surface, we calculate selected invariants. Starting from a desired observable, we narrow the possible constructions and identify the additional choices. We will reconstruct the T_3 row, change a puncture, compare two irregular singularities and follow three different physical operations. The prerequisites are the regular-puncture dictionary, the anomaly formulas, the proposed star mirrors and the global-line discussion of those chapters. The collection contains twelve selected records. It is an entry to these examples rather than a classification of class-S theories.

XVI.12.1 Choosing a theory from geometry

Suppose we want an isolated rank-one building block. The geometry is a useful starting point because it separates a coupling from a vacuum coordinate. The ultraviolet curve C supports the compactification; its marked points carry defects. A spectral cover Σ above C describes the Coulomb geometry. For type A_{N-1} its characteristic equation and differential are

$$\Sigma \subset T^*(C \setminus \{P_i\}), \qquad x^N + \sum_{k=2}^{N} c_k x^{N-k} = 0, \qquad \lambda = x\,dz. \tag{XVI.12.1}$$

Here x is the local cotangent coordinate and c_k denotes the coefficient of a meromorphic k-differential in this chart. The choice of the interacting A_{N-1} parent removes the free center tensor. It does not choose an absolute theory or a set of genuine lines. Figure XVI.12.1 separates these roles.

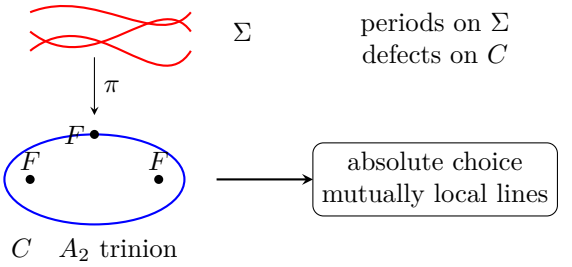


Figure XVI.12.1: The decorated ultraviolet curve C supplies the parent type and three defect labels. The cover Σ supplies periods and Coulomb coordinates. A separate choice of mutually local lines completes the appropriate relative construction. The vertical arrow is a covering map, whereas the horizontal arrow indicates extra information rather than an equivalence.

For regular punctures, first set the masses to zero when counting Coulomb variations. A Nahm partition Y lists descending Jordan block sizes; the Hitchin diagram is its transpose. In the examples needed here, the full and simple labels give

$$Y_F = [1^N], \quad p_k(F) = k - 1, \qquad Y_S = [N-1, 1], \quad p_k(S) = 1, \qquad 2 \le k \le N. \tag{XVI.12.2}$$

The pole orders refer to variable Coulomb coefficients with fixed masses. Highest polar coefficients fixed by masses are not additional vacuum coordinates. On $C = \mathbb{P}^1$ the allowed degree-k variations belong to

$$H^0\left(\mathbb{P}^1, K^k\Big(\sum_i p_k^{(i)} P_i\Big)\right), \qquad \deg K^k\Big(\sum_i p_k^{(i)} P_i\Big) = -2k + \sum_i p_k^{(i)}. \tag{XVI.12.3}$$

A line bundle of degree d on the sphere has $d+1$ sections for $d \ge 0$ and none for $d < 0$. Thus the arithmetic count is

$$d_k = \max\left(0, 1 - 2k + \sum_i p_k^{(i)}\right), \qquad r_{\mathrm{CB}} = \sum_{k=2}^{N} d_k, \qquad \{\Delta\}_{\mathrm{CB}} = \coprod_{k=2}^{N} \{k\}^{d_k}. \tag{XVI.12.4}$$

These formulas count sections. A negative virtual value before taking the maximum is a warning about the proposed fixture, not a negative number of operators. Physical fixture existence is supplied by the puncture construction in the previous chapters.

For three full A_2 punctures, the degree-two line bundle has degree -1 and the degree-three bundle has degree zero. The result is

$$(p_2, p_3) = (1, 2) \text{ at each puncture}, \qquad (d_2, d_3) = (1 - 4 + 3, 1 - 6 + 6) = (0, 1). \tag{XVI.12.5}$$

This is the sourced T_3 fixture. We can see its single coordinate without relying on a count. Place the punctures at $0, 1, \infty$. Use the positive cubic differential $\varphi_3 = -c_3(dz)^3$

of Chapter 4. A basis for its variation is

$$\delta\varphi_3 = \frac{u\,(dz)^3}{z^2(z-1)^2}, \qquad z = w^{-1} \implies \delta\varphi_3 = -\frac{u\,(dw)^3}{w^2(1-w)^2}. \tag{XVI.12.6}$$

The infinity chart has precisely the allowed double pole. Multiplying the numerator by z would create a cubic pole at infinity and would change the defect condition. Since $[\lambda] = 1$, this coordinate has dimension three.

Now replace the third full puncture with $[2,1]$. The last pole pair becomes $(1,1)$, so

$$T_3 \longrightarrow FFS, \qquad (d_2, d_3) = (1{-}4{+}3, 1{-}6{+}5) = (0,0), \qquad \{\Delta\}_{FFS} = \varnothing. \tag{XVI.12.7}$$

The residual fixture is a sourced free bifundamental sector with nine hypermultiplet dimensions. An empty Coulomb spectrum therefore does not mean an empty theory. It means there is no Coulomb modulus of this fixture. Exercise 1 asks the reader to reconstruct the pole replacement from the partitions.

There is a separate domain issue for the torus. The stable pants construction requires

$$2g - 2 + n > 0, \qquad (g,n) = (0,3) \text{ is allowed}, \qquad (g,n) = (1,0) \text{ lies on the boundary.} \tag{XVI.12.8}$$

The flat unpunctured torus with periodic fermions and trivial R holonomy has enhanced $\mathcal{N} = 4$ supersymmetry. Its three line choices will appear below, but its anomalies are not obtained by applying a stable $\mathcal{N} = 2$ pants formula outside its domain. A value absent from our finite collection is written as not tabulated. A calculated zero and an empty spectrum retain their actual meanings.

XVI.12.2 Comparing recurring constructions

The rank-one cubic coordinate does not yet tell us the anomalies of T_3. For that purpose use the integrated anomaly of Chapter 7 together with the full-puncture terms. Write n_v, n_h for effective counts and $H = N(N^2-1)$. In the closed-curve convention used there, the bulk pair and full-puncture pair are

$$\begin{aligned} (n_v, n_h)_{\text{bulk}} &= (g-1)\left(N - 1 + \frac{4}{3}H, \frac{4}{3}H\right), \\ v_F = \sum_{k=2}^{N}(2k-1)(k-1), &\qquad h_F = v_F + \frac{N^2-N}{2}. \end{aligned} \tag{XVI.12.9}$$

These local terms must be combined with that same bulk convention. For $N = 3$, the bulk pair on the sphere is negative, while each defect contributes positively,

$$\begin{aligned} (n_v, n_h)_{\text{bulk}} = (-34,-32), \qquad (v_F, h_F) = (3+10, 13+3) = (13,16), \\ (n_v, n_h)_{T_3} = (-34,-32) + 3(13,16) = (5,16). \end{aligned} \tag{XVI.12.10}$$

The negative bulk term alone is not the anomaly of a physical isolated sphere theory. After including its three defects we find

$$a = \frac{5n_v + n_h}{24}, \quad c = \frac{2n_v + n_h}{12}, \qquad (a,c)_{T_3} = \left(\frac{41}{24}, \frac{13}{6}\right), \quad 4(2a-c) = 5 = 2\cdot 3 - 1. \tag{XVI.12.11}$$

The last equality agrees with the single Coulomb dimension three. It does not infer the enhanced $\mathfrak{e}_6$ flavor algebra. That enhancement is physical information supplied by the T_3 construction and its operator analysis.

The proposed star mirror supplies another comparison with a different physical premise. Its gauge nodes have central rank three and three tails of ranks two and one. Removing the diagonal $U(1)$ gives

$$r_{\text{mirror}} = 3 + 3(2 + 1) - 1 = 11, \qquad \dim_{\mathbb{H}} \mathcal{H}(T_3) = 11. \tag{XVI.12.12}$$

The Higgs interpretation is conditional on mirror symmetry and Higgs protection. The subtraction removes a common abelian gauge factor, not the six-dimensional center tensor. Figure XVI.12.2 makes it visible. This rank calculation uses the sourced mirror proposal. It proves neither equality of rings nor equality of metrics. For T_4 the same rank operation gives $4 + 3(3 + 2 + 1) - 1 = 21$. The regular pole formula now yields $(d_2, d_3, d_4) = (0, 1, 2)$, so it has three Coulomb coordinates rather than one.

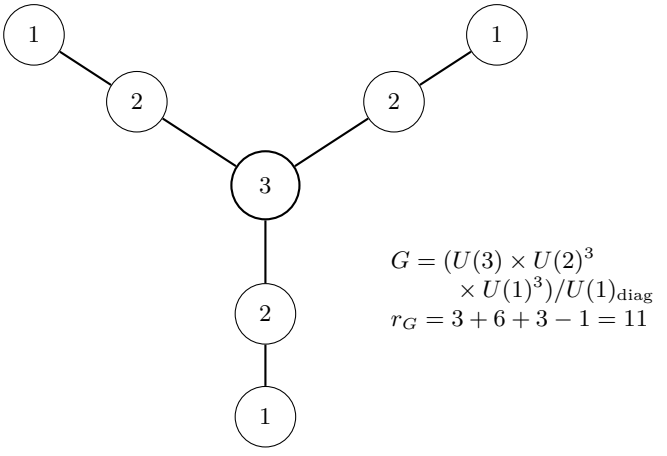


Figure XVI.12.2: The proposed T_3 star mirror has a $U(3)$ center and three $U(2)$–$U(1)$ tails. Edges are bifundamental hypermultiplets. The common diagonal $U(1)$ is removed from the product gauge group. Adding the node ranks and subtracting one gives eleven; interpreting this as a four-dimensional Higgs dimension requires the mirror and protection premises.

For a direct field-count comparison take $SU(2)$ with four fundamental hypermultiplets. Each full fundamental contributes two hypermultiplet dimensions and the vector contributes the dimension of $\mathfrak{su}(2)$,

$$(n_v, n_h) = (3, 4 \cdot 2) = (3, 8), \qquad (a, c) = \left(\frac{23}{24}, \frac{7}{6}\right), \qquad \dim_{\mathbb{H}} \mathcal{H} = 8 - 3 = 5. \tag{XVI.12.13}$$

The last equation is the generic fully Higgsed hyperkahler quotient. Its Coulomb dimension is two. Thus even the two familiar regular rank-one theories already have different scaling dimensions and anomalies.

Irregular examples sharpen the distinction. For a local curve $x^2 = z^p + \sum_{j=0}^{p-2} u_j z^j$ and $\lambda = x\,dz$, homogeneity and the differential normalization require

$$2[x] = p[z], \qquad [x] + [z] = 1, \qquad [z] = \frac{2}{p+2}, \quad [x] = \frac{p}{p+2}, \quad [u_j] = \frac{2(p-j)}{p+2}. \tag{XVI.12.14}$$

The coordinate shift has removed the z^{p-1} term. For the cubic and quartic, respectively, the ordered deformation weights and roles are

$$\begin{aligned} &p = 3 \quad ([u_0], [u_1]) = (6/5, 4/5), && \text{(Coulomb vev, relevant coupling)},\\ &p = 4 \quad ([u_0], [u_1], [u_2]) = (4/3, 1, 2/3), && \text{(Coulomb vev, mass, relevant coupling)}. \end{aligned} \tag{XVI.12.15}$$

Both examples have rank one. Their Coulomb spectra retain only the entry above one. The mass and relevant coupling must remain in a deformation description but must not inflate that rank. The local scaling match with an IIB singularity does not establish equivalence of complete theories, and it supplies no missing anomaly or flavor entry in this collection.

Two selected twisted D_4 gluings illustrate another source of different spectra. The sourced building block is a half-hypermultiplet in $(\mathbf{8}, \mathbf{6})$ of $\mathfrak{so}(8) \oplus \mathfrak{usp}(6)$. Thus

$$n_h^{\text{half}} = \frac{1}{2} \cdot 8 \cdot 6 = 24, \qquad n_h^{\text{two}} = 48, \qquad \dim \mathfrak{so}(8) = 28, \quad \dim \mathfrak{usp}(6) = 21. \tag{XVI.12.16}$$

The source's $Sp(3)$ means $USp(6)$. The two cylinders gauge different algebras with different external decorations. Write the one-loop gauge beta-function coefficient as $b_0 = 2h^\vee - \frac{1}{2}\sum_i k_i$, where $h^\vee$ is the dual Coxeter number and k_i is the flavor-current level of each sector being gauged. In the inherited index convention, $T_{\mathfrak{so}(8)}(\mathbf{8}) = 1$ and $T_{\mathfrak{usp}(6)}(\mathbf{6}) = 1/2$. One half-hyper in the product representation therefore supplies

$$k_{D_4} = 2\dim(\mathbf{6}) T_{D_4}(\mathbf{8}) = 12, \qquad k_{C_3} = 2\dim(\mathbf{8}) T_{C_3}(\mathbf{6}) = 8. \tag{XVI.12.17}$$

Using $h^\vee(D_4) = 6$ and $h^\vee(C_3) = 4$, their invariant degrees and one-loop matter sums are

$$\begin{aligned} &D_4 \quad \{2, 4, 4, 6\}, \quad b_0 = 2 \cdot 6 - \tfrac{1}{2}(12 + 12) = 0,\\ &C_3 \quad \{2, 4, 6\}, \qquad b_0 = 2 \cdot 4 - \tfrac{1}{2}(8 + 8) = 0. \end{aligned} \tag{XVI.12.18}$$

The repeated degree four in D_4 is essential. Gauging the other cylinder is not an operation that preserves the external punctures. These examples are not presented as dual frames, and their algebra labels do not specify global gauge groups.

Table XVI.12.1 gathers the twelve records. The regular fixture identities and flavor assignments, the twisted half-hyper construction and the torus interpretation are source premises. Numerical section counts, anomaly arithmetic, scaling weights and finite line sets are calculations conditional on those premises. Higgs entries obtained from star quivers are conditional on the mirror proposal CONJ+. A blank physical prediction is never replaced by zero.

For completeness the finite charges of those torus choices are pairs $(e, m) \in \mathbb{F}_2^2$ with

Construction	CB dimensions	a	c	$\dim_{\mathbb{H}} \mathcal{H}$
T_2	$\varnothing$	$\frac{1}{6}$	$\frac{1}{3}$	4
T_3	3	$\frac{41}{24}$	$\frac{13}{6}$	11
T_4	$3, 4, 4$	$\frac{45}{8}$	$\frac{13}{2}$	21
$SU(2),\ N_f = 4$	2	$\frac{23}{24}$	$\frac{7}{6}$	5
A_2 full-full-simple	$\varnothing$	$\frac{3}{8}$	$\frac{3}{4}$	9
Cubic AD	$\frac{6}{5}$	n.t.	n.t.	n.t.
Quartic AD	$\frac{4}{3}$	n.t.	n.t.	n.t.
Twisted D_4 gauging	$2, 4, 4, 6$	$\frac{47}{6}$	$\frac{26}{3}$	n.t.
Twisted C_3 gauging	$2, 4, 6$	$\frac{51}{8}$	$\frac{15}{2}$	n.t.
Torus $SU(2)$	n.t.	n.t.	n.t.	n.t.
Torus $SO(3)_+$	n.t.	n.t.	n.t.	n.t.
Torus $SO(3)_-$	n.t.	n.t.	n.t.	n.t.

Table XVI.12.1: Selected constructions from the preceding chapters, regenerated from one common collection. "n.t." means not tabulated and no value is supplied here. The empty spectrum of T_2 and FFS is a calculated result. Regular Higgs dimensions use the sourced mirror/protection proposal, with direct free-field or quotient comparisons where available. The torus rows concern the enhanced periodic $\mathcal{N} = 4$ compactification and retain only the line choices used here.

pairing $em' - me'$. Their maximal mutually local sets are

$$\begin{aligned} L_{SU(2)} &= \{(0,0),(1,0)\}, \\ L_{SO(3)_+} &= \{(0,0),(0,1)\}, \\ L_{SO(3)_-} &= \{(0,0),(1,1)\}. \end{aligned} \tag{XVI.12.19}$$

They distinguish absolute completions of the same local torus construction. Their line-preserving subgroups do not by themselves prove an anomaly-free action of the full duality group. They also cannot be transferred to the four-fundamental theory, where fundamental matter changes screening and representation descent.

XVI.12.3 Searching backwards from observables

Suppose a calculation calls for a rank-one theory. Which surface should we use? Let $\mathcal{A}$ denote precisely the twelve rows of Table XVI.12.1. For a supplied Coulomb rank $r(t)$ and spectrum $S(t)$, define two finite selections,

$$\begin{aligned} R_q &= \{t \in \mathcal{A} \mid r(t) \text{ is supplied and } r(t) = q\}, \\ D_\delta &= \{t \in \mathcal{A} \mid S(t) \text{ is supplied and } \delta \in S(t)\}. \end{aligned} \tag{XVI.12.20}$$

The first question has four answers in this collection,

$$R_1 = \{T_3,\ SU(2)\ N_f = 4,\ \text{cubic AD},\ \text{quartic AD}\}. \tag{XVI.12.21}$$

The torus ranks are not supplied here and hence do not enter this set. This is a limitation of the recorded fields, not a statement that the enhanced torus theory lacks a Coulomb branch.

To choose among these four candidates, the scaling dimension is more informative than rank. From the calculations above,

$$\begin{aligned} S(T_3) = \{3\}, \qquad & S(SU(2)\ N_f = 4) = \{2\}, \\ S(\text{cubic AD}) = \{6/5\}, \qquad & S(\text{quartic AD}) = \{4/3\}. \end{aligned} \tag{XVI.12.22}$$

Each dimension leads to a different next calculation. Dimension three selects a regular A_2 trinion in this collection. Dimension 6/5 instead selects a local irregular scaling construction. Figure XVI.12.3 organizes this distinction.

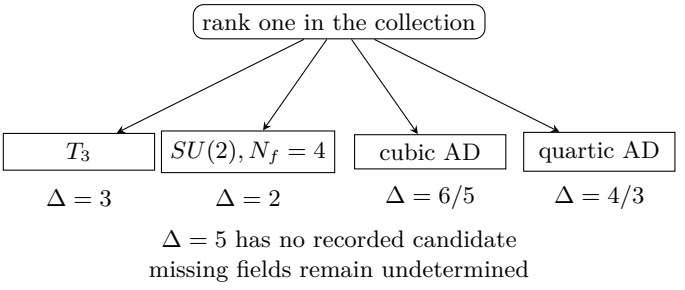


Figure XVI.12.3: A rank-one request leaves four recorded candidates. Their Coulomb scaling dimensions separate them in this finite collection. The labels describe vacuum coordinates; the quartic's dimension-one mass and dimension-2/3 coupling are not additional leaves. An empty branch at dimension five means that the present collection supplies no candidate.

The order of the restrictions matters conceptually even when set intersection commutes. T_4 also contains a dimension-three coordinate, but has rank three. Consequently

$$D_3 = \{T_3, T_4\}, \qquad R_1 \cap D_3 = \{T_3\}, \qquad R_1 \cap D_5 = \varnothing. \tag{XVI.12.23}$$

The singleton says that T_3 is the only current recorded candidate for this pair of conditions. The empty set says that no recorded candidate meets the other pair. Neither is a theorem about all class-S theories.

Flavor gives a further restriction only when its identity is supplied. Let $F_{\mathfrak{f}}$ select rows with a supplied flavor assignment containing $\mathfrak{f}$ in the stated sense. With the enhanced flavor labels of Chapter 6 and the four-fundamental example,

$$R_1 \cap F_{\mathfrak{e}_6} = \{T_3\}, \qquad R_1 \cap F_{\mathfrak{so}(8)} = \{SU(2)\ N_f = 4\}. \tag{XVI.12.24}$$

The AD rows have no flavor assignment in this collection. Failing this filter cannot be read as a computation of their flavor symmetry. Similarly, the manifest $\mathfrak{su}(3)^2 \oplus \mathfrak{u}(1)$ of FFS should be interpreted with its stated manifest status rather than promoted to an exhaustive enhanced algebra.

Missing entries require a third logical possibility. For any requested field value v, define the finite predicate by

$$P_v(t) = \begin{cases} \text{true}, & f(t) \text{ supplied and equal to } v, \\ \text{false}, & f(t) \text{ supplied and unequal to } v, \\ \text{undetermined}, & f(t) \text{ not supplied.} \end{cases} \tag{XVI.12.25}$$

This prevents a search for zero anomaly from returning rows whose anomalies have simply not been calculated here. It also keeps an empty list of Coulomb operators distinct from an absent list. In particular,

$$r(T_2) = r(FFS) = 0, \quad S(T_2) = S(FFS) = \varnothing, \qquad (a,c)_{\text{cubic AD}} = \text{not supplied here.} \tag{XVI.12.26}$$

Exercise 4 asks the reader to execute these restrictions and explain the undetermined cases. The physical lesson is that inverse selection is a choice of a useful next construction. Its output becomes a theory only through the original parent, defect and global premises, which remain attached to the selected row.

XVI.12.4 Gluing, closure and collision

After selecting a theory, we often want to move to another description or another theory. Three operations recur in the preceding chapters. They have different domains and different effects on observables. We begin with gauging, whose input includes two sectors and a specified common flavor group. For two T_2 blocks joined by an $SU(2)$ cylinder,

$$T_2 \overset{SU(2)}{\longleftrightarrow} T_2 \quad \Longrightarrow \quad (n_v, n_h) = (0,4) + (0,4) + (3,0) = (3,8). \tag{XVI.12.27}$$

The vector is part of the output. Forgetting it would give the anomaly of eight free hypermultiplet dimensions, not the gauged theory. On the surface, gluing two three-punctured spheres along one puncture each gives

$$g = 0, \quad n = 3 + 3 - 2 = 4, \qquad d_2 = 1 - 4 + 4 = 1, \qquad \Delta = 2. \tag{XVI.12.28}$$

The four remaining punctures label external flavor factors. Their cross-ratio supplies a marginal coupling. Choosing a different degeneration is a candidate dual frame through the class-S construction; equality of the two anomaly columns alone would not establish that identification.

Partial closure instead changes a defect through a moment-map vev. For the chosen A_2 closure $[1,1,1] \to [2,1]$, the complex nilpotent orbit can be counted from the transpose partition. If $Y^t = [2,1]$, then

$$\begin{gathered} \dim_{\mathbb{C}} Z_{\mathfrak{sl}_3}(e) = 2^2 + 1^2 - 1 = 4, \qquad \dim_{\mathbb{C}} \mathcal{O}_{[2,1]} = 8 - 4 = 4, \\ n_{\text{Goldstone}} = \tfrac{1}{2} \dim_{\mathbb{C}} \mathcal{O}_{[2,1]} = 2. \end{gathered} \tag{XVI.12.29}$$

The residual FFS fixture has nine hypermultiplet dimensions. The two Goldstone dimensions are a separate local sector along the chosen Higgs vacuum. Conditional on the Higgs-dimension dictionary, the dimension comparison is

$$11 = 9 + 2, \qquad (n_v, n_h)_{T_3} = (5, 16), \qquad (n_v, n_h)_{FFS} = (0, 9). \tag{XVI.12.30}$$

The equality of dimensions does not conserve the Coulomb spectrum or the conformal anomalies. A Higgs flow selects a vacuum and changes the infrared sectors. It is not a duality equating two conformal descriptions. The Goldstones are not already included in the residual fixture's nine.

The third operation sends a heavy flavor mass to infinity while tuning the coupling. It produces an irregular end. To expose the required correlated scaling, let H be the large mass, L a fixed scale and $q = L/H$. In the fixed chart of Chapter 9 the tuned finite-H coefficient is

$$\begin{aligned}\varphi_H(z) = &-\frac{U}{z(z-1)(z-L/H)} + \frac{b^2}{(z-1)^2} + \frac{-b^2+c^2}{z(z-1)} \\ &+ \frac{L^2(1+m/H)^2/4 - Lmz}{z^2(z-L/H)^2}.\end{aligned} \tag{XVI.12.31}$$

The quadratic differential is $\varphi_H(z)(dz)^2$. The parameters b, c are spectator masses, m is the surviving mass, and U is the finite Coulomb coordinate after the tuning. This combined expression comes from the four-pole family, so taking its limit retains the cancellation between the approaching poles. At fixed $z \neq 0, 1$,

$$\lim_{H\to\infty} \varphi_H(z) = \frac{L^2}{4z^4} - \frac{Lm}{z^3} - \frac{U}{z^2(z-1)} + \frac{b^2}{(z-1)^2} + \frac{-b^2+c^2}{z(z-1)}. \tag{XVI.12.32}$$

Use $-1/[z^2(z-1)] = 1/z^2 - 1/[z(z-1)]$ to rewrite it as the sourced three-flavor differential,

$$\varphi_3(z) = \frac{L^2}{4z^4} - \frac{Lm}{z^3} + \frac{U}{z^2} + \frac{b^2}{(z-1)^2} - \frac{U+b^2-c^2}{z(z-1)}, \qquad \lim_{H\to\infty} \varphi_H - \varphi_3 = 0. \tag{XVI.12.33}$$

The fourth-order pole is the new irregular end. Omitting the correlated tuning of the Coulomb parameter would leave a divergent contribution before this limit. This calculation establishes the selected four-to-three confluence of differentials. It does not produce all lower-flavor theories, a full punctured charge-lattice equivalence or an AD fixed point.

Figure XVI.12.4 keeps the arrows distinct. To compare any two outputs we first ask which operation was performed and what was held fixed. Exercise 5 practices the vector count, the orbit count and the finite rational limit independently.

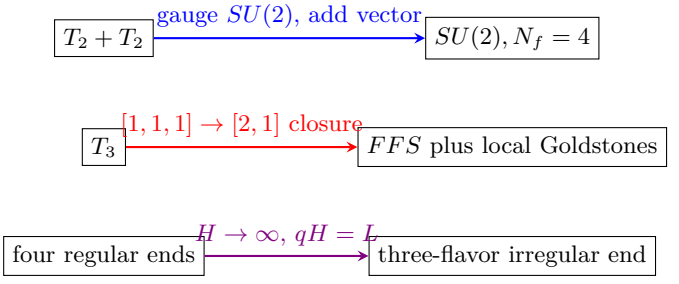


Figure XVI.12.4: Three operations with different physical meanings. Gauging consumes two flavor legs and adds a vector. Closure replaces one full puncture by a simple one and separates local Goldstones from the residual fixture. Collision takes the correlated heavy-mass limit $qH = L$ and creates an irregular end. The arrows indicate constructions and flows, not a common equivalence relation.

XVI.12.5 Inputs for protected calculations

Selecting T_3 does not select a protected observable. A BPS spectrum, an AGT quantity and an index ask different questions of the same theory. Each requires choices that are absent from the anomaly and rank columns. We can make this incompleteness precise without pretending to evaluate the observable. Let $\mathcal{R}$ denote a selected theory record and $\mathcal{C}_X$ the necessary choices for a target X. The task is to supply

$$(\mathcal{R}, \mathcal{C}_X) \longmapsto \text{a specified calculation of } X, \qquad X \in \{\mathrm{BPS}, \mathrm{AGT}, \mathrm{index}\}. \tag{XVI.12.34}$$

This notation defines the requested calculation, not a theorem that the displayed information is sufficient for its existence. Figure XVI.12.5 separates the three targets.

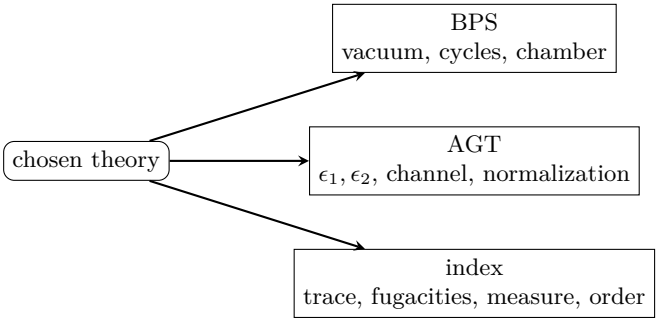


Figure XVI.12.5: One chosen theory leads to three separate questions after further choices. The BPS branch needs a vacuum and stability information. The AGT branch needs deformation parameters, a channel and normalization. The index branch needs a trace, fugacities and a gluing prescription. No arrow equates these observables or the different two-dimensional structures that can organize them.

For the BPS problem we need a smooth point of the Seiberg–Witten geometry, a charge lattice, oriented cycles, a chamber and information determining occupied charges. The necessary list used here is

$$\begin{aligned}\mathcal{C}_{\mathrm{BPS}} = \{&\text{smooth SW point},\ \text{charge lattice},\ \text{oriented cycles},\\ &\text{stability chamber},\ \text{occupancy input}\}.\end{aligned} \tag{XVI.12.35}$$

The role of orientations is visible in the central charge itself. In the period convention of Chapter 4, one fixed nonzero constant c_{SW} converts geometric periods into physical central charges,

$$Z_\gamma = c_{\mathrm{SW}} \oint_\gamma \lambda, \qquad Z_{-\gamma} = -Z_\gamma, \qquad |Z_{-\gamma}| = |Z_\gamma|. \tag{XVI.12.36}$$

The mass alone loses this sign and the associated phase. Specifying a charge and its central charge also does not determine whether a BPS state occupies it in a chosen chamber. In particular, the torus's finite center-line pair (e, m) is not the complete

particle charge lattice with multiplicities. Importing the three torus line sets would not complete the BPS problem for T_3.

For AGT we must first specify which partition function or conformal block is requested. The necessary choices retained here are

$$\begin{aligned}\mathcal{C}_{\mathrm{AGT}} = \{&\text{observable definition},\ \Omega \text{ parameters},\\ &\text{mass dictionary},\ \text{channel and internal momenta},\\ &\text{normalization}\}.\end{aligned} \tag{XVI.12.37}$$

The anomaly pair is insensitive to the values of the two deformation parameters. Keeping a record fixed while changing them gives distinct requests,

$$\mathcal{R}' = \mathcal{R}, \qquad (\epsilon_1', \epsilon_2') \neq (\epsilon_1, \epsilon_2) \quad \Longrightarrow \quad (\mathcal{R}, \mathcal{C}'_{\mathrm{AGT}}) \neq (\mathcal{R}, \mathcal{C}_{\mathrm{AGT}}). \tag{XVI.12.38}$$

Likewise, a channel is a specified decomposition used to organize the calculation. It is not supplied by the isolated trinion's Coulomb dimension three. A normalization is required to distinguish a block comparison from a full correlator comparison. The next volume establishes the appropriate correspondence for explicit examples rather than inferring it from this list.

For an index we need the definition of the trace and the convention for fugacities, puncture wavefunctions, the gluing measure and the desired series order,

$$\begin{aligned}\mathcal{C}_{\mathrm{index}} = \{&\text{trace and fugacity convention},\\ &\text{puncture wavefunctions},\ \text{gluing measure},\ \text{series order}\}.\end{aligned} \tag{XVI.12.39}$$

The trace convention determines which protected states and charges enter. A finite series order determines the comparison actually being requested. Matching a truncated series at one order cannot become equality of complete functions merely by increasing the number of theories in a table.

A useful final exercise is to remove one necessary choice. Let I_X be a proposed set of supplied choices and define its missing set,

$$M_X = \mathcal{C}_X \setminus I_X, \qquad I_X = \mathcal{C}_X \setminus \{f\} \implies M_X = \{f\}, \qquad I_X = \mathcal{C}_X \implies M_X = \varnothing. \tag{XVI.12.40}$$

The last condition detects no omission from this particular list. It does not prove physical sufficiency. A choice can be present but inconsistent, such as cycles that do not belong to the specified smooth cover. Establishing consistency and carrying out the protected calculation remain the tasks of the next volume.

We have now closed the construction route begun with the six-dimensional parent. A decorated surface, spectral data, defect contributions and an appropriate global choice serve different purposes. The finite collection makes them available for calculation while retaining the physical assumptions that connect them. The next step is to choose an observable and supply its additional data, rather than asking the table to determine information it does not contain.

Exercises

1. For T_3 and the residual A_2 full-full-simple fixture submit the three ordered pole vectors (p_2, p_3), the ordered multiplicities (d_2, d_3) and the Coulomb spectra. Derive the infinity-pole condition and explain why the residual fixture has fields despite rank zero. Keep punctures in full, full, changed order.

2. Construct $SU(2)$ with four full fundamentals. Submit (n_v, n_h), (a, c) and its generic fully Higgsed quaternionic dimension. Derive the representation count and explain why removing the free center tensor and choosing genuine lines are different operations. Explain why the torus's three absolute labels cannot be assigned to fundamental matter unchanged.

3. For $p = 3, 4$ submit the ordered weights $([x], [z])$, deformation weights in increasing monomial power j, and their ordered roles. Use the labels `CB`, `mass`, `coupling`. Derive the weights from the differential and explain why equal rank or matching local weights would not prove a full physical equivalence.

4. Return the exact row-name sets for rank one, rank one with a dimension-three coordinate, all rows containing dimension three, all rows containing dimension five and rank one with supplied $\mathfrak{e}_6$ flavor. Identify rows by the construction names in the atlas table. Explain the difference between an empty answer, an absent field and a computed zero. Explain why T_4 enters only one of the dimension-three selections.

5. Submit the gauged anomaly pair, the complex orbit dimension for $[2, 1]$, the quaternionic Goldstone count and the residual fixture's hypermultiplet count. Also substitute the finite-H differential's limit and submit its difference from φ_3 as a rational expression in z, L, m, U, b, c. Derive each result and explain why gauging, closure and collision do not share a single list of preserved observables.

6. For the BPS, AGT and index lists above, the benchmark asks for the missing field in each of three supplied choice lists. The instructor must provide those lists to complete this part of the question. Give a concrete physical consequence of omitting that field, then describe one additional consistency requirement beyond mere field presence. Explain why the result is a necessary-choice test rather than an evaluation or sufficiency theorem.

For benchmark submissions, see `benchmark/PROTOCOL.md`. Equivalent rational expressions and reorderings of sets are accepted. Keep pole vectors, deformation weights and role labels in the specified order. Include the requested written derivations and explanations.

Sources and scope

Section 12.1. The compactification, twist and physical spectral dictionary are inherited [GEO-E] premises of Chapters 1–4. The characteristic-map anchor is Gaiotto, Moore,

et al. (2013, arXiv v2, §4.2.2, eq. (166) and following paragraph); its §4.1, eqs. (155)–(158), concerns boundary behavior. Regular partitions and fixed-mass poles use Gaiotto (2009, arXiv v1, §§2.1, 3.1, pp. 41–42). Sphere section counts and the infinity-chart transformation are [MATH]. Existence of the named fixtures and the residual full-full-simple assignment remain sourced premises. Missing values mean uncomputed here.

Section 12.2. Effective anomalies use the [ANOM] dictionary of Chapter 7 and Gaiotto and Maldacena (2009, arXiv v4, pp. 5–6, eqs. (2.1)–(2.4)), together with Chacaltana and Distler (2010, arXiv v2, §§5.2–5.3). Their arithmetic and the selected scaling weights are [MATH]. The $SU(4)$ full puncture locator is Fig. 37e of Gaiotto v1; Fig. 36c concerns $SU(3)$. Fixture identities and T_3 enhancement are [GEO-E]; they are not inferred from equal numerical columns. Mirror and Higgs protection retain [CONJ+], using Benini et al. (2010, arXiv v1, p. 5, pp. 7–10, eqs. (3.1), (3.3)–(3.5)) and Cremonesi et al. (2014, arXiv v2, pp. 1–2, 10). The node-rank calculation establishes no ring, metric or global-group equality. AD local scaling uses Xie (2013, arXiv v2, §4.1.1, eqs. (4.1)–(4.5)) and Xie and Yau (2015, arXiv v1, §§2.1–2.2). The source half-hyper and distinct cylinder decorations use Chacaltana, Distler, and Trimm (2013, arXiv v1, §4.1, pp. 59–60) and Tachikawa (2009, arXiv v2, §3, pp. 9–11). The D_4 and C_3 degrees are sourced invariant spectra; representation dimensions and half-hyper counts are explicit arithmetic. Torus line assignments use Tachikawa (2013, arXiv v2, §§3, 4.1) and Aharony et al. (2013, arXiv v3, §§1.2, 2.4), graded [GEO-E]. Their finite line sets are [MATH], within the enhanced periodic spin-torus setup.

Section 12.3. Finite intersections and missing-value distinctions are [MATH]. Flavor filters use the sourced assignments from Chapters 5–6 and 10. A singleton or empty selection describes only the twelve supplied rows.

Section 12.4. Gauging and closure use the sourced [GEO-E] premises of Chapters 3 and 5–7. The vector sum, centralizer, orbit and rational limit are [MATH]. The confluence target is Gaiotto, Moore, et al. (2013, arXiv v2, p. 134, eq. (10.19)). Only the tuned four-to-three limit is used. The residual fixture excludes its two local Goldstone dimensions. No conservation of anomalies under closure, or new duality under collision, is asserted.

Section 12.5. The AGT, index and BPS lists specify necessary input choices for the next volume. Missing-set calculations are [MATH]; list completeness is not a physical sufficiency theorem or a new protected correspondence. Period orientation recalls Chapter 4. No protected observable is evaluated in this chapter.

References

Aharony, O., N. Seiberg, and Y. Tachikawa (2013). "Reading between the lines of four-dimensional gauge theories". In: arXiv: `1305.0318 [hep-th]`.

Benini, F., Y. Tachikawa, and D. Xie (2010). "Mirrors of 3d Sicilian theories". In: arXiv: `1007.0992 [hep-th]`.

Chacaltana, O. and J. Distler (2010). "Tinkertoys for Gaiotto Duality". In: arXiv: `1008.5203 [hep-th]`.

Chacaltana, O., J. Distler, and A. Trimm (2013). "Tinkertoys for the Twisted D-Series". In: arXiv: `1309.2299 [hep-th]`.

Cremonesi, S. et al. (2014). “Coulomb branch Hilbert series and Three Dimensional Sicilian Theories”. In: arXiv: 1403.2384 [hep-th].

Gaiotto, D. (2009). “N=2 dualities”. In: arXiv: 0904.2715 [hep-th].

Gaiotto, D. and J. Maldacena (2009). “The Gravity duals of N=2 superconformal field theories”. In: arXiv: 0904.4466 [hep-th].

Gaiotto, D., G. W. Moore, and A. Neitzke (2013). “Wall-crossing, Hitchin Systems, and the WKB Approximation”. In: *Adv. Math.* 234, pp. 239–403. DOI: 10.1016/j.aim.2012.09.027. arXiv: 0907.3987 [hep-th].

Tachikawa, Y. (2009). “Six-dimensional D N theory and four-dimensional SO-USp quivers”. In: arXiv: 0905.4074 [hep-th].

Tachikawa, Y. (2013). “On the 6d origin of discrete additional data of 4d gauge theories”. In: arXiv: 1309.0697 [hep-th].

Xie, D. (2013). “General Argyres-Douglas Theory”. In: *JHEP* 01, p. 100. DOI: 10.1007/JHEP01(2013)100. arXiv: 1204.2270 [hep-th].

Xie, D. and S.-T. Yau (2015). “4d N=2 SCFT and singularity theory Part I”. In: arXiv: 1510.01324 [hep-th].